Volume 66A
Number 2
Mar.–Apr. 1962

Physics and Chemistry

U.S. DEPARTMENT OF COMMERCE

SECTION A

JOURNAL OF RESEARCH

NATIONAL BUREAU OF STANDARDS

Journal of Research

of the

National Bureau of Standards

A. Physics and Chemistry

MAR.–APR. • 1962

VOLUME • 66A

NUMBER • 2

Editor: C. W. Beckett

Associate Editors: D. D. Wagman
J. M. Richardson

Publication dates:
Feb. 1, Apr. 1, June 1, Aug. 1, Oct. 1, Dec. 1, 1962.

JOURNAL OF RESEARCH

The National Bureau of Standards Journal of Research reports research and development in the fields of activity shown at right. Also included from time to time are survey articles on topics closely related to the Bureau's scientific and technical program.

The Journal is published in four separate sections as follows:

A. Physics and Chemistry

Contains papers of interest primarily to scientists working in these fields. Issued six times a year. Annual subscription: domestic, $4.00; foreign, $4.75.

B. Mathematics and Mathematical Physics

Presents studies and compilations designed mainly for the mathematician and the theoretical physicist. Issued quarterly. Annual subscription: domestic, $2.25; foreign, $2.75.

C. Engineering and Instrumentation.

Reports research and development results of interest chiefly to the engineer and the applied scientist. Issued quarterly. Annual subscription: domestic, $2.25; foreign, $2.75

D. Radio Propagation and Atmospheric Physics

Reports work in radio propagation, upper atmospheric physics and communications. Issued six times a year. Annual subscription: domestic, $4.00; foreign, $4.75.

U.S. DEPARTMENT OF COMMERCE
Luther H. Hodges, Secretary

NATIONAL BUREAU OF STANDARDS
A. V. Astin, Director

Functions and Activities

The functions of the National Bureau of Standards are set forth in the Act of Congress, March 3, 1901, as amended. These include the development and maintenance of the national standards of measurement and the provision of means and methods for making measurements consistent with these standards; the determination of physical constants and properties of materials; the development of methods and instruments for testing materials, devices, and structures; advisory services to government agencies on scientific and technical problems; invention and development of devices to serve special needs of the Government; and the development of standard practices, codes, and specifications. The work includes basic and applied research, development, engineering, instrumentation, testing, evaluation, calibration services, and various consultation and information services. The Bureau also serves as the Federal technical research center in a number of specialized fields. The scope of activities of the National Bureau of Standards is suggested in the following listing of the divisions and sections engaged in technical work.

Washington, D.C.

Electricity. Resistance and Reactance. Electrochemistry. Electrical Instruments. Magnetic Measurements. Dielectrics. High Voltage.

Metrology. Photometry and Colorimetry. Refractometry. Photographic Research. Length. Engineering Metrology. Mass and Scale. Volumetry and Densimetry.

Heat. Temperature Physics. Heat Measurement. Cryogenic Physics. Equation of State. Statistical Physics.

Radiation Physics. X-ray. Radioactivity. Radiation Theory. High Energy Radiation. Radiological Equipment. Nucleonic Instrumentation. Neutron Physics.

Analytical and Inorganic Chemistry. Pure Substances. Spectrochemistry. Solution Chemistry. Standard Reference Material. Applied Analytical Research.

Mechanics. Sound. Pressure and Vacuum. Fluid Mechanics. Engineering Mechanics. Rheology. Combustion Controls.

Organic and Fibrous Materials. Rubber. Textiles. Paper. Leather. Testing and Specifications. Polymer Structure. Plastics. Dental Research.

Metallurgy. Thermal Metallurgy. Chemical Metallurgy. Mechanical Metallurgy. Corrosion. Metal Physics. Electrolysis and Metal Deposition.

Mineral Products. Engineering Ceramics. Glass. Refractories. Enameled Metals. Crystal Growth. Physical Properties. Constitution and Microstructure.

Building Research. Structural Engineering. Fire Research. Mechanical Systems. Organic Building Materials. Codes and Safety Standards. Heat Transfer. Inorganic Building Materials.

Applied Mathematics. Numerical Analysis Computation. Statistical Engineering. Mathematical Physics. Operations Research.

Data Processing Systems. SEAC Engineering Group. Components and Techniques. Digital Circuitry. Digital Systems. Analog Systems. Applications Engineering.

Atomic Physics. Spectroscopy. Infrared Spectroscopy. Solid State Physics. Electron Physics. Atomic Physics.

Instrumentation. Engineering Electronics. Electron Devices. Electronic Instrumentation. Mechanical Instruments. Basic Instrumentation.

Physical Chemistry. Thermochemistry. Surface Chemistry. Organic Chemistry. Molecular Spectroscopy. Molecular Kinetics. Mass Spectrometry.

Office of Weights and Measures.

Boulder, Colorado

Cryogenic Engineering. Cryogenic Equipment. Cryogenic Processes. Properties of Materials. Gas Liquefaction.

Ionosphere Research and Propagation. Low Frequency and Very Low Frequency Research. Ionosphere Research. Prediction Services. Sun-Earth Relationships. Field Engineering. Radio Warning Services.

Radio Propagation Engineering. Data Reduction Instrumentation. Radio Noise. Tropospheric Measurements. Tropospheric Analysis. Propagation-Terrain Effects. Radio-Meteorology. Lower Atmosphere Physics.

Radio Standards. High Frequency Electrical Standards. Radio Broadcast Service. Radio and Microwave Materials. Atomic Frequency and Time Interval Standards. Electronic Calibration Center. Millimeter-Wave Research. Microwave Circuit Standards.

Radio Systems. Applied Electromagnetic Theory. High Frequency and Very High Frequency Research. Modulation Research. Antenna Research. Navigation Systems. Space Telecommunications.

Upper Atmosphere and Space Physics. Upper Atmosphere and Plasma Physics. Ionosphere and Exosphere Scatter. Airglow and Aurora. Ionospheric Radio Astronomy.

Order all publications from the Superintendent of Documents
U.S. Government Printing Office, Washington 25, D.C.

Use of funds for printing this publication approved by the Director of the Bureau of the Budget (June 19, 1961).

JOURNAL OF RESEARCH of the National Bureau of Standards—A. Physics and Chemistry
Vol. 66A, No. 2, March–April 1962

Correction Factors for the Calibration of Encapsulated Radium Sources

R. M. Lee and T. P. Loftus

(December 7, 1961)

Several aspects of the procedure and corrections for the calibration of encapsulated radium sources at NBS have recently been investigated. It was found that a chamber equipped with a guard-ring type electrode system allowing the use of a vibrating reed electrometer as a current detector provides more versatility and precision than the gold-leaf electroscope now in use for routine calibrations. Absorption corrections for the U.S. primary national radium standards have been determined for the NBS chamber: 0.78 percent for standard 5440 and 1.01 percent for standard 5437. The Owen-Naylor integral equation for absorption of rays in the walls of cylindrical radium sources has been evaluated by a power series expansion of the integrand. Absorption coefficients and correction factors for platinum and Monel metal (materials commonly used for source capsules) have been computed for the NBS chamber.

1. Introduction

Encapsulated radium sources are calibrated at the National Bureau of Standards by a comparison, through secondary working standards, with primary national standards prepared by Hönigschmid [1][1] in 1934. A gold-leaf electroscope with lead and aluminum walls is used for measuring the gamma rays emitted by the sources. The ratio of the measurements with the standard and tested source multiplied by the weight of radium element present in the standard is certified as the "equivalent weight" of the source. A correction factor for the absorption of gamma rays by the wall of the source being calibrated is also given.

Several aspects of the calibration procedure and corrections have recently been investigated. These include the instrument used for comparing sources, absorption corrections for the Hönigschmid standards, and corrections for the wall absorption of the tested source. It was found that a chamber (with walls similar to those used for the gold-leaf electroscope) equipped with a guard-ring type electrode system allowing the use of a vibrating reed electrometer as a current detector provides more versatility and precision. Absorption corrections for the Hönigschmid standards were determined so that the true weight of radium instead of the "equivalent weight" might be determined. The capsule wall absorption corrections were determined through the use of an evaluation of the integral for the absorption of parallel gamma rays by a cylindrical wall. This integral was evaluated by a term-by-term integration of the integrand expanded in a power series. Using the new current detector for the measurements and this evaluation of the integral, an effective absorption coefficient for platinum (commonly used for capsule walls) and its dependence on several factors was determined. Measurements were also made with Monel metal which is used to a lesser extent for encapsulations.

[1] Figures in brackets indicate the literature references at the end of this paper.

2. Equipment and Method

The measurements were performed with a lead-walled cubical ionization chamber equipped with a guard-ring type electrode system allowing the use of a vibrating reed electrometer as a current detector. The chamber walls are of the same construction as those used for the gold-leaf electroscope, the instrument used for routine radium calibrations. They consist of 5-mm-thick inner aluminum walls and 10-mm-thick outer lead walls, and are 10 cm on a side. Ionization currents were measured using the capacitance method, with a nulling potentiometer and electronic timer to determine the rate of change of potential with time. Only comparisons of ionization currents resulting from different source conditions are involved in the measurements, so that with capacitance and null voltage constant, only the time need be determined accurately. Saturation curves were plotted and the voltage difference between the electrodes of the chamber was set at an appropriate value.

As in ordinary calibrations, the sources were measured with their axes horizontal and parallel to the front face of the chamber. The source and chamber were at the same height so that the rays could pass horizontally into the chamber. In most cases, the distance between the source and chamber has been made as small as possible since the larger currents can be measured with more precision. The distance cannot be made too small, however, because the correction factors which have been computed depend on the assumption that the gamma rays going from the source to the detector are parallel.

Several experiments, such as the result of one depicted in figure 2, have been performed to determine the minimum distance which may be used for the measurement of a particular quantity.

Long-term changes in measuring conditions such as temperature and pressure were avoided by performing the comparisons over short periods of time and in an ABBA sequence. Where possible, conditions were arranged so that ionization currents were large enough to make background correction unnecessary. If the currents were too small, it was found that the measurements were affected by pulses in the background current. These background pulses were studied by making a continuous recording of the electrometer readings. About 130 of these pulses are observed per hour and their magnitude is approximately 1×10^{-4} statcoulomb. The charge produced in air by the passage of alpha particles from radionuclides such as Rn^{222} is of this order of magnitude.

3. National Standard Correction Factors

3.1. Description of the Standards

The National radium standards used at NBS are two of twenty sources prepared by Hönigschmid in 1934 for use as international and national standards. The sources acquired by the United States were designated as numbers 5437 and 5440 by Hönigschmid, who determined their radium element content by careful weighing to be 38.23 and 20.45 mg respectively as of June 2, 1934. They are also assigned the roman numerals XIV and XV, respectively, by the International Radium Standards Commission as a result of a comparison with the Paris and Vienna 1911 standards. The weights derived from this comparison are 38.13 and 20.38 mg, respectively, as of June 1934. The encapsulation is Thüringen glass tubing of 0.27 mm wall thickness and internal diameter of 3 mm and lengths of 36.7 and 36.3 mm [2] respectively. More information and photographs of the sources are given by Loftus et al. [2] and Davenport et al. [3].

3.2. Corrections Proposed by Other Authors

Although there is no information available on the absorption corrections for the Hönigschmid standards using the NBS type chamber, several values have been proposed for use with other types for the horizontal orientation shown in figure 1. Perry [4] has estimated the correction for the standards in general to be about 0.5 percent for a chamber with a 5-mm wall of lead and no aluminum wall. Weiss [5] lists wall and salt absorption corrections for Hönigschmid standards and a chamber similar to the one used by Perry, but the sources measured are enclosed in an additional tube of glass. The method used for computing the salt absorption is given by Fränz and Weiss [6].

Another analysis of the correction factors is given by Geiger [7] for a chamber with composite walls of 6 mm lead and 6 mm aluminum. The value for this chamber should be nearly the same as one for the NBS chamber, since the walls are of similar construction. He computed total absorption corrections of 1.13 percent and 1.09 percent for the Hönigschmid standards 5425 (Canadian) and 5440 (U.S.) respectively by a graphical integration. The calculation is based on the assumption that the salt is fine grained and uniformly distributed along the bottom of the glass tube. Examination of enlarged photographs of the standard 5440 indicates, however, that the average grain size is about 0.3 mm, 20 percent of the inner radius of the tube itself. The grains are large enough so that most of them appear to be along the bottom of the tube in a single layer four or five grains across. In order to avoid making this assumption, other methods of determining the correction factors were developed.

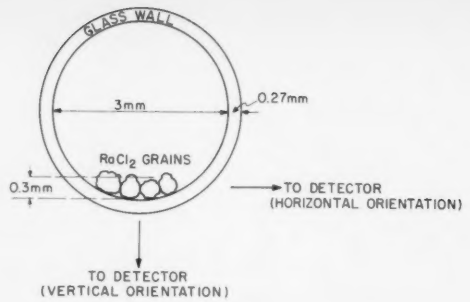

FIGURE 1. *Diagram defining the vertical and horizontal orientation of the radium source and detector.*

The arrows indicate the position of the detector which is the lead and aluminum walled ionization chamber. The horizontal orientation is normally used, but in the vertical orientation there is less salt and wall absorption and the correction factors can be computed more easily.

3.3. Absorption Correction for Standard 5440

It is considerably easier to compute the correction factors for a vertical orientation, that is, with the axis of the source being parallel to the floor and the rays being directed downward into the chamber. The source geometry in this position is more clearly defined and the absorption corrections are smaller than for the horizontal position which is normally used. Figure 1 shows the vertical and horizontal orientations. By measuring the difference in the ionization current for radiation coming from the primary source placed in the vertical and horizontal orientations, the difference in their absorption corrections can be found. The absorption correction for the horizontal position is, then, the sum of this difference and the absorption correction computed for the vertical position.

The experimental procedure for determining this difference was to compare the primary standard 5440 in both orientations to a radially symmetric source. The percent difference in these comparisons is equal to the percent difference in the absorption corrections. The average of 19 determinations of this quantity is 0.37 percent and the standard error of the mean is 0.06.

The wall absorption for rays passing downward from the source to the chamber was computed from an effective wall thickness of 0.279 mm as determined by a graphical integration assuming that the width of the salt along the axis of the tube is 1.4 mm, as estimated from the enlarged photograph. The mass absorption coefficient for the glass was taken to be 0.032 cm^2/g which is the coefficient for elements with Z less than 57, given by Michel [8]. This figure was determined for the Canadian National Research Council chamber, but its construction is similar enough to the NBS chamber that the error incurred in its use should be negligible.[2] The density of the glass, computed from dimensions listed on the source certificate, is 2.39 g/cm^3. The linear absorption coefficient is then 0.076 cm^{-1}, and the computed absorption is 0.21 percent.

The computation of the salt absorption as opposed to the wall absorption for the vertical orientation is more uncertain and several different approaches to the problem have been considered. In the computations outlined below, the following quantities are estimated to have an accuracy of better than 5 percent: the density of the individual $RaCl_2$ grains is 4.9 g/cm^3 [9], the volume of the salt with the tube on end is 11.9 mm^3 (by actual measurement using a cathetometer), the density as computed from this volume is 2.26 g/cm^3 (Michel and Whyte [10] give 2.2 g/cm^3), and the mass absorption coefficient[3] for $RaCl_2$ is 0.047 cm^2/g. The percent absorption corrections are based on the formula, $100(1-e^{-\mu x})$, where μ is the product of the mass absorption coefficient and the density of the salt and x is taken to be one-half the length of the salt through which the rays pass.

A value for the salt absorption in the vertical direction may be calculated assuming a uniform distribution of fine grains and a density of 2.26 g/cm^3. Such a calculation provides an absorption correction of 0.12 percent for primary 5440. Calculation of the salt absorption using a more realistic description of the salt configuration provides values which are somewhat higher.

An estimate of the depth of the salt grains may be made from the volume measurement with the tube on end and length and width measurements from an enlarged photograph. With the salt evenly distributed through the length of the tube the dimensions are 32.75 and 1.38 mm giving a depth of 0.263 mm. Using this depth, and the density 2.26 g/cm^3, the absorption is 0.14 percent.

From the photograph, an average grain diameter of 0.3 mm was estimated. If the effective shape of the grains is assumed to be spherical, the salt absorption calculated from a formula given by Dixon [11] and using 4.9 g/cm^3 for the salt density, is 0.26 percent. The average of these two values is 0.20 percent and the estimated error is taken to be ± 0.06, one-half the difference between the values.

[2] This is assumed since the absorption coefficient for Monel metal (composed of elements with Z less than 57) reported in this paper is 0.0335 cm^2/g, only 5 percent different from Michel's value. In this paper and also in Keyser [16] it is shown that the absorption coefficient for platinum is also approximately the same for both chambers.

[3] This value is given by Geiger [7]. It was measured with the Canadian chamber and its use here is discussed in footnote 2.

The total absorption correction using the average value of 0.20 percent ± 0.06 for the salt absorption and 0.21 percent (with a negligible error) for the wall absorption, is 0.41 percent ± 0.06. Adding this to the measured difference of 0.37 percent ± 0.06, the correction for the horizontal orientation is 0.78 percent for national standard 5440 and the estimated error is $(0.06^2+0.06^2)^{1/2}=0.09$.

3.4. Absorption Corrections for Standard 5437

Mann [12] has developed a calorimeter, called a radiation balance, for comparing the energy emission from radioactive sources. Absorption corrections for radium sources in a calorimetric calibration are quite small[4] and in many cases need not be determined for 0.1 percent accuracy. If a source is calibrated with a standard using both the calorimetric and ionization chamber method, a difference in values will result which depends upon the absorption corrections for the standard and source calibrated. By correcting this difference for the absorption of gamma rays in the calibrated source, the remaining discrepancy can be used as a measure of the absorption correction for the standard.

Attix and Ritz [13] give the result of a calibration of a secondary NBS standard N–100 with the primary standard 5437 carried out by W. B. Mann using a Peltier-effect twin microcalorimeter [14] specially designed for the comparison of Hönigschmid standards. The value, 99.6_2 mg $\pm$00.3, was obtained as of October 1956. The result of a recent calibration using the vibrating reed electrometer method described above is 100.63 mg (corrected for absorption in the secondary standard and for decay since October 1956) with a 0.05 percent standard error of the mean. The difference between the two determinations is then 1.01 percent which represents the absorption correction for the standard 5437.

3.5. Summary

The corrections derived from the two methods described above are 0.78 percent for the 5440 and 1.01 percent for the 5437. This difference in absorption corrections of 0.23 percent occurs because standard 5440 contains 20 mg of radium element and the 5437 contains 38 mg, making the geometries different. Loftus et al. [2] compared several of the Hönigschmid standards with both the calorimeter and the electroscope. Table 1 lists the pertinent data. The differences in the ratio obtained by the two methods should be a measure of the differences in gamma ray absorption since the calorimetric method is independent of corrections. The difference in weight for the 5440 and 5437 standards is 18 mg which corresponds to a percent difference of about 0.25, in good agreement with the difference of 0.23 percent for the two methods.

[4] The size of the absorption corrections depends upon the amount of energy which is not absorbed in the calorimeter, usually several percent. If, for example, it is 5 percent, then absorption corrections for the calorimetric method will be 5 percent of those for the ionization chamber method.

TABLE 1. *Difference in calorimetric and electroscope methods of measuring Hönigschmid standards from Loftus et al.*

Sources compared	Difference in weight of two standards	Ratio of radiation balance ratio to electroscope ratio
	mg	
C/D	04	1.000
D/B	04	1.002
D/G	05	1.002
A/C	14	1.003
A/D	18	1.002
A/D	18	1.000
A/D	18	1.003
A/B	22	1.003
A/G	23	1.002

4. Evaluation of the Owen-Naylor Integral

Owen and Naylor [15] have derived an integral equation for the absorption of gamma rays in a cylindrical capsule having its axis at right angles to a line drawn between the source and the detector. It is assumed that the rays leaving the source are parallel and that the capsule is completely filled with radium salt. That integral is:

$$I/I_0=\frac{4}{\pi}\int_0^{\pi/2}\cos^2 x\cdot e^{-\mu a(\sqrt{(b/a)^2-\sin^2 x}-\cos x)}\,dx$$

where a=internal radius
b=external radius
μ=linear absorption coefficient
x=an angle
I_0=intensity of unattenuated radiation
I=intensity after wall absorption

Using a planimeter, Owen and Naylor evaluated this integral for specific wall thicknesses and external diameters. To gain more accuracy and flexibility in its application, it was decided to integrate the equation by expanding the exponential in a power series. The exponent is usually of the order of 0.1 or less so that three terms in the expansion is sufficient, the contribution of the fourth term being of the order of 0.01 percent. The result of the expansion is seven terms which may be integrated term by term. The integration of one of these terms was performed by another expansion (in four terms). The result is:

$$\begin{aligned}I/I_0=1+\mu[5a^6/1024b^5+a^4/64b^3+a^2/8b+8a/3\pi-b]\\+\mu^2[b^2/2+a^2/4+(b^2/\pi)(b^2/2a^2-2)\arcsin(a/b)\\-1/\pi\sqrt{(b/a)^2-1}(b^2/2+a^2)]+\ \ldots\end{aligned}\quad(1)$$

It may be noticed that eq (1) is of the form:

$$I/I_0=A(a,b)\mu^2+B(a,b)\mu+1. \quad (2)$$

The result was checked to better than 0.1 percent for specific cases using Simpson's rule and by comparison with Owen and Naylor's graphical evaluation.

5. Linear Absorption Coefficient for Platinum and Monel Metal

5.1. Previous Measurements

It is important to note that the effective absorption coefficients determined are highly dependent upon the thickness and composition of the walls of the chamber used for the measurement. Platinum (actually 90 percent platinum and 10 percent iridium) is most widely used for the capsules of radium sources which are submitted for calibration, but there have been few measurements of the platinum absorption coefficient for the type of chamber used at NBS. Keyser [16] has made measurements using the same type of chamber, but flat absorbers were used to measure the absorption coefficient of platinum, instead of cylindrical sleeves which more nearly approximate the condition under which the coefficient will be used. The determinations for three different flat absorber thicknesses are 1.000 ± 0.050, 0.960 ± 0.050, and 0.960 ± 0.060 cm^{-1}, averaging 0.973 cm^{-1}. The value 0.93 cm^{-1} was given to Attix and Ritz [11] in a private communication from G. N. Whyte, but no details on the type of absorbers used were given.

5.2. Procedure

The linear absorption coefficients were computed from measurements using right cylindrical sleeves of the material in question and two secondary standard sources, nominally 50 and 100 mg, which fit snugly in and were the same length as the sleeves. The wall thickness of the sleeves, the critical value, was computed indirectly from their density, weight, length, and external diameter, quantities which could be measured very accurately. This method has an advantage over more direct means because it accounts for irregularities in the internal diameter and gives an average wall thickness for the whole length and circumference of the tube. An average sleeve thickness is important since many measurements are taken using random orientations of source and sleeve. Errors in the sleeve wall thicknesses are estimated to be no greater than a few tenths of a percent. The dimensions used for the sources are certified by the manufacturer to be correct to 1 percent.

The ratio, R, of the electrometer measurements with the sleeve on the source to those with the sleeve off was found experimentally as described above. Using the internal radius, a, and the external radius, b, of the source, the coefficients, A and B in eq (2),

$$I/I_0=A(a,b)\mu^2+B(a,b)\mu+1,$$

could be computed. For the combination of the sleeve and source, a new eq (2) may be determined, using the internal radius of the source for a, and the sum of the external radius of the source and the wall thickness of the sleeve for b:

$$I'/I_0 = A(a,b')\mu^2 + B(a,b')\mu + 1.$$

Since the ratio of I' to I is R, μ may be computed from

$$R = \frac{A(a,b')\,\mu^2 + B(a,b')\,\mu + 1}{A(a,b)\,\mu^2 + B(a,b)\,\mu + 1}. \quad (3)$$

5.3. Dependence of μ on Several Factors

The linear absorption coefficient, μ, for platinum was measured under various conditions to obtain information on its constancy.

It was assumed in deriving the integral for wall absorption that the rays coming from the source were parallel. The effect of having nonparallel rays was determined by measuring the sleeve wall absorption for different distances between the source and the front of the detector (a 10-cm square) and making the computation for the linear absorption coefficient. Figure 2 shows the range of constancy for μ as a function of distance for a sleeve of wall thickness 0.934 mm. The graph shows that μ remains reasonably constant for distances greater than 20 cm.

Four sleeves having different wall thicknesses were used for the determination of μ, and the average values for several determinations with each sleeve are listed in table 2. The table indicates that there is a slight downward trend in μ with decreasing wall thickness. The magnitude of this trend makes it reasonable to assume that it is caused by such factors as the error in eq (1) due to the omission of the remaining terms in the expansion and the change in energy due to the absorption of softer gamma rays by the sleeve wall. These factors would all become negligible if a sleeve of very small thickness were used so that the best estimate of μ would be given by an extrapolation of μ to zero sleeve thickness. The use of a secondary standard source nominally 50 mg or one nominally 100 mg (having the same dimensions) had negligible effect on the data. The fact that these measurements were in such good agreement indicates that μ is independent of wall thickness in the range used, that there was good precision in the dimensions, and that errors due to a looseness of fit of the source in the sleeve (this varied appreciably among the different combinations of sources and sleeves) were negligible.

Several different geometries were used in the measurements and it was noted that the effects of scattering objects on the ratio, R, were not appreciable except if located near the axis of the source so that rays passing out through the ends are scattered and detected.

TABLE 2. *Linear absorption coefficient for platinum measured with different sleeve wall thicknesses*

Sleeve wall thickness	Linear absorption coefficient
mm	*cm*$^{-1}$
1.892	0.944
1.343	.940
0.934	.941
.438	.939

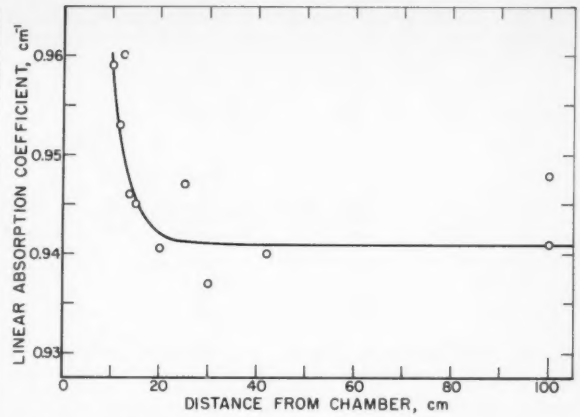

FIGURE 2. *Dependence of the linear absorption coefficient of platinum on the distance between source and chamber.*

5.4. Final Result

Twenty-one values, measured under various conditions (except where the divergence of the beam was considered to have an appreciable effect), were averaged in the determination of μ with the four platinum sleeves listed in table 2. It was pointed out above that the best estimate of μ is given by an extrapolation of μ to zero sleeve thickness. The result of this extrapolation is $\mu = 0.939$ cm^{-1} and the estimated error is 0.2 percent, one-half the range of values. Since the source used for the measurements had a 0.5-mm platinum wall, this value of μ is applicable to gamma rays from radium filtered by 0.5 mm platinum, 10 mm lead and 5 mm aluminum. Table 2 shows that μ remains reasonably constant for wall thicknesses up to approximately 1.5 mm so that it can be used in that range. A check on this value was performed using the gold-leaf electroscope. The mean of six measurements was 0.95 cm^{-1} with a 1 percent standard error of the mean.

In different laboratories, ionization chambers having varying wall thicknesses are used for calibrations. So that comparisons may be made, μ for platinum was measured as a function of chamber wall thickness by replacing the outer wall with lead filters of different thickness. Table 3 lists these values and figure 3 shows the shape of the curve. These measurements were performed with a source having a 0.5-mm platinum wall to which was added a cylindrical sleeve having a 0.934-mm platinum wall so that the values listed are for these filtrations.

The linear absorption coefficient for Monel metal was also measured using three sleeves and a value of 0.296 cm^{-1} with a 0.8 percent standard error of the mean. Correction factors for filled capsules of various wall thickness and external diameter were computed for Monel metal and platinum using eq (1), the result of the evaluation of the Owen-Naylor integral. Tables 4 and 5 list these correction factors and figure 4 shows the shape of some representative curves.

TABLE 3. *Linear absorption coefficient of platinum for chambers having 5-mm inner aluminum walls and different thicknesses of lead outer walls*

Lead wall thickness	Linear absorption coefficient
mm	*cm*$^{-1}$
00	1.381
02	1.152
04	1.056
06	0.993
08	.965
10	.941
12	.914
14	.910
16	.908
18	.901
30	.873

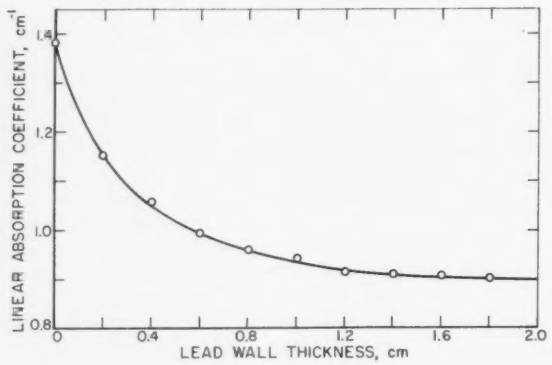

FIGURE 3. *Dependence of the linear absorption coefficient of platinum on the lead wall thickness of the ionization chamber.*

The ionization chamber has 5-mm inner walls of aluminum to which varying thicknesses of lead were added. A 1.0-cm lead wall is used at NBS.

TABLE 4.—*Platinum wall correction factors for filled cylindrical radium sources*

Wall thickness	Outside diameter, mm						
	1	2	3	4	5	6	7
mm							
0.1	1.0108	1.0114	1.0118	1.0119	.....	.....	.....
.2	1.0207	1.0220	1.0229	1.0234	.....	.....	.....
.3	1.0299	1.0323	1.0337	1.0346	.....	.....	.....
.4	1.0391	1.0423	1.0441	1.0450	.....	.....	.....
.5	1.0481	1.0522	1.0541	1.0552	1.0561	.....	.....
.6	.....	1.0615	1.0640	1.0652	1.0658	.....	.....
.7	.....	1.0710	1.0744	1.0764	1.0778	.....	.....
.8	.....	1.0806	1.0848	1.0872	1.0891	.....	.....
.9	.....	1.0895	1.0941	1.0971	1.0993	.....	.....
1.0	.....	1.0985	1.1038	1.1072	1.1095	1.1114	.....
1.1	.....	.....	1.1135	1.1172	1.1197	1.1218	.....
1.2	.....	.....	1.1229	1.1271	1.1300	1.1322	.....
1.3	.....	.....	1.1324	1.1373	1.1408	1.1438	.....
1.4	.....	.....	1.1417	1.1471	1.1509	1.1541	1.1570
1.5	.....	.....	1.1512	1.1572	1.1614	1.1645	1.1674

TABLE 5.—*Monel wall correction factors for filled cylindrical radium sources*

Wall thickness	Outside diameter, mm						
	1	2	3	4	5	6	7
mm							
0.1	1.0034	1.0037	1.0038	1.0039	.....	.....	.....
.2	1.0065	1.0069	1.0071	1.0073	.....	.....	.....
.3	1.0094	1.0101	1.0106	1.0108	.....	.....	.....
.4	1.0122	1.0132	1.0139	1.0143	.....	.....	.....
.5	1.0149	1.0163	1.0168	1.0172	1.0174	.....	.....
.6	.....	1.0192	1.0199	1.0201	1.0205	.....	.....
.7	.....	1.0220	1.0230	1.0235	1.0238	.....	.....
.8	.....	1.0248	1.0260	1.0267	1.0271	.....	.....
.9	.....	1.0274	1.0289	1.0298	1.0303	.....	.....
1.0	.....	1.0300	1.0317	1.0327	1.0335	1.0339	.....
1.1	.....	.....	1.0344	1.0356	1.0364	1.0370	.....
1.2	.....	.....	1.0372	1.0386	1.0395	1.0401	.....
1.3	.....	.....	1.0401	1.0416	1.0426	1.0432	.....
1.4	.....	.....	1.0427	1.0444	1.0456	1.0463	1.0469
1.5	.....	.....	1.0454	1.0473	1.0486	1.0494	1.0501

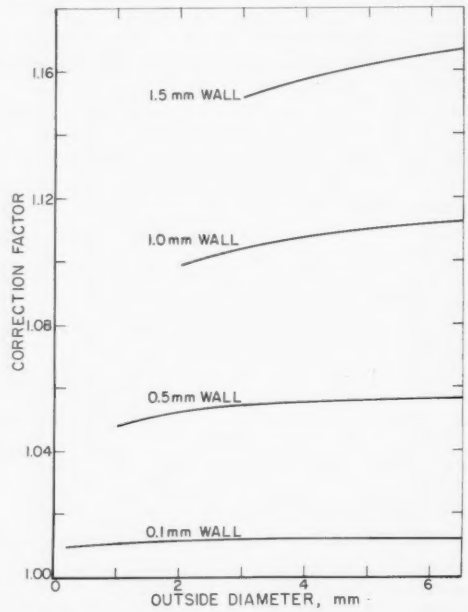

FIGURE 4. *Correction factors for gamma ray absorption in cylindrical platinum walls.*

Four representative curves for wall thicknesses of 0.1, 0.5, 1.0, and 1.5 mm are shown. The factors were computed from an absorption coefficient of 0.939 cm^{-1} using the evaluation of the Owen-Naylor integral given in this paper. They are applicable only for measurements with an NBS type chamber.

6. Discussion

As a result of an investigation of the radium calibration procedure, measurements can be performed with greater precision, more accurate wall absorption corrections have been developed, and through the use of absorption corrections determined for the primary standards, the "true weight" of radium element in a source can be specified. If the current reading for the source being calibrated is I_x (which is increased by a factor A_x for wall and salt absorption in the source), the current reading for the standard is I_s (with corresponding factor A_s),

and the weight of radium element in the standard is M_s, then the "true weight" of radium element in the source being calibrated is:

$$M_x = \frac{I_x A_x}{I_s A_s} M_s \qquad (4)$$

In this equation, $M_s\, I_x/I_s$ is the "equivalent weight."

In table 6, the accuracy with which each quantity in eq (4) can be determined is listed. The total estimated error is the square root of the sum of the individual errors squared and is equal to 0.17 percent.

TABLE 6. *Accuracy with which a typical radium source can be calibrated at NBS*

see eq (4)

Quantity	Estimated error	Range for error	Source of quantity
	%		
I_x/I_s	0.07	10 to 250 mg RaEl	Experimentally determined by the new method with four readings on each source.
A_s	.09	All sources	Determined in this paper. 0.78% for standard 5440 and 1.01% for standard 5437.
A_x:			
wall	.06	Less than 1.5-mm wall thickness.	Determined in this paper. $\mu = 0.939$ cm^{-1} for Pt-Ir.
salt	.05	Less than 2 mm *ID*	From the equation for μ_e given by Michel [8]* and the method of Paterson et al. [17]
M_s	.1	All sources	"Best estimates" determined by Connor (Report of ICRU 1959 [18]).
Combined error = 0.17%			

*The use of this equation for the computation of absorption coefficients for radium salts is discussed in footnote 2.

The significant contribution of R. Cantor who performed the evaluation of the Owen-Naylor integral presented in this paper is gratefully acknowledged.

7. References

[1] O. Hönigschmid, Anz. Akad. Wiss. Wien **82,** 30 (1945).
[2] T. P. Loftus, W. B. Mann, L. F. Paolella, L. L. Stockmann and W. J. Youden, J. Research NBS **58,** 169 (1957) RP2749.
[3] T. I. Davenport, W. B. Mann, C. C. McCraven, and C. C. Smith, J. Research NBS **53,** 267 (1954) RP2544, pt. 1.
[4] W. E. Perry, Proc. Phys. Soc. **68,** 924 (1955).
[5] C. Weiss, Z. Physik **120,** 652 (1943).
[6] H. Fränz and C. Weiss, Phys. Z. **41,** 345 (1940).
[7] K. W. Geiger, National Research Council of Canada, Divisional Report No. APXNR–435 (1957).
[8] W. S. Michel, National Research Council of Canada, Divisional Report No. APR–271, NRC No. 3675 (1955).
[9] Handbook of Chemistry and Physics, 33d Ed. (1951) p. 555, Chemical Rubber Publishing Company, Cleveland.
[10] W. S. Michel and G. N. Whyte, Can. J. Phys. **33,** 521 (1955).
[11] W. R. Dixon, Nucleonics **8,** No. 4, 68 (1951).
[12] W. B. Mann, J. Research NBS **52,** 177 (1954) RP2486.
[13] F. H. Attix and V. H. Ritz, J. Research NBS **59,** 293 (1957) RP2801.
[14] W. B. Mann, J. Research NBS **53,** 277 (1954) RP2545.
[15] E. A. Owen and B. Naylor, Proc. Phys. Soc. (London) **34,** 92 (1922).
[16] G. M. Keyser, Can. J. Phys. **29,** 301 (1951).
[17] C. C. Paterson, J. W. T. Walsh, W. F. Higgins, Proc. Phys. Soc. **29,** 215 (1917).
[18] Report of ICRU 1959, NBS Handb. 78 (1961).

(Paper 66A2–145)

JOURNAL OF RESEARCH of the National Bureau of Standards—A. Physics and Chemistry
Vol. 66A, No. 2, March–April 1962

Description and Analysis of the Second Spectrum of Tantalum, Ta II

C. C. Kiess

(October 23, 1961)

The spectrum has been observed from 2000.73 to 7813.40 A. There are 2,629 lines listed, of which 1,890 have been classified. Observed Zeeman patterns are recorded, as well as g-values. These have aided greatly in the work on analysis. The 61 known even levels have been grouped into 26 terms from the $5d^3\ 6s$, $5d^2\ 6s^2$ and $5d^4$ configurations. The odd levels number 164; they have no assigned term designations. No series have been found, but the ionization potential is estimated to be between 16.0 and 16.5 electron volts.

1. Introduction

During the period 1930–1940 the concave-grating and quartz-prism spectrographs of the National Bureau of Standards were used to record photographically the spectra of several elements throughout the region from 1950 A in the ultraviolet to approximataly 13000 A in the infrared. The purpose of the investigations was to acquire data for descriptions of the spectra sufficiently extensive and homogeneous to serve for the analysis of their term-structures. These descriptions as finally tabulated comprise the wavelengths of the spectral lines, their estimated intensities, and their Zeeman effects. Thus far results have been published for the first and second spectra of chromium, Cr I and Cr II, [1],[1] and for the second spectrum of molybdenum, Mo II [2]. This paper presents similar results for the second spectrum of tantalum, Ta II. A subsequent paper will present results for Ta I. It is of interest to note that no detailed description of this spectrum has appeared since the publication of volume 6 of Kayser's Handbuch der Spectroscopie in 1912 [3], although the M.I.T. Tables of Wavelengths [4] do contain new wavelengths and estimated intensities for some of the stronger lines of Ta II.

2. Experimental Procedures

In the spectroscopy laboratory of this Bureau it was a common practice, whenever a spectrograph was adjusted for a given spectral region, to photograph the spectra of several elements during a period of observation. Thus, tantalum was one of the elements investigated concurrently with chromium and molybdenum. It is, therefore, unnecessary to repeat the statements, in the earlier papers, concerning the instruments, techniques, and accessories employed in making the observations. The electrodes used in the light-sources for this investigation were tantalum rods of high purity procured from the Fansteel Co. The only impurities detected in them, from measurements of the spectrograms, were a small amount of niobium (columbium), and a possible trace of wolfram (tungsten).

[1] Figures in brackets indicate the literature references at the end of this paper.

The first observations of the Zeeman effect for this Bureau's work on the spectra of tantalum were made for us by B. E. Moore who used the electromagnet and grating-spectrograph of the Brace Laboratory of the University of Nebraska. His first results showed well-resolved patterns for many of the stronger lines of both Ta I and Ta II. However, his untimely death in 1925, brought to an end his cooperation in the work. With the acquisition of a Weiss water-cooled magnet by the NBS the work was continued here. Our first observations were made with the 21-ft concave grating ruled by Rowland with 20,000 lines per inch. The low reflectance of this instrument in the short-wave regions limited its use to the visible spectrum. Subsequently additional observations were made with the large Hilger E 185 quartz-prism spectrograph, and with the grating-spectrograph carrying the concave grating ruled by R. W. Wood with 30,000 lines per inch. Thus observations of the Zeeman effect, at fields of approximately 35,000 oersteds were obtained for lines of Ta I and Ta II in the spectral range from 2180 to 8300 A. Subsequently the excellent plates obtained at M.I.T. under the direction of G. R. Harrison were sent to the NBS for measurement and study. All lines from 2300 to 7700 A, showing magnetic broadening or splitting, were measured even though many of them were overlaid by the Zeeman patterns of adjacent lines.

3. Results

3.1. Wavelengths, Intensities, and Zeeman Effects

The results of this investigation are presented in tables 1, 2, and 3. The wavelengths listed in the first column of table 1 are, in general, mean values derived from measurements of two or more spectrograms. A few lines, measured only once on a more-strongly exposed plate, have been kept because their reality has been indicated by the term-analysis. Many of the lines exhibit hyperfine structure, which is designated by the letter c after the estimated intensity in the second column. The wavelengths adopted for such lines are weighted means of the

623381—62——2

components measured in the complex patterns. It is recognized that this is not a strictly legitimate procedure because in most of the complex lines the fainter components are not fully resolved; but the adopted wavelength is sufficiently close to the undetermined real value to serve the requirements for identification and classification.

The intensities of the lines are estimated values based on the strength of photographic blackening they produce. The number 1 is assigned to the weakest lines measurable on a spectrogram, the stronger ones being graded on a linear scale relative to the faintest. It is obvious that intensities derived in this manner are not comparable in spectral regions that require different types of photographic emulsions to record them. The lines owe their complexity to a nuclear spin of 7/2, measured by McMillan and Grace [5], for the isotope 181, in which all but 0.01 of the nuclear mass is concentrated.

The wave-numbers of the lines in the third column were taken from Kayser's Tabelle der Schwingungszahlen, but have been corrected by the small amounts necessary for conformity with Edlén's [6] formula for the index of refraction of air. These numbers are the basis for the analysis of the term-structure of Ta II, and are equal to the differences between the energy-levels of the Ta atom involved in the production of the spectral lines. These level-differences are given in column 4. In the last column are given the Zeeman patterns from either the M.I.T. or the NBS spectrograms. Those given to only two places of decimals are from the NBS plates; all others from those made at M.I.T. The type of shading in unresolved magnetic patterns, which gives a clue to the J- and g-values of the combining levels, are indicated by letters with the significance, A=◥◤, B=◤◥, C=∧, D=⊓.

3.2. The Systems of Energy Levels

Analysis of Ta II was begun independently and almost simultaneously at three laboratories. When G. R. Harrison of the M.I.T. Spectroscopy Laboratory learned that the problem had been undertaken at the Spectroscopy Laboratory of the NBS he suggested that a joint announcement be made of the first results that had been obtained, and that the necessary continuation of the work be carried on at the NBS with the aid of the M.I.T. data. This suggestion was realized in part in the paper, "Preliminary list of terms of Ta II," [7]. At the same time a similar and somewhat more extensive paper by van den Berg [8] was issued by the Zeeman Laboratory of the University of Amsterdam. This earlier work showed that the prominent low even terms of Ta II arise in the electron configurations $5d^3\,6s$, $5d^2\,6s^2$, and $5d^4$, the clue to their identity having been found in well-resolved Zeeman patterns that are in very close accord with those from levels with Landé g-values.

The further procedure of unravelling the spectrum has followed the conventional practices of combing the spectrum for pairs and groups of lines separated by established level-differences, and of tying together related lines that exhibit the same g-values. These operations have been somewhat tedious; but as the structure of the spectrum began to unfold the work received guidance from the calculations of Trees et al., [9] which narrowed the limits of search for the levels expected theoretically.

In table 2 are listed the low even terms upon which the spectrum is built. The ground state $a\,^5\mathrm{F}$ arises in the electron configuration $5d^3(^4\mathrm{F})6s$; but interspersed among its components are levels from the $^3\mathrm{F}$ and $^3\mathrm{P}$ terms of $5d^2\,6s^2$, which thus becomes a strong competitor of $5d^3\,6s$ in governing the energetic processes of the atom. All of the $5d^36s$ terms have been found; and likewise all but $^1\mathrm{S}$ of $5d^2\,6s^2$. The configuration $5d^4$ requires more energy to excite its levels, with the result that only six of its 16 theoretically possible terms have been detected completely or partially. Resolved Zeeman patterns of a small number of unclassified lines indicate that transitions to undetected $5d^4$ levels do occur, but the connecting links have not yet been found.

The g-values that are assigned to the levels in table 2 are, for most of them, mean values derived from two to twenty well-resolved Zeeman patterns. They are sufficiently close to LS-values to justify the designation of the levels with the LS notation, although a study, by Trees [9, 10, 11] of the configuration interaction in tantalum indicates that most of the levels of table 2 are of mixed parentage.

The odd levels in table 3 reveal the extent to which the excited states of the ionized atom have departed from LS-coupling. A few of the lowest odd levels might be uniquely designated with LS-symbols, but to apply this mode of designation to the others would be meaningless. It has seemed best, therefore, for sake of brevity, to give as the designation of the line in table 1 the first three figures of the level-value and the appropriate inner quantum number.

3.3. Series and Ionization Potential

No high levels have been found that can be ascribed unambiguously to the configurations $5d^3\,ns$ and $5d^2\,6s\,ns$. It is impossible, therefore, at this stage of the analysis of Ta II, to calculate an ionization-potential from series-forming terms. An ionization potential of 7.88 ev has been found for the neutral Ta atom; for neutral W this value is 7.98 ev. For the homologous atoms Nb and Mo the estimated second ionization potentials are a little more than twice the first. If this ratio is of physical significance we may expect, therefore, that the ionization potential of singly ionized tantalum lies between 16 and 16.5 ev, which is essentially the same as the interpolated value given by Finkelnburg and Humbach [12].

During its progress the work described above has been aided with observational material from various individuals, and consultations with others. As stated previously, the late B. E. Moore, of the University of Nebraska, made the first magnetic observations that were of significance in analyzing the

spectra Ta I and Ta II. Later G. R. Harrison and W. J. Hitchcock of M.I.T. made available their Zeeman observations and the results which they had obtained from them. At the NBS, R. E. Trees has made numerous theoretical calculations to verify and identify the levels found for the low configurations and to predict the probable positions of others; R. Zalubas has obtained and measured several spectrograms to improve the description of Ta II in the region 2500 to 1950 A; and Mrs. Ruth Peterson has made extensive calculations and tabulations of the data. It is a pleasure for me to acknowledge my indebtedness to them and also to others who have made contributions to this work.

TABLE 1. *Wavelengths, term combinations, and Zeeman effects of* Ta II

Wave length λair	Intensity and notes	Wave number	Term combination	Zeeman pattern
7813. 40	2	12795. 01		
7733. 92	2	12926. 05		
7606. 07	4	13143. 78		
7510. 64	2	13310. 78	*c* $^3P_2$—413(1)	
6736. 86	1	14839. 61		
11. 75	1	14895. 13	*c* $^3F_3$—385(2)	
6598. 80	4	15150. 08		(**0.00,** 0.22, 0.46) 0.54 *A*
97. 09	5	15154. 03	*c* $^3P_0$—385(1)	
67. 94	3	15221. 27		
34. 22	2	15299. 82	*d* $^3F_4$—468(3)	
00. 81	5	15378. 45	*b* $^3G_5$—466(4)	
6496. 20	1	15389. 36		
05. 76	3	15606. 64	*c* $^3F_2$—385(1)	
6374. 86	10	15682. 38		(**0.00,** 0.27) **1.21,** 1.44
69. 04	18	15696. 61	*a* $^1D_2$—292(2)	(0.59, **1.19**) 0.00, **0.52, 1.10,** 1.72
11. 50	1	15839. 71	*b* $^3G_4$—440(4)	
6286. 85	1	15901. 82		
80. 22	4	15918. 61	*c* $^3P_1$—421(2)	
73. 54	1	15935. 55	*c* $^1D_2$—489(3)	
39. 91	1	16021. 44	*b* $^3D_3$—466(4)	
6187. 75	3	16156. 49		
61. 00	2	16226. 64		
57. 50	5	16235. 86	*b* $^3G_3$—430(2)	
46. 46	3	16265. 03	*b* $^3G_4$—444(3)	
34. 82	10	16295. 89		(0.00) 1.10
22. 58	3	16328. 46	*c* $^1G_4$—514(4)	
10. 37	1	16361. 09	*b* $^3H_5$—417(4)	
6079. 18	3	16445. 03	*b* $^3D_2$—468(2)	
42. 47	1	16544. 94	*b* $^3D_3$—471(3)	
17. 71	2	16613. 02	*c* $^3F_3$—402(2)	
5989. 34	1	16691. 70		
80. 86	5	16715. 37	*b* $^3G_3$—435(3)	
79. 61	1	16718. 87		
72. 96	1	16737. 48	*b* $^1G_4$—421(4)	
63. 72	1	16763. 41	*b* $^3D_2$—471(3)	
53. 85	1	16791. 20	*c* $^3P_2$—448(3)	
19. 99	1	16887. 24	*b* $^3D_1$—468(2)	
5891. 18	1	16969. 83	*c* $^1G_4$—521(3)	
78. 31	7	17006. 98	*d* $^3F_2$—468(2)	
62. 27	1	17053. 51		
38. 98	3	17121. 50	*b* $^3H_4$—415(3)	
33. 85	1	17136. 59		
5798. 32	2	17241. 59		
94. 35	1	17253. 41	*a* $^1F_3$—421(4)	
90. 78	2	17264. 04		
86. 72	1	17276. 17	*b* $^3H_4$—417(5)	
82. 90	1	17287. 57	*c* $^1D_2$—503(3)	
53. 43	3	17376. 12	*c* $^3F_2$—403(1)	
51. 78	15	17381. 10	*a* $^5P_2$—292(2)	(0.91, **1.80**) . . . , **0.52, 1.40,** 2.34
38. 10	1	17422. 54		

TABLE 1. *Wavelengths, term combinations, and Zeeman effects of* Ta II—Continued

Wave length λair	Intensity and notes	Wave number	Term combination	Zeeman pattern
5735. 53	8	17430. 34	*b* $^3G_3$—442(2)	(**0.00,** 0.39) **0.00***w*, 0.46, 0.85
35. 21	2	17431. 32	*d* $^3F_4$—489(3)	
30. 44	4	17445. 83		
18. 33	8	17482. 77	*a* $^1H_5$—417(5)	
16. 07	3	17489. 69	*a* $^3G_3$—292(2)	
04. 72	12	17524. 48	*c* $^3F_3$—411(2)	(0.000) 0.964
5688. 62	1	17574. 08	*b* $^1G_4$—429(3)	
60. 32	1	17661. 95		
57. 40	3	17671. 06	*d* $^3F_2$— 475(2)	
49. 61	1	17695. 43		
37. 82	1	17732. 43		
36. 43	8	17736. 81	*a* $^5D_1$—312(1)	
35. 95	8	17738. 32		
20. 19	2	17788. 06	*b* $^3G_5$—490(5)	
04. 46	1	17837. 98	*b* $^3D_1$—478(0)	
00. 63	18	17850. 18	*b* $^1D_2$—411(2)	
5576. 61	1	17927. 06	*a* $^3H_5$—361(4)	
74. 46	15	17933. 98	*c* $^3F_3$—415(3)	
72. 20	1	17941. 25		
69. 80	10	17948. 98	*a* $^1P_1$—413(1)	
62. 18	4	17973. 57	*c* $^3P_0$—413(1)	
57. 32	4	17989. 29	*a* $^5D_3$—337(2)	
52. 64	8	18004. 46	*d* $^3F_4$—495(3)	
52. 10	5	18006. 20	*b* $^3G_3$—448(3)	
51. 65	4	18007. 66		
51. 27	3	18008. 90		
05. 39	7	18158. 97	*b* $^1G_4$—435(3)	
5494. 42	7	18195. 23	*a* $^1F_3$—430(2)	
92. 94	2	18200. 13	*c* $^3P_1$—444(0)	
71. 74	5	18270. 65		
63. 22	8	18299. 14	*c* $^1D_2$—513(1)	
51. 98	3	18336. 87		
41. 98	3	18370. 56	*b* $^3D_2$—487(1)	
39. 40	10	18379. 27	*d* $^3F_2$—482(2)	
16. 62	1	18456. 57	*b* $^3D_3$—490(2)	
09. 67	6	18480. 28	*b* $^3G_4$—466(4)	
5378. 90	4	18585. 99		
77. 45	3	18591. 01	*b* $^3H_5$—440(4)	
73. 62	2	18604. 26		
69. 73	5	18617. 73	*b* $^3G_3$—454(2)	
69. 19	4	18619. 64	*b* $^3G_5$—498(5)	
67. 44	4	18625. 66	*c* $^3F_2$—415(3) *c* $^3F_4$—417(5)	
55. 82	7	18666. 09	*b* $^3G_4$—468(3)	
51. 10	2	18682. 55		
44. 57	8	18705. 38		
37. 24	1	18731. 07		
32. 66	1	18747. 15	*a* $^1P_1$—421(2)	
27. 06	1	18766. 86		
21. 15	7	18787. 71		
20. 69	2	18789. 33		
18. 66	7	18796. 50		
06. 67	1	18838. 97		
01. 53	2	18857. 23		
01. 16	3	18858. 55	*b* $^1D_2$—421(2)	
5292. 44	2	18889. 62		
90. 32	7	18897. 19	*c* $^1G_4$—540(5)	
86. 15	2	18912. 10	*b* $^3D_3$—495(3)	
66. 48	7	18982. 72		(0.00 *W*) 0.93 *A*
60. 67	25	19003. 70	*b* $^3G_4$—471(3)	(0.000 *W*) 0.999
55. 47	4	19022. 48	*b* $^3D_3$—496(3)	(0.59) 1.16

TABLE 1. *Wavelengths, term combinations, and Zeeman effects of* Ta II—Continued

Wave length λair	Intensity and notes	Wave number	Term combination	Zeeman pattern
5250. 60	5	19040. 14	*c* $^3F_4$—421(4)	
49. 29	7	19044. 91	*b* $^1G_4$—444(3)	(0.00 *w*) 1.56
48. 62	3	19047. 31		
46. 44	4	19055. 23	*c* $^1G_4$—542(4)	
37. 53	125*c*	19087. 66	*a* $^3D_1$—337(2)	(0.00) 0.77 *w*
30. 97	12	19111. 60	*b* $^3H_4$—435(3)	(0.00 *w*) 0.94 *w*
29. 91	5	19115. 47	*b* $^3G_4$—472(4)	(0.51 *B*) 1.22 *w*
29. 38	4	19117. 39	*b* $^3D_1$—490(2)	(**0.00,** 0.36) 1.45
28. 96	4	19118. 92	*d* $^3F_2$—489(3)	
03. 70	15*c*	19211. 74	*a* $^5D_2$—337(1) *b* $^3H_5$—446(4)	(**0.00,** 1.33) 1.58, **2.74**
01. 38	12	19220. 31	*a* $^5D_2$—337(2)	(0.72, **1.40**) 0.08, **0.81, 1.52,** 2.25
5196. 91	6	19236. 83	*d* $^3F_2$—490(2)	(0.46, **0.98**) 0.39, **0.89, 1.39,** . . .
93. 80	10*c*	19248. 36	*d* $^3P_1$—511(2)	(0.00) 1.14*W*
70. 09	6	19336. 65	*a* $^5P_2$—312(1)	(0.00) 1.35
65. 88	7	19352. 38		(0.00) 1.12
41. 39	5	19444. 59	*c* $^3F_3$—430(2)	(0.00) 1.13
40. 06	1	19449. 60	*b* $^1G_4$—448(3)	
39. 40	3	19452. 12		(0.00) 1.44
35. 55	2	19466. 69		(0.00) 1.07
22. 54	5	19516. 11		(0.00) 0.77
11. 51	3	19558. 22	*b* $^3G_3$—463(2)	
09. 36	90*c*	19566. 49	*b* $^3F_2$—292(2)	(0.534, **1.071** *W*) 0.000, **0.523, 1.064,** 1.600*w*
04. 33	1	19585. 74	*d* $^3P_1$—515(2)	
03. 80	5	19587. 80		(0.00) 1.14
01. 85	40	19595. 26	*a* $^3D_2$—367(3)	(0.00 *W*) 1.10*w*
5097. 24	20*c*	19613. 00	*b* $^3P_1$—369(1) *a* $^3G_4$—323(3)	(0.00 *w*) 1.031*w*
85. 35	4	19658. 86	*a* $^1P_1$—430(2)	(0.00) 1.06
84. 36	2	19662. 70	*a* $^1P_1$—430(0)	
56. 70	25	19770. 22	*b* $^3P_2$—382(3) *b* $^1D_2$—430(2)	(0.508) 1.111
44. 87	150	19816. 59	*b* $^3G_3$—466(4)	(**0.000,** 0.389, 0.751, 1.125) 0.508, 0.892, 1.245, 1.618, 1.986, **2.363**
34. 98	4*c*	19855. 51	*b* $^3P_1$—372(2)	
29. 59	12	19876. 80	*c* $^3F_4$—429(3)	(0.000 *w*) 0.799*wA*
13. 62	3	19940. 11	*c* $^3P_1$—461(1)	(0.000 *w*) 1.354*w*
4999. 20	15	19997. 63	*b* $^3H_4$—444(3)	(0.000) 1.075*B*
93. 24	15	20021. 48	*b* $^3G_3$—468(2)	
89. 98	10	20034. 56	*b* $^3P_2$—385(1)	(**0.000,** 0.973) 1.442, **2.415**
64. 78	12*c*	20136. 28	*c* $^3F_2$—430(2)	(0.67) 0.96
62. 34	8*c*	20146. 16	*a* $^1D_2$—337(1)	
59. 58	15*c*	20157. 35		(0.183*W*) 1.187*W*
53. 87	1	20180. 62		
52. 94	1	20184. 38		
50. 77	3	20193. 23	*b* $^3H_4$—446(4)	
46. 04	8	20212. 57	*b* $^3G_5$—514(4)	(0.000) 1.129
41. 55	12	20230. 93	*a* $^5D_1$—337(1)	(1.232) 0.275, 1.512
39. 36	2	20239. 89	*a* $^5D_1$—337(2)	
34. 03	10*c*	20261. 74	*a* $^3H_4$—361(4)	(0.00*W*) 1.19
06. 94	4	20373. 61	*a* $^3G_4$—330(5)	
03. 76	3	20386. 84	*a* $^5D_3$—361(4)	
4895. 40	8	20421. 64		
91. 37	1	20438. 47	*c* $^1D_2$—534(3)	
90. 27	3	20443. 05	*a* $^5P_2$—323(3)	
88. 66	7	20449. 80	*b* $^3D_3$—510(3)	(0.24) 1.25
88. 35	6	20451. 07	*a* $^5D_3$—361(2)	(**0.000,** 0.533, 1.038) 1.460, 1.978, **2.477**
85. 79	7	20461. 82	*b* $^3P_2$—389(3) *c* $^3F_4$—435(3)	(0.00*w*) 0.47*w*
79. 88	6	20486. 59	*b* $^3G_5$—517(5)	(0.000) 1.170

TABLE 1. *Wavelengths, term combinations, and Zeeman effects of* Ta II—Continued

Wave length λair	Intensity and notes	Wave number	Term combination	Zeeman pattern
4876. 40	2	20501. 18		(0.00) 1.07
73. 19	3	20514. 70		
66. 79	2	20541. 70	$c\ ^3P_1$—467(2)	
64. 48	50*c*	20551. 42	$a\ ^3G_3$—323(3)	(0.00*W*) 0.93 *w*
61. 03	3	20566. 03		(0.000) 0.986
60. 51	3	20568. 24	$b\ ^3D_1$—505(1)	
59. 29	2	20573. 38	$b\ ^3D_3$—511(2)	(0.00) 1.12
58. 38	7	20577. 27	$a\ ^1F_3$—454(2)	(**0.000,** 0.189, 0.372) **0.613,** 0.783, 0.959, . . .
55. 51	8	20589. 42	$d\ ^3F_4$—521(3)	(0.000*W*) 1.114*w*
43. 84	5	20639. 00	$c\ ^3F_3$—442(2)	(**0.000,** 0.174, 0.351) **0.719,** 0.906, 1.070, . . .
38. 54	1	20661. 60		(0.000*W*) 1.225
37. 00	2	20668. 20	$b\ ^3D_2$—510(3)	
32. 95	1	20685. 50	$b\ ^3G_3$—475(2)	
32. 50	1	20687. 43	$d\ ^3F_2$—505(1)	
29. 67	10	20699. 56	$b\ ^3P_0$—369(1)	(0.000) 0.686*w*
24. 98	4	20719. 70	$c\ ^1D_2$—537(1)	
08. 26	6	20791. 72	$b\ ^3D_2$—511(2)	(0.592) 1.045, 1.367
06. 37	3	20799. 92	$a\ ^1P_1$—442(1)	
05. 87	12	20802. 09	$b\ ^3F_4$—392(3)	
04. 03	10	20810. 03	$c\ ^3F_3$—444(3)	(0.129, 0.254, **0.390**) 0.683, 0.819, **0.939, 1.065,** 1.213, 1.333
4798. 57	2	20833. 72		
94. 09	15	20853. 18	$a\ ^1P_1$—442(2)	(0.000) 1.302*w*
93. 28	3	20856. 73		
89. 43	4	20873. 47	$b\ ^3H_5$—462(4)	(0.00) 1.57
85. 68	4	20889. 82	$b\ ^3G_4$—490(5)	
78. 25	8	20922. 33	$c\ ^3F_4$—440(4)	(0.306*w*) 0.974*w*
65. 18	4	20979. 70		
64. 71	4	20981. 77		
61. 42	7	20996. 24	$b\ ^3G_3$—478(3)	(0.360, 0.698, **1.036**) 0.488, **0.844, 1.200,** 1.552, 1.913
60. 79	5	20999. 04		(0.000*w*) 1.252*w*
59. 31	2	21005. 59	$c\ ^3F_2$—446(4)	
52. 36	3	21036. 76	$c\ ^3P_2$—490(2)	
51. 96	7	21038. 03	$a\ ^5D_3$—367(3)	(0.559, **0.937**) . . ., **1.159, 1.458,** 1.754
36. 75	35	21105. 60	$a\ ^5D_0$—337(1)	(0.000) 0.270
31. 27	8	21130. 05		(0.000*w*) 0.704*w*
28. 96	5	21140. 39	$b\ ^3P_1$—385(2)	(0.000) 0.996*B*
26. 84	5*c*	21149. 89		
24. 54	3	21160. 15	$b\ ^3P_1$—385(1)	
17. 93	8	21189. 80	$a\ ^3D_3$—397(4)	
15. 28	7*c*	21201. 71		
12. 37	2	21214. 83	$c\ ^3F_3$—448(3)	
11. 79	1	21217. 42		
08. 66	10	21231. 52	$b\ ^3H_5$—466(4)	(**0.000,** 0.152, 0.315, 0.465, 0.620) **0.425,** 0.588, 0.744, 0.898, 1.056, 1.208
08. 07	1	21234. 17	$b\ ^3D_1$—511(2)	
04. 54	3	21250. 12	$b\ ^3F_4$—397(4)	(0.000*W*) 1.231*w*
4698. 46	3	21277. 63	$c\ ^3F_2$—442(1)	(**0.000,** 0.442) 0.699, **1.158***w*
86. 79	5	21330. 60	$c\ ^3F_2$—442(2)	
84. 04	3	21343. 10		
83. 07	20	21347. 54	$a\ ^3D_2$—385(2) $c\ ^3F_4$—444(3)	(0.235, **0.402**) 0.864, **1.040, 1.232,** 1.404
79. 64	3	21363. 20	$b\ ^3D_1$—513(1)	(0.057) 1.017
78. 01	10	21370. 64	$c\ ^1G_4$—565(5) $b\ ^3G_4$—495(3)	(0.00*W*) 1.47*B*
74. 93	2	21384. 70		
70. 78	2	21403. 72		
67. 24	4	21419. 96		
65. 94	1	21425. 89		

TABLE 1. *Wavelengths, term combinations, and Zeeman effects of* Ta II—Continued

Wave length λair	Intensity and notes	Wave number	Term combination	Zeeman pattern
4657. 75	3	21463. 57		
57. 03	2	21466. 89		
37. 45	5	21557. 52	*a* $^3H_5$—397(4)	(0.000*w*) 0.541*A*
29. 24	5*c*	21595. 76	*b* $^3F_3$—361(2)	(0.000*w*) 1.004*A*
23. 67	5	21621. 78	*c* $^1D_2$—546(3) *a* $^1F_3$—464(2)	(**0.000,** 0.123, 0.252) **0.702***w*, 0.813
10. 79	10	21682. 17	*a* $^5D_2$—361(2)	(0.511, **1.029**) 0.430 **0.951, 1.471,** 1.992
4591. 74	10	21772. 16	*b* $^3G_4$—499(4)	(0.315, 0.472, **0.637**) 0.647, 0.819, 0.979, **1.129, 1.283,** 1.454, 1.593, 1.769.
89. 32	8	21783. 61	*b* $^1G_4$—471(3	(0.000) 1.092
85. 03	10	21803. 99	*b* $^3P_2$—403(1)	(**0.000,** 0.212) 1.404, **1.619**
81. 89	10	21818. 94	*b* $^3H_6$—478(6)	(0.478, 0.640, 0.798, **0.961**) . . ., 1.088, **1.257, 1.406,** 1.576, 1.740
80. 03	10	21827. 81	*a* $^1P_1$—452(1)	(0.353*W*) 1.191*W*
79. 45	12	21830. 56		(0.000) 1.396
79. 32	25	21831. 18	*a* $^5P_2$—337(1)	
78. 21	2	21836. 47	*c* $^1G_4$—569(4)	
77. 52	4	21839. 79	*a* $^5P_2$—337(2)	
74. 85	6	21852. 52	*c* $^3P_0$—452(1)	(0.000) 1.463
62. 99	3	21909. 31	*c* $^1G_4$—570(3)	
57. 65	3	21934. 98		
56. 81	3	21939. 03	*b* $^1D_2$—452(1)	(**0.000,** 0.353) **0.761,** 1.100
50. 90	2	21967. 54	*b* $^3G_5$—532(5)	(0.00) 1.06
49. 93	4	21972. 19		
48. 08	7	21981. 12	*a* $^1F_3$—468(2)	(**0.000,** 0.118, 0.239) **0.799,** 0.916, 1.035
35. 77	8	22040. 78	*a* $^5P_1$—454(2)	(0.000) 0.485
30. 00	12	22068. 89	*a* $^1H_5$—462(5)	(0.376, 0.580, **0.776**) 0.616, 0.815, **1.014, 1.212,** 1.398, 1.595
18. 03	5	22127. 32	*a* $^3D_2$—392(3)	(0.000*W*) 1.014*A*
14. 16	4	22146. 32		
13. 57	10	22149. 22	*b* $^3G_4$—503(3)	(**0.000,** 0.224, 0.435, 0.649) **0.394,** 0.615, 0.842, 1.045
06. 74	12	22182. 77	*b* $^3F_3$—367(3)	(0.303, **0.555**) 0.835, **0.997, 1.168,** . . .
00. 64	10	22212. 85	*b* $^3H_4$—466(4)	(0.445, 0.676, **0.906**) 0.432, 0.656, 0.873, **1.093, 1.320,** 1,553, 1.760
4493. 45	2	22248. 89		(0.000*w*) 0.962*w*
92. 82	2	22251. 47	*b* $^3G_3$—490(2)	
89. 30	40	22268. 94	*a* $^5D_2$—367(3)	(**0.000,** 0.300, 0595*w*) **0.562***w*, 0.871*w*, 1.172, 1.466
88. 25	1	22274. 13		
87. 84	1	22276. 20		
86. 92	1	22280. 75		
82. 00	4	22305. 22	*c* $^3F_2$—452(1)	(**0.00,** 0.80) **0.00,** 0.80
79. 82	2	22316. 04		
79. 18	3	22319. 23		
78. 05	3	22324. 88		
77. 61	4	22327. 07		
74. 67	7	22341. 75	*b* $^3G_4$—505(5)	(0.000*W*) 1.214*W*
65. 65	6	22386. 87	*b* $^3D_3$—530(2)	(**0.000,** 0.211, 0.434) **0.817,** 1.031, 1.252, 1.466
63. 34	3	22398. 46	*b* $^3H_4$—468(3)	
60. 80	5	22411. 22	*a* $^1F_3$—472(4)	(**0.000,** 0.215, 0.428, 0.652) 0.983, 1.197, 1.397, 1.612, **1.827**
59. 15	6	22419. 52	*a* $^1H_5$—466(4) *a* $^3H_4$—382(3)	(**0.000,** 0.205, 0.400, 0.585) **0.239,** 0.407, . . .
57. 95	4	22425. 53	*a* $^3F_3$—292(2)	
40. 71	4	22512. 62	*a* $^5D_4$—397(4)	(0.000*W*) 1.276
39. 64	4	22518. 04	*c* $^3F_2$—454(2)	
37. 81	3	22527. 32		(**0.000***W*, 0.109) 1.684*W B*?
25. 34	2	22590. 78	*a* $^3D_3$—411(2)	(0.00) 1.02
22. 94	10	22603. 05	*a* $^3D_1$—372(2)	(**0.000,** 0.222*w*) 0.445*w*, **0.632**
22. 49	3	22605. 35	*b* $^3D_2$—530(2)	
21. 36	1	22611. 14		
20. 24	6	22616. 88	*a* $^1D_2$—361(2)	(0.168, **0.320**) 0.777, **0.942, 1.115,** 1.272
18. 06	4	22628. 01	*b* $^3F_2$—323(3)	

TABLE 1. *Wavelengths, term combinations, and Zeeman effects of* Ta II—Continued

Wave length λair	Intensity and notes	Wave number	Term combination	Zeeman pattern
4413. 89	8	22649. 39	$\left\{\begin{array}{l} a\ ^3H_5—408(6) \\ b\ ^3F_3—372(2) \end{array}\right.$	
08. 92	3	22674. 90	$d\ ^3F_4—542(4)$	(0.000) 1.160*w*
03. 73	25	22701. 66	$a\ ^5D_1—361(2)$	(**0.000,** 0.562) **0.399,** 0.950, 1.509
01. 13	4	22715. 06		
00. 32	5	22719. 24	$b\ ^3D_3—533(4)$	(**0.000,** 0.148, 0.310, 0.469) **0.644,** 0.794
4398. 85	3	22726. 84		
97. 06	8	22736. 09	$\left\{\begin{array}{l} a\ ^5D_2—372(2) \\ b\ ^3H_4—471(3) \end{array}\right.$	(**0.000,** 0.113, 0.240, . . .) 0.842*w A*
91. 79	2	22763. 37	$b\ ^3G_3—495(2)$	
90. 84	12	22768. 28	$a\ ^1P_1—461(1)$	(0.000*w*) 0.852*w*
86. 77	4	22789. 43	$a\ ^5D_3—385(2)$	(**0.000,** 0.459) 1.455, 1.876, **2.309**
81. 39	8	22817. 40	$b\ ^3G_3—476(3)$	(0.198, 0.379, **0.560**) 0.478, 0.665, **0.849, 1.034,** 1.222, 1.390
76. 75	5	22841. 60	$b\ ^3D_3—534(3)$	(0.069) 1.208
74. 47	20	22853. 50	$a\ ^3H_6—408(6)$	(0.434) 1.120
74. 21	50	22854. 83	$b\ ^3P_2—413(1)$	(**0.000,** 0.432) **1.007,** 1.328
73. 06	3	22860. 84	$b\ ^3D_1—528(1)$	
71. 48	1	22869. 10		
71. 11	2	22871. 08	$c\ ^3F_3—464(2)$	
63. 96	8	22908. 51	$b\ ^3G_4—510(3)$	(**0.000,** 0.101, 0.206, 0.314) **0.781,** 0.848, 0.959
62. 51	2	22916. 13		
60. 02	4	22929. 24	$b\ ^3P_1—403(1)$	(0.000*w*) 1.282*B*
58. 14	40	22939. 13	$b\ ^3G_5—542(4)$	(0.000) 1.126
56. 42	2	22948. 16		
54. 27	3	22959. 50		
50. 21	8	22980. 94	$\left\{\begin{array}{l} d\ ^3F_2—528(1) \\ a\ ^1P_1—463(2) \end{array}\right.$	(0.00) 1.48
47. 88	15	22993. 24	$a\ ^5P_1—337(1)$	
46. 53	10	23000. 39	$a\ ^3D_3—415(3)$	(0.138, 0.285, **0.466**) 0.944, 1.085, **1.214, 1.365,** 1.495, . . .
41. 85	2	23025. 17	$c\ ^3F_3—466(4)$	(0.00) 1.78*B*
41. 00	8	23029. 68	$c\ ^3P_2—510(3)$	(**0.000,** 0.211) **0.764,** 1.005, 1.203, 1.387, . . .
38. 24	12	23044. 36	$b\ ^3H_6—490(5)$	(**0.000,** 0.096, 0.198, 0.290) **0.657,** 0.747, 0.835, 1.032, 1.105, . . .
37. 61	4	23047. 69	$b\ ^3D_1—530(2)$	
35. 21	2	23060. 44	$b\ ^3F_4—415(3)$	
31. 15	6	23082. 07		
28. 79	7	23094. 67		
27. 58	5	23101. 13		
26. 21	3	23108. 42	$b\ ^3G_3—499(4)$	
24. 65	5	23116. 77	$d\ ^3F_4—546(3)$	
21. 05	4	23136. 04	$a\ ^3D_2—403(1)$	(0.000) 1.228*w*
20. 38	2	23139. 62		
17. 86	2	23153. 09	$c\ ^3P_2—511(2)$	(0.000) 1.319
11. 12	2	23189. 33		
09. 77	1	23196. 58	$b\ ^1D_2—464(2)$	
07. 11	4	23210. 88	$c\ ^3F_3—468(3)$	
06. 83	15	23212. 43	$c\ ^3F_4—462(5)$	(**0.000,** 0.170, 0.334, 0.516) 0.842, 1.018, 1.199, 1.366, 1.548, 1.722, **1.913**
05. 28	3	23220. 77		
03. 52	15	23230. 25	$c\ ^3F_3—468(2)$	(0.000) 1.054
4294. 02	12	23281. 65	$b\ ^3F_4—417(4)$	(0.000) 1.250
82. 01	8	23346. 96		(0.000) 0.996
80. 85	3	23353. 28	$a\ ^1F_3—482(2)$	(0.00) 0.59
79. 96	2	23358. 13	$c\ ^3P_1—495(2)$	
75. 69	2	23381. 45		
73. 68	3	23392. 48	$b\ ^3H_4—478(3)$	(0.00) 0.34*A*
71. 09	7	23406. 62		
67. 30	30	23427. 45	$a\ ^1D_2—369(1)$	(**0.00,** 0.35) 0.63, 1.18, **1.59**
65. 05	2	23439. 80		
64. 43	1	23443. 18		

TABLE 1. *Wavelengths, term combinations, and Zeeman effects of* Ta II—Continued

Wave length λair	Intensity and notes	Wave number	Term combination	Zeeman pattern
4263. 50	3	23448. 32		
62. 95	4	23451. 32		(0.00) 1.26
61. 63	4	23458. 59	$c\ ^3F_2$—463(2)	
55. 92	2	23490. 04	$c\ ^3P_2$—515(2)	(0.00) 1.41
42. 74	20	23563. 02	$c\ ^3F_2$—464(2) $c\ ^3F_4$—466(4)	(0.357, 0.546, **0.721**) 0.667, 0.874, **1.032, 1.214,** 1.385, 1.562, 1.745
41. 59	8	23569. 15	$a\ ^3D_3$—421(4)	(0.000) 1.132
35. 93	15	23600. 91	$a\ ^1F_3$—484(4)	(**0.000,** 0.286, 0.572, 0.859) 0.996, 1.272, 1.554, 1.826, **2.115**
35. 51	7	23603. 26	$d\ ^3P_1$—555(2) $a\ ^1H_5$—478(6)	(0.00) 1.42
30. 87	40	23629. 16	$b\ ^3F_4$—421(4)	(0.000 *W*) 1.248
23. 49	6	23670. 44	$a\ ^1D_2$—372(2)	(0.48, **0.98**) 0.11, **0.63, 1.16,** 1.65
20. 09	3	23689. 53	$b\ ^3F_3$—382(3)	
19. 70	1	23691. 71		(0.00) 1.06
18. 44	12	23698. 79		(0.102) 1.186
13. 43	4	23726. 93	$a\ ^3H_6$—417(5)	(0.00*W*) 0.92
13. 02	2	23729. 27		(0.16) 0.85
09. 57	6	23748. 71	$c\ ^3F_4$—468(3)	(**0.00,** 0.16, 0.36, 0.53) **0.50,** 0.69, . . .
08. 42	12	23755. 20	$a\ ^5D_1$—372(2)	(**0.000,** 0.892) −**0.267***w*, +0.611, 1.493
01. 02	15*c*	23797. 06	$a\ ^1F_3$—486(2)	(0.00*w*) 0.81*w*
00. 30	2	23801. 10	$d\ ^3F_2$—536 (2)	(0.00) 1.19
4190. 51	10	23856. 70		(0.000*w*) **1.244,** 1.738
87. 43	10	23874. 27	$b\ ^1D_2$—471(3)	(0.000) 1.076
85. 06	7	23887. 81	$a\ ^3D_1$—385(2)	(**0.000,** 0.169) **1.080,** 1.234
83. 93	7	23894. 22	$c\ ^3F_3$—475(2)	(**0.000,** 0.220, 0.428) **0.636,** 0.815
82. 43	8	23902. 80	$c\ ^3F_2$—468(3)	(**0.00,** 0.50, 1.03) 1.13, 1.65, **2.18**
81. 64	8*c*	23907. 35	$a\ ^3D_1$—385(1)	(0.00) 1.20
79. 06	15*c*	23922. 07	$c\ ^3F_2$—468(2)	(0.392, **0.792***w*) **1.098,** 1.497*w*
76. 93	25*c*	23934. 30	$b\ ^3F_3$—385(2)	(0.000) 0.988
76. 62	1	23936. 09	$a\ ^3H_5$—421(4)	(0.00) 0.98*B*
69. 03	15*c*	23979. 62	$b\ ^3P_1$—413(1)	
62. 67	60*c*	24016. 28	$b\ ^3F_2$—337(1)	
62. 45	8*c*	24017. 54	$a\ ^5D_3$—397(4)	
61. 20	12*c*	24024. 77	$b\ ^3D_3$—546(3) $b\ ^3F_2$—337(2)	(0.282, **0.532**) . . . ?, 0.536, **0.807, 1.061**
59. 02	3	24037. 34	$b\ ^3H_4$—484(4)	
58. 51	3	24040. 31	$a\ ^5D_2$—385(1)	
55. 40	7*c*	24058. 29	$a\ ^3G_4$—367(3)	(0.162*W*) 0.754*W*
52. 19	5	24076. 89	$c\ ^3P_2$—521(3)	
39. 52	7	24150. 58	$b\ ^1G_4$—495(3)	(**0.000,** 0.220, 0.432, 0.652) **0.438,** 0.657, 0.868, 1.090, 1.310
33. 35	5	24186. 65	$a\ ^3D_2$—413(1)	(**0.00,** 0.71) **0.55,** 1.15
30. 22	4	24204. 95	$c\ ^3F_3$—478(3)	(0.261, **0.382**) 1.18
24. 65	8	24237. 67	$b\ ^3G_5$—555(5)	(0.000*W*) 0.871*A*
20. 67	8	24261. 03	$b\ ^1G_4$—496(3)	(0.000) 1.196*w*
10. 10	5	24323. 44	$a\ ^5D_4$—415(3)	(0.000) 1.183*B*
09. 40	4	24327. 57	$b\ ^3G_4$—524(4) $a\ ^5P_3$—367(3)	(0.121) 1.062
4099. 42	8*c*	24386. 81	$a\ ^5D_0$—369(1)	(0.000) 0.682*w*
95. 53	8*c*	24409. 97	$a\ ^3G_3$—361(2)	(0.000) 0.913*B*
94. 60	3	24415. 52		(**0.00,** 0.36, 0.75, 1.13) **0.73,** 1.10, . . .
86. 17	2*c*	24465. 88	$b\ ^3F_4$—429(3)	(0.000) 0.797*w*
85. 07	1	24472. 48	$b\ ^3H_5$—498(5)	(0.30, **0.52**) 0.27
84. 13	2	24478. 12	$a\ ^5D_4$—417(5)	(0.000) 1.291*A*
75. 50	10	24529. 94	$b\ ^3H_4$—489(3) $b\ ^1D_2$—478(3)	(**0.00,** 0.30, 0.60, 0.91) **0.08,** 0.38, 0.68, 1.00
74. 43	1	24536. 38	$c\ ^3P_2$—525(3)	(0.000) 1.454*w*
73. 13	7*c*	24544. 20	$a\ ^5D_4$—417(4)	(0.00*W*) 1.19*W*
66. 22	4	24585. 95	$c\ ^3F_2$—475(2)	(0.58, **1.19**) 0.00*w*, **0.71, 1.30,** 1.88
60. 21	4	24622. 33	$b\ ^3H_4$—490(5)	(**0.000,** 0.237, 0.488, 0.739, 0.991) . . ., 1.702, 1.950, **2.195**
54. 15	2	24659. 14		

TABLE 1. *Wavelengths, term combinations, and Zeeman effects of* Ta II—Continued

Wave length λair	Intensity and notes	Wave number	Term combination	Zeeman pattern
4050.00	3	24684.41		(0.073) 1.062
49.09	1	24689.91	*d* $^3F_2$—545(2)	
48.31	2	24694.70		(**0.000,** 0.291, 0.580) 1.149, 1.426, **1.712**
45.02	3*c*	24714.76	*b* $^3F_2$—392(3)	
40.47	4*c*	24742.61	*c* $^3F_4$—478(3)	(**0.000,** 0.168, 0.344, 0.522) **0.497,** 0.671, 0.846, 1.020, . . .
34.66	2*c*	24778.25	*b* $^3P_1$—421(2)	(0.00) 1.23
30.96	10*c*	24801.00	*a* $^5D_2$—392(3)	(**0.000,** 0.336, 0.662) **0.470***w*, 0.804, 1.137, 1.470
29.08	2	24812.58		(**0.000,** 0.427, 0.845) **0.077,** 0.548, 0.964, . . .
16.82	5	24888.27	*a* $^5P_2$—367(3)	(**0.000,** 0.252, 0.502) **0.666,** 0.914, 1.162, . . .
16.28	7	24891.64	*a* $^5D_4$—421(4)	(0.193*WA*) 1.234*W*
10.49	3	24927.55	*b* $^3D_3$—555(2) *b* $^1D_2$—482(2)	
10.24	5	24929.08	*b* $^1G_4$—503(3)	(**0.000,** 0.224, 0.451, 0.663) **0.640,** 0.849, 1.052
05.97	5	24955.69		(**0.000,** 0.269, 0.518) **0.696,** 0.950, 1.212, . . ., . . .
04.83	3	24962.77	*c* $^3P_1$—511(2)	(0.000*w*) 1.347*w*
3999.39	3*c*	24996.74	*a* $^3G_3$—367(3)	(0.358, **0.880**) 0.811, **1.314, 1.815,** 2.332
92.44	10	25040.26	*a* $^5D_1$—385(2)	(**0.000,** 0.489) **0.513,** 1.007, 1.497
92.15	1	25042.05	*c* $^1D_2$—580(1)	(0.000) 0.850
90.76	10	25050.83	*b* $^3F_4$—435(3)	(**0.000,** 0.158, 0.329, 0.484) 0.952, 1.083, 1.229, 1.370, **1.504**
89.32	2	25059.81	*a* $^5D_1$—385(1)	(1.04) 0.50, 1.39
87.96	3	25068.41	*a* $^1F_3$—499(4)	(**0.000,** 0.260, 0.505) 1.073, 1.356, 1.578, **1.830**
87.82	2	25069.29	*b* $^3G_4$—532(5)	
86.21	3	25079.37		(0.000) 1.023
84.58	2	25089.65	*b* $^3H_4$—495(5) *c* $^1G_4$—602(3)	(0.00*wD*) 0.80*A*
84.26	12	25091.68	*c* $^3P_1$—513(1)	(0.623) 1.046, 1.336
80.99	25*c*	25112.28	*a* $^5P_2$—369(1)	(**0.000,** 0.868) 0.680, 1.418, **2.151**
75.64	8	25146.06	*b* $^3D_2$—555(2)	(0.000) 1.049
74.19	6	25155.22		(0.496) 1.225*W*
72.99	18*c*	25162.84	*b* $^3F_3$—397(4)	(**0.000,** 0.217, 0.442*w* 0.781*w*) 0.768, 0.996, 1.213, 1.399, 1.637*w*, **1.875***w*
70.57	10	25178.16	*b* $^3G_4$—533(4)	(0.148) 1.099*W*
69.70	2	25183.72	*b* $^3G_5$—564(5)	
64.96	4	25213.80	*b* $^3H_4$—496(3)	(0.000) 0.890
61.60	20	25235.18	*b* $^3D_3$—558(2)	
58.55	3	25254.63	*b* $^3G_5$—565(5)	(0.00*W*) 0.58
57.62	4	25260.58	*a* $^1P_1$—486(2)	(0.000) 1.130
56.35	2	25268.66		
54.68	5	25279.37	*b* $^3H_5$—506(6)	
52.70	7	25292.04	*b* $^3G_3$—521(3)	(0.478, **0.738**) 0.358, 0.593, **0.841, 1.094,** 1.329
51.50	10*c*	25299.67	*c* $^3P_1$—515(2)	(**0.000,** 0.113) 1.196, **1.310**
44.85	10	25342.31	*c* $^3F_3$—489(3)	(0.195, 0.394, **0.602**) 0.675, 0.874, **1.071, 1.271,** 1.462, 1.674
43.78	10	25349.23		(0.000) 0.867
42.84	5	25355.26	*a* $^5P_2$—372(2)	(0.84, **1.58**) 0.16, **0.64,** . . .
41.86	3	25361.52		(**0.00,** 0.22, 0.42) 0.89*A*
41.65	3	25362.91		
40.52	4	25370.20	*a* $^1P_1$—487(1)	(0.44) 0.75, 1.37
40.26	6	25371.86	*b* $^1D_2$—486(2)	(0.069) 1.133
36.68	10	25394.90	*c* $^3P_0$—487(1)	(0.000) 1.818
35.90	3	25399.93		
35.57	12	25402.11	*a* $^1D_2$—389(3)	(**0.000,** 0.122, 0.230) **0.763,** 0.874, 1.007, 1.142
32.85	1	25419.66		
27.92	5	25451.56	*a* $^3D_3$—440(4)	(**0.000,** 0.843) 1.600
26.48	7	25460.90		
26.02	12*c*	25463.88	*a* $^3G_3$—372(2) *a* $^5P_1$—361(2)	(0.00) 0.85*w*
24.56	5*c*	25473.38	*b* $^3D_2$—558(1)	(0.000) 1.066
24.15	2	25476.00		
22.44	60*c*	25487.09	*a* $^3F_3$—323(3)	(0.226, **0.359**) 0.817, **0.940, 1.074,** 1.214

TABLE 1. *Wavelengths, term combinations, and Zeeman effects of* Ta II—Continued

Wave length λair	Intensity and notes	Wave number	Term combination	Zeeman pattern
3917. 62	8	25518. 48	*b* $^3D_3$—561(4)	(0.000) 1.316
15. 97	2	25529. 20	*d* $^3F_4$—570(3)	(**0.000,** 0.284, 0.557, 0.846) **0.335,**, 0.590, 0.853, 1.142, 1.420, . . .
14. 05	7	25541. 78		
12. 14	1	25554. 22	*a* $^3P_2$—312(1)	
10. 48	5	25565. 03	*b* $^3D_1$—555(1) *a* $^3G_4$—382(3)	(0.00) 1.24
06. 01	2	25594. 32		
03. 15	1	25613. 07	*b* $^3D_2$—560(2)	(0.000) 1.066
02. 10	2	25619. 97		(0.000*w*) 0.000*w*
3899. 91	2	25634. 33		(0.00) 0.00
98. 48	1	25643. 73		
96. 61	10*c*	25656. 04		
95. 97	2	25660. 29	*a* $^1H_5$—498(5)	
95. 50	2	25663. 39	*b* $^3G_3$—524(4)	(**0.000,** 0.247) 1.592
93. 31	8	25677. 82		(0.00) 0.95
92. 10	2	25685. 77		
91. 90	2	25687. 08		
91. 55	10	25689. 43	*b* $^3P_1$—430(2)	(**0.000,** 0.187) 0.844, **1.061**
90. 16	1	25698. 59		
89. 42	20*c*	25703. 52	*a* $^3H_4$—415(3)	(0.000*W*) 1.071*wA*
88. 68	20	25708. 39	*d* $^3F_2$—552(2)	(0.394*W*) 1.060*WD*
88. 20	4	25711. 56	*a* $^1H_5$—499(4)	
85. 32	8	25730. 63		
84. 56	3	25735. 62	*a* $^1D_2$—392(3)	(0.000*w*) 1.172*w*
84. 18	2	25738. 19	*c* $^3F_2$—486(2) *a* $^5D_2$—402(2)	
77. 02	4	25785. 03	*b* $^1D_2$—490(2)	(0.204, **0.411**) 0.902, **1.111, 1.315,** 1.518
73. 38	10	25809. 92	*a* $^5D_2$—403(1)	(**0.000,** 0.242) 1.233, 1.466, **1.700**
72. 01	2	25819. 07	*a* $^3H_5$—440(4)	(0.00) 1.04
70. 64	35*c*	25828. 20	*a* $^5D_3$—415(3)	(0.254, 0.504, **0.778**) 0.687, 0.948, **1.202, 1.454,** 1.711, 1.959
67. 74	10	25847. 56	*c* $^3F_2$—487(1)	(0.000) 0.671
66. 24	50*c*	25857. 57	*a* $^3H_4$ 417(5)	
62. 89	2*c*	25880. 03	*c* $^3F_4$—489(3)	(**0.000,** 0.250, 0.523, 0.800, . . .) **0.530,** 0.790, 1.036, 1.258
62. 62	2	25881. 82		
61. 95	3	25886. 30		
60. 50	7	25896. 07	*b* $^3D_1$—558(2) *a* $^3D_2$—430(2)	
59. 36	2*c*	25903. 69		
57. 56	15	25915. 79	*b* $^3D_1$—558(1) *c* $^3F_3$—495(3)	(0.243, 0.475, **0.716**) 0.589, 0.836, **1.072, 1.308,** 1.544, 1.771
56. 93	3	25920. 03		
56. 33	10*c*	25924. 05	*a* $^3H_4$—417(4)	
54. 83	2*c*	25934. 11	*a* $^5D_0$—385(1)	(0.000) 0.127, **0.476**
54. 15	1	25938. 71		
52. 61	1	25949. 06		
51. 84	4	25954. 24	*c* $^1G_4$—611(4)	(0.137*w*) 1.049*w*
49. 15	4	25972. 42	*c* $^3F_4$—490(5) *c* $^3F_3$—495(2)	
45. 62	3	25996. 24		(0.000*W*) 1.067 *A*
43. 02	2	26013. 80		
42. 70	2	26015. 99	*d* $^3F_2$—558(2)	
37. 48	1	26051. 37		
35. 36	12	26065. 75	*b* $^3H_5$—514(4)	(0.000*WD*) 0.791 *A*
34. 13	2	26074. 11	*b* $^3H_4$—505(5)	
33. 74	100*c*	26076. 80	*a* $^3F_2$—292(2)	(0.220, **0.460**) 0.278, **0.517, 0.743,** 0.977
31. 17	15	26094. 28	*b* $^3G_4$—514(4)	(0.102*w*) 1.113*w*
30. 00	2*c*	26102. 28		(0.000*W*) 1.531 *A*
28. 07	2	26115. 40		
25. 58	6*c*	26132. 40	*b* $^3F_4$—446(4)	(0.000*W*) 1.238*w*
23. 82	8	26144. 43		(0.000) 1.135

TABLE 1. *Wavelengths, term combinations, and Zeeman effects of* Ta II—Continued

Wave length λair	Intensity and notes	Wave number	Term combination	Zeeman pattern
3822. 72	5	26151. 97	*c* $^3F_2$—490(2)	(0.603, **1.222**) 0.081, **0.696, 1.303,** 1.917
21. 96	1	26157. 14		
21. 76	1	26158. 54		
19. 80	2	26171. 93		
14. 07	6	26211. 30		(0.00) 0.88 *A*
09. 39	2	26243. 50		(0.00*w*) 1.00
08. 09	7	26252. 40		
07. 79	3	26254. 51		
07. 49	5	26256. 54	*a* $^3G_4$—389(3)	(0.000) 1.013 *A*
04. 92	5*c*	26274. 29	*a* $^5P_1$—369(1)	
04. 06	3	26280. 23		
03. 11	4	26286. 80		(0.00) 0.88
02. 10	1	26293. 78		
01. 75	4	26296. 20		
3798. 71	12	26317. 25	*c* $^3F_3$—499(4)	(**0.000,** 0.137, 0.281, 0.433) 1.219, 1.348, 1.490, **1.631**
97. 62	4	26324. 79	*c* $^1D_2$—593(2)	(0.18) 1.16
96. 21	15*c*	26334. 60	*b* $^3P_2$—448(3)	(**0.000,** 0.194, 0.442) **0.823,** 1.058, 1.258, 1.430
95. 20	20*c*	26341. 62	*b* $^3F_4$—448(3)	(0.000*w*) 1.228 *B*
91. 60	15*c*	26366. 59	*a* $^3F_4$—361(4)	(0.229*w*) 1.225*w*
88. 98	2	26384. 81	*a* $^3D_2$—435(1)	(0.000) 0.985
88. 44	1	26388. 57		(0.00*w*) 1.52 *B*
87. 26	25*c*	26396. 83	*a* $^5D_3$—421(4)	(**0.000,** 0.197, 0.412, 0.650) **0.581,** 0.799, 1.053, 1.266, 1.455, 1.655
86. 94	2	26399. 07	*a* $^3H_5$—445(5)	
85. 84	3	26406. 69		
85. 36	4	26410. 03		
83. 58	2	26422. 46		
82. 91	50	26427. 20	*a* $^5D_2$—421(2)	(**0.000,** 0.248, 0.500) 1.003, 1.212, 1.453, 1.703, **1.955**
82. 19	1	26432. 22		
81. 54	2	26436. 73	*c* $^1G_5$—615(6) *b* $^3D_3$—570(3)	(0.28) 1.36
81. 08	2	26439. 96	*c* $^3F_4$—495(5) *a* $^3H_5$—446(4)	(**0.000,** 0.178, 0.364, 0.534, 0.693) **0.159,** 0.339, 0.503, 0.660, 0.834, 0.940
79. 14	20	26453. 53	*c* $^3F_4$—495(3)	**0.000,** 0.282, 0.571, 0.852) **0.179,** 0.459, 0.744, 1.020, 1.308, 1.596
75. 25	8	26480. 77	*a* $^1P_1$—498(1)	(0.815*w*) 1.283, 1.990
74. 41	15*c*	26486. 68	*b* $^3F_2$—361(2)	(0.107, **0.216**) 0.837, **0.954, 1.067,** 1.187
73. 98	2	26489. 70	*c* $^3P_2$—545(2)	
71. 17	5	26509. 42	*d* $^3F_4$—580(4)	
70. 45	3	26514. 53	*b* $^3G_3$—533(4)	
70. 03	7*c*	26517. 43	*a* $^3D_1$—411(2) *a* $^5P_1$—372(2)	(**0.000,** 0.508) 0.610, **1.124**
68. 98	5	26524. 86		
68. 70	20	26526. 79	*a* $^5P_3$—389(3)	
66. 43	10	26542. 80	*c* $^1G_4$—616(3)	(**0.000,** 0.152, 0.305, 0.459) 0.921, 1.082, 1.228, 1.391, **1.539**
65. 67	12	26548. 18	*a* $^5D_1$—400(0)	(0.000) 1.504
63. 44	60*c*	26563. 89	*b* $^3F_3$—411(2) *c* $^3F_4$—496(3)	(**0.000,** 0.170, 0.377) **0.593,** 0.802, 0.998, 1.159
59. 42	2	26592. 30	*b* $^1D_2$—498(1)	
57. 70	5	26604. 48	*c* $^3P_2$—546(3)	
57. 29	10*c*	26607. 35	*d* $^3F_2$—564(3) *c* $^3F_2$—495(3)	(**0.00,** 0.58, 1.16) 0.74, 1.38, 1.94, **2.47**
56. 88	20	26610. 28	*a* $^1F_3$—514(4)	(**0.000,** 0.139, 0.283, 0.432) 0.983, 1.114, 1.255, 1.397, **1.545**
56. 27	4*c*	26614. 57	*a* $^5F_3$—292(2)	(**0.00**, 0.75) 0.29
53. 32	5	26635. 51		
52. 70	6	26639. 90	*a* $^5P_2$—385(2)	(0.463, **0.824**) 0.602, **1.002, 1.404,** . . .
52. 53	5	26641. 13	*b* $^3H_4$—510(3)	(0.00*W*) 0.67
51. 36	6	26649. 41		
50. 51	3	26655. 44	*b* $^3D_2$—570(3)	
49. 92	10*c*	26659. 66	*a* $^5P_2$—385(1)	
49. 13	5	26665. 25		(00.0) 0.88*w*
48. 02	15*c*	26673. 14	*a* $^1D_2$—402(2)	(0.000*W*) 1.100 *A*

TABLE 1. *Wavelengths, term combinations, and Zeeman effects of* Ta II—Continued

Wave length λair	Intensity and notes	Wave number	Term combination	Zeeman pattern
3746.00	2	26687.56		
45.07	3	26694.16	*c* $^3F_3$—503(3)	(0.196, 0.414, **0.613**) . . . ?
43.80	1	26703.27		
40.55	4	26726.47		
37.50	15*c*	26748.22	*a* $^3G_3$—385(2)	(0.000*W*) 0.798*w*
33.95	4	26773.68	*b* $^3G_5$—580(4) *a* $^5D_4$—440(4)	(0.292) 1.169*w*
33.41	8	26777.57		(0.000, 0.194, 0.383, 0.560, **0.750**) 0.602, 0.845, 1.033, **1.219, 1.404,** 1.588, 1.738, . . .
21.94	25*c*	26860.10	*a* $^5P_3$—392(3) *a* $^5D_2$—413(1)	(**0.000,** 0.293, 0.547) **0.917,** 1.169, 1.463, 1.768, 1.976
18.60	12*c*	26884.18	*a* $^3F_3$—337(2) *b* $^3P_1$—442(2)	(**0.000,** 0.309, 0.581) 0.047, 0.429, 0.865, 1.176, 1.395, 1.457, **1.651**
17.49	4	26892.24	*a* $^5F_5$—330(5)	
07.52	6	26964.56	*c* $^1G_4$—621(4)	(0.084*w*) 1.058*wD*
00.26	20*c*	27017.41	*a* $^3F_4$—367(3)	(0.000*W*) 1.324*w*
3699.98	8	27019.46	*b* $^1D_2$—503(3)	(0.00) 1.16
96.20	7	27047.10	*b* $^3H_4$—514(4)	(0.124, 0.265, 0.411, **0.560**) . . ., **0.999, 1.141,** 1.265, 1.406, 1.535
95.26	25*c*	27053.97	*c* $^1G_4$—622(5)	
94.50	50*c*	27059.53	*a* $^5D_2$—415(3) *b* $^3P_1$—444(0)	(**0.000,** 0.266, 0.531) **0.673,** 0.941, 1.201, 1.460, 1.710
92.62	12*c*	27073.32	*b* $^3F_2$—367(3)	(**0.000,** 0.113, 0.236) 1.174, 1.286, **1.404**
91.85	25	27078.98	*b* $^3H_5$—524(4)	(0.000) 0.969*w*
91.13	4	27084.24	*c* $^3P_2$—551(3)	(0.26) 1.13
90.77	10	27086.92	*a* $^5P_2$—389(3)	(**0.000,** 0.420, 0.840) **0.155,** 0.584, 1.013
90.23	1	27090.87	*a* $^3D_2$—442(2)	(0.00) 1.32*B*
89.60	8	27095.52		
89.25	3	27098.04		(**0.00,** 0.59) . . . , 1.41, **1.74**
88.25	2	27105.41		
82.22	12	27149.82	*c* $^3P_0$—505(1)	(0.000) 1.359
79.83	3	27167.47	*b* $^3D_3$—577(2)	(**0.000,** 0.202, 0.436) . . ., 1.464, **1.666**
76.09	10*c*	27195.05	*b* $^1G_4$—525(3) *a* $^3G_3$—389(3)	(0.289*W*) 0.941*w*
73.28	8	27215.91	*b* $^3G_4$—553(4)	(0.109) 1.028*w*
73.07	4	27217.42	*d* $^3F_2$—570(3)	
70.96	5	27233.07	*b* $^3D_1$—571(1)	
69.84	2	27241.42		(0.00) 0.90
67.08	10	27261.89	*a* $^3D_2$—444(3)	
62.34	50	27297.19	*b* $^3F_2$—369(1)	(**0.000,** 0.377) 0.393, 0.687, 1.055, **1.424**
59.18	6	27320.72	*b* $^3H_4$—517(5)	(0.00*W*) 1.52*B*
58.40	2	27326.56		
56.64	5	27339.72	*b* $^3G_4$—555(5)	(**0.000,** 0.459) 1.119
56.51	10	27340.71		
54.81	50	27353.41	*a* $^5D_4$—445(5)	(0.000*W*) 1.440*W*
51.54	7	27377.87	*b* $^3G_3$—542(4) *b* $^3G_4$—555(3)	
49.32	7*c*	27394.58	*a* $^5D_4$—446(4)	(0.145, **0.522**) 1.201*w*
48.18	4	27403.14	*d* $^3P_1$—593(2)	(0.00) 1.29
45.88	10	27420.41	*a* $^5P_2$—392(3)	(**0.000,** 0.284) **0.574,** 0.866, 1.140
45.44	20	27423.69		(0.000*W*) 1.330
44.31	25	27432.20	*b* $^3H_5$—528(6)	(**0.000,** 0.098, 0.206, 0.309, 0.418, 0.517) 1.393, 1.464, 1.585, **1.675**
41.47	35	27453.60	*c* $^3F_3$—510(3)	(0.260*B*) 1.106*w*
40.79	3	27458.71		(0.000*W*) 1.243*w*
37.69	7*c*	27482.11		(0.000*w*) 0.786
34.34	2	27507.46	*c* $^3P_2$—555(2)	
31.93	25	27525.72	*a* $^3D_1$—421(2)	(**0.000,** 0.369) 0.838, 1.207, **1.573**
31.71	20	27527.41	*a* $^1H_5$—517(5)	(0.355, 0.473, **0.593**) . . . **0.988, 1.102,** 1.201
31.48	10	27529.14	*a* $^3G_3$—392(3)	(0.517, **0.762**) 0.687, **0.914, 1.139,** 1.380
30.01	15	27540.25	*b* $^3F_2$—372(2)	(0.438, **0.867**) 0.185, **0.613, 1.050,** 1.462
28.68	50*c*	27550.41		(0.407*B*) 0.782, **1.583***W*
26.10	5	27569.95	*a* $^1G_4$—417(4)	
24.17	25	27584.64	*a* $^1D_2$—411(2)	(0.101*B*) 1.129*w*

TABLE 1. *Wavelengths, term combinations, and Zeeman effects of* Ta II—Continued

Wave length λair	Intensity and notes	Wave number	Term combination	Zeeman pattern
3622.37	1	27598.35		
21.62	8	27604.04	*a* $^5D_4$—448(3)	(0.000*w*) 1.001*A*
19.96	4	27616.76		(0.000*W*) 0.672*A*
19.08	8	27623.47	*a* $^1F_3$—524(4)	(**0.000,** 0.113, 0.230, 0.346) 1.217, 1.328, **1.430**
14.51	15	27658.40	*a* $^5D_2$—421(2)	(0.255, **0.509**) 0.959, **1.212, 1.467,** 1.719
13.41	30*c*	27666.83	*a* $^3D_2$—448(3)	(0.000*W*) 1.305*w*
13.05	7	27669.56	*a* $^5D_1$—411(2)	(**0.000,** 0.345) **0.811,** 1.156, 1.513
10.60	40	27688.35	*b* $^3H_4$—521(3)	(**0.000,** 0.112, 0.232, 0.343) **0.632,** 0.756, 0.863, 0.980, 1.077
10.23	4	27691.20		
09.95	60*c*	27693.33	*a* $^3H_4$—435(3)	(0.000*w*) 1.219*w*
08.56	10	27703.96	*a* $^5D_0$—403(1)	(0.000) 1.253
3599.20	8	27776.04		(0.000*D*) 0.708*w*
90.80	7	27779.08	*b* $^1D_2$—510(3)	(0.000*w*) 1.234 *B*
95.79	20*c*	27802.38	*a* $^5P_1$—385(2)	(**0.000,** 1.356*WD*) **0.350***WD*, 1.005, 2.355
94.13	4	27815.19	*c* $^3P_2$—558(2)	(0.00) 1.30
93.73	10	27818.31	*a* $^5D_3$—435(3)	(0.379, **0.751**) 0.328, 0.715, **1.087, 1.461,** 1.837, 2.205
93.53	8	27819.87	*b* $^3G_3$—546(3)	(0.273) 0.936
93.14	7	27822.90		
92.44	5	27828.29	*b* $^3D_1$—577(2)	(0.098) 1.143
91.61	5	27834.73	*c* $^3P_2$—558(1)	(0.000*w*) 1.315*w*
90.50	8	27843.34	*c* $^1D_2$—608(2)	(0.144) 1.072*w*
89.74	10	27849.22	*a* $^3H_4$—437(5) *b* $^1G_4$—532(5)	(0.000) 1.356*B*
88.42	7	27859.48	*b* $^3P_1$—452(1) *c* $^3F_3$—514(4)	(0.000*w*) 1.244*B*
87.14	3	27869.41	*b* $^3D_2$—582(2)	
85.83	8*c*	27879.60	*a* $^5D_1$—413(1)	(0.387) 1.491
82.86	4	27902.72	*a* $^5F_4$—323(3) *b* $^1D_2$—511(2)	(**0.000,** 0.363, 0.730, 1.083) . . ., 1.709, **2.018**
80.89	10	27918.03	*b* $^3P_0$—442(1) *a* $^1G_4$—421(4)	(0.000) 0.257, 1.717
79.42	200	27929.48	*b* $^3H_5$—533(4)	(0.000*w*) 0.895*A*
77.42	5	27945.10	*c* $^3P_0$—513(1)	(0.000) 1.045
75.78	20	27957.98	*b* $^1G_4$—533(4)	(0.000) 1.089
73.42	125*c*	27976.39	*a* $^3G_3$—397(4)	(**0.000,** 0.308, 0.610*w*, 0.924*w*) 0.000, . . ., 0.598, 0.912, 1.212, 1.500, 1.839*w*, **2.118***w*.
71.52	25	27991.29	*c* $^3F_4$—510(3)	(**0.000,** 0.088, 0.266, 0.393) **0.628,** 0.766, 0.898, 1.033, 1.168
71.15	20	27994.21	*a* $^1D_2$—415(3)	(**0.000,** 0.100, 0.191) 1.400*B*
69.82	10	28004.64	*a* $^3G_5$—408(6)	
66.84	10	28028.02		
66.37	6	28031.74	*b* $^1D_2$—513(1)	(0.000) 1.14
65.57	250	28037.98	*b* $^3H_6$—540(5)	(0.000 *W*) 0.782*A*
64.22	40*c*	28048.62	*a* $^3P_2$—337(1)	(**0.000,** 1.039*w*) 1.324, **2.418***w*
63.12	3	28057.31	*a* $^3P_2$—337(2)	
62.08	10	28065.50	*a* $^3D_2$—452(1)	(**0.000,** 0.248) **0.954,** 1.209, 1.463
61.27	15*c*	28071.88	*b* $^3P_1$—454(2)	(0.000) 1.161*w*
60.87	20*c*	28075.04		
60.20	7	28080.26	*b* $^1G_4$—534(3)	(**0.000,** 0.127, 0.258, 0.393) 0.749*w*
58.73	45*c*	28091.89	*a* $^3D_3$—466(4)	(**0.000,** 0.148, 0.326, 0.503) **0.709,** 0.896, 1.040, 1.215, 1.358
56.94	3	28106.05	*b* $^3D_1$—580(1)	(0.137) 1.005, 1.160
54.14	3	28128.18	*a* $^1P_1$—515(2)	(0.000) 1.408
53.16	4*c*	28135.93		
52.83	3	28138.53		
52.45	7	28141.52	*a* $^1F_3$—530(2)	(**0.00,** 0.47) **0.63,** 1.10
51.98	12	28145.26	*c* $^3F_2$—510(3)	(**0.000,** 0.451, 0.899) 1.600, **2.053**
51.12	60*c*	28152.10	*b* $^3F_4$—466(4)	(0.000*W*) 1.219*w*
50.91	30*c*	28153.74	*a* $^3H_4$—440(4)	(0.000*W*) 1.44*W*
50.05	8	28160.55	*d* $^3F_4$—596(5)	(0.150, 0.302, **0.449**) . . .?
42.22	75	28222.83		(0.000) 1.129
41.88	70	28225.52	*a* $^5F_2$—292(2)	(0.489, **0.971**) 0.000, **0.513, 1.002,** 1.487

TABLE 1. *Wavelengths, term combinations, and Zeeman effects of* Ta II—Continued

Wave length λair	Intensity and notes	Wave number	Term combination	Zeeman pattern
3539.20	7	28246.88		
37.98	2	28256.65		
36.96	3	28264.80		(**0.00,** 0.32, 0.65) 0.78, 1.14, 1.48, **1.81**
36.71	8	28266.81	*a* $^1H_5$—524(4)	(0.000) 0.736
35.40	35	28277.25	*a* $^3D_3$—468(3)	(0.316*W*) 0.800, 0.92*C*, 1.071, **1.198, 1.351,** . . .
34.36	3	28285.57	*b* $^3G_4$—564(5)	(0.00*W*) 0.73*A*
32.66	20*c*	28299.16	*c* $^3P_1$—545(2) *b* $^3G_3$—551(3)	(**0.000,** 0.297) **0.717,** 1.000
31.80	4*c*	28306.06	*d* $^3F_4$—598(5)	
31.13	10*c*	28311.47	*b* $^3D_1$—582(2)	
30.30	1	28318.07		
30.03	1	28320.27		
28.74	45*c*	28330.65	*b* $^3P_2$—468(3)	(**0.000,** 0.236, 0.430) **0.794***w*, 1.215, 1.484, . . .
28.27	4	28334.39	*c* $^1G_4$—634(4)	(0.000) 1.212
26.34	20*c*	28349.92	*b* $^3P_2$—468(2)	(0.346, 0.594, **0.810**) 0.760, **1.088, 1.435,** 1.733, 1.965
25.52	15	28356.50	*b* $^3G_4$—565(5)	(0.000*W*) 0.881 *A*
25.07	3	28360.11		
24.72	2	28362.96		
24.55	6	28364.31		
23.16	90*c*	28375.47	*a* $^3P_1$—337(1)	(1.284) 0.267, 1.547
22.64	3	28379.65		
22.16	2	28383.55		
22.04	6	28384.49	*a* $^3P_1$—337(2)	(0.000) 0.920
21.47	50	28389.13		(0.000) 0.830
19.27	10	28406.87	*c* $^3P_2$—564(3)	(**0.000,** 0.178, 0.356) **0.840,** 1.015, 1.197
17.82	2	28418.53		
17.01	10	28425.10	*b* $^3G_5$—596(5)	(**0.000,** 0.150, 0.311, 0.477) 1.282, 1.440, **1.596**
15.04	3	28441.04	*a* $^3D_1$—430(0)	(0.000) 0.857
12.01	7*c*	28465.58	*a* $^5D_2$—429(3) *a* $^3G_3$—402(2)	
06.66	2	28508.98		
01.35	10	28552.28	*c* $^1G_4$—637(5) *b* $^3G_3$—553(4)	(**0.000,** 0.180, 0.356, 0.518) 0.837, 1.017, 1.200, 1.371, **1.566**
3499.06	25	28570.92	*b* $^3G_5$—598(5)	(0.000*w*) 1.010*w*
96.36	12	28592.98	*a* $^1D_2$—421(2)	(0.125, **0.207**) 1.057, **1.162, 1.260,** 1.361
95.98	10	28596.12	*a* $^1F_3$—534(3)	(0.258, 0.495, **0.732**) . . . ?
94.80	20*c*	28605.79	*c* $^3F_2$—515(2)	(0.600, **1.192**) 0.108, **0.699, 1.313,** 1.891
93.82	3	28613.76		
93.04	75	28620.14	*a* $^1H_5$—528(6)	(**0.000,** 0.156, 0.299, 0.449, 0.592, 0.767) 1.005, 1.148, 1.302, 1.446, 1.587, 1.769, **1.918**
87.80	25	28663.16	*a* $^5F_4$—330(5) *b* $^1G_4$—540(5)	(**0.000,** 0.110, 0.222, 0.332, 0.445) . . . , 1.541, 1.648, 1.766, **1.875**
87.31	20	28667.21	*c* $^1D_2$—616(3)	
87.16	20*c*	28668.38	*b* $^3P_2$—471(3)	(**0.000,** 0.350) 0.906
86.85	25	28670.96	*c* $^3F_4$—517(5)	(**0.000***W*) 1.189, 1.312, 1.407, **1.498**
86.29	8	28675.58	*b* $^3F_4$—471(3)	
86.01	30	28677.85	*a* $^5D_1$—421(2)	(**0.000,** 0.297) **0.914,** 1.208, 1.504
82.82	8	28704.18	*a* $^5D_3$—444(3)	(0.539, 1.038, **1.559**) −0.093, 0.430, **0.941, 1.452,** 1.970, 2.477
81.74	5	28713.07		
80.04	15*c*	28727.10	*a* $^3D_3$—472(4)	(**0.000,** 0.162, 0.365) . . . ?
78.59	7	28739.04		
75.07	2	28768.15		
74.25	200*c*	28774.98	*c* $^3P_0$—521(1) *a* $^3H_4$—446(4) *a* $^1F_3$—536(2)	(0.471*W*) 0.832, **1.031, 1.209,** 1.362
71.98	3	28793.73	*d* $^3F_4$—603(3)	(0.00) 1.17
70.99	50	28801.98	*b* $^3H_4$—532(5)	(**0.000,** 0.166, 0.341, 0.503, 0.677) . . . , 0.976, 1.146, 1.318, 1.488, 1.649, **1.831**
70.10	3	28809.34		
68.67	20	28821.21	*b* $^1G_4$—542(4)	(0.175 *B*) 1.117*w*
68.51	4	28822.57	*b* $^3G_4$—569(4)	(0.28) 1.11
68.05	4	28826.39	*b* $^1D_2$—521(3)	(0.000) 1.080
67.19	1	28833.53		

TABLE 1. *Wavelengths, term combinations, and Zeeman effects of* Ta II—Continued

Wave length λair	Intensity and notes	Wave number	Term combination	Zeeman pattern
3466. 75	7	28837. 19		
65. 82	20*c*	28844. 94	*b* $^3F_2$—385(1)	(0.000) 1.055
62. 49	50	28872. 66	*c* $^3F_3$—524(4)	(0.000) 1.107
61. 83	3*c*	28878. 19	*a* $^3G_5$—417(5)	(0.00) 1.19
60. 84	8	28886. 46		(**0.00,** 0.28, 0.56) 0.74, 0.99, 1.29, **1.55**
59. 22	35*c*	28900. 00	*a* $^5D_3$—448(3)	(**0.000,** 0.197, 0.417, 0.667) **0.548,** 0.779, 1.030, 1.252, 1.447, 1.659
54. 47	6	28939. 71		
53. 70	12*c*	28946. 12	*b* $^3P_0$—452(1) *b* $^3D_2$—593(2)	(0.18) 1.11
50. 89	10	28969. 76		(0.000 *WD*) 0.802 *A*
49. 50	4	28981. 38		
46. 86	150*c*	29003. 62	*a* $^3G_4$—417(5)	(**0.000,** 0.213, 0.476, 0.743, 1.014) 0.801, 1.016, 1.234, 1.420, . . . **2.305**
46. 27	25	29008. 60	*a* $^1H_5$—532(5)	
45. 20	7	29017. 57	*d* $^3F_4$—605(5)	(0.000) 1.332
43. 37	12	29033. 00	*b* $^3H_4$—534(3)	(**0.000,** 0.241, 0.487, 0.733) **0.250,** 0.490, 0.722, 0.970, 1.212, 1.456
42. 72	12	29038. 50	*c* $^3F_4$—521(3)	(0.000*w*) 0.857*A*
41. 40	35	29049. 62	*a* $^3D_2$—435(3)	(**0.000,** 0.377, 0.765) **0.313,** 0.702, 1.087, 1.469, . . .
40. 32	85*c*	29058. 74	*a* $^5D_2$—435(1)	(0.000) 1.471; (0.268) 0.827
39. 70	20*c*	29063. 99	*a* $^5D_4$—462(5)	(0.000) 1.192*w*
39. 00	80*c*	29069. 90	*a* $^3G_4$—417(4)	(0.216, 0.408, 0.796, **1.093**) 0.791, **1.017, 1.248,** 1.479
37. 24	10	29084. 74		
34. 36	35	29109. 16	*a* $^5D_3$—448(3)	(0.000, 0.203, 0.411, **0.629**) 0.852, 1.044, **1.252, 1.473,** 1.668, 1.879
33. 39	20	29117. 39	*a* $^1H_5$—533(4)	(0.00) 0.77
33. 25	25*c*	29118. 56	*a* $^5P_3$—415(3)	(0.403, 0.799, 1.118, **1.276**) 0.430, 0.801, **1.193, 1.583,** 1.980, 2.299
30. 94	100	29138. 18	*a* $^3F_2$—323(3)	(**0.000,** 0.229, 0.479) 0.000, 0.227, 0.511, 0.744, 0.967, 1.189, **1.476**
30. 49	2	29141. 97		
29. 91	3	29146. 95		
29. 39	10	29151. 38	*c* $^3P_2$—571(1)	(**0.000,** 0.407) **0.986,** 1.365, 1.721
28. 78	15	29157. 53		
28. 36	5	29160. 14		
27. 39	2	29168. 36		
25. 74	4	29182. 44		(0.00) 1.00
25. 55	2	29184. 02		
24. 57	15	29192. 38	*c* $^3F_2$—521(3)	(**0.000,** 0.401, 0.817) 0.714, 1.091, 1.475, 1,848, **2.238**
23. 87	2	29198. 37		
22. 35	4	29211. 31		
21. 80	40*c*	29216. 01	*a* $^3F_4$—389(3)	(**0.000,** 0.226, 0.448, 0.693) 0.770, 0.992, 1.221, 1.437, 1.662, **1.896**
20. 93	7	29223. 46		
18. 83	3	29241. 40		
17. 50	2	29252. 75		
17. 02	40*c*	29256. 86	*a* $^5F_1$—292(2)	(**0.000** *W*, 0.489*w*) 0.000*w*, 0.510, **1.003***w*
16. 22	1	29263. 73		
15. 58	10	29269. 24	*c* $^1D_2$—622(1) *a* $^5P_2$—411(2)	(0.000, 0.202, **0.488**) 0.916, 1.139, . . .
15. 27	75	29271. 87	*a* $^3D_3$—478(3) *b* $^3F_2$—389(3)	(0.000) 0.912
14. 13	200*c*	29281. 65	*a* $^3F_3$—361(4) *b* $^3G_5$—605(5)	(0.000*WD*) 1.292*w*
13. 06	2	29290. 78	*c* $^1D_2$—623(2)	
12. 88	10	29292. 38	*a* $^3G_5$—421(4)	
12. 74	10	29293. 53	*c* $^3P_1$—555(1)	(0.000) 1.459
10. 74	7*c*	29310. 72	*a* $^5P_1$—400(0)	(0.000) 2.416
10. 42	15	29313. 51	*b* $^3G_3$—561(4)	(**0.000,** 0.433, 0.860, 1.287) 0.000, 0.412, 0.851, 1.288, 1.706, **2.140, 2.555**
08. 28	20*c*	29331. 92	*b* $^3F_4$—478(3)	(0.000) 1.249
07. 67	10	29337. 18	*a* $^1F_3$—542(4)	(0.00 *W*) 1.67*B*
07. 40	55*c*	29339. 46	*a* $^1G_4$—435(3) *a* $^5P_3$—417(4)	(**0.000,** 0.341, 0.689, 1.032) **0.212,** 0.556, 0.877, 1.252
06. 68	75	29345. 71	*a* $^3F_3$—361(2)	(**0.000,** 0.131, 0.262) 0.941, 1.073, 1.201, **1.341**
02. 93	40	29377. 99	*a* $^3G_3$—411(2)	(**0.000,** 0.243, 0.510) **0.408,** 0.678, 0.910, 1.153, 1.383
01. 69	7	29388. 71	*b* $^3D_1$—593(2)	(**0.000,** 0.147) 1.005, 1.147, **1.285**

TABLE 1. *Wavelengths, term combinations, and Zeeman effects of* Ta II—Continued

Wave length λair	Intensity and notes	Wave number	Term combination	Zeeman pattern
3400. 45	3	29399. 44	*a* $^1D_2$—429(3)	(0.000) 1.127
3399. 20	45*c*	29410. 29	*c* $^3F_4$—524(4)	(0.238) 1.071*w*
98. 72	5	29414. 42	*a* $^5D_4$—466(4)	
98. 37	90*c*	29417. 43	*a* $^3G_4$—421(4)	
97. 60	10*c*	29424. 14	*b* $^3F_3$—440(4)	(0.000) 1.346
96. 69	1	29431. 94		
96. 17	15	29436. 46		(**0.000,** 0.100, 0.191) 1.172, 1.258, **1.344**
95. 39	35	29443. 25	*c* $^3P_0$—528(1)	(0.000) 0.916
91. 22	15	29479. 47	*a* $^5P_2$—413(1)	(**0.000,** 0.466) **0.954,** 1.430, 1.909
90. 46	10	29486. 09		(0.000 *W*) 1.259*w*
90. 20	50	29488. 34		(0.389*w*) 1.158 *W D*
89. 51	8	29494. 36	*b* $^3H_6$—555(5) *a* $^1G_4$—437(5)	(0.000 *W D*) 1.373
89. 12	5	29497. 74	*c* $^3F_4$—525(3)	
88. 62	8	29502. 05	*c* $^1G_4$—646(3)	(0.000) 1.088
88. 33	40	29504. 62	*a* $^1D_2$—430(2)	(0.119) 1.099
87. 91	2	29508. 25	*d* $^3F_2$—593(2)	
86. 53	20*c*	29520. 24	*a* $^5P_1$—402(2)	(**0.000,** 1.219) −**0.078,** +1.139
85. 44	8*c*	29529. 76	*b* $^1D_2$—528(1)	(**0.000,** 0.199) 0.907, 1.115, **1.313**
83. 18	15	29549. 54	*a* $^3F_4$—392(3)	(0.00) 1.38
82. 31	2	29557. 07		(0.36, 0.75) . . .
80. 37	2	29574. 10	*d* $^3F_4$—611(4)	(0.00) 0.93
79. 51	100*c*	29581. 58	*a* $^3P_0$—337(1)	(0.00) 0.00, **0.31**
78. 58	10	29589. 74	*a* $^5D_1$—430(2)	(**0.000,** 0.448) **0.638,** 1.074
78. 17	20	29593. 29	*a* $^5D_1$—430(0)	(0.000) 1.500*w*
77. 18	5	29601. 97		
76. 78	6	29605. 49	*b* $^3F_2$—392(3)	(0.00) 0.62
76. 47	75	29608. 26	*a* $^3D_2$—467(2)	(**0.000,** 0.307, 0.613) **0.127,** 0.412, 0.713, 1.033, 1.333
75. 75	4	29614. 52		
75. 60	20	29615. 86	*a* $^3H_4$—454(5) *b* $^3H_4$—540(5)	(**0.000,** 0.216, 0.454, 0.665, 0.889) . . ., 1.626, 1.833, **2.067**
75. 47	5	29617. 03	*b* $^3D_3$—602(3)	(0.14) 1.36
73. 68	2	29632. 69		
72. 42	4*c*	29643. 79	*c* $^3P_1$—558(1) *a* $^3H_5$—478(6)	(**0.000,** 0.208, 0.396, 0.610, . . .) 1.107, 1.295, 1.477, 1.728, . . .
71. 53	50*c*	29651. 62	*c* $^3F_2$—525(3)	
69. 55	2	29669. 02	*a* $^3D_3$—482(2)	
69. 27	12	29671. 50	*a* $^3H_5$—478(5)	
68. 74	20	29676. 19	*a* $^5F_3$—323(3)	(0.251, **0.516**) 0.473, 0.711, **0.960, 1.237,** 1.501, 1.765
68. 44	40	29678. 84	*a* $^5P_2$—415(3)	(**0.000,** 0.222, 0.452) **0.766,** 0.991, 1.213, . . .
67. 50	40*c*	29687. 07	*a* $^5P_3$—421(4)	(**0.000,** 0.339, 0.675, 1.037) **0.256,** 0.586, 0.917, 1.248, 1.593
67. 08	5	29690. 78		(**0.00,** 0.57) 1.40
64. 74	8*c*	29711. 42	*a* $^5D_2$—442(1)	(**0.000,** 1.222) 1.460, **2.671**
64. 19	4	29716. 30	*b* $^1D_2$—530(2)	(0.37, **0.73**) 1.24
63. 71	15*c*	29720. 53	*a* $^5D_2$—454(2)	(**0.000,** 0.304, 0.590) 1.150, 1.460, 1.768, **2.061**
63. 42	35	29723. 10	*b* $^3P_2$—482(2) *c* $^3F_3$—533(4)	(0.000) 1.129
60. 67	8	29747. 41	*c* $^3P_2$—577(2)	(0.315, **0.643**) 0.686, **1.013, 1.352,** 1.667
58. 76	40*c*	29764. 34	*a* $^5D_2$—442(2)	(0.216) 1.468, 1.733
57. 69	40	29773. 81	*b* $^3H_4$—542(4)	(0.170, 0.319, 0.476, **0.641**) 0.490, 0.648, 0.791, **0.959, 1.092,** 1.272, 1.435, . . .
56. 20	15*c*	29787. 06	*a* $^3G_3$—415(3)	(0.64, **0.98**) 0.58, **0.90, 1.22,** 1.58
53. 92	3	29807. 33	*a* $^3D_1$—444(0)	(0.000) 0.852
53. 06	2	29814. 97		
52. 20	15*c*	29822. 63	*a* $^1H_5$—540(5)	(0.785, **0.978**) 0.670, 0.855, **1.040, 1.227,** 1.449, 1.646
50. 74	15	29835. 53	*b* $^3D_2$—602(3)	(0.00) 1.35
49. 21	150*c*	29849. 22	*a* $^3H_6$—478(6) *b* $^3F_3$—444(3)	(0.000 *W D*) 0.971*w*
48. 65	10	29854. 21		(0.00) 1.23
46. 26	35	29875. 54	*b* $^3G_4$—580(4) *a* $^3H_6$—478(5)	(0.000) 1.046
43. 73	5	29898. 13		(**0.00,** 0.69) 0.78

TABLE 1. *Wavelengths, term combinations, and Zeeman effects of* Ta II—Continued

Wave length λair	Intensity and notes	Wave number	Term combination	Zeeman pattern
3341.35	4	29919.38	*b* $^3D_2$—603(3)	
40.87	20	29923.73	*b* $^3G_3$—567(4)	(**0.000,** 0.354, 0.721, 1.069) 1.194, 1.552, 1.912, **2.272**
39.91	100*c*	29932.33	*a* $^3F_3$—367(3)	(0.253 *B*) 1.131*w*
39.56	5	29935.48	*a* $^5D_2$—444(3)	(**0.00,** 0.54) 1.02, **1.60**
39.29	20	29937.90	*a* $^5D_4$—471(3)	(0.000*w*) 1.371*w*
38.69	3	29943.23		
34.96	35*c*	29976.73	*b* $^3F_4$—484(4)	(0.000 *W*) 1.249
34.14	25	29984.14	*a* $^1D_2$—435(3)	(0.000) 1.065
33.10	45*c*	29993.50	*a* $^1D_2$—435(1)	(0.000*w D*) 0.925 *W*
32.85	30*c*	29995.74	*b* $^1G_4$—553(4)	(0.230 *B*) 0.992 *D*
32.68	50*c*	29997.24	*a* $^3F_4$—397(4)	(0.000) 1.221
32.29	12	30000.76	*a* $^3D_2$—471(3)	(0.00) 0.94
31.48	15*c*	30008.10	*a* $^3G_3$—417(4)	(**0.000,** 0.349, 0.687, 1.048) 0.911, 1.248, 1.563, . . .
30.99	250*c*	30012.51		(0.000 *W D*) 1.197 *W*, 1.582 *W B*
28.63	2	30033.76	*c* $^1D_2$—630(2)	(0.09) 1.05
26.86	25	30049.68	*a* $^5D_4$—472(4)	(0.000*w*) 1.186
24.61	3	30070.06		(0.147) 1.061
23.68	12*c*	30078.50	*a* $^5D_1$—435(1)	(0.000) 1.498 *B*
23.23	5*c*	30082.59	*c* $^3F_2$—530(2)	
23.06	8	30084.04	*c* $^1G_4$—652(4)	(0.54) 1.10
22.30	25	30091.00	*b* $^3H_5$—555(5)	(0.108) 1.045
19.15	10	30119.56	*b* $^1G_4$—555(5)	(0.000) 1.037
16.95	15*c*	30139.52	*b* $^3P_1$—475(2)	(0.000) 1.322
15.58	3	30152.00	*c* $^3F_4$—532(5)	(0.000 *W*) . . . ; (0.00) 1.50
14.85	15*c*	30158.60	*b* $^3G_3$—569(4)	(**0.000,** 0.285, 0.583, 0.907) 1.133, 1.430, 1.725, **1.971**
14.41	10	30162.57	*d* $^3F_4$—616(3)	(**0.000,** 0.192, 0.399, 0.573) 0.810, 0.959, 1.116, 1.293, **1.467,** . . .
14.06	50*c*	30165.79	*b* $^3P_2$—486(2)	(0.304, **0.622**) 0.833, **1.142,** 1.446, 1.744
13.49	5	30171.00	*b* $^1D_2$—534(3)	(**0.000,** 0.111, 0.217) 1.313, **1.420**
07.58	3	30224.87	*a* $^1G_4$—444(3)	(0.00) 1.05
06.04	8	30238.98	*a* $^1P_1$—536(2)	(0.000 *W D*) 1.362 *W D*
05.69	3	30242.15		
05.23	2	30246.34		(0.00) 1.35
04.37	25	30254.24	*a* $^3G_4$—429(3) *b* $^3F_3$—448(3)	
03.65	8	30260.82	*c* $^3F_4$—533(4)	(0.256 *B*) 0.935
02.54	12	30271.01		(0.00) 1.42
01.78	3	30278.00	*a* $^5P_2$—421(2)	(0.00) 1.40
01.08	12	30284.41	*a* $^3H_5$—484(4)	(**0.000,** 0.171, 0.345, 0.529, 0.692) **0.386,** 0.575, 0.747, 0.923, . . .
3298.86	7*c*	30304.81		(0.00) 1.40
95.45	7	30336.12		(0.27) 0.94
94.92	15*c*	30341.06	*a* $^1P_1$—537(1)	(0.00) 1.29
94.20	6	30347.61	*d* $^3P_1$—622(1)	(0.36) 0.60, 0.99
93.93	25	30350.17	*b* $^1D_2$—536(2)	(**0.000,** 0.469) **0.926,** 1.340
93.32	20*c*	30355.73	*a* $^3G_3$—421(4)	(**0.000,** 0.351, 0.694) 1.257, 1.638, 2.15
92.25	1	30365.59	*c* $^3P_0$—537(1)	
91.57	5	30371.90	*c* $^3F_2$—533(2)	
90.76	12	30379.33	*a* $^1G_4$—445(5)	(0.00) 1.20
90.02	10	30386.19	*a* $^3G_3$—421(2)	(**0.000,** 0.282, 0.544) **0.330,** 0.623, 0.910
88.98	8*c*	30395.84		
88.80	10	30397.52	*d* $^3F_2$—602(3)	(**0.000,** 0.343, 0.681) 0.862, 1.188, 1.533, **1.877**
88.57	10	30399.63	*a* $^3F_3$—372(2)	(**0.000,** 0.192, 0.559, 0.926) 1.415, 1.758, **2.113**
87.76	15*c*	30407.06	*b* $^3G_4$—585(5)	(0.000 *W*) 1.339*w*
86.31	8*c*	30420.52	*a* $^1G_4$—446(4)	
85.61	20	30426.98	*a* $^3D_2$—475(1)	(0.594 *B*) 1.201 *D*
85.10	50*c*	30431.74	*a* $^5P_1$—411(2)	(**0.000,** 1.074) **0.000***w*, 1.160
83.73	10*c*	30444.44	*a* $^3H_4$—462(5)	(0.00) 0.72 *A*
82.93	4*c*	30451.85	*b* $^1D_2$—537(1)	(0.00) 1.08
82.20	2	30458.60		(0.000) 1.352
81.82	2	30462.13	*b* $^3P_2$—489(3)	(0.00) 1.25
81.52	10	30464.89	*b* $^3D_2$—608(2)	(0.00) 1.11
81.23	20*c*	30467.57		(0.00 *W*) 0.89

TABLE 1. *Wavelengths, term combinations, and Zeeman effects of* Ta II—Continued

Wave length λair	Intensity and notes	Wave number	Term combination	Zeeman pattern
3281.08	3	30469.04	$b\ ^3F_4$—489(3)	
80.60	2	30473.40		
80.01	4	30478.91		(0.00) 1.05
79.72	7	30481.61	$d\ ^3F_2$—603(3)	(**0.00,** 0.31, 0.61) 1.12, 1.50, **1.83**
78.26	5*c*	30495.21		(0.00) 1.52
77.44	1	30502.88		(0.00) 0.99
77.03	8	30506.68	$c\ ^1G_4$—656(3)	(0.00) 1.19
76.51	30*c*	30511.46	$a\ ^1F_3$—553(4)	(0.000*w*) 1.132*w*
75.97	10	30516.48	$b\ ^3D_1$—604(1)	(0.34) 0.75, 1.06
75.66	60*c*	30519.36	$a\ ^3P_2$—361(2)	(0.383, **0.782**) 0.559, **0.963, 1.344,** 1.755
74.92	90*c*	30526.34	$a\ ^3F_2$—337(1) $a\ ^3D_3$—490(2)	(**0.000,** 0.582) **0.748,** 1.491
73.96	75	30535.23	$a\ ^3F_2$—337(2)	
73.13	20	30543.01	$b\ ^3F_2$—402(2)	(0.199 *B*) 1.211*w*
71.13	50*c*	30561.65	$b\ ^3F_4$—490(5)	(0.000) 1.214
69.34	20*c*	30578.41		(0.000*w*) 1.041*w*
69.16	12	30580.04	$b\ ^3P_2$—490(2)	(0.154, **0.280**) 1.175, **1.300, 1.472,** 1.625
68.72	15*c*	30584.23	$d\ ^3F_4$—621(4)	(0.00) 1.01
66.28	5	30607.06		(0.00) 0.97
65.51	50	30614.25	$b\ ^3F_2$—403(1)	(**0.000,** 0.200) **0.840,** 1.057, 1.246
62.64	25*c*	30641.22		
62.53	18*c*	30642.21	$a\ ^5P_1$—413(1)	(0.495) 1.825*w*, 2.365*w*
62.14	7	30645.92	$a\ ^1D_2$—442(1)	(**0.00,** 0.85) 1.08, **1.96**
61.49	35*c*	30652.01	$b\ ^3H_6$—566(6)	(0.181) 1.091*W*
60.97	18	30656.92	$a\ ^3D_2$—478(3)	(0.000) 1.195
60.55	15	30660.83	$a\ ^5D_3$—463(2)	(**0.000,** 0.179, 0.375) 1.475, 1.650, **1.837**
59.19	5	30673.61	$a\ ^1F_3$—555(3)	
57.50	5	30689.58	$b\ ^3P_1$—480(0)	(0.000) 1.186
56.85	25	30695.62	$b\ ^3H_4$—551(3)	(**0.000,** 0.266, 0.539, 0.795) **0.187,** 0.457, 0.719, 0.996, 1.249, 1.509
56.50	12	30699.00	$a\ ^1D_2$—442(2)	(0.147, **0.279**) 0.978, **1.112, 1.257,** 1.381
56.28	2	30701.07		
55.76	12	30705.94		(0.000) 0.617
53.36	20	30728.61	$b\ ^3H_5$—561(4)	(**0.000,** 0.215, 0.438, 0.657, 0.895) **0.150,** 0.379, 0.618, 0.851, 1.060
53.12	50	30730.86	$a\ ^5D_1$—442(1)	(1.261) 0.247, 1.501
52.26	60*c*	30738.98	$a\ ^5D_2$—452(1)	(0.000) 1.477
50.94	4	30751.44		
50.47	8	30755.95		(0.00) 1.71*B*
48.83	1	30771.46		
47.29	2	30786.05		
41.69	12	30839.23	$a\ ^3G_4$—435(3)	(0.000) 0.954
40.94	250	30846.37	$a\ ^3P_1$—361(2)	(**0.000,** 0.611) **0.339,** 0.944, 1.527
40.70	15	30848.64	$b\ ^3G_5$—621(4) $b\ ^3P_1$—482(2)	
38.90	10*c*	30865.79	$b\ ^3F_3$—454(2)	(0.00) 0.94
38.54	25	30869.20	$a\ ^3G_5$—437(5) $a\ ^3H_5$—490(5)	(0.128, 0.269, 0.412, 0.568, **0.712**) 0.582, 0.719, 0.879, 1.011, **1.147, 1.297,** 1.426, 1.567, 1.710, 1.834
38.27	3	30871.76		(0.00) 1.17
35.13	5	30901.70		(0.000*WD*) 0.662*A*
34.68	10	30906.04	$d\ ^3P_1$—628(1)	
33.91	25	30913.44	$c\ ^3F_3$—545(2)	(0.000*w*) 1.098*w*
31.98	10	30931.89	$d\ ^3F_4$—624(4)	(0.000*w*) 1.115
31.34	12	30937.94	$b\ ^3G_5$—622(5)	(0.000*w*) 0.917*w*
29.89	100	30951.83	$a\ ^5D_2$—454(2)	(0.302, **0.613**) 0.870, **1.160, 1.479,** 1.775
29.10	10	30959.46	$a\ ^5D_1$—444(0)	(0.000) 1.488
28.77	12	30962.59	$b\ ^3G_3$—577(2)	
28.42	35	30965.98	$c\ ^3F_4$—540(5)	(**0.000,** 0.172, 0.357, 0.533, 0.730) 1.279, 1.453, 1.650, 1.834, **2.031**
26.93	100*c*	30980.30	$a\ ^3H_4$—468(3)	(0.000*WD*) 1.036*WD*
25.94	10	30989.77	$a\ ^1F_3$—558(2)	(**0.000,** 0.333, 0.696) **0.275,** 0.646, . . .
22.22	20	31025.56		(0.000*w*) 0.949*B*
21.12	15	31036.12	$b\ ^3P_2$—495(3)	(0.000*W*) 0.938, 1.382*W*
19.21	15	31054.59	$a\ ^3D_2$—482(2)	(0.218, **0.461**) 0.978, **1.208, 1.443,** 1.665
18.08	3	31065.51	$b\ ^1G_4$—564(5)	(0.00) 0.94
17.61	2	31070.03	$b\ ^3D_3$—616(3)	

TABLE 1. *Wavelengths, term combinations, and Zeeman effects of* Ta II—Continued

Wave length λair	Intensity and notes	Wave number	Term combination	Zeeman pattern
3217.37	12	31072.27	$b\ ^3H_4$—555(5) $a\ ^5F_3$—337(2)	(0.000*WD*) 1.228*WD*
17.22	6	31073.71		(0.00) 1.20
16.15	75	31084.06	$a\ ^5P_2$—429(3)	(**0.000,** 0.300, 0.615) **0.512,** 0.818, 1.114, 1.396
15.32	15*c*	31092.16	$b\ ^3P_2$—495(2)	(0.00*W*) 1.54
15.13	10	31093.99		(0.00) 1.33
13.91	150	31105.80	$a\ ^5D_3$—468(3) $a\ ^3P_2$—367(3)	(**0.000,** 0.172, 0.364) **0.788,** 1.012, . . .
13.70	20	31107.78	$b\ ^3H_5$—565(5)	(0.31) 1.13*D*
13.29	1	31111.80	$d\ ^3P_1$—630(2)	
12.00	2	31124.22	$c\ ^3F_4$—542(4) $a\ ^5D_3$—468(2)	
11.62	2	31127.89	$a\ ^1P_1$—545(2)	(0.000) 1.027
10.73	10	31136.58	$b\ ^1G_4$—565(5)	(0.000*W*) 1.100*D*
09.76	50*c*	31145.98	$b\ ^3P_2$—496(3)	(**0.000,** 0.430, 0.862) **0.190,** 0.624, 1.043
09.42	5	31149.30	$a\ ^1F_3$—560(2)	(0.00) 1.00
09.03	25	31153.08	$b\ ^3F_4$—496(3)	(**0.000,** 0.201, 0.399, 0.596) . . .
08.83	10	31155.00	$a\ ^1H_5$—553(4)	(0.000) 0.676
08.08	1	31162.31		
05.28	20*c*	31189.49	$a\ ^5P_2$—430(2)	
04.58	10	31196.28	$b\ ^3G_5$—624(4)	(0.000) 1.087
02.96	2	31212.08	$a\ ^5F_1$—312(1)	
00.18	90*c*	31239.23	$b\ ^1D_2$—545(2) $a\ ^5D_4$—484(4)	(0.183 *W*, 0.228) 1.200 *W D*
3199.21	60	31248.70	$b\ ^3H_5$—566(6)	(0.000*w* 1.271 *B*
98.93	75	31251.43		(0.000*w*) 0.885 *A*
96.72	8	31273.06	$a\ ^1F_3$—561(4)	
96.52	15	31275.02	$a\ ^1D_2$—448(3)	(**0.000,** 0.153, 0.297) . . ., 1.179, 1.322, **1.469**
96.08	25*c*	31279.32	$a\ ^1H_5$—555(5)	(0.293*w*) 0.852, 1.132*w*
95.28	20*c*	31287.12	$a\ ^5F_2$—323(3)	(0.000*w*) 0.940*w*
95.13	6	31288.63	$b\ ^3D_2$—616(3)	(0.00) 0.86
94.83	75*c*	31291.48	$b\ ^3P_1$—486(2)	(0.000) 1.114
94.19	2	31297.83	$a\ ^3G_3$—430(2)	
93.97	7*c*	31299.97	$a\ ^3G_4$—440(4)	(0.129, 0.280, 0.437, **0.569**) 1.032 *W D*
93.16	15	31307.89	$c\ ^3P_2$—593(2) $b\ ^3P_0$—475(1)	(0.000) 1.502
92.55	2	31313.89		
90.92	7	31329.85	$a\ ^3P_2$—369(1)	(**0.000,** 0.640) . . ., 1.337, **1.981**
90.00	7	31338.94	$b\ ^3H_5$—567(4)	(0.00 *D*) 0.58 *A*
89.19	20	31346.87		(0.000) 1.144
87.09	10	31367.48	$b\ ^1G_4$—567(4)	(0.380*w*) 1.146*w D*
85.17	25*c*	31386.39	$b\ ^3P_2$—498(1)	(**0.000,** 0.548) **0.905***w*, 1.442, 1.989
84.73	2	31390.74		
82.95	8	31408.33		(0.000*w*) 1.109*w*
79.73	25*c*	31440.12	$a\ ^5P_1$—421(2)	(0.00) 1.24
79.44	12	31443.02	$a\ ^5D_3$—471(3)	(0.42, 0.80, **1.14**) 0.37, 0.75, **1.11, 1.50,** 1.87, 2.17
79.12	8	31446.13	$b\ ^3G_3$—582(2)	(**0.00,** 0.84, 1.56) −**0.80,** +0.06, 1.64, 2.44
77.56	10	31461.55		(0.00) 0.63*w*
77.27	2	31464.45		(0.00) 0.86 *A*
75.53	10	31481.68		(0.000) 0.737
74.49	2	31492.05	$b\ ^3D_3$—621(4)	(0.00 *W*) 0.46
72.88	25	31508.01	$c\ ^3F_3$—551(3)	
70.77	8	31529.00		(0.00) 1.14
68.96	15*c*	31547.01	$a\ ^3D_1$—461(1)	(0.517) 0.912, 1.390
68.17	75	31554.81	$a\ ^5D_3$—472(4)	(**0.000,** 0.271, 0.503, 0.836) **0.367,** 0.653, 0.919, 1.197, 1.468, 1.727, 1.988
66.71	50*c*	31569.40	$a\ ^5P_3$—440(4)	(**0.000,** 0.491, 0.972, 1.457) −0.354, +0.141, 0.639, **1.118**
66.36	40	31572.83	$a\ ^3P_2$—372(2)	(0.000, 0.719, **1.436**) −0.113, **0.610, 1.333,** 2.053
65.80	4*c*	31578.43		
65.50	3	31581.47		(0.433, **0.653**) . . .?
64.34	15	31592.97		(0.00) 1.19

TABLE 1. *Wavelengths, term combinations, and Zeeman effects of* Ta II—Continued

Wave length λair	Intensity and notes	Wave number	Term combination	Zeeman pattern
3163. 12	40*c*	31605. 22	*c* $^3F_2$—545(2) *a* $^5D_0$—442(1)	(**0.098,** 0.316) **1.071,** 1.269, 1.454
62. 86	20*c*	31607. 86	*a* $^3D_2$—487(1)	(**0.000,** 0.428) 0.712, 1.149, **1.576**
61. 90	2	31617. 36		
61. 72	4	31619. 20		
57. 95	70*c*	31656. 95	*a* $^3P_1$—369(1)	(0.877) 0.670, 1.546
57. 64	50*c*	31660. 03		(0.447, 0.675, **0.929**) 0.582, 0.818, 1.039, **1.267,** 1.504, 1.743, 1.949
57. 19	5	31664. 59	*b* $^3F_2$—413(1)	(**0.00,** 0.86) 0.23, . . .
56. 74	50*c*	31669. 05	*a* $^5P_2$—435(3)	(**0.000,** 0.356, 0.698) **0.408***w*, 0.750, 1.075
56. 58	10	31670. 65		(0.00) 1.04)
56. 37	2	31672. 79	*b* $^3G_4$—598(5)	(0.00) 1.18
56. 14	4	31675. 10	*b* $^1G_4$—570(3)	
55. 69	6	31679. 66	*a* $^5D_2$—461(1)	(0.000*w*) 1.498 *A*
55. 35	5	31682. 99		(0.00) 1.17
55. 24	50	31684. 16	*a* $^3F_3$—385(2)	(0.000 *W D*) 1.181*w B*
53. 92	12	31697. 42	*a* $^5F_4$—361(4)	(. . ., 0.334, 0.509, **0.696**) . . ., 1.484, 1.662, 1.839
53. 76	15*c*	31698. 98		(0.00 *W*) 0.92
53. 07	5*c*	31705. 94	*b* $^3F_3$—462(4)	(0.000 *W*) 1.109 *A*
52. 69	7	31709. 78	*b* $^3H_4$—561(4)	(0.96, **1.20**) . . ., 1.15, 1.55, 1.83, 2.23
51. 65	15	31720. 21	*c* $^3F_2$—546(3)	(**0.000,** 0.227, 0.468) 0.716, 0.942, **1.160**
51. 16	50*c*	31725. 12	*a* $^3G_4$—444(3)	(0.000 *W*) 1.182*w*
50. 54	20*c*	31731. 37	*a* $^5D_4$—489(3)	(0.000 *WD*) 1.057*w*
47. 70	20*c*	31760. 03	*a* $^3D_1$—463(2)	(0.00) 0.210*B*
45. 99	20*c*	31777. 28	*a* $^3G_3$—435(3)	(0.166, 0.337, **0.531**) 0.651, **0.834, 1.008,** 1.257
44. 86	30*c*	31788. 70	*a* $^5D_3$—475(2)	(**0.000,** 0.169, 0.361) 1.288, 1.462, 1.631, **1.824**
44. 32	10	31794. 13	*a* $^3D_2$—489(3)	(0.000) 1.358*B*
42. 95	75	31808. 07	*a* $^3F_4$—415(3)	(0.000) 1.243
42. 36	20*c*	31814. 01	*b* $^3P_2$—503(3)	(**0.000,** 0.201, 0.410) **0.772,** 1.039
41. 69	8	31820. 77	*b* $^3F_4$—503(3)	(0.000) 1.226
41. 37	80*c*	31824. 00	*a* $^5D_4$—490(5)	(0.000*w*) 1.327*w*
40. 33	4	31834. 56	*c* $^3P_1$—580(1)	(0.180) 1.134, 1.342
39. 84	20	31839. 57	*b* $^3D_3$—624(4)	(0.268*w*) 1.193*w*
38. 75	7	31850. 63	*d* $^3F_2$—616(3)	(0.000*WD*) 1.042
38. 04	5	31857. 76		(0.000) 1.026
37. 43	75	31863. 95	*a* $^3D_1$—464(2) *b* $^3F_2$—415(3)	(**0.000,** 0.163, 0.331) 0.892, 1.051, 1.198, 1.358, **1.521**
36. 72	4	31871. 19		(0.33) 1.67
35. 83	120*c*	31880. 22	*a* $^3G_4$—445(5)	(**0.000,** 0.253, 0.551, 0.877, 1.187) 1.017, 1.272, 1.525, 1.860, 2.153, **2.469**
35. 53	5	31883. 30	*a* $^1F_3$—567(4)	
35. 20	15	31886. 65	*a* $^1D_2$—454(2)	(0.123) 1.111*w*
34. 80	5	31890. 71	*b* $^3D_2$—622(1)	(**0.00,** 0.48) 0.58, 1.13, **1.55**
33. 89	50	31899. 95	*a* $^3P_1$—372(2)	(**0.000,** 0.949) −**0.309,** +0.631, 1.556
32. 86	3	31910. 46	*b* $^3F_3$—464(2)	
31. 85	90*c*	31920. 73	*a* $^3G_4$—446(4)	(0.220, **0.772**) . . . ?
31. 60	90*c*	31923. 33	*c* $^3F_3$—555(3)	
30. 80	8	31931. 46	*c* $^3F_3$—555(2)	(0.00*w*) 1.13
28. 59	10	31954. 04	*d* $^3F_4$—634(4)	(0.29) 1.10*w*
27. 74	100*c*	31962. 74	*a* $^3F_4$—417(5)	(0.000*w*) 1.264*w*
26. 87	7	31971. 58	*a* $^5D_1$—454(2)	(**0.000,** 0.341) **0.781,** 1.148, 1.503
26. 59	7*c*	31974. 45	*a* $^3H_4$—478(3)	(0.000*w*) 1.107
24. 62	50*c*	31994. 66	*a* $^5P_3$—444(3)	(0.670, 1.326, **1.976***w*) . . . 0.327, **0.936, 1.560,** 2.237, 2.912
23. 46	3	32006. 55	*a* $^3H_4$—478(5)	
22. 78	15*c*	32013. 42	*b* $^3F_4$—505(5)	(**0.000,** 0.156, 0.330) 1.17*B*
22. 32	18	32018. 22	*b* $^3H_4$—564(5)	(**0.000,** 0.205, 0.410, 0.622) **0.352,** 0.568, 0.778, 0.976, 1.186
21. 26	40*c*	32029. 03	*a* $^3F_4$—417(4)	(0.139) 1.236*A*
21. 09	7	32030. 79	*b* $^3P_2$—505(1)	
20. 13	2	32040. 62	*c* $^3P_1$—582(2)	
19. 64	5	32045. 73	*c* $^3F_4$—551(3)	(0.000) 1.302*B*
19. 12	10	32050. 99		(**0.000,** 0.188) 1.231, 1.397, **1.582**
17. 74	10	32065. 24	*b* $^3F_3$—466(4)	(**0.000,** 0.210, 0.421, 0.645) **0.960,** 1.188, 1.377
16. 70	15	32075. 96	*b* $^3G_4$—602(3)	(**0.000,** 0.123, 0.265, 0.387) **0.655,** 0.803, 0.927
15. 42	20	32089. 12	*b* $^3H_4$—565(5) *a* $^1G_4$—462(5)	(0.000) 1.005

TABLE 1. *Wavelengths, term combinations, and Zeeman effects of* Ta II—Continued

Wave length λair	Intensity and notes	Wave number	Term combination	Zeeman pattern
3114.45	8	32099.13	$a\ ^5D_3$—478(3)	(0.269, 0.523, **0.804**) 0.932, **1.186, 1.447,** 1.699
12.88	50	32115.27		(0.247) 1.088*WD*
12.58	6	32118.35	$a\ ^1F_3$—569(4)	(**0.000,** 0.165, 0.319, 0.475) . . . , 1.266, 1.434, **1.626**
11.35	2	32131.11	$a\ ^3F_3$—389(3)	(0.242) 0.633, **0.865, 1.111,** 1.340.
10.81	90*c*	32136.69		(0.263*w*) 1.185*w*
09.93	6*c*	32145.72	$a\ ^1P_1$—555(2)	(0.00) 0.94
09.81	10	32146.98	$c\ ^3P_0$—555(1)	(0.000) 1.395
09.04	3*c*	32154.98		(**0.00,** 0.38) **0.77,** 1.14
08.58	45*c*	32159.66	$b\ ^3G_4$—603(3)	(0.000*w*) 0.832
06.11	3	32185.27		
05.63	50	32190.20	$a\ ^5P_3$—446(4)	(**0.000,** 0.345, 0.675, 1.033) **0.230,** 0.575, 0.909, 1.251, 1.603
04.70	6*c*	32199.89	$c\ ^3F_2$—551(3)	(**0.00,** 0.55, 1.13) . . . , 0.72, 1.22, 1.81, **2.48**
02.90	7	32218.56	$b\ ^3P_1$—495(2) $b\ ^3G_5$—634(4)	(0.00) 1.15
01.47	10	32233.46	$b\ ^1D_2$—555(1)	(0.000, 0.293) **0.822,** 1.097, 1.423
01.22	7	32236.02		
01.04	100*c*	32237.86	$a\ ^3G_3$—440(4)	(**0.000,** 0.205, 0.448, 0.713) 0.683, 0.916, 1.117, 1.346, 1.598, **1.857**
3099.83	20*c*	32250.43	$b\ ^3F_3$—468(3)	(0.211, 0.406, **0.668**) 0.564, 0.784, **1.003, 1.209,** 1.436, 1.667
99.22	2	32256.86	$b\ ^1D_2$—555(2)	(0.00) 1.10
97.98	25*c*	32269.69	$b\ ^3F_3$—468(2)	(0.000*w*) 0.875*w*
96.88	8*c*	32281.19	$c\ ^3P_2$—603(3)	(**0.000,** 0.218, 0.444) **0.692,** 0.943
96.13	10	32289.04	$d\ ^3F_4$—638(4)	(0.000) 1.128
95.50	15	32295.56	$a\ ^1H_5$—565(5)	(0.000) 1.008
95.21	10	32298.61	$c\ ^3F_4$—553(4)	(0.000) 1.033
94.60	40*c*	32304.94	$a\ ^5D_4$—495(3)	(**0.000,** 0.149, 0.306, 0.470) **0.717,** 0.889, 1.066
93.14	7	32320.20	$b\ ^3H_4$—567(4)	(0.49, **0.76**) 0.43, **0.85, 1.29,** 1.79
91.90	8	32333.19	$b\ ^3D_1$—622(1)	(0.39) 0.60, 1.00
91.58	15	32336.50	$a\ ^5D_2$—468(3)	(**0.000,** 0.253, 0.550) **0.656,** 0.948, 1.240
90.48	10	32348.04	$a\ ^5F_4$—367(3)	(**0.000,** 0.185, 0.341, 0.501) 1.317, 1.501, **1.663**
90.14	20*c*	32351.59	$a\ ^5P_1$—430(2)	(0.000) **0.251,** 1.056
89.85	5	32354.64	$b\ ^3D_1$—623(2)	
89.74	15*c*	32355.83	$a\ ^5D_2$—468(2)	(0.75*B*) 0.68, **1.07, 1.49,** 1.89, 2.38
88.84	4	32365.22		
88.69	10	32366.77		(0.00) 1.15
88.60	10	32367.73	$a\ ^3D_2$—495(3)	(0.000) 1.059
87.76	100*c*	32376.57	$a\ ^3F_4$—421(4)	(0.020*w*) 1.254*w*
87.08	4	32383.65	$a\ ^5P_2$—442(2)	
85.65	10	32398.68	$c\ ^3F_3$—560(2)	(**0.00,** 0.70) 1.13
84.06	10	32415.40	$a\ ^5D_4$—496(3)	(**0.000,** 0.147, 0.291, 0.439) 1.030, 1.171, 1.312, 1.460, **1.613**
83.39	25	32422.40	$c\ ^3F_4$—555(5)	(0.000 *w*) 0.098 *w*
83.19	6	32424.50	$a\ ^3D_2$—495(2)	(0.34, **0.73**) 0.88, **1.26, 1.64**, . . .
82.06	90*c*	32436.42	$b\ ^3G_5$—637(5) $b\ ^3D_3$—630(2) $a\ ^1H_5$—566(6)	(0.00*w*) 1.40*w*
80.53	1	32452.55	$d\ ^3F_2$—622(1)	
79.56	75*c*	32462.80	$b\ ^3F_2$—421(2)	(0.124, **0.323**) 0.846, **1.035, 1.215,** 1.391
79.40	4	32464.43	$a\ ^3F_3$—392(3)	(0.00) 1.11
78.47	10	32474.19	$d\ ^3F_2$—623(2)	(0.157, **0.326**) 0.673, **0.829, 0.988,** 1.138
78.10	25*c*	32478.17	$a\ ^3D_2$—496(3)	(0.58) 0.71*w*
76.80	8*c*	32491.88	$a\ ^3G_3$—442(2)	(**0.00,** 0.39) . . .?
76.32	20	32496.89	$a\ ^5D_3$—482(2)	(0.000) 1.468
75.31	2	32507.60	$a\ ^3H_5$—506(6)	(0.000*WD*) 1.350*B*
74.90	20*c*	32511.94	$b\ ^3P_1$—498(1)	(0.809) 1.922
74.23	25	32519.02		
74.13	15*c*	32520.04	$a\ ^3D_3$—510(3)	(0.424*W*) 1.316*W*
73.87	20	32522.87	$b\ ^3G_3$—593(2)	(**0.000,** 0.284, 0.604) **0.252,** 0.573, 0.846
73.50	8	32526.72	$a\ ^1H_5$—567(4)	(0.00) 0.77
70.96	15	32553.69	$b\ ^3G_5$—638(4)	(0.000) 1.127
69.93	8	32564.55	$b\ ^1D_2$—558(2)	(0.229, **0.433**) 0.947, **1.162, 1.368,** 1.554
68.77	8	32576.92		(0.00) 0.99
68.45	7	32580.32		(0.000*w*) 1.349
67.60	5	32589.29		
65.58	5	32610.78		

TABLE 1. *Wavelengths, term combinations, and Zeeman effects of* Ta II—Continued

Wave length λair	Intensity and notes	Wave number	Term combination	Zeeman pattern
3065. 25	8	32614. 27	$\left\{\begin{array}{l} a\ ^1D_2—461(1) \\ c\ ^3F_2—555(3) \end{array}\right.$	(**0.000,** 0.252) **0.869,** 1.105, 1.352
64. 79	125*c*	32619. 20	*a* $^3H_4$—484(4)	(0.445) 1.186
64. 17	6*c*	32625. 78	*a* $^1G_4$—468(3)	(0.00) 1.22
64. 08	8	32626. 77	*b* $^3H_5$—580(4)	(0.00) 1.35
63. 68	1	32631. 00	*c* $^1D_2$—656(3)	
63. 49	8	32633. 02	*a* $^5D_0$—452(1)	(0.00) 1.45
62. 52	35*c*	32643. 40	*a* $^3D_3$—511(2)	(0.000) 1.278
61. 44	20	32654. 92	*b* $^3D_2$—630(2)	(0.082) 0.755
60. 65	50*c*	32663. 26	*a* $^3G_3$—444(3)	(0.000*w*) 0.910*w*
59. 63	15	32674. 17	*a* $^5D_2$—471(3)	(**0.000,** 0.377, 0.751) **0.336,** 0.707, 1.102, 1.487
58. 73	12	32683. 83	*a* $^5F_2$—337(2)	(0.000, **0.341**) 0.537, **0.869, 1.176,** 1.482
57. 23	150*c*	32699. 88	$\left\{\begin{array}{l} a\ ^5D_1—461(1) \\ b\ ^3F_3—472(4) \end{array}\right.$	(**0.000,** 0.198, 0.413, 0.656) 0.988, 1.176, 1.382, 1.616, **1.849**
56. 62	75*c*	32706. 37	*a* $^5D_4$—499(4)	(0.167*w*) 1.216*w*
56. 12	40	32711. 68	*a* $^3H_6$—506(6)	(0.000*wD*) 1.153 *B*
55. 48	2	32718. 53	*a* $^3D_2$—498(1)	(**0.00,** 0.81) **0.46,** 1.32, 2.03
53. 10	50	32744. 12	*a* $^5D_3$—484(4)	(**0.000,** 0.195, 0.399, 0.615) **0.840,** 1.067, 1.265, 1.458, 1.656, 1.856
52. 59	125	32749. 52		(0.000*WD*) 0.624*A*
51. 46	15	32761. 63	$\left\{\begin{array}{l} a\ ^3G_4—454(5) \\ a\ ^1H_5—569(4) \end{array}\right.$	(**0.000,** 0.128, 0.251, 0.392, 0.525) **0.450,** 0.620, 0.739, 0.864, 1.004
45. 51	2	32825. 68	*b* $^3P_2$—513(1)	
45. 37	25*c*	32827. 20	*a* $^1D_2$—463(2)	(0.224, **0.440**) 0.913, **1.112, 1.316,** . . .
44. 13	3*c*	32840. 55	*a* $^5P_1$—435(1)	(0.98) 1.50
42. 92	4	32853. 63		(0.00) 1.16
42. 45	100*c*	32858. 73	*a* $^3G_3$—446(4)	(**0.000,** 0.336, 0.679) 0.232, 0.568, 0.916, 1.256, 1.537, . . .
42. 07	100*c*	32862. 79	*a* $^3P_0$—369(1)	(0.000) 0.679
40. 72	50*c*	32877. 44	*a* $^3P_2$—385(1)	(**0.000,** 0.878) 0.477, 1.326, **2.187***w*
39. 85	50	32886. 83	*a* $^3D_1$—475(2)	(**0.000,** 0.444) 0.863, 1.272, **1.736**
39. 44	4	32891. 25	*b* $^3D_1$—628(1)	
37. 51	100*c*	32912. 12	$\left\{\begin{array}{l} a\ ^3F_3—397(4) \\ a\ ^5D_1—463(2) \end{array}\right.$	(0.102, 0.308, **0.470**) . . .?
36. 61	50	32921. 84	*a* $^1F_3$—577(2)	(0.000*w*) 0.923 *A*
35. 53	7*c*	32933. 57	*b* $^3F_3$—475(2)	(**0.000,** 0.288, 0.593) **0.429,** 0.710
34. 91	10	32940. 29	$\left\{\begin{array}{l} b\ ^3G_4—611(4) \\ a\ ^5D_3—486(2) \end{array}\right.$	(**0.000,** 0.328, 0.628) 1.471, 1.784, **2.105**
34. 01	5*c*	32950. 08	*c* $^3F_2$—558(1)	(**0.00,** 0.74) **0.00,** 0.74
33. 12	15*c*	32959. 78	*a* $^5P_2$—448(3)	(**0.000,** 0.183, 0.385) **0.892,** 1.069, 1.246
32. 77	1	32963. 55	*a* $^1G_4$—471(3)	(0.000) 1.021
32. 34	6	32968. 24	*a* $^3D_1$—475(1)	(0.652) 0.865, 1.507
31. 22	40*c*	32980. 63	*a* $^3D_3$—515(2)	(0.000*w*) 1.324 *A*
30. 68	8	32986. 25	*b* $^3F_4$—514(4)	(0.365*w*) 1.274*w*
29. 70	2	32996. 98	*a* $^3F_2$—361(2)	(0.44) 0.93 *D*
28. 44	25	33010. 74	*a* $^5P_3$—454(2)	(0.00) 0.84
27. 62	30	33019. 63	*a* $^5D_2$—475(2)	(0.213, **0.370**) 1.105, **1.273, 1.480,** 1.652
24. 29	2	33056. 02	*b* $^1D_2$—563(3)	
23. 94	2	33059. 81	*c* $^3F_4$—561(4)	
23. 20	5	33067. 88	*a* $^3G_3$—448(3)	(0.00) 1.11
22. 56	50	33074. 90	*a* $^1G_4$—472(4)	(0.496 *B*) 1.110
21. 80	70	33083. 28	*a* $^5D_4$—503(3)	(0.000 *W*) 1.031*w*
21. 18	4	33090. 04	*c* $^3F_2$—560(2)	
20. 52	5	33097. 22	*b* $^3D_1$—630(2)	(0.000) 1.225*w*
20. 17	50	33101. 06	*a* $^5D_2$—475(1)	(0.000) 1.460
19. 34	8	33110. 22		
18. 70	5	33117. 24	*c* $^3P_1$—593(2)	(**0.000,** 0.197) **0.919,** 1.150, 1.360
18. 29	10	33121. 66	*d* $^3F_4$—646(3)	(0.125) 1.086
16. 07	25	33146. 10	*a* $^3D_2$—503(3)	(0.000*w*) 1.363 *B*
15. 84	4	33148. 56	*c* $^1G_4$—682(3)	(0.00) 1.17
15. 17	10	33156. 01	$\left\{\begin{array}{l} b\ ^1D_2—564(1) \\ b\ ^3P_1—505(1) \end{array}\right.$	(0.000*w*) 1.306*w*
14. 94	20	33158. 45	*b* $^3H_5$—585(5)	(0.304) 1.088 *W*

TABLE 1. *Wavelengths, term combinations, and Zeeman effects of* Ta II—Continued

Wave length λair	Intensity and notes	Wave number	Term combination	Zeeman pattern
3013.78	3	33171.26	$a\ ^1F_3$—580(4)	(0.00) 1.16
12.55	125*c*	33184.84	$a\ ^3P_1$—385(2)	(**0.000,** 0.561) **0.460,** 1.012, 1.544; (0.957) 2.046*w*
11.87	10	33192.25	$b\ ^3G_4$—613(5)	(0.76) 1.26
11.49	15	33196.52	$b\ ^3D_3$—638(4)	(0.00) 0.84
10.80	125*c*	33204.09	$a\ ^3P_1$—385(1) $a\ ^3H_4$—490(5)	(0.376 *W*) 1.289, 1.750 *W*
09.97	7	33213.27	$a\ ^3F_4$—429(3)	(0.000*w*) 1.533 *B*
09.65	2	33216.80	$a\ ^1D_2$—467(2) $d\ ^3F_2$—630(2)	(0.279, **0.554**) 0.550, **0.816, 1.118,** 1.376
09.16	1	33222.21		(**0.000,** 0.93) 1.53, **2.42**
05.74	40	33259.97	$b\ ^3F_4$—517(5)	(**0.000** *W D*) 0.683 *W*
04.92	50	33269.06	$b\ ^3F_2$—429(3)	(0.000*w*) 1.229
04.72	10	33271.30	$a\ ^1D_2$—468(3)	(0.000*w*) 1.385*w*
04.32	5*c*	33275.71	$a\ ^5D_4$—505(5)	(0.000) 1.084*w*
02.98	50	33290.51	$a\ ^1D_2$—468(2)	(0.000) 1.108
02.68	5	33293.86	$a\ ^3H_5$—514(4)	(0.000*w*) 1.009*w*
01.73	1	33304.45	$a\ ^3P_2$—389(3)	
2999.38	125*c*	33330.53	$a\ ^5D_2$—478(3)	(**0.000,** 0.266, 0.564) **0.624,** 0.931, 1.196, 1.460, 1.728
98.69	3	33338.18		(0.262 *W*) 1.147 *W*
97.28	75*c*	33353.85	$a\ ^5D_3$—490(2)	(0.312*w*) 1.192 *W D*
96.88	7	33358.33	$a\ ^5P_2$—452(1)	(0.000) 1.408*w*
96.49	25	33362.70	$a\ ^3D_2$—505(1)	(**0.000,** 0.163) **0.754,** 0.898, 1.067
95.99	3	33368.18	$c\ ^3F_4$—564(5)	(**0.000,** 0.166, 0.322, 0.482) . . .?
95.43	30	33374.48	$b\ ^3F_2$—430(2)	(0.000) 1.061
92.95	12	33402.11	$a\ ^3F_3$—402(2)	(0.000 *W*) 1.017 *B*
92.69	10	33404.97	$a\ ^1F_3$—582(2)	(0.000) 0.989
92.01	4	33412.56		
89.83	5	33437.01	$a\ ^3D_1$—480(0)	(0.000) 0.856
89.63	20	33439.19	$c\ ^3F_4$—565(5)	(0.000) 0.890
88.72	10	33449.38		(0.000) 0.915
87.12	2	33467.30		(0.00) 1.04
86.81	50*c*	33470.73	$a\ ^5F_3$—361(4)	(0.000*W*) 0.907*A*
84.83	12*c*	33492.98	$a\ ^5P_1$—442(1)	(0.135) 0.255, 2.376
84.55	10	33496.07	$b\ ^3G_3$—603(3)	
83.73	2	33505.32		
80.78	1	33538.51	$a\ ^3D_1$—481(2)	
80.12	15*c*	33545.92	$a\ ^5P_1$—442(2)	(**0.00,** 1.13) **0.00***w*, 1.24
79.14	10*c*	33556.94	$a\ ^5F_5$—397(4)	(0.00) 1.81
78.20	50	33567.52	$a\ ^3D_3$—521(3) $a\ ^3H_5$—517(5)	
77.85	10*c*	33571.50	$a\ ^5P_2$—454(2)	(0.53) 1.32*w*
76.99	50*c*	33581.16	$a\ ^3G_4$—462(4)	(0.000*w*) 1.004*W*
76.76	10	33583.79	$a\ ^3F_2$—367(3)	(**0.000,** 0.420, 0.842) 0.945, 1.374, 1.814, **2.265**
76.22	200*c*	33589.80	$a\ ^3G_4$—462(5)	(**0.000,** 0.187, 0.406, 0.606, 0.823) 1.004, 1.202, 1.409, 1.611, 1.795, **2.050**
75.74	1	33595.29	$a\ ^3D_1$—482(2)	
74.88	2	33605.05		
74.54	50	33608.86	$a\ ^1D_2$—471(3)	
73.65	10	33618.85		(**0.000,** 0.347, 0.658) **0.453,** 0.713, 0.997, 1.303
73.52	8*c*	33620.41	$b\ ^3P_2$—521(3)	(**0.00,** 0.40) . . . ?
72.90	8	33627.37	$b\ ^3F_4$—521(3)	(0.00*W*) 1.41*w*
72.85	6	33627.93		
72.75	7	33629.07		(0.00) 1.08
71.96	15	33637.99	$a\ ^3P_2$—392(3)	(0.00*W*) 0.77*A*
71.62	10	33641.83	$b\ ^3F_3$—482(2) $b\ ^3G_5$—649(6)	(0.00) 1.31*B*
71.48	8	33643.46		(0.00) 0.98
70.90	1	33650.01	$c\ ^3P_2$—616(3)	
70.46	6	33654.97	$b\ ^3P_2$—521(1)	(**0.000,** 0.183) 1.281*w*
69.04	40*c*	33671.04	$c\ ^3F_4$—567(4)	(0.000*WD*) 1.794*WD*

TABLE 1. *Wavelengths, term combinations, and Zeeman effects of* Ta II—Continued

Wave length λair	Intensity and notes	Wave number	Term combination	Zeeman pattern
2968. 64	10	33675. 66		(**0.000,** 0.165, 0.345, 0.519) **0.370,** 0.522, 0.668
68. 29	75*c*	33679. 60	*a* $^3G_3$—454(2)	(**0.000,** 0.250, 0.568, 0.850) . . . ?
67. 81	5*c*	33685. 01	*a* $^3H_4$—495(3)	(**0.000,** 0.197, 0.391, 0.615) **0.699,** 0.929, 1.134, 1.319, 1.501
66. 18	3	33703. 60	*d* $^3F_4$—652(4)	(0.000*w*) 1.369*W*
65. 93	50*c*	33706. 39	*a* $^5F_1$—337(1)	(0.269) 0.165, 0.383
65. 14	250*c*	33715. 33	*a* $^5F_1$—337(2)	(**0.000,** 0.748) 0.771, **1.554***W*
64. 02	50*c*	33728. 16	*a* $^5D_2$—482(2)	(0.000*w*) 1.453
62. 20	2	33748. 84		(0.00) 1.55
61. 47	3	33757. 12		(0.000) 0.669
60. 71	3	33765. 78	*b* $^1D_2$—570(3)	(**0.000,** 0.283, 0.571) 1.369, 1.695, . . .
60. 37	7	33769. 72		(0.000*w*) 0.951*w*
60. 12	7	33772. 53		(0.000*w*) 0.787*B*
58. 61	3*c*	33789. 74	*a* $^1P_1$—571(1)	(0.572*w*) 2.082
58. 12	10	33795. 37	*a* $^3H_4$—496(3)	(0.000*w*) 1.339*W*
57. 88	50	33798. 09	*a* $^3F_4$—435(3)	(**0.000,** 0.150, 0.272, 0.416) 0.945, 1.082, 1.215, 1.358, 1.501, **1.650**
56. 84	100*c*	33810. 07	*a* $^5D_3$—495(3)	(0.171, 0.355, **0.493**) 0.975, 1.141, **1.304, 1.473,** 1.637, 1.802
56. 43	10	33814. 73	*c* $^3P_0$—571(1) *a* $^3G_5$—466(4) *a* $^1H_5$—580(4)	(0.000*w*) 0.894*A*
55. 79	3	33822. 04	*b* $^3P_1$—511(2)	(0.00) 1.31*A*
55. 32	50	33827. 38	*b* $^3H_6$—598(5)	(0.000*WD*) 1.319*B*
54. 92	8*c*	33831. 97		
53. 97	1	33842. 84	*a* $^5D_4$—510(3)	(**0.000,** 0.150) . . . ?
53. 00	100	33853. 96	*b* $^3F_2$—435(3)	(0.000*w*) 1.116
51. 90	75	33866. 56	*a* $^5D_3$—495(2)	(0.000*w*) 1.372*WD*
49. 92	70*c*	33889. 26	*b* $^3F_3$—484(4)	(**0.000,** 0.263, 0.541, 0.884) 0.726, 1.003 ,1.264, 1.521, 1.884, **2.176**
49. 02	30	33899. 66		(0.000*WD*) 1.451
48. 53	10	33905. 28	*a* $^3D_2$—510(3) *c* $^3F_4$—569(4)	(0.414) 0.903
47. 21	4	33920. 50	*a* $^5D_3$—496(3)	(0.43, 0.93, **1.36**) 0.22, 0.60, **1.09, 1.60,** . . .
45. 59	60	33939. 09	*a* $^3D_3$—524(4)	(**0.000,** 0.241, 0.489, 0.752) **0.347,** 0.604, 0.845, 1.080
44. 83	100	33947. 89		(0.000) 1.166
44. 57	50*c*	33950. 86	*b* $^3G_4$—621(4) *b* $^3P_1$—513(1)	(0.000) 1.065
44. 27	3	33954. 40	*a* $^1D_2$—475(2)	(0.40) 1.04
43. 48	5*c*	33963. 44	*d* $^3F_4$—654(3)	(0.00*w*) 1.06*w*
43. 09	20	33967. 95	*b* $^3G_5$—652(4)	(0.376 *B*) 1.174 *D*
38. 02	75*c*	34026. 60	*a* $^3D_3$—525(3)	(0.216 *B*) 1.349 *D*
37. 80	12	34029. 14	*a* $^3D_2$—511(2) *b* $^3D_3$—646(3)	(0.179, 0.350, **0.549**) 0.717, 0.897, **1.062, 1.240,** 1.417, 1.614
36. 95	50	34039. 00	*a* $^5D_1$—475(2) *a* $^3D_1$—486(2)	(**0.000,** 0.209) **1.044,** 1.296*w* (**0.000,** 0.222) 1.434*w*
36. 74	10	34041. 38	*b* $^3G_3$—608(2)	(**0.000,** 0.273, 0.546) **0.292,** 0.584, 0.857, 1.123
35. 95	10	34050. 61	*a* $^3F_2$—372(2)	(0.138, **0.257**) 0.475, **0.608, 0.745,** 0.872
35. 62	10	34054. 42		(0.059) 1.023
32. 91	30*c*	34085. 88	*b* $^3F_3$—486(2)	(**0.000,** 0.175, 0.337) **0.607,** 0.786, 0.954, 1.104, 1.285, 1.419
31. 69	5	34100. 00		(**0.000,** 0.094) **0.439,** 0.532
29. 93	20	34120. 55	*a* $^5D_1$—475(1)	(0.000) 1.506
29. 45	15	34126. 14	*d* $^3F_4$—656(3) *a* $^3G_4$—468(3)	(**0.000,** 0.203, 0.376, 0.560) **0.467,** 0.643, 0.844
28. 94	2	34132. 06	*c* $^3F_2$—570(3)	
28. 29	3	34139. 68	*b* $^3H_4$—585(5)	
27. 51	15	34148. 72	*a* $^3D_1$—487(1)	(0.107) 0.798
26. 72	20*c*	34158. 00	*a* $^3D_2$—513(1)	(**0.000,** 0.184) **1.077,** 1.251, 1.422
26. 60	7	34159. 35	*b* $^3P_1$—515(2)	(0.00) 1.32
25. 55	8	34171. 63	*c* $^3F_3$—577(2) *a* $^5D_2$—486(2)	(0.341, **0.644**) 0.835, **1.126, 1.492,** 1.781
22. 85	50*c*	34203. 12		(0.000*w*) 0.885 *D*
22. 28	30*c*	34209. 78	*a* $^5P_3$—466(4)	
22. 13	40	34211. 39	*a* $^5D_3$—499(4)	(**0.000,** 0.248, 0.494, 0.747) **0.449,** 0.694, 0.955, 1.202, 1.436, 1.692, 1.968
21. 44	8	34219. 66		(0.000) 0.818
18. 96	200*c*	34248. 75	*a* $^5D_4$—514(4)	(0.239*w*) 1.131 *W*
18. 09	12	34258. 92	*a* $^3F_4$—440(4)	(0.402 *B*) 1.168 *D*

TABLE 1. *Wavelengths, term combinations, and Zeeman effects of* Ta II—Continued

Wave length λair	Intensity and notes	Wave number	Term combination	Zeeman pattern
2917. 56	50	34265. 16	$a\ ^1G_4$—484(4) $a\ ^1D_2$—478(3)	(0.000*w*) 1.360 *B*
16. 81	1	34274. 02	$c\ ^3P_2$—623(2)	
16. 55	15*c*	34277. 10		(**0.00,** 0.34) 1.25, **1.52**
14. 73	50	34298. 43	$b\ ^3G_4$—624(4)	(0.000 *WD*) 0.847*w*
14. 66	20*c*	34299. 28	$a\ ^5P_2$—461(1)	(0.000) 1.475 *D*
14. 10	4	34305. 81		(**0.000,** 0.230) 1.405, 1.616, **1.858**
13. 99	30	34307. 14	$a\ ^3H_5$—524(4)	(0.000) 1.101
13. 44	30	34313. 63	$a\ ^3F_3$—411(2)	(0.000*w*) 0.970 *A*
12. 41	40	34325. 77	$a\ ^5D_1$—478(0)	(0.000) 1.515
11. 88	2	34332. 02		
10. 86	3	34344. 05		(0.000) 1.466 *B*
10. 67	2	34346. 29	$a\ ^1H_5$—585(5)	(0.00) 1.22
09. 02	12	34365. 80	$a\ ^3D_2$—515(2)	(0.158) 1.232
07. 33	30*c*	34385. 72	$a\ ^1P_1$—577(2)	(**0.000,** 0.217) **0.889,** 1.055
06. 92	3	34390. 63		(0.000) 1.014
05. 24	100	34410. 51	$a\ ^3P_0$—385(1)	(0.000) 0.472
04. 88	20	34414. 76	$a\ ^5P_3$—468(2)	(**0.000,** 0.498) 1.127, 1.600, 2.079, **2.597**
04. 41	2	34420. 34	$c\ ^3F_3$—580(4)	
04. 08	20*c*	34424. 20	$b\ ^3H_5$—598(5)	(0.00*w*) 1.09
01. 87	50	34450. 46	$a\ ^3G_5$—472(4)	(0.141) 1.087
01. 67	4	34452. 84	$a\ ^3D_1$—490(2)	
01. 31	15*c*	34457. 14	$a\ ^3D_3$—530(2)	
00. 74	75	34463. 84	$a\ ^3G_4$—471(3)	(0.000*w*) 0.875*w*
2899. 20	50	34482. 18	$a\ ^1F_3$—593(2)	(**0.000,** 0.174, . . .) **0.622,** 0.799, 0.996, 1.179
98. 69	3	34488. 25		(0.18) 1.13
97. 99	2	34496. 61	$b\ ^1D_2$—577(2)	(0.00) 1.13
97. 73	4	34499. 65	$b\ ^3F_3$—490(2)	(**0.000,** 0.313, 0.644) **0.345,** 0.673, 0.996, 1.320
96. 84	2	34510. 28	$b\ ^3P_2$—530(2)	(0.000*w*) 1.461
96. 38	20	34515. 74	$b\ ^3F_2$—442(1)	(**0.000,** 0.799) 0.248, 1.049, **1.843**
96. 04	7	34519. 78	$a\ ^3G_3$—462(4)	
95. 48	30	34526. 41		(**0.000,** 0.155, 0.297) **0.960,** 1.139, 1.289
93. 77	10	34546. 83	$a\ ^5F_4$—389(3)	(**0.000,** 0.342, 0.681, 1.013) 0.827, 1.162, 1.497, 1.840, **2.175**
91. 99	2	34568. 08		(0.23) 1.11
91. 36	15	34575. 64	$a\ ^3G_4$—472(4) $a\ ^3P_2$—402(2)	(0.188, **0.385**) . . ., **1.149, 1.336,** 1.524, 1.719
90. 53	3	34585. 63	$a\ ^3D_2$—490(2)	(0.31) **1.57**
90. 26	50*c*	34588. 85	$a\ ^5F_3$—372(2) $a\ ^5D_1$—480(0)	(**0.000,** 0.622, 1.247) 0.000, 0.614, 1.240, 1.866, **2.491**
88. 40	20	34611. 12	$b\ ^3D_3$—652(4)	(0.000) 1.179
87. 69	2	34619. 60	$a\ ^3G_3$—463(2)	
87. 16	2	34625. 96		
86. 34	6	34635. 81	$c\ ^3P_1$—608(2)	(**0.000,** 0.209) **0.923,** 1.137, 1.330
85. 40	40*c*	34647. 03	$a\ ^3P_2$—403(1)	(0.097) 1.395
84. 65	25*c*	34656. 06	$a\ ^3H_4$—505(5)	(0.000) 1.123*w*
84. 30	12	34660. 26	$a\ ^3H_5$—528(6)	(0.000*w*) 1.467*B*
82. 83	8	34678. 01		
82. 32	25	34684. 09	$a\ ^3F_4$—444(3)	(**0.000,** 0.278, 0.562, 0.835) 0.659, 0.939, 1.222. 1.496, **1.777, 2.051**
82. 00	8	34687. 95	$c\ ^3P_0$—580(1)	(0.000) 1.133
81. 60	50	34692. 82	$a\ ^3P_1$—400(0)	(0.000) 1.549
80. 57	4	34705. 14		(0.000) 0.508
79. 09	35	34722. 99	$a\ ^3F_3$—415(3)	(0.246, **0.385**) 0.824, 0.936, **1.083, 1.208,** 1.347, 1.462
78. 21	18*c*	34733. 65	$a\ ^5P_3$—471(3) $a\ ^5P_1$—454(2)	(0.000) 1.117 *W D*
77. 67	100	34740. 19	$b\ ^3F_2$—444(3)	(0.000*w*) 0.992*w B*
77. 54	25	34741. 71	$b\ ^3F_4$—532(5)	
77. 06	25	34747. 53	$a\ ^5D_1$—482(2)	(0.000) 1.385
74. 83	12	34774. 45		(0.000) 1.081
74. 33	30*c*	34780. 54	$b\ ^3P_1$—521(1)	(0.409) 1.17, 1.608

TABLE 1. *Wavelengths, term combinations, and Zeeman effects of* Ta II—Continued

Wave length λair	Intensity and notes	Wave number	Term combination	Zeeman pattern
2873. 56	40	34789. 82	*a* $^3D_3$—533(4)	(0.00*w*) 1.64
72. 16	1	34806. 79		
71. 89	1	34810. 06	*d* $^3F_2$—646(3) *c* $^3P_2$—628(1)	
71. 59	5	34813. 72		(0.00) 1.20
70. 87	6	34822. 47		(0.000) 0.956
69. 51	15*c*	34838. 98	*a* $^3F_4$—445(5)	(0.000*W*) 1.399*w*
69. 02	6	34844. 93	*a* $^5P_3$—472(4)	(**0.000,** 0.396) **0.775,** 1.197, 1.602
68. 64	25	34849. 53	*b* $^3F_4$—533(4) *a* $^1G_4$—490(5)	(0.392*B*) 1.132*D*
68. 14	20	34855. 52	*b* $^1G_4$—602(3)	(0.000*w*) 0.893*B*
67. 83	7*c*	34859. 39		(**0.000,** 0.176, 0.369, 0.539) . . .?
67. 41	150*c*	34864. 40	*a* $^3H_6$—528(6)	(0.000*W*) 1.163*w*
66. 85	7	34871. 20	*b* $^3D_3$—654(3)	(0.00) 1.42
66. 26	18*c*	34878. 47	*a* $^3G_3$—466(4)	(**0.000,** 0.280, 0.586) 1.223, 1.499, 1.789, **2.102**
66. 14	35*c*	34879. 84	*a* $^5F_4$—392(3) *a* $^3F_4$—446(4)	(0.000*w*) 1.282*w*
65. 70	50	34885. 23		(0.000*w*) 1.035*A*
65. 32	85	34889. 85	*a* $^5D_4$—521(3)	(0.000*w*) 1.328*W*
64. 26	7	34902. 82	*a* $^3P_1$—402(2)	(**0.000,** 0.395) **0.751,** 1.159, 1.571
63. 54	10	34911. 56	*a* $^3D_3$—534(3)	(0.00*w*) 1.24
63. 44	20	34912. 80		(0.264*B*) 1.105*D*
62. 52	12	34923. 96		(0.000) 1.112
61. 24	10	34939. 65	*b* $^1G_4$—603(3)	(0.00) 1.01
60. 88	75	34943. 99	*a* $^3F_3$—417(4)	(**0.000,** 0.172, 0.358, 0.542) . . ., 0.901, 1.075, 1.259, 1.436, 1.637, **1.829**
59. 94	8	34955. 55	*b* $^3F_3$—495(3) *a* $^5P_2$—468(3)	(**0.000,** 0.221, 0.453) **0.766,** 0.984
59. 72	12	34958. 17	*c* $^3F_4$—580(4)	(0.059) 1.056
59. 14	20*c*	34965. 28	*b* $^3P_2$—534(3) *a* $^3D_1$—495(2)	(0.000) 0.755 (0.000) 2.305
58. 75	20	34970. 05		
58. 43	125	34973. 99	*a* $^3P_1$—403(1)	(0.317) 1.223, 1.556
57. 34	8	34987. 33	*a* $^3D_2$— 52i(1)	(**0.000,** 0.399) **0.853,** 1.227
56. 68	50	34995. 40	*a* $^5D_0$—475(1)	(0.000) 1.502
55. 85	2	35005. 55		(0.00) 1.21
55. 34	20*c*	35011. 75	*b* $^3F_3$—495(2)	(**0.000,** 0.587, 1.155, 1.678) **0.441,** 0.984, 1.581
55. 18	5	35013. 75	*d* $^3F_4$—665(4)	(0.00) 1.10
54. 79	6	35018. 60		(0.000) 0.846
54. 21	2	35025. 68		(0.00) 0.90*A*
53. 54	8	35033. 85	*b* $^3D_3$—656(3)	(0.264, 0.504, **0.753**) 0.501, 0.766, **1.032, 1.274,** 1.492, 1.754
53. 18	10	35038. 26	*b* $^3P_0$—513(1)	(0.00) 1.046
52. 94	10	35041. 32	*a* $^5D_2$—495(3)	(**0.000,** 0.161, 0.335) **0.989,** 1.120, 1.288, 1.466
52. 34	150	35048. 68	*a* $^3H_5$—532(5)	(0.274*B*) 1.109 *W D*
50. 98	40	35065. 40	*b* $^3F_3$—496(3)	(0.389*B*) 1.239 *W D*
49. 92	10	35078. 40	*d* $^3F_4$—66b(5)	
49. 86	12	35079. 08	*a* $^5P_3$—475(2)	(**0.000,** 0.325, 0.654) 0.967, 1.297, **1.604,** . . . ?
49. 51	1	35083. 43	*a* $^3G_3$—468(2)	
49. 06	8	35089. 02	*a* $^3F_4$—448(3)	(0.000) 1.172
48. 89	20*c*	35091. 13	*a* $^3D_3$—536(2)	(0.000*w*) 1.350*w*
48. 33	15	35097. 98	*a* $^5D_2$—495(2)	(0.197) 1.513*D*
47. 65	20	35106. 31	*a* $^1D_2$—486(2)	(0.000) 1.114
46. 54	5*c*	35120. 05	*a* $^3G_4$—478(3)	
44. 60	10	35144. 00	*b* $^3P_2$—536(2)	
44. 46	200	35145. 75	*a* $^5F_2$—361(2)	(0.139*B*) 0.988*w*
43. 98	4	35151. 68	*a* $^5D_2$—496(3)	
43. 51	110*c*	35157. 50	*a* $^3H_5$—533(4)	(0.000) 1.083
41. 61	8	35180. 95		(0.000) 1.112
40. 79	8	35191. 13	*a* $^5D_1$—486(2)	(**0.000,** 0.368) **0.770,** 1.143
40. 39	75	35196. 13		(0.000) 1.038
39. 91	10	35202. 01		(0.000*w*) 0.889*w*

TABLE 1. *Wavelengths, term combinations, and Zeeman effects of* Ta II—Continued

Wave length λair	Intensity and notes	Wave number	Term combination	Zeeman pattern
2838. 78	2	35216. 06	$a\ ^1D_2$—487(1)	(**0.000,** 0.362) 0.795, 1.104, **1.477**
38. 23	175*c*	35222. 87	$a\ ^3H_4$—510(3)	(0.000*w*) 1.101*w*
37. 11	7	35236. 82		
36. 35	7	35246. 16	$b\ ^3P_2$—537(1)	(**0.000,** 0.199) 1.407, **1.633**
35. 84	30*c*	35252. 60	$a\ ^3H_6$—532(5)	(0.000*w*) 1.069*WB*
35. 29	25*c*	35259. 39	$a\ ^3D_1$—498(1) $b\ ^3H_4$—596(5)	(1.209) 1.995 (**0.000,** 1.081) 0.880
35. 10	20*c*	35261. 78	$a\ ^5D_4$—524(4)	(0.283) 1.081*B*
33. 78	7	35278. 20	$b\ ^3G_5$—665(4)	(0.000) 1.314
33. 06	1	35287. 19	$b\ ^3G_3$—621(4)	
32. 70	50*c*	35291. 63	$a\ ^3F_3$—421(4)	(**0.000,** 0.191, 0.380, 0.581) 0.893, 1.074, 1.258, 1.460, 1.639, **1.866**
32. 54	15	35293. 62	$a\ ^5P_2$—471(3)	
31. 97	8	35300. 76	$a\ ^5D_1$—487(1)	(0.751) 0.751, 1.491
31. 75	2	35303. 47		
31. 47	4	35307. 01		
30. 40	10	35320. 28	$b\ ^3G_4$—634(4)	
30. 26	25	35321. 99	$a\ ^3F_3$—421(2)	(**0.000,** 0.126, 0.289, 0.492) **0.798,** 0.934, 1.081, 1.214
29. 79	30	35327. 97	$a\ ^5F_4$—397(4)	(0.478*B*) 0.841, **1.059, 1.316,** 1.572
29. 19	12	35335. 41	$a\ ^3F_2$—385(2)	(0.277, **0.525**) . . . ?
28. 58	75	35343. 04	$b\ ^3G_5$—666(5)	(0.000*WD*) 1.028
28. 09	12*c*	35349. 20	$a\ ^5D_4$—525(3)	
27. 59	60*c*	35355. 38	$a\ ^3F_2$—385(1)	(**0.000,** 0.243) 0.457, 0.746, **1.032***w*
27. 47	10*c*	35356. 90	$b\ ^3F_3$—499(4)	(**0.000,** 0.209, 0.430, 0.680) 0.996, 1.202, 1.427, 1.664, **1.902**
26. 30	3	35371. 54	$a\ ^1F_3$—602(3)	
25. 75	1	35378. 42		
24. 64	12	35392. 28	$a\ ^5D_2$—498(1)	(**0.000,** 0.532) **0.934,** 1.485, 2.024
24. 36	5	35395. 83		
23. 82	20*c*	35402. 55	$a\ ^3G_3$—471(3) $a\ ^1D_2$—489(3)	(0.254) 1.002
23. 61	3	35405. 24	$b\ ^3H_4$—598(5)	
23. 07	15	35412. 05	$a\ ^3D_2$—525(3)	(**0.000,** 0.201, 0.403) 1.226, 1.411, 1.597, **1.792**
20. 71	6	35441. 61	$b\ ^1G_4$—496(3)	(**0.000,** 0.341, 0.695) **0.325,** 0.671, 0.998, 1.309
20. 08	3	35449. 58	$b\ ^3P_1$—528(1)	(0.258) 1.449
19. 93	1	35451. 44		
19. 52	15*c*	35456. 62		
19. 13	70*c*	35461. 51	$a\ ^5P_1$—461(1)	(1.026) 1.365, 2.362
18. 35	20	35471. 29	$a\ ^5D_3$—511(2)	(0.000*w*) 1.655*B*
17. 10	200	35487. 11	$a\ ^3P_2$—411(2)	(0.171, **0.369**) 0.959, **1.160, 1.352,** 1.567
15. 72	2	35504. 44		
15. 00	25	35513. 55	$a\ ^3G_3$—472(4)	
14. 46	20	35520. 28	$a\ ^1D_2$—490(2)	(0.147, 0.332, **0.508**) 0.985, **1.216, 1.403,** 1.600
14. 30	90*c*	35522. 35	$a\ ^5F_5$—417(5)	(0.715) 1.605*W*
13. 52	3	35532. 19		
13. 05	2	35538. 19	$b\ ^3G_4$—637(5)	
12. 63	6	35543. 44	$b\ ^3F_2$—452(1)	(**0.000,** 0.408) **0.657,** 1.055, 1.451
11. 70	125*c*	35555. 20	$b\ ^3F_4$—540(5)	(0.000*W*) 1.212*B*
11. 33	15	35559. 83		(**0.000,** 0.173, 0.341) **0.899,** 1.060, 1.240
10. 48	3	35570. 62		
09. 94	15	35577. 44	$b\ ^3H_6$—615(6)	(0.208*w*) 1.147
09. 06	15*c*	35588. 61	$a\ ^5F_5$—417(4)	(0.000*W*) 0.472*w*
08. 31	25	35598. 13	$b\ ^3H_6$—616(6)	(0.000) 1.185
07. 75	12	35605. 17	$a\ ^5D_1$—490(2)	(**0.000,** 0.193) **1.113,** 1.312, 1.508
07. 39	30	35609. 73		(0.000*w*) 0.872*A*
07. 23	5	35611. 79	$a\ ^1H_5$—598(5)	
05. 90	15*c*	35628. 67	$a\ ^5F_5$—382(3) $a\ ^3H_4$—514(4)	(0.000*w*) 1.109
05. 46	3	35634. 28	$b\ ^3G_3$—624(4)	
05. 33	15*c*	35635. 96	$b\ ^3P_1$—530(2)	(**0.000,** 0.299) 1.774

TABLE 1. *Wavelengths, term combinations, and Zeeman effects of* Ta II—Continued

Wave length λair	Intensity and notes	Wave number	Term combination	Zeeman pattern
2805. 07	8	35639. 21	$a\ ^5P_2$—475(2) $a\ ^3G_3$—484(4)	(0.242*B*) 1.342*D*
04. 58	3	35645. 46		
04. 01	20	35652. 71	$a\ ^3D_3$—542(4)	(**0.000,** 0.198, 0.430, 0.639) **0.531,** 0.738, 0.940, 1.145, 1.349
03. 80	10	35655. 38	$b\ ^3G_4$—638(4) $a\ ^3D_2$—528(1)	
02. 93	3	35666. 44		
02. 34	10	35673. 93	$a\ ^5P_1$—463(2)	
00. 53	15	35697. 01	$a\ ^3P_2$—413(1)	(**0.000,** 0.548) **0.782,** 1.322, 1.893
2799. 27	35	35713. 05	$b\ ^3F_4$—542(4)	(0.328*Wd*) 1.034*D*
98. 72	40	35720. 13	$a\ ^5P_2$—475(1) $b\ ^1G_4$—611(4)	(0.206*B*) 0.865*D*
97. 76	200	35732. 40	$a\ ^1G_4$—499(4) $a\ ^5F_2$—367(3)	(**0.000,** 0.170, 0.355) 0.820, 0.995, 1.176, 1.351, **1.523**
96. 58	5	35747. 41	$a\ ^3G_3$—475(2)	
96. 08	20	35753. 80	$a\ ^5D_3$—514(4)	(**0.000,** 0.343, 0.670, 1.005) **0.105,** 0.413, . . .
95. 20	70*c*	35765. 01	$a\ ^3G_4$—484(4)	(0.235, 0.482, 0.818, **1.100**) 0.205, 0.501, 0.778, **1.014, 1.254,** 1.501, 1.771, 2.040.
94. 10	8	35779. 15		(0.000*w*) 1.087*w*
93. 86	20	35782. 25	$a\ ^3F_2$—389(3)	(**0.000,** 0.251, 0.519) 0.480, 0.735, 0.992, 1.241, **1.509**
93. 47	4	35787. 19	$a\ ^5P_3$—482(2)	(**0.000,** 0.096, 0.198) . . .?
91. 84	10	35808. 14	$a\ ^5D_3$—515(2) $b\ ^3H_4$—602(3)	(**0.000,** 0.239, 0.453, 0.664) **0.193,** 0.414, 0.593, 0.774, 0.976, 1.176
91. 37	50	35814. 18	$a\ ^3P_1$—411(2) $d\ ^3F_2$—656(3)	(**0.000,** 0.392) **0.754,** 1.164, 1.551
89. 16	30	35842. 58	$a\ ^3D_2$—530(2)	(0.246, **0.522**) 0.941, **1.212, 1.474,** 1.727
88. 95	3	35845. 20		
86. 77	25	35873. 20	$a\ ^5F_3$—385(2)	(**0.000,** 0.229, 0.476) 0.775, 1.004, 1.242, 1.484, **1.736**
85. 29	8	35892. 28	$b\ ^3H_4$—603(3)	(**0.000,** 0.168, 0.328, 0.513) **0.471,** 0.660, 0.843, 0.991, 1.139, 1.288, 1.453
84. 96	75	35896. 60	$a\ ^3P_2$—415(3)	(0.000*w*) 0.903*A*
84. 46	2	35903. 04	$a\ ^3D_1$—505(1)	
83. 04	3	35921. 38	$b\ ^3D_3$—665(4)	(0.000*WD*) 0.693*A*
81. 90	12	35936. 05	$a\ ^5F_5$—421(4)	(0.000*WD*) 1.841*B*
81. 35	1	35943. 20	$b\ ^3H_5$—613(5)	
81. 14	7	35945. 92	$a\ ^1P_1$—593(2)	(0.000*w*) 1.123
80. 83	10	35949. 92	$a\ ^5P_2$—478(3)	(**0.000,** 0.225, 0.435) **0.749,** 0.979, 1.196
80. 34	50	35956. 21	$a\ ^5F_2$—369(1)	(**0.000,** 0.333) 0.696, 0.995, **1.336**
79. 46	2	35967. 65		
79. 06	2	35972. 84	$b\ ^1G_4$—613(5)	
78. 81	30	35976. 02	$a\ ^1D_2$—495(3)	(**0.000,** 0.209, 0.413) 0.898, 1.099, 1.299, 1.497, **1.719**
76. 91	6	36000. 60	$a\ ^1F_3$—608(2)	(**0.000,** 0.160, 0.319) **0.653,** 0.802, 0.958, 1.145
76. 70	20	36003. 30	$a\ ^5D_4$—532(5)	(0.000*w*) 1.086
76. 23	5	36009. 42		
75. 38	8	36020. 52	$a\ ^3H_5$—542(4)	(0.000*w*) 0.940
75. 10	30	36024. 16	$a\ ^3P_1$—413(1)	(0.336) 1.530
74. 56	40	36031. 17		(**0.000,** 0.137, 0.286, 0.430, 0.562, 0.732) **0.288,** 0.412, 0.576, 0.711, 0.874, 1.024, 1.145
74. 18	15	36036. 10	$a\ ^5D_2$—505(1)	(0.000*wD*) 1.490
73. 60	5	36043. 65		
72. 47	10	36058. 25	$a\ ^3G_3$—478(3)	(0.258, 0.755*W*) 0.335, 0.632, **0.919, 1.182,** 1.470, 1.787
72. 24	2	36061. 33	$c\ ^3P_1$—622(1)	
72. 06	2	36063. 66	$a\ ^5P_1$—467(2)	
71. 82	75	36066. 68	$a\ ^3H_6$—540(5)	(0.000*w*) 1.070*w*
70. 54	1	36083. 34	$c\ ^3P_1$—623(2)	
70. 32	4	36086. 28	$c\ ^1D_2$—496(3)	(0.000*w*) 0.909*A*
70. 10	15	36089. 19	$c\ ^1G_4$—712(5)	(**0.000,** 0.200, 0.423, 0.631, 0.892) **1.027,** 1.223, 1.430, 1.630, 1.840, **2.097.**
69. 65	5	36094. 99	$a\ ^3D_3$—546(3)	(0.396, 0.574, 0.824, 1.217*w*) . . ., **0.928,** 1.320, 1.762
68. 07	12	36115. 54	$a\ ^3F_2$—392(3)	(**0.000,** 0.395, 0.788) 0.339, 0.732, 1.136, 1.532, 1.922

TABLE 1. *Wavelengths, term combinations, and Zeeman effects of* Ta II—Continued

Wave length λair	Intensity and notes	Wave number	Term combination	Zeeman pattern
2767. 92	2	36117. 51	$a\ ^5D_1$—495(2)	
67. 10	15	36128. 20	$a\ ^3F_3$—429(3)	(0.132) 1.083
66. 79	1	36132. 27	$a\ ^3D_2$—533(2)	
66. 40	12	36137. 39	$a\ ^5P_1$—468(2)	(**0.000,** 1.286*w*) −**0.197,** +1.091, 2.357
65. 59	2	36147. 95	$b\ ^3P_2$—546(3)	(**0.000,** 0.515, 1.048) **0.429,** 0.929, 1.437
65. 04	2	36155. 19	$b^3\ F_4$—546(3)	(**0.000,** 0.295, 0.600, 0.907) 1.224, 1.525, 1.833, **2.124**
63. 36	30	36177. 16	$a\ ^5F_1$—361(2)	(**0.000,** 0.934) 0.000, 0.934, **1.866**
62. 05	75	36194. 27	$b\ ^3H_6$—622(5) $b\ ^3H_5$—616(6)	(0.000 *W*) 1.464
61. 75	75	36199. 54	$a\ ^5F_2$—372(2)	(0.384, **0.770**) 0.249, **0.612, 1.005,** 1.385
59. 28	20	36230. 59	$a\ ^5P_3$—486(2)	(**0.000,** 0.473, 0.990) 0.575, 1.130, 1.610, 2.067, **2.538**
59. 05	25	36233. 65	$a\ ^3F_3$—430(2)	(0.000) 1.097
58. 16	2	36245. 36		
57. 26	40	36257. 20	$a\ ^3G_4$—489(3)	(**0.000,** 0.259, 0.549, 0.871) **0.149,** 0.455, 0.774, 1.015, 1.269, 1.535, . . .
56. 30	25	36269. 75	$b\ ^3P_1$—536(2) $a\ ^3H_4$—521(3)	(0.000*w*) 1.149*A*
54. 21	2	36297. 27	$a\ ^3D_2$—534(3)	(0.000) 1.228
53. 46	3	36307. 20		
52. 49	100	36319. 96	$a\ ^5F_3$—389(3)	(0.240, 0.475, **0.762**) 0.486, 0.744, **0.997, 1.239,** 1.490, 1.768
51. 98	3	36326. 79	$a\ ^1D_2$—498(1)	(0.00) 0.93
50. 35	100	36348. 24	$a\ ^5P_2$—482(2)	(0.176) 1.125*W*
48. 58	20	36371. 70	$b\ ^3P_1$—537(1)	(0.098) 1.217
46. 83	75	36394. 81	$a\ ^5D_3$—521(3)	(0.000*W*) 1.197*D*
45. 57	3	36411. 50	$a\ ^5D_1$—498(1)	(0.485) 1.512, 1.984
43. 98	1	36432. 64		(0.000) 1.011, 1.294
42. 23	15	36455. 83	$a\ ^3G_3$—482(2)	(**0.000,** 0.524, 1.048) **0.000** *w*, 0.404, 0.913, 1.454
40. 69	30	36476. 34	$a\ ^3D_2$—536(2)	(0.162, **0.279**) 1.042, **1.191, 1.343,** 1.476
40. 11	25	36484. 09	$b\ ^3F_2$—461(1)	(0.00) 1.22
39. 26	75	36495. 42	$a\ ^3P_2$—421(2)	(0.175, **0.310**) 1.045, **1.184, 1.371,** 1.528
38. 20	1	36509. 61		
37. 20	2	36522. 89		
36. 91	15	36526. 69	$a\ ^5P_3$—489(3)	(0.332, 0.647, **0.999**) 0.623, 0.944, **1.275, 1.598,** 1.927, . . .
35. 26	50	36548. 83	$a\ ^3F_4$—462(5)	
33. 67	2	36569. 98	$a\ ^3D_1$—511(2)	
33. 33	25	36574. 54	$a\ ^3D_3$—551(3)	(0.260 *B*) 1.257*D*
31. 26	8	36602. 32		(0.000) 0.930
30. 98	2	36606. 11		
30. 74	50	36609. 30	$c\ ^3P_2$—646(3) $c\ ^3F_4$—596(5)	(0.000*W*) 1.151*B*
30. 25	1	36615. 86	$b\ ^3F_3$—511(2)	
29. 93	3	36620. 19	$c\ ^3P_1$—628(1)	(0.424) 0.911, 1.340
29. 37	1	36627. 69	$b\ ^3P_2$—551(3)	
28. 79	15	36635. 41		(0.000) 1.176
28. 32	2	36641. 78	$a\ ^3H_4$—524(4)	
27. 44	75	36653. 62	$a\ ^5F_3$—392(3)	(0.309) 1.198
26. 85	4	36661. 47		
26. 41	2	36667. 42		
26. 01	15	36672. 80	$b\ ^3H_4$—611(4)	(0.204) 1.038*D*
25. 44	75	36680. 49		(0.000W) 1.032*D*
24. 09	12	36698. 69	$a\ ^3D_1$—513(1)	(0.207) 0.841, 1.000
23. 85	40	36701. 83	$b\ ^3H_5$—621(4)	(0.00) 0.98
23. 67	1	36704. 30	$c\ ^3F_3$—603(3)	
23. 49	2	36706. 70		(0.000) 0.845
22. 20	1	36724. 09		
21. 82	3	36729. 22	$a\ ^3H_4$—525(3)	
21. 16	1	36738. 12		
20. 05	10	36753. 13		(0.113) 1.043
19. 89	2	36755. 26		
19. 28	1	36763. 60		

TABLE 1. *Wavelengths, term combinations, and Zeeman effects of* Ta II—Continued

Wave length λair	Intensity and notes	Wave number	Term combination	Zeeman pattern
2718. 95	8	36768. 01	$d\ ^3F_4$—682(3)	
17. 26	2	36790. 94	$b\ ^3H_5$—622(5) $a\ ^5P_2$—486(2)	
16. 49	25	36801. 36	$a\ ^5P_1$—475(2) $b\ ^3P_2$—464(2)	(**0.000,** 0.988*w*) **0.213,** 1.276, 2.357*w*
15. 31	10	36817. 30	$a\ ^3G_4$—495(5)	(0.000) 1.229*w*
15. 14	3	36819. 56	$b\ ^1G_4$—622(5)	(0.000) 1.017
14. 79	3	36824. 38	$a\ ^1F_3$—616(3)	
14. 67	12	36826. 02	$c\ ^3P_1$—630(2)	(0.000) 1.28
14. 28	8	36831. 20	$a\ ^3G_4$—495(3) $a\ ^5D_2$—513(1)	(**0.000,** 0.426) 1.064, 1.444, **1.879**
13. 44	1	36842. 64		(0.000*W*) 1.115*w*
12. 59	3	36854. 24	$a\ ^5D_3$—525(3)	(0.000*W*) 1.451
11. 71	2	36866. 12		(0.000) 1.072
10. 73	40	36879. 55	$a\ ^1H_5$—611(4)	(0.000) 0.947
10. 12	12	36887. 81	$b\ ^3F_4$—553(4)	(0.00) 1.19
09. 27	125	36899. 34	$a\ ^3G_3$—486(2) $a\ ^3F_4$—466(4)	(**0.000,** 0.228) **0.452,** 0.702, 0.935 (0.474) 1.215
08. 73	1	36906. 72	$a\ ^3D_1$—515(2)	
05. 83	4	36946. 31	$b\ ^1D_2$—602(3) $b\ ^3G_5$—682(5)	(0.000*D*) 1.267*w*
05. 32	12	36953. 22	$b\ ^3F_3$—515(2)	(**0.000,** 0.305, 0.620) **0.352,** 0.676, 0.985, 1.295, 1.608
03. 99	15	36971. 45	$a\ ^1D_2$—505(1)	(**0.000,** 0.257) **0.847,** 1.130, 1.398
03. 69	15	36975. 50	$a\ ^5D_4$—542(4)	(0.000*W*) 1.134*w*
02. 78	35	36987. 90	$a\ ^5F_1$—369(1)	(0.658) 0.000, 0.685
02. 66	25	36989. 64	$a\ ^3D_3$—555(3)	(0.300*w*) 1.396*D*
02. 08	10	36997. 61	$a\ ^3D_3$—555(2)	(**0.000,** 0.274, 0.570) 1.019, 1.308, . . ., . . .
01. 07	25	37011. 36	$b\ ^3F_4$—555(5)	(**0.000,** 0.171, 0.353, 0.528, 0.710) **0.359,** 0.522, 0.685, 0.869, 1.057, 1.230, 1.400, 1.603
2699. 90	2	37027. 45	$b\ ^3P_2$—555(1)	(0.000) 1.473
99. 69	4	37030. 33	$b\ ^1D_2$—603(3)	(0.000) 1.180
98. 80	15	37042. 48	$b\ ^3P_2$—555(3)	(0.000) 1.396
98. 52	20	37046. 34		(0.000) 1.259
98. 30	10	37049. 31	$b\ ^3H_5$—624(4) $b\ ^3F_4$—555(3)	(0.000) 1.044
98. 01	3	37053. 33	$a\ ^3F_2$—402(2)	(0.399, . . .) 0.749, 1.155
97. 84	2	37055. 70	$a\ ^3G_5$—498(5) $a\ ^5D_1$—505(1)	(0.000) 1.284
97. 39	10	37061. 88		
96. 81	5	37069. 79	$b\ ^3G_4$—652(4)	
96. 52	1	37073. 79	$a\ ^1P_1$—604(1)	
96. 22	8	37077. 93	$b\ ^1G_4$—624(4)	(0.000) 0.512
95. 70	12	37085. 04	$a\ ^3F_4$—468(3)	(0.000) 1.242
95. 54	2	37087. 31	$a\ ^5P_2$—489(3) $a\ ^5P_1$—478(0)	(**0.000,** 0.143, 0.305) **0.968,** 1.124, 1.289 (0.000) 1.157, 1.246*w*
94. 52	100	37101. 35	$a\ ^5F_3$—397(4)	(0.000*w*) 1.190*w*
92. 83	20	37124. 66	$a\ ^3F_2$—403(1)	(**0.000,** 0.489) **0.263,** 0.740, 1.230
91. 80	25	37138. 78	$a\ ^5F_4$—415(3)	(0.000*w*) 1.729*B*
90. 79	1	37152. 78		
90. 49	2	37156. 89	$a\ ^5P_3$—495(2)	(0.000) 1.585
90. 36	3	37158. 66	$b\ ^3P_1$—545(2)	(0.000*w*) 0.891
90. 20	5	37160. 91		(0.068) 0.992
89. 81	1	37166. 37		
89. 27	50	37173. 80	$a\ ^3F_3$—440(4)	(0.000*w*) 1.175*w*
88. 75	1	37180. 99	$a\ ^3G_4$—498(5)	
88. 46	3	37184. 95		(**0.000,** 0.445) 0.676, 1.101, **1.559**
87. 46	4	37198. 76		
87. 00	2	37205. 18	$a\ ^5P_2$—490(2)	(0.222) 1.333
86. 59	2	37210. 87	$a\ ^5P_3$—496(3)	

TABLE 1. *Wavelengths, term combinations, and Zeeman effects of* Ta II—Continued

Wave length λair	Intensity and notes	Wave number	Term combination	Zeeman pattern
2685. 16	150	37230. 64	$a\ ^3P_0$—413(1) $a\ ^5F_1$—372(2)	(0.000) 1.890 (**0.000,** 0.613w) 0.000w, 0.600w **1.212**w
84. 04	1	37246. 22	$a\ ^1F_3$—621(4)	
83. 77	4	37249. 91	$c\ ^3F_3$—608(2)	(0.000w) 1.028
82. 96	4	37261. 26	$b\ ^3H_4$—616(3)	(0.000w) 1.094w
81. 25	25	37284. 91	$a\ ^5D_3$—530(2)	(0.000) 1.464
80. 66	75	37293. 17	$a\ ^5F_4$—417(5)	(0.000w) 0.815A
80. 06	75	37301. 59	$a\ ^3P_2$—429(3)	(**0.000,** 0.233, 0.461) **0.661,** 0.902, 1.126, 1.361, 1.586
79. 77	2	37305. 52	$a\ ^3D_3$—558(2)	
79. 26	5	37312. 60	$c\ ^3F_2$—602(3)	
78. 81	50	37318. 94	$a\ ^3H_5$—555(5)	(0.000) 1.086
76. 48	20	37351. 44	$a\ ^5P_1$—480(0)	(0.000) 2.394w
75. 90	100	37359. 45	$a\ ^5F_4$—417(4)	(0.292w) 1.324D
75. 73	50	37361. 92	$a\ ^1H_5$—615(6)	(0.000) 1.484D
75. 54	3	37364. 53		
74. 85	3	37374. 15		
74. 19	30	37383. 45	$a\ ^3H_4$—532(5)	(0.000w) 1.158A
73. 16	2	37397. 74		
72. 50	50	37406. 97	$a\ ^3P_2$—430(2)	(0.266, **0.563**) 0.563, 0.787, **1.056, 1.330,** 1.625, . . .
71. 76	2	37417. 44	$a\ ^5D_4$—546(3)	
71. 40	5	37422. 38	$a\ ^3F_4$—471(3)	
71. 00	5	37427. 97	$a\ ^3F_3$—442(2)	(**0.000,** 0.173, 0.349) **0.750,** 0.921, 1.103, 1.282
69. 57	40	37448. 07	$a\ ^1F_3$—623(2)	(0.000) 0.953
68. 40	5	37464. 52	$a\ ^3D_3$—560(2)	(0.000w) 1.124
67. 40	5	37478. 53	$b\ ^3F_2$—471(3)	(0.000) 1.148
67. 29	5	37480. 15	$a\ ^3D_2$—546(3)	(**0.000,** 0.265, 0.604) **0.352,** 0.648, 0.950
67. 00	12	37484. 17	$a\ ^5F_2$—385(2)	(0.000) 1.000
66. 41	30	37492. 40	$a\ ^3H_4$—533(4)	(0.000w) 1.076D
65. 60	50	37503. 81	$a\ ^5F_2$—385(1)	(**0.000,** 0.520) 0.480, 0.998, **1.520**
64. 25	75	37522. 91	$a\ ^3H_6$—555(5)	(0.000W) 1.743B
63. 88	25	37528. 00	$a\ ^3D_1$—521(1)	(0.758) 0.845, 1.620
63. 41	1	37534. 73	$a\ ^3F_4$—472(4)	
63. 07	10	37539. 42		
63. 00	20	37540. 47	$b\ ^3F_3$—521(3)	(0.000) 1.048
62. 96	8	37541. 03		(0.000w) 1.048w
62. 27	8	37550. 79	$c\ ^3F_2$—604(1)	(0.000) 0.714
60. 81	3	37571. 36		
59. 40	40	37591. 23	$a\ ^5F_3$—402(2)	(0.000w) 1.320A
58. 86	75	37598. 99	$a\ ^3F_3$—444(3)	(0.137, 0.277, **0.414**) 0.650, 0.780, **0.923, 1.086,** 1.247, 1.370
58. 14	50	37609. 07	$a\ ^3G_4$—503(3)	(**0.000,** 0.246, 0.511, 0.831) **0.138,** 0.542, 0.767, 1.015, 1.274, . . .
57. 76	5	37614. 42	$a\ ^3H_4$—534(3)	(0.000D) 0.972w
56. 16	20	37637. 11	$a\ ^1D_2$—511(2)	(0.245, **0.498**) 0.848, **1.107, 1.358,** 1.594
55. 34	25	37648. 76	$b\ ^3F_4$—561(4)	(0.000D) 1.271w
54. 88	6	37655. 34		(**0.000,** 0.338) **0.551,** 0.874, 1.208
54. 51	3	37660. 47	$a\ ^5D_2$—521(1)	
54. 34	3	37662. 91		
53. 45	6	37675. 63	$b\ ^3D_3$—682(3)	
52. 46	3	37689. 63		
51. 23	125	37707. 17	$a\ ^5F_4$—421(4)	(0.280B) 1.330D
50. 52	4	37717. 27	$a\ ^5P_2$—495(2)	(0.160, **0.303**) 1.305, **1.453, 1.617,** 1.788
48. 54	5	37745. 48		
47. 10	3	37766. 00	$a\ ^1D_2$—513(1)	
46. 90	20	37768. 78	$a\ ^3G_3$—495(3)	(. . ., 0.391, 0.787, **1.246**) 0.070, 0.508, **0.894, 1.316,** . . .
46. 74	20	37771. 02	$a\ ^5P_2$—496(3)	(**0.000,** 0.457, 0.840) **0.161,** 0.678, . . .
45. 91	15	37782. 96		(0.270) 1.059
45. 09	30	37794. 61	$a\ ^3F_3$—446(4)	(**0.000,** 0.196, 0.383, 0.577) 0.739, 0.911, 1.080, 1.252, 1.475, 1.682, **1.856**
44. 58	100	37801. 87	$a\ ^3G_4$—505(5)	(0.000W) 1.168A
43. 43	15	37818. 37	$a\ ^5F_5$—440(4)	(**0.000,** 0.260, 0.535, 0.779) 1.175, 1.379, 1.645, 1.931, 2.158, **2.428**
43. 03	12	37824. 12	$b\ ^3F_2$—475(2) $b\ ^3G_3$—646(3)	(0.247, **0.468**) 0.807, **1.058, 1.285,** 1.524
42. 91	2	37825. 78	$a\ ^3G_3$—495(2)	
42. 70	5	37828. 79		(0.000) 0.852

TABLE 1. *Wavelengths, term combinations, and Zeeman effects of* Ta II—Continued

Wave length λair	Intensity and notes	Wave number	Term combination	Zeeman pattern
2642.06	3	37838.04		
41.16	8	37850.85	*b* $^3P_2$—563(3) *a* $^5D_1$—513(1)	(0.463) 1.048, 1.508
40.61	12	37858.82		(0.000) 1.513
40.13	2	37865.64	*c* $^1D_2$—708(2)	(0.336, **0.622**) 0.412, **0.716, 1.017,** 1.331
39.19	40	37879.16	*a* $^3G_3$—496(3)	
38.68	25	37886.45	*a* $^3P_2$—435(3)	(**0.000,** 0.246, 0.521) **0.546,** 0.827, 1.073, 1.315
37.94	30	37897.05	*a* $^5D_4$—551(3)	(0.000*W*) 1.026*A*
37.34	3	37905.72	*b* $^3F_2$—475(1)	(**0.000,** 0.454) . . .?
36.90	8	37912.09	*b* $^3F_3$—524(4)	(0.00) 1.49
36.67	3	37915.38	*a* $^1G_4$—521(3)	
36.46	2	37918.42	*a* $^5D_3$—536(2)	
36.30	2	37920.66		
35.59	200	37930.92	*a* $^5F_2$—389(3)	(0.000*W*) 0.979*w*
34.25	3	37950.20	*b* $^3P_2$—564(3)	(**0.000,** 0.254) **1.195,** 1.428
33.78	75	37956.94	*a* $^3H_5$—561(4) *b* $^3F_4$—564(5)	(**0.000,** 0.249, 0.434, 0.661, 0.846, 1.002) **0.316,** 0.511, 0.710, 0.856, 1.030
33.29	10	37964.02		(0.000) 1.247
32.60	2	37973.97	*a* $^1D_2$—515(2)	(0.192, **0.385**) 0.922, **1.116, 1.299,** 1.528
32.27	25	37978.76	*a* $^1H_5$—622(5)	(0.280) 1.066
30.84	12	37999.29	*b* $^3F_3$—525(3)	(0.451, 0.720, **1.451**) 0.633, **1.016, 1.414,** 1.850, 2.278
30.53	25	38003.88	*a* $^3F_3$—448(3)	(0.148, 0.354, **0.540**) 0.714, 0.906, **1.084, 1.246,** 1.426, 1.602
30.18	3	38008.85		
29.99	2	38011.62	*a* $^5P_2$—498(1)	(**0.000,** 0.582) **0.850,** 1.401
29.21	1	38022.96	*c* $^3F_4$—611(4)	
28.84	50	38028.28	*b* $^3F_4$—565(5)	(**0.000,** 0.253, 0.495, 0.762, 1.049) **0.147,** 0.481, 0.733, 0.968, 1.220, 1.465, 1.758, 2.020
26.74	3	38058.67	*a* $^5D_1$—515(2)	
26.44	2	38063.00	*a* $^5P_1$—487(1)	
25.70	3	38073.80	*c* $^3F_3$—616(3)	
25.33	6	38079.06	*a* $^3F_4$—478(3)	(0.000) 1.314
21.49	5	38134.92	*b* $^3F_2$—478(3)	(**0.000,** 0.149, 0.285) 1.213, 1.360, **1.479**
20.45	5	38150.06	*a* $^5D_4$—553(4)	(0.307, 0.476, **0.630**) 0.558, 0.691, 0.849, **1.004, 1.174,** 1.351, 1.534, . . .
19.04	2	38170.54	*a* $^3G_3$—499(4)	
18.98	20	38171.47		(**0.000,** 0.283, 0.575, 0.890, 1.169) 1.209, 1.476, 1.759, 2.067, **2.362**
18.87	2	38173.02		(0.000*w*) 1.091*A*
18.62	1	38176.59	*b* $^3P_1$—555(2)	(0.000*w*) 0.996*B*
17.65	8	38190.86	*a* $^1F_3$—630(2)	
17.22	30	38197.14	*a* $^3D_1$—528(1)	(0.000*w*) 0.875
16.12	2	38213.21		
15.46	3	38222.80	*a* $^3P_1$—435(1)	(0.000) 0.884
14.94	25	38230.35		
13.50	1	38251.45		(0.000*w*) 1.162
12.62	50	38264.39	*a* $^5F_2$—392(3)	(0.000*W*) 1.423*B*
11.99	20	38273.56	*a* $^5D_4$—555(5)	(0.000*w*) 0.782*w*
10.92	12	38289.27	*b* $^3H_5$—637(5)	(0.237) 1.076*w*
09.37	6	38311.94	*a* $^5D_4$—555(3)	(**0.000,** 0.269, 0.512, 0.804) **0.462,** 0.687, 0.924, 1.182, 1.431. 1.696
08.18	3	38329.52	*a* $^5D_2$—528(1)	(0.000) 1.098
07.84	100	38334.48		(0.000 *W*) 1.241*w*
06.43	100	38355.20	*a* $^3H_4$—542(4)	(0.000) 1.144
06.12	30	38359.73	*a* $^1D_2$—555(1)	(**0.000,** 0.228) **0.975,** 1.173, 1.392
05.58	1	38367.72	*a* $^5P_1$—490(2)	
05.11	10	38374.63	*a* $^3D_2$—555(3) *a* $^3F_2$—415(3)	
04.74	4	38380.11	*b* $^3G_4$—665(4)	
04.52	20	38383.29	*a* $^3D_2$—555(2)	(**0.000,** 0.615) 0.853, 1.464, **2.080**
03.49	125	38398.48	*a* $^5F_5$—445(5)	(0.442) 1.330*D*
02.96	15	38406.37	*b* $^3H_5$—638(4) *b* $^3G_3$—652(4)	(0.000*w*) 0.848*A*
01.68	3	38425.15		(**0.000,** 0.168, 0.358) **0.877,** 1.055

TABLE 1. *Wavelengths, term combinations, and Zeeman effects of* Ta II—Continued

Wave length λair	Intensity and notes	Wave number	Term combination	Zeeman pattern
2601.04	20	38434.72	*b* $^1G_4$—638(4)	(0.00) 0.99
00.73	20	38439.26	*a* $^5P_2$—503(3) *a* $^5F_5$—446(4)	(0.000*D*) 1.839*WB*
2598.72	1	38468.97	*a* $^3H_6$—564(5)	
98.19	75	38476.80	*a* $^3H_5$—566(6)	(0.000) 1.127
97.80	5	38482.61		
97.75	10	38483.35		(**0.000,** 0.128) **1.160,** 1.292
97.71	2	38484.00	*b* $^3P_1$—558(2)	(**0.000,** 0.182) 1.349, **1.525**
96.99	2	38494.65		(0.000) 1.018
96.46	75	38502.53	*a* $^5F_3$—411(2)	(0.000*w*) 1.325
96.14	10	38507.18	*a* $^3D_3$—570(3)	(0.00) 1.39
95.58	50	38515.46	*a* $^5F_1$—385(2)	(**0.000***w*, 0.963) 0.000*w*, 0.957, **1.950**
94.43	10	38532.53	*b* $^3F_2$—482(2)	(0.362, **0.756**) 0.689, **1.089, 1.461,** 1.800
94.25	20	38535.28	*a* $^5F_1$—385(1)	(0.000) 0.455*A*
93.95	4	38539.78	*a* $^3H_6$—565(5)	
93.68	50	38543.67	*a* $^5F_4$—429(3)	(**0.000,** 0.212, 0.448, 0.677) 0.779, 0.999, 1.224, 1.446, 1.650, 1.888, **2.111**
93.45	15	38547.12	*a* $^3G_3$—503(3)	(0.391, 0.763, **1.135**) 0.509, **0.891, 1.280,** 1.636
92.54	50	38560.62	*a* $^1D_2$—521(3)	(0.000) 1.079
92.13	2	38566.84	*a* $^3H_5$—567(4)	(0.000*w*) 0.741*w*
91.06	2	38582.69		(0.000) 1.353
90.20	20	38595.53	*a* $^1D_2$—521(1)	(**0.000,** 0.520) **0.616,** 1.110, 1.613
89.81	25	38601.27	*a* $^3P_2$—442(2)	(0.169) 1.361
89.12	3	38611.66	*c* $^3F_4$—616(3)	
88.88	15	38615.24	*a* $^3F_3$—454(2)	(0.000*w*) 0.958
88.08	4	38627.16		
87.35	10	38638.05	*a* $^5P_3$—510(3)	(0.452, 0.885, **1.353**) 0.286, 0.707, **1.143, 1.605,** 2.042, 2.518
86.98	10	38643.52	*b* $^3P_1$—560(2)	(0.000*w*) 0.891*w*
86.41	10	38652.07		
85.47	2	38666.18	*b* $^3G_3$—654(3)	
84.49	75	38680.76	*a* $^5D_1$—521(1) *a* $^3H_6$—566(6)	(0.342) 1.168*W D*
84.02	75	38687.84		(0.000*w*) 1.195*w*
82.52	10	38710.21	*a* $^3D_2$—558(1)	(**0.000,** 0.211) **1.007,** 1.219, 1.438
81.61	15	38723.90	*a* $^3F_4$—484(4)	(0.156) 1.232
81.50	4	38725.61	*a* $^5D_0$—513(1)	(0.000) 1.047
80.60	25	38739.16		(**0.000,** 0.230, 0.458, 0.688, 0.918) **0.218,** 0.454, 0.682, 0.912, 1.144, 1.366, 1.603, . . .
79.06	40	38762.26	*a* $^5P_3$—511(2) *b* $^3F_3$—533(4)	(0.000*W*) 1.323*WB*
78.25	40	38774.44	*a* $^3G_4$—514(4)	(0.346*W*) 1.070*WD*
77.37	100	38787.63		(0.000*w*) 1.407
76.75	8	38796.98	*a* $^3H_4$—546(3)	
76.44	25	38801.60	*a* $^3H_5$—569(4)	(0.000*w*) 1.025
76.06	8	38807.43	*a* $^5D_3$—545(2)	(**0.000,** 0.433, 0.868) 1.023, 1.460, **1.889**
75.23	12	38819.86		(0.000*W*) 1.403*w*
74.64	3	38828.78	*b* $^3G_3$—656(3)	
74.09	1	38837.06		
73.70	2	38842.95	*c* $^3F_3$—624(4)	
73.20	8	38850.44	*a* $^3D_2$—560(2)	(0.205, **0.440**) 0.773, **1.008, 1.250,** 1.467
71.52	20	38875.86	*a* $^3P_1$—442(1)	(1.308) 0.255, 1.554
71.28	3	38879.49	*a* $^5P_1$—495(2)	
70.94	3	38884.63	*b* $^3F_3$—534(3)	
70.82	3	38886.44	*c* $^3P_2$—669(1)	
70.60	6	38889.78	*a* $^1P_1$—622(1)	
69.99	2	38898.97	*b* $^3H_6$—649(6)	(0.000*w*) 1.224*A*
69.13	40	38912.07	*a* $^1P_1$—623(2) *a* $^5F_3$—415(3)	(0.133) 1.213*w*
68.04	15	38928.49	*a* $^3P_1$—442(2)	(**0.000,** 0.301) **0.936,** 1.245, 1.538
66.52	1	38951.53	*a* $^1F_3$—638(4)	
65.11	4	38973.06	*a* $^3F_2$—421(2)	(**0.000,** 0.168) **0.670,** 0.826

TABLE 1. *Wavelengths, term combinations, and Zeeman effects of* Ta II—Continued

Wave length λair	Intensity and notes	Wave number	Term combination	Zeeman pattern
2564.91	5	38976.09	*b* $^3F_2$—486(2)	(0.160) 1.104
62.63	6	39010.75		
62.22	15	39017.00	*a* $^3D_1$—536(2)	(**0.000,** 0.484) 0.892, 1.344, **1.834**
61.82	1	39023.05	*b* $^1D_2$—623(2)	
61.16	10	39033.14	*c* $^3F_4$—621(4)	(0.121) 1.056
60.44	5	39044.05	*a* $^5P_3$—514(4)	(**0.000,** 0.488) **0.374,** 0.881
60.16	4	39048.38	*a* $^3G_4$—517(5)	(0.225) 1.182*W*
59.87	20	39052.84	*b* $^3H_4$—634(4)	(0.000) 0.948
59.15	3	39063.82	*b* $^3F_3$—536(2)	(**0.000,** 0.351, 0.723) **0.295,** 0.662, 1.013
58.34	15	39076.10		(0.000) 1.181
57.71	50	39085.81	*b* $^3F_2$—487(1)	(**0.000,** 0.303) 0.745, 1.040, **1.389**
57.26	4	39092.64		(0.000) 0.850
56.88	2	39098.38	*a* $^5P_3$—515(2)	(**0.000,** 0.306, 0.624) 1.287, 1.578, 1.903, **2.248**
56.51	30	39104.10	*a* $^3P_1$—444(0)	(0.000) 1.547
55.53	4	39119.15	*a* $^3D_1$—537(1)	(0.404) 0.846, 1.261
55.34	4	39122.08	*c* $^3F_4$—622(5)	
54.90	30	39128.68	*a* $^5F_4$—435(3)	(**0.000,** 0.256, 0.516) 0.579, 0.836, 1.098, 1.350, 1.560, 1.914, **2.203**
54.63	50	39132.94	*a* $^5F_3$—417(4)	(0.000) 1.285
54.02	2	39142.14		(**0.000,** 0.176) 1.263, **1.406**
53.52	12	39149.85	*a* $^5D_2$—536(2)	(0.243) 1.412*D*
53.19	40	39154.97		(0.000*w*) 0.940*D*
52.61	3	39163.81		
52.00	1	39173.20	*a* $^5P_1$—498(1)	
51.73	25	39177.28	*a* $^3P_2$—448(3)	(0.000*w*) 1.139
50.36	5	39198.42	*a* $^5P_2$—510(3)	(**0.000,** 0.257) **0.619,** 0.894, 1.155, 1.414
50.11	7	39202.25	*a* $^5F_2$—402(2)	(0.143, **0.292**) 0.856, **1.010, 1.147,** 1.311
49.20	10	39216.16	*a* $^3F_4$—489(3)	(0.000) 1.148
48.97	1	39219.78	*a* $^5D_4$—564(5)	(0.000) 1.165
47.81	1	39237.66	*a* $^3D_3$—577(2)	
47.66	5	39239.96	*b* $^3P_0$—555(1)	(0.000) 1.406
46.32	6	39260.58	*b* $^1G_4$—534(3)	(**0.000,** 0.224) **0.907,** 1.138
45.68	1	39270.45	*b* $^3H_4$—637(5)	
45.50	75	39273.25	*a* $^5F_2$—403(1)	(**0.000,** 0.251) **0.741,** 1.003, 1.252
44.91	3	39282.36	*a* $^3D_2$—564(3)	
44.37	75	39290.60	*a* $^5D_4$—565(5)	(**0.000,** 0.209, 0.391, 0.628, 0.873) **0.169,** 0.345, 0.558, 0.786, 0.937, 1.158
43.33	2	39306.76	*a* $^3G_3$—510(3)	(0.749, 0.999, **1.269**) 0.922, 1.176, **1.430, 1.680,** 1.925, 2.162
43.18	3	39308.98	*a* $^3F_4$—490(5)	
42.74	6	39315.93		
42.36	25	39321.76	*a* $^5P_2$—511(2)	(0.180*w*) 1.336*w*
40.60	10	39348.99	*a* $^5D_1$—528(1)	(0.596) 0.914, 1.501
39.37	1	39368.01	*c* $^3F_2$—622(1)	(0.000) 0.747
38.75	2	39377.65		
38.56	2	39380.50	*c* $^3F_4$—624(4)	(0.000*W*) 1.087*w*
37.96	75	39389.95	*b* $^3F_2$—490(2)	(0.240, **0.546**) 0.761, **1.043, 1.311,** 1.576
37.16	6	39402.34	*a* $^5D_3$—551(3)	(0.176, 0.408, **0.644**) 0.821, 1.025, **1.254, 1.477,** 1.703, 1.928
36.30	20	39415.64	*a* $^3G_4$—521(3)	(0.000*W*) 0.855
35.36	4	39430.20	*a* $^3G_3$—511(2)	(**0.000,** 0.438, 0.868) **0.000***w*, 0.511, 0.941
34.73	2	39440.11	*c* $^3F_3$—630(2)	
34.22	1	39448.04	*a* $^1P_1$—628(1)	
34.04	25	39450.79	*a* $^1D_2$—530(2) *a* $^5P_2$—513(1)	(**0.000,** 0.390) 1.048, 1.404, **1.818**
33.76	2	39455.23	*a* $^3F_3$—462(4)	(**0.000,** 0.200) 1.366, **1.545**
32.37	20	39476.90	*a* $^1H_5$—637(5)	(0.433*w*) 1.086*W*
32.13	100	39480.58	*a* $^5F_3$—421(4)	(0.000) 1.293
31.71	2	39487.13	*a* $^3D_3$—580(4)	
31.10	3	39496.69		(0.000*w*) 1.027*A*
30.18	6	39511.03	*a* $^5F_3$—421(2)	(0.000*w*) 1.259*A*
29.50	12	39521.62	*a* $^5D_4$—567(4)	(0.101) 1.189
29.16	6	39526.86		(0.214) 1.106
28.62	10	39535.39	*a* $^5D_1$—530(2)	(0.000) 1.447
27.85	1	39547.42	*b* $^3F_4$—580(4)	

TABLE 1. *Wavelengths, term combinations, and Zeeman effects of* Ta II—Continued

Wave length λair	Intensity and notes	Wave number	Term combination	Zeeman pattern
2527.34	30	39555.46	$a\ ^3F_3$—463(2)	(**0.000,** 0.251) **0.589,** 0.846, 1.032
27.06	2	39559.80	$b\ ^1D_2$—628(1)	(**0.000,** 0.206) . . . ?
26.03	50	39575.91	$a\ ^3P_2$—452(1)	(0.000*w*) 1.212*A*
25.50	6	39584.25		
25.11	10	39590.33	$b\ ^3P_0$— 558(1)	(0.000) 1.414
24.84	8	39594.48	$a\ ^1H_5$—638(4)	
23.90	5	39609.24		
23.56	4	39614.63		(**0.000,** 0.372, 0.735, 1.122) 0.288, 0.649, 1.056, 1.444
22.88	3	39625.30	$b\ ^3F_3$—542(4)	(0.000*w*) 2.163*w*
21.05	25	39654.10	$a\ ^3H_4$—555(5)	(0.000*w*) 0.943*w*
20.75	2	39658.83	$a\ ^5P_2$—515(2)	
20.08	10	39669.31		
19.04	15	39685.78	$a\ ^5P_3$—521(3)	
18.88	1	39688.24		
18.64	5	39692.06	$a\ ^3H_4$—555(3)	
18.33	2	39696.92		
18.16	1	39699.65		
17.58	12	39708.77	$d\ ^3F_4$—712(5)	(0.000) 1.101
17.34	1	39712.52	$a\ ^3G_3$—514(4)	
17.21	4	39714.55		(0.000) 1.216
16.78	3	39721.43	$a\ ^3D_3$—582(2)	(**0.000,** 0.300) 0.955, **1.313**
15.58	5	39740.27	$a\ ^1D_2$—533(2)	(0.249, **0.519**) 0.882, **1.131, 1.377,** 1.639
14.55	12	39756.53	$a\ ^5D_4$—569(4)	(0.173*w*) 1.147*w*
13.89	30	39766.97	$a\ ^3G_3$—515(2)	(**0.000,** 0.381, 0.788) **0.160,** 0.530, 0.907, 1.293
13.43	2	39774.29	$b\ ^3P_2$—582(2)	
13.10	15	39779.52	$a\ ^3F_2$—429(3)	(**0.000,** 0.368, 0.741) 0.368, 0.754, 1.127, 1.491, **1.863**
12.83	5	39783.76	$a\ ^1F_3$—646(3)	
12.60	2	39787.48	$a\ ^3G_4$—524(4)	
12.49	12	39789.17	$a\ ^3P_2$—454(2)	(0.340*w*) 0.910*w*
11.64	50	39802.65		(0.00) 1.49
11.10	2	39811.12		
10.90	3	39814.43	$a\ ^3F_3$—466(4)	
10.68	75	39817.89	$a\ ^5P_1$—505(1)	(1.014) 1.335, 2.390W
10.49	3	39820.93	$b\ ^3H_5$—652(4) $b\ ^3P_1$—571(1)	
09.94	15	39829.56	$a\ ^5D_4$—570(3)	
08.92	15	39845.76	$b\ ^3F_2$—495(3)	(**0.000,** 0.252, 0.524) 0.809, 1.052, 1.309, 1.563, **1.822**
08.35	4	39854.84	$a\ ^3H_5$—580(4)	(0.000*w*) 1.209*w*
07.69	15	39865.28	$c\ ^3F_3$—634(4)	(0.174) 1.027
07.08	20	39875.09	$a\ ^3G_4$—525(3)	(**0.000,** 0.390, 0.782) **0.226,** 0.618, 1.010
06.45	10	39884.99	$a\ ^3F_2$— 430(2)	(0.322, **0.636**) 0.420, **0.741, 1.041,** 1.346
06.13	2	39890.10		
05.98	2	39892.47	$a\ ^3D_2$—570(3)	
05.48	2	39900.51	$a\ ^3F_4$—496(3)	(**0.000,** 0.188, 0.388) . . ., 1.417, 1.589, **1.787**
05.32	15	39903.01	$a\ ^3P_1$—452(1)	(0.116) 1.493
05.13	2	39906.06	$a\ ^1D_2$—534(3) $a\ ^3D_1$—545(2)	(**0.000,** 0.181) 0.844, 1.016, **1.201**
03.88	3	39925.97	$c\ ^3F_2$—628(1)	(**0.000,** 0.203) **0.495,** 0.707, 0.906
03.01	50	39939.85		(0.000) 1.060
02.21	2	39952.66	$b\ ^3F_3$—545(2)	(0.000) 0.968
02.11	2	39954.23		
01.99	50	39956.14	$b\ ^3F_2$—496(3)	(0.000) 1.008
00.92	4	39973.20	$b\ ^3G_5$—712(5)	(0.000) 1.109
00.58	1	39978.70		
2499.74	1	39992.14		
99.24	3	40000.11	$a\ ^3F_3$—468(3)	(0.372*B*) 1.117*D*
98.34	12	40014.48	$a\ ^5F_4$—444(3)	(**0.000,** 0.397, 0.796, 1.195) 0.557, 0.949, 1.353, 1.725, 2.111, **2.521**

TABLE 1. *Wavelengths, term combinations, and Zeeman effects of* Ta II—Continued

Wave length λair	Intensity and notes	Wave number	Term combination	Zeeman pattern
2498.04	5	40019.32	$a\ ^3F_3$—468(2)	(0.000) 1.018*w*
97.77	10	40023.65	$a\ ^5F_1$—400(0)	(0.118) 0.000*w*, 1.018
97.51	2	40027.81	$a\ ^3D_2$—571(1)	
97.15	2	40033.58		(0.090, **0.276**) . . . ?
96.24	10	40048.18	$b\ ^3G_4$—682(5)	(0.000) 1.173
95.03	3	40067.60	$b\ ^3F_3$—546(3)	(0.178*B*) 0.965*w*
94.33	8	40078.84	$b\ ^3F_4$—585(5)	(0.000*D*) 0.761*A*
94.17	6	40081.41	$a\ ^3P_0$—442(1)	(0.000) 0.262
93.97	7	40084.62	$a\ ^1D_2$—536(2)	(0.224, **0.477**) 0.856, **1.091, 1.329,** 1.562
93.56	2	40091.22		
93.14	2	40097.97		(0.00) 1.20
92.51	4	40108.10	$a\ ^5F_5$—462(5)	(0.427, 0.661, **0.894**) 0.471, 0.617, 0.850, 1.026, **1.207, 1.383,** 1.590, 1.810 . . .
92.16	12	40113.74	$a\ ^5F_2$—411(2)	(0.295*B*) 1.093*D*
92.01	12	40116.15	$a\ ^3P_1$—454(2)	(**0.000,** 0.397) **0.776,** 1.157, 1.542
90.74	2	40136.60		
90.27	20	40144.18	$a\ ^5P_3$—525(3)	(0.406*w*) 1.165*D*
88.71	20	40169.40	$a\ ^5F_4$—445(5) $a\ ^5D_1$—536(2)	(0.000*W*) 1.049*A*
87.65	15	40186.49	$a\ ^1D_2$—537(1)	(0.000*W*) 0.997*A*
87.34	8	40191.38	$a\ ^3F_4$—499(4)	(0.000) 1.592
87.26	3	40192.76		
87.04	8	40196.34	$b\ ^3F_2$—498(1)	(0.000) 1.049
86.81	5	40199.98	$c\ ^3F_3$—638(4)	(0.000) 1.151
86.18	3	40210.21	$a\ ^5F_4$—446(4)	(0.268*B*) 1.282*D*
85.37	4	40223.38	$a\ ^5D_0$—528(1)	
84.75	10	40233.32	$a\ ^5F_1$—402(2)	(**0.000,** 1.170) 1.097, 2.301
83.48	3	40253.89		(**0.000,** 0.228) 1.580, 1.775, **1.992**
82.60	30	40268.26	$b\ ^3D_3$—708(2)	(0.000*W*) 1.621*B*
82.39	3	40271.60		
81.87	30	40280.04	$a\ ^5P_2$—521(1)	(**0.000,** 0.231) **1.142,** 1.373, 1.604
81.15	3	40291.76	$a\ ^3H_4$—561(4)	(**0.000,** 0.476, 0.945) 0.987, **1.487**
80.61	2	40300.46		
80.37	3	40304.43	$a\ ^5F_1$—403(1)	(1.206) 0.000*D*, 1.281
79.59	12	40317.07	$a\ ^5F_3$—429(3)	(0.378*B*) 1.202*D*
79.22	10	40323.17	$a\ ^5F_2$—413(1)	(**0.000,** 0.877) **0.118,** 0.986, 1.883
78.45	1	40335.60		
78.33	3	40337.50	$a\ ^3F_3$—471(3)	(0.000) 1.103
77.18	5	40356.28		(0.259) 1.200
76.69	40	40364.26	$a\ ^3F_2$—435(3)	(**0.000,** 0.352, 0.689) 0.379, 0.745, 1.080, 1.414, **1.767**
76.11	3	40373.76	$a\ ^3F_2$—435(1)	
75.32	50	40386.55	$a\ ^3H_5$—585(5)	(0.257*B*) 1.103
74.33	5	40402.74	$c\ ^3F_4$—634(4)	(0.000) 0.872
73.32	15	40419.30	$a\ ^5F_4$—448(3)	(0.000*w*) 1.510*D*
73.12	15	40422.57	$a\ ^5F_3$—430(2)	(**0.000,** 0.186, 0.376) 0.946, 1.166, 1.394, **1.622**
72.33	6	40435.47		
71.90	4	40442.49	$a\ ^1G_4$—546(3)	
71.48	4	40449.36	$a\ ^3F_3$—472(4)	
70.90	50	40458.82	$a\ ^5F_5$—466(4)	(**0.000,** 0.166, 0.377, 0.592, 0.798) 1.024, 1.174, 1.408, 1.594, 1.822, 2.031, **2.214**
70.69	3	40462.29		
69.37	25	40483.96	$a\ ^5P_1$—511(2)	(**0.000,** 1.021) **0.337,** 1.353, 2.376
68.42	40	40499.48	$a\ ^3H_4$—563(3)	(**0.000,** 0.202, 0.436, 0.633) **0.364,** 0.546, 0.766. 0.995, 1.210, 1.417
68.10	2	40504.74		
67.38	15	40516.60	$a\ ^3P_2$—461(1)	(0.000) 1.333
66.99	15	40522.98	$a\ ^5F_2$—415(3)	(**0.000,** 0.200, 0.409) 0.812, 0.998, 1.189, 1.396, **1.621**
66.66	3	40528.46		
65.52	10	40547.20	$b\ ^3F_3$—551(3)	(0.248, 0.520, **0.792**) 0.470, 0.743, **0.995, 1.256,** 1.506, 1.758

TABLE 1. *Wavelengths, term combinations, and Zeeman effects of* Ta II—Continued

Wave length λair	Intensity and notes	Wave number	Term combination	Zeeman pattern
2464.92	3	40557.00		(**0.000,** 0.313, 0.606) 0.716, 1.036, **1.333**
64.24	10	40568.16	*a* $^3F_4$—503(3)	(0.000*w*) 1.122*A*
63.83	50	40574.93	*a* $^5P_3$—530(2)	(0.000*w*) 1.963*B*
62.88	12	40590.60	*a* $^3H_6$—585(5)	(0.000*w*) 1.180
62.34	2	40599.58	*b* $^3H_6$—666(5) *a* $^3H_4$—564(5)	(0.000*w*) 1.119*A*
61.58	7	40612.03	*a* $^5P_1$—513(1)	
61.06	15	40620.68	*c* $^3F_4$—637(5)	(0.000) 2.375*D*
60.91	7	40623.05	*a* $^3D_2$—577(2)	(0.156, **0.352**) 0.859, **1.033, 1.213,** 1.414
60.00	10	40638.13	*a* $^3G_4$—533(4)	(0.278) 1.067*D*
58.19	12	40668.03		(0.000) 0.851
58.02	7	40670.78	*a* $^3H_4$—565(5)	
57.27	8	40683.32	*a* $^1H_5$—649(5) *a* $^3F_3$—475(2)	(**0.000,** 0.213, 0.433) **0.653,** 0.872, 1.081, 1.287, 1.468
56.62	5	40694.05	*b* $^3P_1$—580(1)	(0.000) 1.161
55.97	8	40704.86	*a* $^5P_2$—525(3)	(0.000) 1.391
54.70	15	40725.80	*a* $^3G_3$—524(4)	(**0.000,** 0.193, 0.416, 0.629) 0.700, 0.904, 1.090, 1.328, 1.537, **1.726**
54.50	2	40729.18	*a* $^3P_2$—463(2)	(0.000) 1.274
53.98	15	40737.86	*c* $^3F_4$—638(4)	(0.302*B*) 1.077*D*
52.60	10	40760.78	*a* $^3G_4$—534(3)	(0.000*W*) 0.817*w*
51.64	2	40776.69		(0.000) 1.166
51.51	1	40778.84		
50.99	4	40787.42		
50.23	7	40800.19	*b* $^3F_3$—553(4)	(0.000) 1.080
49.84	8	40806.67		
49.65	2	40809.80	*a* $^5D_4$—580(4)	
49.45	25	40813.18	*a* $^3G_3$—525(3)	(0.483, 0.974, **1.492**) 0.000, 0.411, **0.894, 1.403,** 1.884, 2.365
48.99	10	40820.83	*a* $^5P_1$—515(2)	(0.000) 1.300
47.79	4	40840.74		
47.61	10	40843.88	*a* $^3P_1$—461(1)	(0.199) 1.359, 1.567
47.16	25	40851.24	*b* $^3P_2$—593(2)	(0.286, **0.626**) 0.820, **1.131, 1.444,** 1.764
45.56	20	40878.04		(0.000) 1.226
45.18	1	40884.40		
44.69	50	40892.59		(0.000*w*) 0.000*w*
44.24	4	40900.12	*b* $^3P_1$—582(2)	
44.13	25	40901.93	*a* $^3H_4$—567(4) *a* $^5F_3$—435(3)	(0.357*D*) 1.109*D*
43.78	8	40907.77	*a* $^5P_3$—533(4)	(0.000) 1.723
43.00	7	40920.88		
42.81	7	40924.03	*a* $^3D_1$—555(2)	(**0.000,** 0.225) 0.844, 1.078, **1.300**
42.60	3	40927.53		
41.85	15	40940.08		(0.000*w*) 1.069*A*
41.34	12	40948.73	*a* $^5P_2$—528(1)	(**0.000,** 0.514) 0.914, 1.407, **1.869**
40.53	12	40962.24	*b* $^3F_3$—555(3)	(0.446, 0.868, **1.349**) 0.561, **0.992, 1.418,** 1.842
40.04	12	40970.60	*b* $^3F_3$—555(2)	(0.000) 0.942
39.81	10	40974.43		(0.000*w*) 1.023*A*
39.14	1	40985.55		
38.93	3	40989.09		
38.64	20	40994.03	*a* $^3F_3$—478(3)	(0.334*B*) 1.141*D*
38.21	25	41001.20		
38.04	2	41004.12		
37.75	15	41009.02	*a* $^1H_5$—652(4)	(0.000*w*) 1.038*WA*
36.89	2	41023.40		
36.73	2	41026.20	*a* $^3F_2$—442(1)	
36.51	25	41029.94	*a* $^5P_3$—534(3)	(0.362, 0.719, **1.178**) 0.454, 0.837, **1.217, 1.588,** 1.975, 2.393
36.31	2	41033.24	*c* $^3F_3$—646(3) *a* $^5D_2$—555(1)	
35.59	4	41045.30		(0.000*w*) 0.680*B*
34.93	5	41056.49	*a* $^3P_1$—463(2) *a* $^5D_2$—555(2)	(**0.000,** 0.247) **1.076,** 1.325, . . .

TABLE 1. *Wavelengths, term combinations, and Zeeman effects of* Ta II—Continued

Wave length λair	Intensity and notes	Wave number	Term combination	Zeeman pattern
2434. 82	5	41058. 34	$a\ ^5D_1$—545(2)	(**0.000,** 0.487) **0.552,** 1.029, 1.514
33. 59	20	41079. 13	$a\ ^3F_2$—442(2)	(0.504, **1.019**) 0.245, **0.744, 1.248,** 1.754
33. 03	8	41088. 57	$a\ ^1D_2$—546(3)	(**0 000,** 0.180, 0.356) **0.569,** 0.772, 0.962, 1.179, 1.368
32. 71	75	41093. 92	$a\ ^5F_5$—472(4)	(**0.000,** 0.199, 0.407, 0.640, 0.849) 0.828, 1.022, 1.179, 1.369, 1.572, 1.820, 2.056, **2.278.**
31. 97	12	41106. 49	$a\ ^3D_2$—582(2)	(0.433, **0.877**) 0.740, **1.208,** 1.643
31. 81	6	41109. 16	$a\ ^3P_0$—452(1)	(0.000) 1.474
31. 06	15	41121. 93	$a\ ^5F_2$—421(2)	(0.201, **0.442**) 0.785, **0.989, 1.213,** 1.435
30. 51	15	41131. 20	$b\ ^3H_5$—665(4)	
30. 22	30	41136. 04	$a\ ^5P_2$—530(2)	(0.000*w*) 1.133
29. 68	25	41145. 16	$a\ ^5F_1$—411(2)	(**0.000***w*, 1.128) 0.000*w*, 1.150, **2.268**
28. 50	30	41165. 19		
28. 00	20	41173. 60	$a\ ^3P_2$—468(3)	(0.000*w*) 0.973*D*
26. 95	4	41191. 46		
26. 86	7	41192. 97	$a\ ^3P_2$—468(2)	(0.393, **0.488**) 0.860, **1.101, 1.334,** 1.596
26. 53	4	41198. 60	$b\ ^3F_4$—596(5)	(**0.000,** 0.265, 0.537, 0.820, 1.106) **0.958,** 1.222, . . .
25. 91	30	41209. 15	$a\ ^5P_3$—536(2)	(**0.000,** 0.258, 0.577) . . ., 1.093, 1.353, 1.532, 1.9, **2.2**
25. 47	10	41216. 61		(0.000*w*) 0.698*A*
25. 20	12	41221. 20		
25. 13	3	41222. 42		(0.000*w*) 1.568
24. 97	3	41225. 09	$b\ ^1G_4$—666(5)	(0.000) 0.966
24. 58	2	41231. 80	$a\ ^3D_1$—558(2)	(**0.000,** 0.486) 1.741
24. 05	3	41240. 70		
23. 89	8	41243. 51	$a\ ^3G_3$—530(2)	(**0.000,** 0.552, 1.102) **0.335,** 0.899, 1.470, 1.980
23. 49	20	41250. 32	$a\ ^3F_2$—444(3)	(**0.000,** 0.196, 0.398) 0.564, 0.753, 0.946, 1.128, **1.340**
21. 85	50	41278. 25	$b\ ^3F_3$—558(2)	(**0.000,** 0.317, 0.670) **0.324,** 0.674, 0.987, 1.306, 1.626
20. 83	2	41295. 67		(0.483) 1.212*C*
20. 35	1	41303. 78		
18. 95	6	41327. 76	$a\ ^3F_4$—510(3)	(**0.000***D*) 1.347*w*
18. 77	20	41330. 77		(0.000) 0.947
18. 54	2	41334. 74	$a\ ^5D_3$—570(3) $a\ ^3F_3$—481(2)	
18. 31	3	41338. 63		
18. 10	10	41342. 31		
17. 85	30	41346. 53		(0.332*w*) 1.138*D*
17. 38	4	41354. 54		
17. 33	5	41355. 39	$a\ ^5F_1$—413(1)	
17. 15	7	41358. 44	$b\ ^1D_2$—646(3)	(0.000) 1.023
16. 89	25	41362. 87	$a\ ^5F_3$—440(4)	(0.000*D*) 0.738*A*
16. 73	1	41365. 66		
15. 83	1	41381. 13		
15. 70	1	41383. 24	$b\ ^3F_2$—510(3)	
15. 24	15	41391. 11	$a\ ^3D_1$—560(2)	(0.000*w*) 1.044*A*
15. 22	12	41391. 48	$a\ ^3F_3$—482(2)	(**0.000.** 0.361, 741) **0.364,** 0.715
13. 78	4	41416. 16		
12. 54	12	41437. 58	$b\ ^3F_3$—560(2)	(0.000) 1.006
12. 27	8	41442. 13	$a\ ^5P_1$—521(1)	(0.764*D*) 1.618, 2.326
10. 61	3	41470. 63	$b\ ^3G_3$—682(3)	(0.539) 0.141, 0.770
09. 80	5	41484. 69		(**0.000,** 0.283, 0.610, 0.895) . . . , 1.475, 1.746, **2.041**
08. 83	8	41501. 24	$a\ ^3G_4$—542(4)	
08. 50	5	41506. 96	$b\ ^3F_2$—511(2)	(0.316, **0.625**) 0.722, **1.045, 1.352,** 1.670
08. 25	20	41511. 27	$a\ ^3P_2$—471(3)	(**0.000,** 0.260, 0.529) **0.578,** 0.849, 1.092
07. 75	10	41519. 89	$a\ ^3P_1$—468(2)	(**0.000,** 0.458) **0.651,** 1.102, 1.562
07. 54	1	41523. 58	$a\ ^5D_2$—560(2)	
06. 87	2	41535. 07		
05. 76	2	41554. 26		
05. 40	3	41560. 52		(0.232) 0.672, 0.948
04. 80	10	41570. 82	$c\ ^3F_4$—646(3)	(0.000) 0.961
04. 48	10	41576. 38	$a\ ^3G_3$—533(4)	(**0.000,** 0.189, 0.381, 0.561) 0.897, 1.115, 1.283, 1.477, **1.643**
03. 68	25	41590. 22	$a\ ^5P_2$—534(3)	(**0.000,** 0.216, 0.455) **0.789,** 0.988, 1.220, 1.442
03. 54	3	41592. 71		(0.000*w*) 1.078
03. 13	10	41599. 70		(0.000*D*) 1.417

TABLE 1. *Wavelengths, term combinations, and Zeeman effects of* Ta II—Continued

Wave length λair	Intensity and notes	Wave number	Term combination	Zeeman pattern
2402. 13	30	41617. 06	$a\ ^5F_3$—442(2)	(0.000) 1.240
01. 04	6	41635. 88	$b\ ^3F_2$—513(1)	(0.000) 1.049
00. 92	6	41638. 03		
00. 62	100	41643. 16	$a\ ^5F_5$—478(6)	(0.000*D*) 1.175*D*
2399. 94	15	41655. 06	$a\ ^3F_2$—448(3)	(**0.000,** 0.516, 1.029) 0.247, 0.744, 1.254, 1.744, **2.248**
98. 74	4	41675. 86	$a\ ^1F_3$—665(4)	(0.000*w*) 1.441
98. 34	6	41682. 85		(0.000*w*) 1.211*w*
98. 10	10	41686. 97	$a\ ^3D_3$—602(3)	(0.390*w*) 1.275*D*
97. 76	5	41692. 81		
97. 52	4	41697. 07		(0.286, 0.609, **0.928**) 0.281, 0.614, **0.928, 1.224,** 1.552, 1.957
97. 44	3	41698. 46	$a\ ^3G_3$—534(3)	
96. 74	1	41710. 59		(0.355) 1.177
95. 94	3	41724. 57	$c\ ^3F_2$—646(3)	(**0.000,** 0.388, 0.751) 1.101, 1.406, **1.807**
95. 40	3	41733. 94	$a\ ^3F_4$—514(4)	(0.393) 1.212
95. 03	12	41740. 42	$b\ ^3P_2$—602(3)	(**0.000,** 0.255, 0.556) **0.615,** 0.914, 1.178, 1.443, 1.732
94. 77	1	41744. 95		
94. 65	5	41747. 01	$b\ ^3F_4$—602(3)	(0.000) 1.320
93. 27	7	41771. 15	$a\ ^3D_3$—603(3)	(0.497*D*) 0.729, 0.941, **1.156, 1.367,** . . .
92. 70	6	41781. 13	$b\ ^3P_0$—580(1)	(0.000) 1.143
92. 29	3	41788. 19	$a\ ^5F_3$—444(3)	(0.304, 0.612, **0.911**) 0.320, 0.636, **0.952, 1.248,** 1.540, 1.851
90. 71	5	41815. 77		
90. 43	2	41820. 80		(0.000) 1.521
90. 22	4	41824. 37	$b\ ^3P_2$—603(3)	(**0.000,** 0.314, 0.635) **0.467,** 0.814, 1.130, 1.430
89. 60	8	41835. 29	$a\ ^3F_3$—486(2)	(0.000*w*) 1.021
89. 11	10	41843. 79	$b\ ^3F_2$—515(2)	(0.235, **0.487**) 0.806, **1.052, 1.299,** 1.554
88. 39	15	41856. 45	$a\ ^5D_2$—563(3) $a\ ^3P_2$—475(2)	(0.000*w*) 1.303
87. 54	5	41871. 39	$a\ ^5F_4$—462(4) $a\ ^5P_2$—537(1)	(0.000) 1.508
87. 35	2	41874. 68	$c\ ^3F_3$—654(3)	
87. 09	50	41879. 28	$a\ ^5F_4$—462(5)	(0.579*D*) 0.627*W*
84. 51	1	41924. 59		
84. 30	12	41928. 21	$a\ ^5F_2$—429(3)	(0.000*w*) 1.314
83. 74	15	41938. 01	$a\ ^3P_2$—475(1)	(0.000*w*) 1.161
83. 15	2	41948. 42		(0.000) 0.985
81. 55	40	41976. 68	$b\ ^3P_1$—593(2)	(0.000) 1.122
81. 14	50	41983. 81	$a\ ^5F_3$—446(4)	(0.000) 1.298
79. 80	2	42007. 54	$a\ ^3F_4$—517(5)	
78. 33	10	42033. 52	$a\ ^5F_2$—430(2)	(0.116) 1.038
78. 20	2	42035. 78		
77. 41	5	42049. 71	$a\ ^3P_0$—461(1)	(0.000) 1.356
77. 18	8	42053. 78	$a\ ^3F_2$—452(1)	(**0.000,** 0.719) **0.000,** 0.741, 1.465
75. 91	3	42076. 22	$a\ ^5D_1$—555(2)	(**0.000,** 0.456) **0.579,** 1.025
74. 69	5	42097. 91	$a\ ^5P_3$—545(2)	(**0.000,** 0.578, 1.145) 0.990, 1.458, 2.140, **2.737**
74. 20	3	42106. 52		
73. 92	20	42111. 51	$a\ ^5P_1$—528(1)	(1.457*B*) 0.906, 2.394*w*
72. 81	12	42131. 23	$a\ ^3F_3$—489(3)	(0.187, 0.433, **0.595**) 0.683, 0.880, **1.072, 1.274,** 1.495, 1.689
71. 58	10	42153. 18	$a\ ^5F_1$—421(2)	(**0.000,** 1.185) **1.185,** 2.340
71. 06	10	42162. 44		(**0.000,** 0.219, 0.453, 0.662) **0.326,** 0.548, 0.767, 1.020, 1.254, 1.487
70. 77	12	42167. 51	$a\ ^3P_2$—478(3)	(0.000*D*) 0.918*A*
70. 52	1	42171. 96	$b\ ^3F_3$—567(4)	
70. 37	8	42174. 64		(0.00) 1.35
69. 85	7	42183. 95	$a\ ^3P_1$—475(2)	(**0.000,** 0.266) **1.028,** 1.291, 1.540
69. 53	4	42189. 54	$a\ ^3H_4$—580(4)	(0.302) 1.058
69. 34	8	42192. 89	$a\ ^5F_3$—448(3)	(0.000) 1.236
68. 78	2	42202. 99	$b\ ^3H_6$—682(5)	
68. 56	2	42206. 85		(0.222) 1.137
68. 22	5	42212. 88	$a\ ^5P_3$—546(3)	(0.676, 1.335, **1.984**) 0.295, **0.954, 1.620,** 2.262
67. 71	4	42222. 00		
67. 26	15	42230. 01	$a\ ^5F_4$—466(4)	(0.437*w*) 1.272*D*
66. 18	1	42249. 25	$a\ ^3F_3$—490(2)	(**0.000,** 0.235, 0.462) 0.633, . . .
65. 29	2	42265. 20	$a\ ^3P_1$—475(1)	(0.000) 1.507

TABLE 1. *Wavelengths, term combinations, and Zeeman effects of* Ta II—Continued

Wave length λair	Intensity and notes	Wave number	Term combination	Zeeman pattern
2364.26	40	42283.58	$a\ ^5F_5$—484(4)	(0.000w) 1.843B
63.47	1	42297.74	$a\ ^5P_1$—530(2)	
62.44	3	42316.20	$a\ ^1G_4$—565(5) $a\ ^3D_3$—608(2)	
62.27	3	42319.21		
61.87	1	42326.43		
61.48	1	42333.44		
60.03	3	42359.39		
59.81	10	42363.30	$a\ ^3H_5$—605(5)	(0.791B) 0.408, 0.560, 0.732, **0.904, 1.081,** 1.253, 1.479, 1.656
59.46	7	42369.62	$b\ ^3P_2$—608(2)	(0.310, **0.619**) 0.777, **1.109, 1.428,** 1.772
59.17	8	42374.76	$a\ ^3F_4$—521(3)	(0.000D) 1.566B
59.08	4	42376.45		
58.68	2	42383.63	$a\ ^5D_1$—558(2)	
58.24	2	42391.56		
56.92	20	42415.24	$a\ ^5F_4$—468(3)	(0.000w) 1.030
56.48	8	42423.15	$a\ ^3G_4$—551(3)	(**0.000,** 0.237, 0.471, 0.700) 0.365A
56.07	20	42430.65	$b\ ^3F_2$—521(3)	(0.000) 1.136
55.67	6	42437.79		
55.58	12	42439.46	$a\ ^3G_3$—542(4)	(**0.000,** 0.229, 0.473, 0.708) 0.681, 0.920, 1.157, 1.416, 1.662, **1.880**
55.07	3	42448.60		
54.59	3	42457.25		
54.52	5	42458.51	$a\ ^1D_2$—560(2)	(0.217) 1.061
54.39	4	42460.82	$a\ ^5D_4$—596(5)	
54.11	4	42465.92	$b\ ^3F_2$—521(1)	(**0.000,** 0.558) **0.533,** 1.057
53.87	10	42470.31	$a\ ^3P_1$—478(0)	(0.000) 1.548
51.99	10	42504.14		(0.000w) 0.962w
51.74	1	42508.70	$a\ ^3P_2$—481(2)	
51.50	1	42513.04	$a\ ^5F_2$—435(3)	
51.16	1	42519.18		
50.92	3	42523.45		(**0.000,** 0.248, 0.513) 0.508A
50.06	3	42539.07		(0.000w) 1.174w
49.84	2	42543.10	$a\ ^5D_1$—560(2)	(**0.000,** 0.503) **0.510,** 0.986
49.52	1	42548.46	$a\ ^5D_3$—582(2)	
49.32	2	42552.52		
49.04	1	42557.56		(0.000w) 0.952w
48.62	7	42565.16	$a\ ^3P_2$—482(2)	(0.000 B) 1.367D
48.55	6	42566.50	$c\ ^3F_2$—654(3)	
48.45	3	42568.24	$a\ ^3D_1$—571(1)	(0.856) 1.762
48.06	3	42575.35		(0.000) 1.080
47.64	8	42582.89		
46.98	20	42594.90		(0.000w) 1.100B
46.44	5	42604.76		
46.32	2	42606.88	$a\ ^5D_4$—598(5)	(0.000w) 0.711, 0.830w
46.04	8	42612.04	$b\ ^3F_4$—611(4)	(0.408, 0.597, **0.813**) 0.425, 0.612, 0.806, **1.029, 1.221,** 1.425, 1.646, 1.855.
45.43	1	42623.05		
44.64	1	42637.41		
43.65	20	42655.38		(0.00w) 0.86w
43.49	7	42658.33	$a\ ^5P_2$—545(2)	(0.384, **0.800**w) 0.628, **1.022, 1.403,** 1.801
42.53	10	42675.87	$a\ ^3G_4$—553(4)	
41.62	12	42692.32	$a\ ^5P_3$—551(3)	(0.357, 0.714, **1.123**) 0.517, 0.881, **1.245, 1.590,** 1.942, 2.316
40.94	10	42704.85	$a\ ^3F_3$—495(3)	(0.222, 0.467, **0.712**) 0.612, 0.846, **1.086, 1.306,** 1.536, 1.760
40.30	10	42716.48		
40.04	10	42721.29	$a\ ^3H_4$—585(5)	(0.000) 1.100
39.34	1	42734.00	$a\ ^3P_1$—480(0)	(0.000) 1.576
38.65	8	42746.54	$a\ ^3F_4$—524(4)	(0.468B) 1.208D
38.28	15	42753.36	$a\ ^5F_4$—471(3)	(**0.000,** 0.238, 0.516, 0.791) . . ., 1.069, 1.324, 1.592, 1.902, **2.167**

TABLE 1. *Wavelengths, term combinations, and Zeeman effects of* Ta II—Continued

Wave length λair	Intensity and notes	Wave number	Term combination	Zeeman pattern
2337. 82	2	42761. 75	*a* $^3F_3$—495(2)	
37. 56	3	42766. 61	*a* $^3G_3$—545(2)	
37. 18	4	42773. 57	*a* $^5P_2$—546(3)	(**0.000,** 0.478, 0.972) **0.000,** 0.451, 0.932, 1.413
36. 55	8	42785. 03		
35. 75	15	42799. 68	*b* $^3H_5$—682(5) *a* $^3G_4$—555(5)	(0.000*w*) 1.146*w*
35. 49	3	42804. 44	*a* $^5F_3$—454(2)	
34. 90	12	42815. 30	*a* $^3F_3$—496(3)	(0.123) 1.057
34. 14	20	42829. 27		(0.000*w*) 1.150*A*
33. 87	12	42834. 15	*a* $^3F_4$—525(3)	(**0.000,** 0.198, 0.301, 0.502) **0.643,** 0.716, 0.887, 1.105, 1.349
33. 08	2	42848. 69	*c* $^3P_2$—708(2)	
32. 19	25	42865. 02	*a* $^5F_4$—472(4)	(0.60) 0.92
32. 00	35	42868. 53	*a* $^5F_5$—490(5)	
31. 30	20	42881. 44	*a* $^3G_3$—546(3)	(0.000) 0.886
30. 82	5	42890. 27	*b* $^3F_2$—525(3)	(0.000*w*) 1.370
30. 70	2	42892. 41	*a* $^3P_1$—482(2)	(0.000) 1.401
29. 88	2	42907. 59		
29. 45	1	42915. 36		
29. 29	1	42918. 37		
29. 20	4	42919. 95	*a* $^3H_5$—611(4)	(0.000*w*) 1.226*w*
28. 96	1	42924. 45		
28. 76	3	42928. 21		(0.189) 1.153
28. 57	1	42931. 64	*a* $^5P_1$—536(2)	
27. 64	6	42948. 79		
27. 00	4	42960. 60		
26. 74	1	42965. 33		
26. 48	6	42970. 29		
25. 70	2	42984. 70		
25. 15	2	42994. 85	*a* $^3F_2$—461(1)	
24. 33	2	43009. 96	*a* $^5D_4$—602(3)	(0.000) 1.221
23. 90	20	43017. 85		(0.00) 0.99
23. 04	3	43033. 75	*a* $^5P_1$—537(1)	(1.128*w*) 1.248, 2.356
22. 21	2	43049. 21		
21. 38	1	43064. 65	*a* $^5F_1$—430(2)	
21. 17	4	43068. 53	*a* $^5F_1$—430(0)	(0.00) 0.00
20. 93	1	43072. 89	*a* $^3D_2$—602(3)	
20. 58	4	43079. 44		
20. 35	2	43083. 75		
19. 79	2	43094. 08	*a* $^5D_4$—603(3)	
19. 51	3	43099. 31		
19. 25	2	43104. 22	*b* $^3P_1$—604(1)	
19. 09	8	43107. 19	*a* $^5P_3$—555(3)	(0.440*D*) 1.526*D*
18. 64	4	43115. 45	*a* $^5P_3$—555(2)	(**0.000,** 0.573, 1.148) 1.568, 2.062, **2.647**
18. 48	2	43118. 46	*a* $^3P_2$—487(1)	
17. 66	2	43133. 77	*b* $^3F_2$—528(1)	(0.000*w*) 1.144
17. 18	1	43142. 59		
17. 03	1	43145. 37		(**0.000,** 0.393) 0.494, 0.884, **1.282**
16. 70	3	43151. 62		
16. 42	4	43156. 76	*a* $^3D_2$—603(3)	(0.000*w*) 0.995
16. 04	5	43163. 81	*a* $^3D_1$—577(2)	(0.000*w*) 0.587*A*
15. 65	3	43171. 15	*a* $^3H_5$—613(5)	
15. 45	10	43174. 90	*a* $^5F_2$—442(1)	(**0.000,** 0.750) 0.253, 0.998, **1.751**
14. 29	3	43196. 52		
14. 08	3	43200. 36	*b* $^3F_4$—616(3)	(**0.000,** 0.307, 0.621, 0.940) 1.554, 1.847, **2.172**
12. 93	2	43221. 92		
12. 62	7	43227. 78	*a* $^5F_2$—442(2)	(0.223, **0.507**) 0.752, **1.008, 1.251,** 1.481
11. 46	1	43249. 34		
11. 20	5	43254. 28		
08. 93	1	43296. 71	*a* $^5D_2$—577(2)	
08. 63	2	43302. 41		
08. 51	4	43304. 74	*a* $^3P_2$—489(3)	(0.000) 1.207*A*

TABLE 1. *Wavelengths, term combinations, and Zeeman effects of* Ta II—Continued

Wave length λair	Intensity and notes	Wave number	Term combination	Zeeman pattern
2308. 16	3	43311. 15	$a\ ^3F_2$—464(2) $a\ ^3D_2$—604(1)	(**0.000,** 0.545) 0.660, 1.192, **1.749**
06. 86	3	43335. 62	$a\ ^3P_1$—486(2) $a\ ^5F_5$—495(5)	(**0.000,** 0.409) **0.720,** 1.129, 1.517
05. 49	1	43361. 38	$a\ ^3G_3$—551(3)	
04. 75	3	43375. 30	$a\ ^3H_6$—613(5)	
03. 48	6	43399. 14	$a\ ^5F_2$—444(3)	(0.000*w*) 0.879*w*
03. 31	1	43402. 42	$a\ ^3H_5$—615(6)	
02. 92	6	43409. 69	$a\ ^5F_4$—478(3)	(0.000*D*) 1.721*B*
02. 39	1	43419. 76		
02. 23	6	43422. 74	$a\ ^3H_5$—616(6) $a\ ^3P_2$—490(2)	(0.000*w*) 1.330
01. 47	8	43437. 04	$a\ ^3G_4$—561(4)	(1.082*B*) 0.240, 0.499, 0.752, **1.008, 1.250,** 1.522, 1.759, 2.012
01. 22	1	43441. 84	$a\ ^5F_4$—478(5)	
01. 07	2	43444. 63		
01. 02	1	43445. 61	$a\ ^3P_1$—487(1)	
00. 27	2	43459. 72	$b\ ^3F_3$—580(4)	(0.000*w*) 1.115*w*
2298. 95	6	43484. 73		(0.000*w*) 0.639*A*
98. 39	1	43495. 32	$b\ ^3P_1$—608(2)	(0.000) 1.114
98. 12	8	43500. 39	$a\ ^1D_2$—570(3)	(**0.000,** 0.295, 0.570) 1.093, 1.378, 1.643, **1.899**
97. 63	2	43509. 67		(0.000) 1.104
96. 81	40	43525. 20		(0.00*w*) 0.99*w*
96. 68	2	43527. 70	$c\ ^3F_4$—666(5)	(0.384*w*) 1.066*D*
95. 55	1	43549. 11	$c\ ^3P_0$—669(1)	(0.000) 0.000, 1.220
95. 22	4	43555. 48		(0.000*w*) 0.895*w*
93. 77	1	43582. 92	$a\ ^5P_3$—560(2)	
92. 56	15	43605. 94	$a\ ^3H_6$—615(6)	(0.362*w*) 1.138*D*
92. 14	4	43613. 98	$a\ ^3G_3$—553(4)	(0.000*D*) 1.297*A*
91. 50	1	43626. 15	$a\ ^5D_3$—593(2)	
91. 47	1	43626. 64	$a\ ^3H_6$—616(6)	
91. 00	1	43635. 61	$a\ ^1D_2$—571(1) $b\ ^1D_2$—669(1)	(**0.000,** 0.628) 0.490, . . .
90. 46	4	43645. 93	$a\ ^3G_4$—563(3)	
89. 93	3	43656. 02		
89. 43	2	43665. 53		
89. 18	15	43670. 28	$a\ ^3F_2$—468(2)	(0.342, **0.723**) 0.389, **0.739, 1.097,** 1.447
88. 88	3	43676. 06	$a\ ^5P_2$—555(2)	
87. 28	12	43706. 57	$a\ ^5P_3$—561(4)	(**0.000,** 0.319, 0.664, 1.023) **0.277,** 0.594, 0.926, 1.268, 1.572
87. 01	1	43711. 73		
86. 60	3	43719. 59	$a\ ^3F_4$—534(3)	(0.000*w*) 1.214
85. 27	20	43744. 97	$a\ ^5F_3$—463(2)	(0.000*w*) 1.171*A*
85. 02	7	43749. 85	$a\ ^3P_1$—490(2)	(**0.000,** 0.257) **1.048,** 1.266, 1.528
83. 67	2	43775. 58	$b\ ^3F_2$—534(3)	(0.00) 1.40
83. 40	1	43780. 91	$b\ ^3H_4$—682(5)	
83. 22	8	43784. 32	$a\ ^3G_3$—555(2)	(0.000) 0.706*A*
83. 07	1	43787. 16		
82. 21	3	43803. 60	$a\ ^5F_2$—448(3)	(**0.000,** 0.271, 0.518) 1.014, 1.264, 1.519, **1.760**
81. 54	4	43816. 44	$a\ ^3G_4$—565(5)	(0.000, 0.912*w*)
81. 32	3	43820. 71	$a\ ^5P_1$—545(2)	(0.000) 1.015
80. 58	5	43834. 92		(0.00*w*) 1.27*w*
78. 92	1	43866. 91	$b\ ^3H_4$—682(3)	
78. 33	2	43878. 21	$a\ ^3P_2$—495(3)	(0.00) 1.25
78. 11	2	43882. 52		(0.00) 1.18
75. 64	10	43930. 11	$a\ ^3H_5$—621(4)	(0.00) 1.19
74. 61	2	43950. 08		
74. 37	2	43954. 66	$b\ ^3F_2$—536(2)	(0.58) 1.16
72. 72	1	43986. 55	$a\ ^3H_4$—598(5)	
72. 59	20	43989. 02	$a\ ^3P_2$—496(3) $a\ ^3F_2$—471(3)	(**0.00,** 0.65) 0.68, **1.33**
71. 86	15	44003. 24	$a\ ^5F_3$—466(4) $a\ ^5P_2$—558(1)	(0.00) 1.16

TABLE 1. *Wavelengths, term combinations, and Zeeman effects of* Ta II—Continued

Wave length λair	Intensity and notes	Wave number	Term combination	Zeeman pattern
2271. 27	1	44014. 63		
71. 05	2	44018. 97	*a* $^3H_5$—622(5)	(0.00) 1.09
70. 90	4	44021. 76		(0.00) 1.09
69. 56	5	44047. 73	*a* $^3G_4$—567(4)	(0.63) 1.15*w*
69. 21	4	44054. 66	*a* $^5F_4$—484(4)	(0.00*w*) 1.29
67. 50	2	44087. 86		(0.00*w*) 0.70*w*
67. 27	4	44092. 31	*a* $^3G_3$—558(2)	(0.00*w*) 0.82*w*
65. 94	1	44118. 23		
64. 45	2	44127. 14		
63. 98	3	44156. 38		(0.00) 1.04
62. 29	25	44189. 28	*a* $^5F_3$—468(3)	(0.00) 1.15
61. 62	12	44202. 45	*a* $^5F_2$—452(1)	(**0.00**, 0.48) **0.48**, 1.00
61. 43	20	44206. 09	*a* $^5F_1$—442(1)	
60. 57	5	44222. 90	*a* $^3H_6$—622(5)	(0.00) 1.43*A*
60. 26	3	44229. 09	*a* $^3P_2$—498(1)	(**0.00**, 0.67) 0.71
59. 59	5	44242. 18	*a* $^3F_3$—510(3)	(0.18) 1.13
59. 12	3	44251. 40	*a* $^3G_3$—560(2)	(0.00) 0.81
58. 74	5	44258. 83	*a* $^5F_1$—442(2)	(**0.00**, 1.24) 0.00, 1.24, **2.53**
57. 55	3	44282. 15		(0.41) 1.09
57. 11	1	44290. 73		
56. 53	12	44302. 07		(0.00) 1.20
55. 77	20	44317. 08	*a* $^5P_3$—567(4).	(0.00*W*) 0.00*W*
55. 60	2	44320. 30	*a* $^5F_5$—505(5)	
54. 88	4	44334. 45	*a* $^3F_2$—475(2)	(1.09) 1.38
53. 47	2	44362. 24		
53. 26	3	44366. 34	*a* $^3F_3$—511(2)	(0.00*w*) 0.78
52. 80	3	44375. 46	*a* $^3G_3$—561(4)	(0.00*w*) 1.42*w*
52. 06	2	44390. 02	*a* $^3H_4$—602(3)	
50. 78	15	44415. 38	*a* $^5F_2$—454(2)	(0.36) 1.13
49. 79	10	44434. 74	*a* $^5F_1$—444(0)	(0.00) 0.00
48. 50	5	44460. 37	*a* $^3F_4$—542(4)	(0.30) 1.22
47. 84	2	44473. 38		
47. 40	1	44482. 11		
46. 16	2	44506. 72	*a* $^3D_3$—630(2) *a* $^5F_5$—506(6)	
43. 87	6	44552. 08	*a* $^5P_3$—569(4)	(0.00*w*) 0.00*w*
43. 47	2	44559. 96	*b* $^3P_2$—630(2)	
42. 68	5	44575. 74	*a* $^5P_2$—564(3)	(0.00*w*) 1.01*w*
41. 72	2	44594. 86	*a* $^5D_0$—571(1)	
39. 48	20	44639. 23	*a* $^5F_4$—490(5) *a* $^5F_3$—472(4)	(0.00) 1.20
39. 01	5	44648. 80	*a* $^3F_3$—514(4)	(0.00) 1.20
38. 60	1	44657. 01	*a* $^3P_2$—503(3)	
37. 46	2	44679. 62	*c* $^3F_3$—682(3)	
36. 29	4	44702. 96	*a* $^3F_3$—515(2)	(0.00) 0.84
35. 94	3	44709. 97		
35. 69	3	44714. 97	*a* $^1D_2$—582(2)	
33. 89	4	44751. 08		
32. 26	1	44783. 81		
31. 46	1	44799. 75	*a* $^5D_1$—582(2)	
30. 86	3	44811. 88		
30. 69	1	44815. 25	*a* $^5P_1$—555(1)	
29. 90	1	44831. 11		
29. 30	1	44843. 27	*b* $^3F_2$—545(2)	
29. 03	1	44848. 62		
27. 85	50	44872. 37	*a* $^5F_3$—475(2)	(0.00) **1.22**
27. 23	10	44884. 82	*a* $^5D_4$—621(4)	

TABLE 1. *Wavelengths, term combinations, and Zeeman effects of* Ta II—Continued

Wave length λair	Intensity and notes	Wave number	Term combination	Zeeman pattern
2226. 52	15	44899. 18		(0.00*w*) 1.05, **1.72**
25. 42	3	44921. 33		
24. 91	1	44931. 62	*a* $^3D_3$—634(4)	
23. 56	1	44958. 94	*b* $^3F_2$—546(3)	
23. 31	10	44963. 91		(0.00*w*) 1.55*w*
22. 80	1	44974. 31		
22. 56	5	44979. 23		
22. 22	4	44986. 05	*a* $^3G_3$—567(4) *a* $^3F_2$—481(2)	
20. 70	15	45016. 79		
19. 41	10	45043. 04	*a* $^3F_2$—482(2)	(1.42) . . .
18. 93	1	45052. 74		
18. 39	6	45063. 75		
17. 84	15	45074. 80		(0.00) 1.07
16. 09	4	45110. 43		
15. 58	20	45120. 77	*a* $^5F_4$—495(3)	(0.00) 1.41
14. 53	25	45142. 21		(0.00*w*) 1.30*w*
14. 33	8	45146. 36	*a* $^5P_1$—558(2)	(0.00) 0.00*w*
13. 39	1	45165. 52	*a* $^5P_1$—558(1)	
12. 42	20	45185. 40	*a* $^5P_2$—570(3)	(0.00) 1.42
11. 96	1	45194. 61		
11. 66	2	45200. 74		
10. 20	6	45230. 78	*a* $^5F_4$—496(3)	
10. 04	5	45234. 01	*a* $^5F_1$—452(1)	(1.45) 0.00, 1.43
09. 03	3	45254. 05	*a* $^3H_4$—611(4)	
07. 99	2	45276. 00		
07. 64	3	45283. 16		
07. 36	3	45288. 78		
07. 13	10	45293. 56	*a* $^3G_3$—570(3)	
07. 04	5	45295. 43		
06. 54	4	45305. 67	*a* $^5P_1$—560(2)	
05. 86	1	45319. 76	*a* $^5P_2$—571(1)	
05. 49	1	45327. 34	*b* $^3F_4$—638(4)	
04. 09	5	45356. 01	*a* $^5P_3$—577(2) *a* $^5F_2$—463(2)	
02. 83	1	45381. 95	*a* $^5F_4$—551(3)	
02. 28	4	45393. 24		
01. 80	3	45403. 22		
01. 15	12	45416. 54	*a* $^3P_2$—510(3)	(0.00) 1.03
00. 43	8	45431. 49		
2199. 67	25	45447. 26	*a* $^5F_1$—454(2)	(**0.00,** 1.12) 1.29, **2.39**
97. 77	1	45486. 46	*a* $^1G_4$—596(5) *a* $^3F_2$—486(2)	
96. 30	3	45516. 90	*a* $^3H_5$—637(5)	
96. 05	50	45522. 04	*a* $^5F_4$—499(4)	(0.41) 1.40
95. 23	1	45539. 09	*a* $^3P_2$—511(2)	
93. 88	25	45567. 19	*a* $^5F_5$—517(5)	
93. 22	15	45580. 90	*a* $^5F_3$—482(2)	
92. 47	2	45596. 34		
91. 99	4	45606. 45		
90. 97	2	45627. 66		
90. 62	2	45634. 80	*a* $^3H_5$—638(4) *a* $^3F_4$—553(4)	
89. 40	1	45660. 38	*b* $^3F_3$—602(3)	
88. 48	8	45679. 57		
86. 44	4	45722. 06		
86. 26	2	45725. 91		
85. 49	2	45742. 00	*a* $^3G_5$—585(5)	
85. 30	2	45746. 10	*a* $^5D_2$—602(3)	

TABLE 1. *Wavelengths, term combinations, and Zeeman effects of* Ta II—Continued

Wave length λair	Intensity and notes	Wave number	Term combination	Zeeman pattern
2185. 15	2	45759. 11	*a* $^3F_3$—525(3)	
84. 68	8	45758. 98	*a* $^3F_4$—555(5)	
83. 44	2	45784. 96		
83. 11	3	45791. 80	*a* $^1D_2$—593(2)	
82. 72	50	45800. 10	*a* $^5F_2$—468(3)	(0.00) 1.53
81. 80	4	45819. 39	*a* $^5F_2$—468(2)	
81. 38	1	45828. 15	*a* $^5F_3$—484(4)	
80. 87	8	45838. 84	*a* $^3H_6$—638(5) *a* $^5P_3$—582(2)	
80. 68	10	45842. 90	*a* $^3H_4$—616(3)	
80. 18	3	45853. 33	*b* $^3F_2$—555(3)	
79. 81	3	45861. 20	*b* $^3F_2$—555(2)	
79. 55	25	45866. 62	*a* $^3P_1$—511(2)	
79. 06	2	45876. 88	*a* $^5D_1$—593(2)	
79. 98	1	45878. 58		
78. 03	4	45898. 63	*a* $^5F_4$—503(3)	
77. 97	25	45899. 94	*a* $^3F_2$—490(2)	
77. 20	1	45916. 06	*a* $^5P_2$—577(2)	
74. 72	3	45968. 46	*a* $^5D_3$—616(3)	
73. 42	2	45996. 02	*a* $^3P_1$—513(1)	
73. 05	5	46003. 81		
72. 85	7	46008. 08	*b* $^3P_0$—622(1)	
72. 15	15	46022. 95	*a* $^1F_3$—708(2)	
72. 08	7	46024. 39	*a* $^5F_3$—486(2) *a* $^3G_3$—577(2)	
71. 02	1	46046. 86		
70. 65	2	46054. 71		
69. 15	10	46086. 55		
67. 02	1	46131. 85		
66. 76	3	46137. 27	*a* $^5F_2$—471(3)	
66. 32	10	46146. 86		
65. 45	3	46165. 29		
65. 26	3	46169. 34		
65. 00	15	46174. 92	*a* $^5F_1$—461(1)	
64. 77	1	46179. 79	*a* $^3F_3$—530(2)	
64. 67	15	46181. 86		
64. 36	5	46188. 45	*b* $^3F_2$—558(1)	
64. 12	1	46193. 66	*a* $^5P_2$—580(1)	
63. 65	8	46203. 65	*a* $^3P_1$—515(2)	
62. 65	5	46225. 05		
62. 45	2	46229. 33		
62. 26	7	46233. 35		
62. 04	4	46238. 09		
61. 88	10	46241. 60	*a* $^3F_4$—569(4)	
61. 82	5	46242. 80	*a* $^3D_1$—608(2)	
61. 26	7	46254. 82	*a* $^5D_4$—634(4)	
60. 79	3	46264. 82	*a* $^3H_4$—621(4)	
60. 36	4	46273. 96		
59. 63	6	46289. 71	*b* $^3F_3$—608(2)	
58. 84	2	46306. 62	*a* $^5F_5$—524(4)	
58. 42	25	46315. 68		
58. 19	3	46320. 57	*a* $^5F_3$—489(3)	
58. 09	8	46322. 71		
57. 83	4	46328. 27	*b* $^3F_2$—560(2)	
57. 66	1	46331. 99		
56. 91	6	46348. 10		
56. 65	1	46353. 64	*a* $^3H_4$—622(5)	

TABLE 1. *Wavelengths, term combinations, and Zeeman effects of* Ta II—Continued

Wave length λair	Intensity and notes	Wave number	Term combination	Zeeman pattern
2156.53	5	46356.28	*a* $^3F_2$—495(2)	
55.09	8	46387.15	*a* $^5F_1$—463(2)	
54.67	10	46396.17	*a* $^3F_4$—561(4)	
54.50	12	46399.85	*a* $^5P_2$—582(2)	
54.20	2	46406.44	*a* $^3P_0$—505(1)	
54.12	10	46408.08		
53.92	2	46412.34		
53.86	15	46413.68		
53.55	10	46420.36		
52.71	20	46438.40	*a* $^5F_3$—490(2)	
51.56	6	46463.29	*a* $^3P_2$—521(3)	
51.40	20	46466.74	*a* $^3F_2$—496(3)	
51.15	2	46472.14	*a* $^5D_4$—637(5)	
50.64	18	46483.12	*a* $^5F_2$—475(2)	
50.47	4	46486.84		
49.96	7	46497.78	*a* $^3P_2$—521(1)	
49.30	2	46512.14	*a* $^3F_3$—533(4)	
48.72	5	46524.71	*b* $^3F_3$—611(4)	
47.20	15	46557.60		
46.87	25	46564.78	*a* $^5F_2$—475(1)	
46.40	2	46575.08		
45.76	5	46588.86	*a* $^5D_4$—638(4)	
45.39	8	46596.94		
43.65	5	46634.67	*a* $^3F_3$—534(3)	
43.16	50	46645.46		
42.52	40	46659.42	*a* $^5F_5$—528(6)	
42.41	7	46661.79		
41.51	20	46681.36	*a* $^3D_3$—652(4)	
40.43	6	46704.86	*a* $^3F_4$—564(5)	
40.34	2	46706.83	*a* $^3F_2$—498(1)	
40.15	50	46711.06		
39.59	1	46723.16	*a* $^3H_5$—649(6)	
39.46	7	46726.10		
38.70	4	46742.62		
37.18	6	46775.88	*a* $^3F_4$—565(5)	
36.35	5	46794.05	*a* $^5F_2$—478(3)	
35.46	4	46813.46	*a* $^3F_3$—536(2)	
35.20	5	46819.16		
34.94	1	46824.95	*a* $^3P_1$—521(1)	
32.88	20	46870.15		
32.80	2	46871.93		
31.80	20	46893.98	*a* $^5F_3$—495(3)	
30.64	4	46919.36	*a* $^1D_2$—604(1)	
30.50	6	46922.48	*a* $^3P_2$—525(3)	
30.29	4	46927.19	*a* $^3H_6$—649(6)	
29.22	7	46950.69	*a* $^5F_3$—495(2)	
26.75	2	47005.25	*a* $^5F_3$—496(3)	
26.68	5	47006.89	*a* $^3F_4$—567(4) *a* $^3G_5$—598(5)	
26.33	3	47014.49	*a* $^1H_5$—712(5)	
24.82	20	47047.96	*a* $^5F_5$—532(5)	
24.56	4	47053.66		
23.45	1	47078.38	*a* $^5P_1$—577(2)	
21.88	2	47113.12	*b* $^3F_3$—616(3)	
20.91	6	47134.71	*a* $^3F_2$—503(3) *a* $^5F_2$—481(2)	
19.91	5	47156.90	*a* $^5F_5$—533(4)	

TABLE 1. *Wavelengths, term combinations, and Zeeman effects of* Ta II—Continued

Wave length λair	Intensity and notes	Wave number	Term combination	Zeeman pattern
2119.48	2	47166.53	*a* $^3P_2$—528(1)	
19.24	5	47171.81		
19.14	1	47174.03		
18.83	6	47180.89		
18.34	6	47191.84	*a* $^5F_2$—482(2)	
15.45	2	47256.35		
13.69	10	47295.65	*a* $^5F_3$—499(4)	
12.85	7	47314.45	*a* $^3F_4$—570(3)	
11.80	6	47337.98	*a* $^5F_4$—517(5)	
11.21	4	47351.16	*a* $^3F_2$—505(1)	
10.36	4	47370.18	*b* $^3F_2$—570(3)	
10.09	3	47376.29		
09.91	1	47380.35		
07.19	1	47441.62		
05.65	1	47476.27	*a* $^5P_2$—593(2)	
05.34	1	47483.19		
04.84	1	47494.38	*a* $^3P_1$—528(1)	
03.72	5	47519.77		
03.12	5	47533.30		
01.85	5	47562.07	*a* $^5P_1$—582(2)	
00.80	1	47585.86		
00.55	2	47591.43		
00.32	5	47596.60	*a* $^5F_1$—475(1)	
2099.63	3	47612.42		
99.29	3	47620.13		
98.66	2	47634.42	*a* $^3H_4$—634(4)	
97.84	1	47652.99		
96.97	3	47672.69		
95.65	3	47702.78	*a* $^3F_3$—545(2)	
94.41	4	47731.00		
91.76	3	47791.44		
91.32	6	47801.47	*a* $^5F_1$—478(0)	
90.61	4	47817.73	*a* $^3F_3$—546(3)	
88.66	7	47862.34	*a* $^5F_5$—540(5)	
87.96	1	47878.45	*a* $^5D_0$—604(1)	
87.84	5	47881.09		
87.80	1	47882.12	*b* $^3F_3$—624(4)	
87.28	4	47894.00	*a* $^3F_2$—510(3)	
85.93	5	47925.06		
84.96	4	47947.36		
83.70	5	47976.28		
80.54	3	48049.16	*a* $^5F_2$—490(2)	
80.08	4	48059.81		
79.31	3	48077.46	*a* $^5F_4$—524(4)	
76.32	5	48146.83	*a* $^3F_2$—513(1)	
75.54	5	48164.94	*a* $^5F_4$—525(3)	
74.45	1	48190.18		
74.11	4	48197.98		
73.94	5	48202.07		
73.42	1	48214.12		
71.01	3	48270.24		
69.91	4	48295.96		
69.13	3	48314.14	*a* $^3P_1$—536(2)	
68.28	8	48333.85		
67.41	3	48354.35	*a* $^3F_2$—515(2)	
67.18	2	48359.68	*a* $^3H_5$—665(4) *a* $^5D_2$—628(1)	
66.63	4	48372.41		
65.30	5	48403.74		
64.76	2	48416.33	*a* $^3P_1$—537(1)	
64.19	4	48429.65	*b* $^3P_2$—669(1)	

TABLE 1. *Wavelengths, term combinations, and Zeeman effects of* Ta II—Continued

Wave length λair	Intensity and notes	Wave number	Term combination	Zeeman pattern
2063. 34	5	48449. 55	*a* $^5P_2$—603(3)	
61. 99	2	48481. 25		
61. 91	10	48483. 13		
60. 99	1	48504. 84	*a* $^5F_2$—495(3)	
60. 05	2	48527. 01	*a* $^3G_5$—613(5)	
59. 08	10	48549. 90	*a* $^3F_3$—553(4)	
58. 84	2	48555. 48	*a* $^5F_3$—511(2)	
58. 59	2	48561. 47	*a* $^5F_2$—495(2)	
57. 61	2	48584. 50	*b* $^3F_2$—582(2)	
56. 78	1	48604. 15	*a* $^5P_2$—604(1)	
55. 76	6	48628. 13	*a* $^3H_6$—666(5)	
55. 26	1	48640. 02		
53. 84	4	48673. 74		
52. 73	2	48699. 99	*a* $^3P_0$—528(1)	
51. 54	2	48728. 21		
51. 17	1	48737. 05		
50. 28	1	48758. 13	*a* $^1D_2$—623(2)	
49. 46	1	48777. 68	*a* $^3G_5$—616(6)	
47. 40	8	48826. 90	*a* $^3F_4$—585(5)	
46. 19	2	48855. 60	*a* $^5F_2$—498(1)	
44. 66	5	48892. 08	*a* $^5F_3$—515(2)	
44. 11	2	48905. 45		
43. 16	5	48927. 99	*a* $^5F_4$—533(4)	
40. 61	5	48989. 13	*a* $^3G_4$—616(3)	
40. 01	5	49003. 53		
38. 10	2	49049. 45	*a* $^5F_4$—534(3)	
35. 89	3	49102. 69	*a* $^3G_3$—608(2)	
34. 19	2	49143. 81		
32. 61	1	49181. 96		
32. 36	2	49187. 94	*a* $^3F_3$—560(2)	
31. 53	2	49208. 06		
31. 17	1	49216. 77		
30. 62	1	49230. 20		
30. 25	1	49239. 20	*b* $^3F_3$—638(4)	
29. 92	1	49247. 05		
28. 40	1	49284. 05		
27. 92	4	49295. 64		
27. 12	1	49315. 16		
24. 00	4	49391. 10		
23. 20	2	49410. 72	*a* $^3G_4$—621(4)	
22. 66	1	49423. 94		
22. 21	1	49434. 96		
20. 74	1	49470. 82	*a* $^3P_2$—551(3)	
19. 56	5	49499. 65	*a* $^5F_2$—505(1) *a* $^3G_4$—622(5)	
19. 18	1	49509. 11	*a* $^5D_3$—652(4)	
17. 71	2	49545. 12		
15. 50	2	49599. 56		
14. 66	2	49620. 17		
13. 17	6	49656. 86		
09. 19	2	49755. 11		
06. 71	6	49816. 60		
05. 86	1	49837. 83		
04. 54	4	49870. 56		
03. 92	4	49885. 92	*a* $^3P_2$—555(3)	
03. 16	1	49904. 84		
02. 28	2	49926. 82	*a* $^3G_3$—616(3)	
01. 81	5	49938. 72	*a* $^5F_3$—525(3)	
01. 17	2	49954. 51		
00. 73	4	49965. 47		

TABLE 2. *Even terms of* Ta II

Electron configuration	Term symbol	Level	Δν	Observed g	Electron configuration	Term symbol	Level	Δν	Observed g
$5d^3(^4F)6s$	$a\ ^5F_1$	0. 00		0. 000	$5d^3(^2D)6s$	$b\ ^3D_1$	29963. 20		1. 004
	$^5F_2$	1031. 36	1031. 36	1. 008		$^3D_2$	30405. 61	442. 41	1. 051
	$^5F_3$	2642. 26	1610. 90	1. 250		$^3D_3$	30624. 09	218. 48	1. 257
	$^5F_4$	4415. 79	1773. 53	1. 350		$c\ ^1D_2$	33027. 18		1. 020
	$^5F_5$	6186. 81	1771. 02	1. 410		$a\ ^3F_2$	3180. 04		0. 750
	$b\ ^3F_2$	9690. 47		1. 047		$^3F_3$	6831. 31	3651. 27	1. 098
	$^3F_3$	14581. 07	4890. 60	0. 988		$^3F_4$	9746. 28	2914. 97	1. 225
	$^3F_4$	18493. 66	3912. 59	1. 227		$a\ ^3P_0$	4124. 85		0. 000
$5d^3(^4P)6s$	$a\ ^5P_1$	10713. 21		2. 353	$5d^2\ 6s^2$	$^3P_1$	5330. 77	1205. 92	1. 550
	$^5P_2$	11875. 47	1162. 26	1. 426		$^3P_2$	5657. 90	327. 13	1. 340
	$^5P_3$	12435. 85	560. 38	1. 594		$a\ ^1D_2$	13560. 24		1. 120
	$b\ ^3P_0$	16288. 04				$b\ ^1G_4$	25385. 49		1. 085
	$^3P_1$	17375. 00	1086. 96	1. 170		$a\ ^1S_0$	. . .		
	$^3P_2$	18500. 62	1125. 62	1. 441		$a\ ^5D_0$	12600. 87		0. 000
$5d^3(^2G)6s$	$a\ ^3G_3$	11767. 16		0. 908		$^5D_1$	13475. 38	874. 51	1. 498
	$^3G_4$	12705. 33	938. 17	1. 013		$^5D_2$	14494. 87	1019. 49	1. 476
	$^3G_5$	12830. 79	125. 46	1. 280		$^5D_3$	15726. 15	1231. 28	1. 455
	$a\ ^1G_4$	14205. 48		0. 994		$^5D_4$	17231. 19	1505. 04	1. 191
$5d^3(^2D)6s$	$a\ ^3D_1$	14627. 64		0. 854		$b\ ^3H_4$	24432. 83		0. 985
	$^3D_2$	17168. 48	2540. 84	1. 204		$^3H_5$	25414. 13	981. 30	1. 060
	$^3D_3$	18553. 83	1385. 35	1. 355		$^3H_6$	26010. 70	596. 57	1. 117
	$b\ ^1D_2$	23294. 77		1. 118		$b\ ^3G_3$	26829. 13		0. 850
$5d^3(^2H)6s$	$a\ ^3H_4$	15851. 12		0. 916	$5d^4$	$^3G_4$	28165. 40	1336. 27	1. 094
	$^3H_5$	18186. 04	2334. 92	1. 100		$^3G_5$	31267. 10	3101. 70	
	$^3H_6$	17982. 00	−204. 04	1. 146		$d\ ^3F_2$	29843. 58		0. 833
	$a\ ^1H_5$	24226. 20		1. 000		$^3F_3$	. . .		
$5d^3(^2F)6s$	$c\ ^3F_2$	22928. 61		0. 700		$^3F_4$	31531. 70		1. 129
	$^3F_3$	23620. 35	691. 74	1. 076		$d\ ^3P_2$	. . .		
	$^3F_4$	23082. 71	−537. 64	1. 026		$d\ ^3P_1$	31948. 68		1. 000
	$a\ ^1F_3$	24869. 58		0. 995		$d\ ^3P_0$	. . .		
$5d^3(^2P)6s$	$c\ ^3P_0$	23381. 28		0. 000		$c\ ^1G_4$	35151. 35		1. 078
	$^3P_1$	26234. 60	2853. 32	1. 332					
	$^3P_2$	28044. 14	1809. 54	1. 358					
	$a\ ^1P_1$	23406. 13							

TABLE 3. *Odd levels of* Ta II

Level	J	Observed g	Level	J	Observed g	Level	J	Observed g	Level	J	Observed g
29256. 87	2	0. 511	45233. 91	1	1. 458	51073. 92	3	1. 156	57195. 81	1	1. 726
31212. 13	1		45446. 85	2	1. 148	51197. 42	2	1. 359	57791. 58	2	1. 050
32318. 44	3	0. 976	45466. 97	5	1. 090	51326. 31	1	1. 047	58040. 89	4	1. 045
33706. 47	1	0. 285	46174. 60	1	1. 367	51479. 86	4	1. 095	58069. 18	1	1. 147
33715. 27	2	0. 823	46286. 90	4		51534. 28	2	1. 299	58274. 85	2	1. 641
36112. 97	4	1. 180	46295. 03	5	1. 200	51753. 70	5	1. 102	58572. 56	5	
36177. 10	2	0. 946	46387. 16	2	1. 323	52121. 15	3	1. 086	59351. 96	2	1. 160
36763. 70	3	1. 169	46491. 44	2	1. 060	52155. 76	1	1. 613	59692. 16	5	
36987. 71	1	0. 685	46645. 70	4	1. 233	52492. 98	4	1. 101	59838. 00	5	
37230. 75	2	0. 623	46776. 78	2	0. 773	52580. 43	3	1. 412	60241. 07	3	1. 176
38270. 63	3	1. 010	46831. 35	3	1. 214	52824. 49	1	0. 907	60325. 15	3	1. 151
38515. 55	2	1. 006	46850. 64	2	1. 110	52846. 28	6	1. 180	60479. 60	1	0. 662
38535. 21	1	0. 472	47168. 90	3	1. 096	53010. 95	2	1. 464	60549. 32	5	0. 904
38962. 32	3	0. 976	47280. 89	4	1. 190	53234. 65	5	1. 146	60870. 30	2	1. 130
39295. 81	3	1. 138	47514. 52	2	1. 284	53300. 59	2	1. 380	61105. 69	4	1. 007
39743. 67	4	1. 223	47595. 98	1	1. 520	53343. 56	4	1. 071	61357. 45	5	
40023. 68	0		47620. 17	1		53465. 79	3	1. 216	61588. 16	6	
40233. 46	2	1. 165	47801. 03	0		53644. 83	2	1. 352	61608. 62	6	
40304. 78	1	1. 225	47825. 41	3	1. 189	53746. 80	1	1. 234	61694. 17	3	0. 937
40835. 45	6		47829. 75	6	1. 300	54048. 81	5	1. 260	62115. 97	4	1. 070
41144. 94	2	1. 152	47857. 60	5		54206. 69	4	1. 157	62204. 91	5	
41355. 11	1	1. 885	48064. 57	0		54533. 78	2	1. 016	62296. 25	1	0. 600
41554. 42	3	1. 207	48166. 15	2		54648. 73	3	0. 943	62317. 92	2	0. 986
41709. 01	5	1. 244	48223. 08	2	1. 446	55128. 38	3	1. 260	62463. 43	4	1. 167
41775. 29	4	1. 249	48470. 41	4	1. 276	55381. 25	4	1. 020	62854. 50	1	0. 908
42122. 91	4	1. 258	48666. 56	2	1. 131	55505. 08	5	1. 054	63060. 46	2	1. 106
42153. 29	2	1. 212	48776. 29	1	0. 746	55528. 22	1	1. 464	63485. 65	4	
42959. 55	3	1. 120	48962. 54	3	1. 283	55543. 11	3	1. 430	63703. 35	5	0. 977
43064. 86	2	1. 041	49055. 18	5	1. 212	55551. 60	2	1. 031	63820. 47	4	1. 01
43068. 72	0		49080. 51	2	1. 320	55859. 32	2	1. 343	64653. 35	3	1. 079
43544. 46	3	1. 059	49522. 55	5	0. 841	55878. 70	1	1. 425	64909. 19	6	
43553. 67	1		49536. 24	3	1. 317	56018. 76	2	1. 002	65225. 24	4	
43700. 05	5	1. 147	49592. 90	2	1. 629	56142. 53	4	1. 270	65495. 18	3	
44005. 20	4	1. 137	49646. 62	3	1. 048	56351. 09	3	1. 200	65657. 89	3	1. 013
44206. 24	1	0. 242	49886. 51	5		56450. 84	5	1. 045	66545. 40	4	
44259. 20	2	1. 256	49886. 97	1	2. 006	56450. 95	3	1. 195	66610. 27	5	
44430. 39	3	0. 940	49937. 74	4	1. 207	56521. 78	5	0. 980	66930. 35	1	1. 746
44434. 79	0		50314. 43	3	1. 281	56662. 76	6		68213. 70	5	
44585. 17	5	1. 297	50507. 12	5	1. 080	56753. 05	4	1. 197	68299. 80	3	
44626. 00	4	1. 265	50531. 17	1	1. 370	56987. 88	4	1. 118	70892. 62	2	0. 719
44835. 20	3	1. 242	50693. 61	6		57060. 81	3	1. 390	71240. 50	5	1. 214

4. References

[1] C. C. Kiess, J. Research NBS **47,** 385 (1951) RP2266; ibid. **51,** 247 (1953) RP2457.
[2] C. C. Kiess, J. Research NBS **60,** 375 (1958) RP 2856.
[3] H. Kayser, Handbuch der Spectroscopie, S. Hirzel and Co., Leipzig (1912).
[4] G. R. Harrison; Wavelength Tables (John Wiley & Sons, Inc., New York, N.Y., 1939).
[5] E. McMillan and N. R. Grace, Phys. Rev. **44,** 949 (1933).
[6] B. Edlén, J. Opt. Soc. Am. **43,** 339 (1953).
[7] C. C. Kiess, G. R. Harrison, and W. J. Hitchcock, J. Research NBS **44,** 245 (1950) RP2075.
[8] G. J. van den Berg, Dissertation, University of Amsterdam (1951).
[9] R. E. Trees, W. F. Cahill, and P. Rabinowitz, J. Research NBS **55,** 335 (1955) RP2639.
[10] R. E. Trees; Phys. Rev. **123,** 1293 (1961).
[11] R. E. Trees, Bull. Am. Phys. Soc. **3,** 29 (1958).
[12] W. Finkelnburg and W. Humbach, Naturwiss. **42,** 35 (1955).

(Paper 66A2–146)

JOURNAL OF RESEARCH of the National Bureau of Standards—A. Physics and Chemistry
Vol. 66A, No. 2, March–April 1962

Vibration-Rotation Bands of Carbonyl Sulfide

Arthur G. Maki, Earle K. Plyler, and Eugene D. Tidwell

(December 8, 1961)

Thirty-two infrared absorption bands of carbonyl sulfide (OCS) have been measured and are reported here, seventeen for the first time. Seven absorption bands due to isotopic molecules were also measured. Rotational constants have been determined and the evaluation of the anharmonicity constants is discussed.

1. Introduction

Although considerable previous work has been done on the infrared spectrum of OCS [1–3],[1] too few absorption bands had been measured to allow a determination of all the anharmonicity constants of this molecule. This work was undertaken to measure enough bands to enable such a determination to be made. When combined with previously published work, the additional bands reported here should be sufficient to determine the quadratic anharmonicity constants provided the Fermi resonance between ν_1 and $2\nu_2$ is the only vibrational perturbation of appreciable size. However, when the constants were calculated, it was found that some of the constants had varying values depending on the bands used in their determination. This discrepancy will be discussed in a later section.

2. Experimental Procedures

The spectra were measured on the NBS high-resolution spectrometer which has a 5 x 8 in. grating with 10,000 lines/in. The optical arrangement of the spectrometer was designed so that the grating could be used double pass for maximum resolution. With favorable conditions, such as low pressure, the spectrometer will partially resolve lines separated by 0.03 cm^{-1}.

The high resolution was made possible by using a cooled PbS cell as detector. Further details concerning the instrument which was designed and built at the Bureau have been given in a previous publication [4].

The high resolution measurements at wavelengths greater than 4.5 μ were obtained using a 7,500 lines/in. grating and a cooled PbSe detector.

A multiple reflection gas cell with a path length of 8 m was used for the measurements. Various pressures were used although whenever possible pressures of a few mm were employed so that the maximum resolution could be attained. Some variation of the gas temperature was also utilized. Temperatures of 60 °C were sometimes used to aid in identification of lines due to "hot bands."

The spectra were measured by using the fringe system of a Fabry-Perot interferometer as a comparison spectrum. The fringe system and absorption spectrum were recorded simultaneously by the use of a double pen recorder [5]. All wavelengths measured were reduced to wavenumbers in vacuum.

The carbonyl sulfide gas was obtained from the Matheson Company. It contained impurities of CS_2, CO_2, and HCN. It was purified by Roland Florin of the Bureau and the mass spectrometer analysis of the final product showed it to be about 99.8 percent pure. There were very small amounts of CS_2 (0.2%) and HCN (0.03%) in the sample.

Thirty-two bands were measured in the spectral range from 1,890 to 6,100 cm^{-1}. Some of these bands had been measured by previous workers at lower resolution, but those bands were remeasured in the attempt to obtain a more consistent set of energy levels. The 001–000 transition was measured by Callomon and Thompson [1]. They reported the band center at 2062.22 cm^{-1}. In the present work the value obtained was 2062.22 cm^{-1} which is in excellent agreement. Likewise, the agreement is very good between the value of 4101.387 cm^{-1} obtained in this work for $2\nu_3$ and the value 4101.384 cm^{-1} obtained by Saksena, Wiggins, and Rank (see ref. 3).

Since the average spacing of the rotational lines in the bands of OCS is about 0.4 cm^{-1}, the overlapping required very good resolution to reveal the true structure and especially the l-type doubling. In figures 1, 2, and 3 are shown the types of bands observed in three regions of the spectrum. In figure 1 is shown on a slow scan (two cm^{-1} per foot of record) the Q branch and part of the P branch through P10 of the 01^11-000 transition. Overlapping these two branches is the R branch of the 300—000 transition. Figures 2 and 3 are records obtained at a much faster scanning rate (1 ft of record per 15 cm^{-1}). In figure 3 a number of lines arising from water vapor of the atmosphere are superimposed on the spectrum of OCS. These water vapor lines have been identified and marked with a small circle on the figure.

[1] Figures in brackets indicate the literature references at the end of this paper.

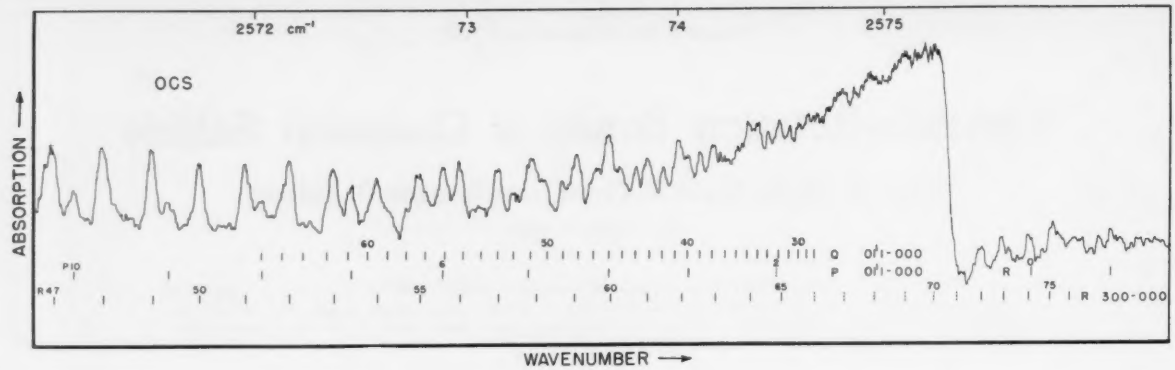

FIGURE 1. *The Q branch of $\nu_2^1+\nu_3$ at 2575.32 cm^{-1}.*
The pressure was 3 cm of Hg with a path of 8 m.

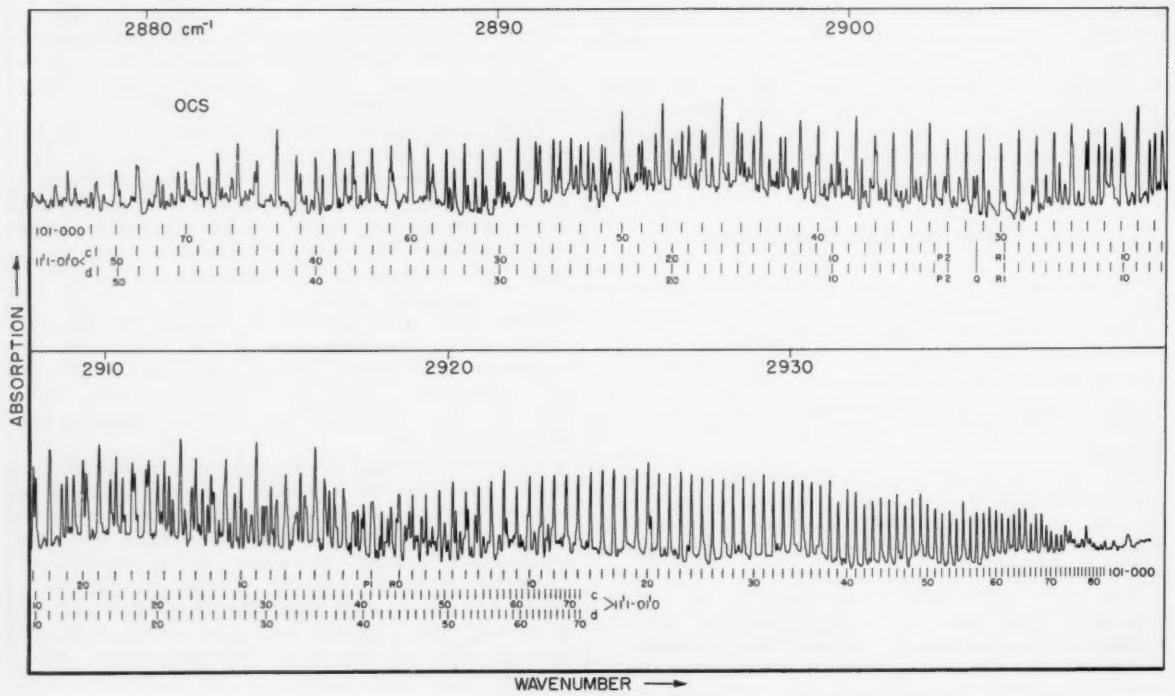

FIGURE 2. *The main band and first "hot band" of the $\nu_1+\nu_3$ transition.*
Path length was 8 m at 1 mm pressure.

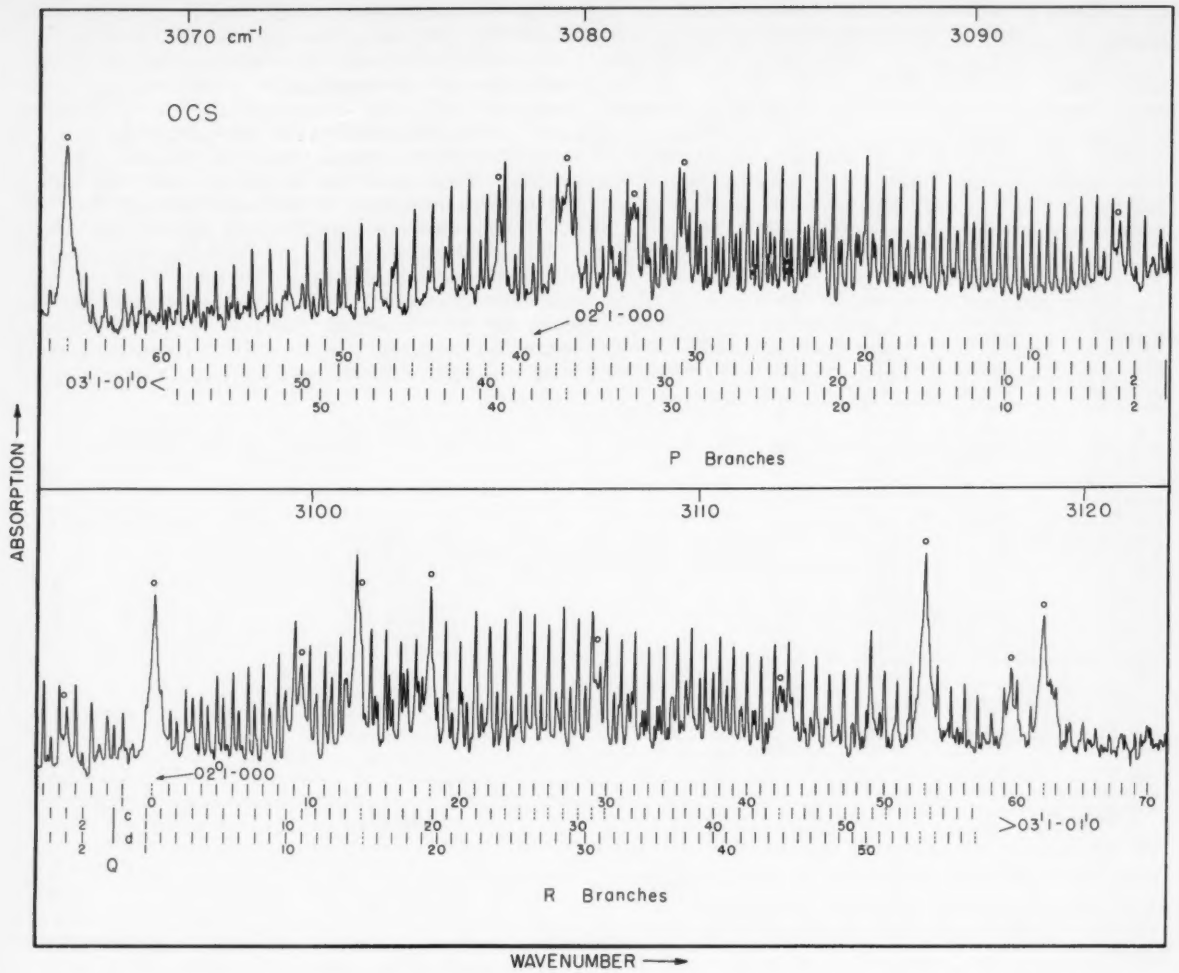

FIGURE 3. *Spectrum of OCS from 3070 cm⁻¹ to 3120 cm⁻¹ obtained at a pressure of 7 mm and a path length of 8 m.*

The circles indicate absorption due to water vapor in the spectrometer.

3. Rotational Analysis

The rotational analyses were made using standard methods of the type described by Herzberg [6]. Since very accurate microwave measurements have been made on all the important isotopic species of OCS in the ground vibrational state and in a number of the lower lying vibrational states [7, 8, 9], no attempt was made to obtain accurate determinations of B″. Table 1 lists the infrared absorption bands of OCS which have been observed. This table also includes a tabulation of the observed values of ΔB. In general the values of ΔB are about what would be estimated for the various bands, but the detailed analysis of the rotational structure gave some ΔB values larger or smaller than expected. This difference may arise from the bands, especially the "hot bands," overlapping thus making the observed position of a line different from the true position.

The microwave rotational data given in references 7, 8, and 9 have been used wherever applicable to this work.

Apparent differences between measured values of α are sufficiently great to warrant investigation of

TABLE 1. *Infrared spectrum of carbonyl sulfide*
All frequencies are in wavenumbers

Upper state	Lower state	Freq. (cm⁻¹)	$B'-B''$	$(D'-D'')\times 10^6$	q'	q''
0 1^1 0	0 0 0	[a] 520.41				
1 0 0	0 0 0	[a] 858.954				
0 2^0 0	0 0 0	1047.1				
2 0 0	0 0 0	[b] 1711.11	−0.00124			
1 3^0 0	0 1^1 0	1891.786	−0.00015			
1 2^0 0	0 0 0	1892.203	+0.000128	−0.41		
0 1^1 1	0 1^1 0	[c] 2054.91	−0.001202			
0 0 1	0 0 0	2062.220	−0.001219	+0.08		
0 4^0 0	0 0 0	2104.830	+0.001150	−0.84		
0 5^1 0	0 1^1 0	[c] 2113.93	+0.00103			
4 0 0	1 0 0	2535.00	−0.00189			
3 1^1 0	0 1^1 0	2536.691	−0.001737			
3 0 0	0 0 0	2556.000	−0.00186	−0.4		
0 2^2 1	0 1^1 0	[d] 2568.38				
0 1^1 1	0 0 0	2575.318	−0.000951 −0.000765	−0.7	0.00019	
2 3^0 0	0 1^1 0	2724.842	−0.000588 −0.000342	1.3 2.0	0.00046	0.00021
2 2^0 0	0 0 0	2731.399	−0.000434	−0.5		
1 1^1 1	0 1^1 0	2903.726	−0.001760 −0.001745	−0.8 −1.1	0.00025	0.00023
2 0 1	1 0 0	2909.511	−0.00129			
1 0 1	0 0 0	2918.116	−0.001765	+0.27		
1 4^0 0	0 0 0	2936.756	+0.000585	−2.90		
0 3^1 1	0 1^1 0	3094.935	−0.000588 −0.000485	+0.9 +1.1	0.00046	0.00025
0 2^0 1	0 0 0	3095.568	−0.0005348	−0.36		
0 6^0 0	0 0 0	3170.636	+0.00157			
0 0 2	1 0 0	3242.439	−0.001814	1.6		
4 0 0	0 0 0	3393.95	−0.00249			
2 0 1	0 0 0	3768.48	−0.00178			
1 2^0 1	0 0 0	[b] 3937.434	−0.001003			
0 1^1 2	0 1^1 0	4086.692	−0.002390 −0.002388	1.3 0.3		
0 0 2	0 0 0	4101.387	−0.002426	[e] −0.115		
0 4^0 1	0 0 0	[e] 4141.216	−0.000032	2.087		
3 0 1	0 0 0	[e] 4609.842	−0.002998	0.034		
2 2^0 1	0 0 0	[e] 4773.222	−0.001493	0.260		
1 1^1 2	0 1^1 0	4932.067	−0.002845 −0.002827		0.00032	0.00028
1 0 2	0 0 0	4953.876	−0.002843	1.8		
2 0 2	0 0 0	[b] 5801.914	−0.00332			
0 1^1 3	0 1^1 0	6095.47	−0.00360			
0 0 3	0 0 0	[e] 6117.572	−0.003618	−0.335		

[a] Obtained by Ritz principle (observed ν_1=859.0).
[b] See reference 2.
[c] See reference 1.
[d] Only Q branch was observed.
[e] See reference 3.

the possible effect of the rotation constants quadratic in v (the γ_{ij} terms). Enough microwave data is available to allow calculation of some of the γ_{ij} terms defined by

$$B_{v_1v_2v_3}=B_e-\sum_i \alpha_i(v_i+\tfrac{1}{2}d_i)+\sum_{ij}\gamma_{ij}(v_i+\tfrac{1}{2}d_i)(v_j+\tfrac{1}{2}d_j)$$

where $j\geq i=1,2,3$ and $d_1=d_3=1$, $d_2=2$. Other γ_{ij} terms may be evaluated from infrared values of ΔB. The resulting constants obtained in this way are tabulated in table 2.

All the γ's which have been found except γ_{13} are of the order of magnitude which one would expect. Both values found for γ_{13} are almost certainly incorrect. The largest value of γ_{13} is obtained from data for the bands $\nu_1+\nu_3$ and $2\nu_2^0+\nu_3$. The precision of this data is very good and the deviation is considered to be somewhat greater than might be expected from experimental error. Since the band $\nu_1+\nu_3$ is only 18.5 cm^{-1} from the band $\nu_1+4\nu_2^0$, resonance between these two bands might be responsible for the discrepancy in the rotational constants, even though the coupling parameter would be expected to be small. Another possibility is that the "l-type resonance" described by Amat and Nielsen [9a] may be creating an apparent error in the ΔB value.

The same situation is found for $\nu_1+\nu_3$ and $2\nu_2^0+\nu_3$ of $OC^{13}S$. By using the microwave value of $\alpha_2=-0.000336$ cm^{-1} and the infrared value of $\alpha_3=0.001142$ cm^{-1} the unperturbed value of α_1 calculated from the ΔB's for $\nu_1+\nu_3$ and $2\nu_2^0+\nu_3$ is 0.000540 cm^{-1}. This is smaller than the perturbed value of α_1 (0.000596) obtained from microwave measurements. This result is, of course, not real and is further evidence that, in both $O^{16}C^{12}S^{32}$ and $O^{16}C^{13}S^{32}$, the Fermi diad $\nu_1+\nu_3$ and $2\nu_2^0+\nu_3$ may be perturbed.

The splitting due to l-type doubling was observed in four $\pi-\pi$ transitions. The measurements were not extensive enough to determine the exact dependence of the doubling constant q on vibrational quantum number. It is quite evident, however, that q is approximately proportional to $(v_2+1)/2$ as expected.

TABLE 2. *Rotational constants for OCS*

$O^{16}C^{12}S^{32}$
$\alpha_2=-0.000348$[a] cm^{-1}
$\alpha_3-2\gamma_{33}-\gamma_{23}-\frac{1}{2}\gamma_{13}=0.001213$ cm^{-1}
$\alpha_1-2\gamma_{11}-\gamma_{12}-\frac{1}{2}\gamma_{13}=0.000683$[a] cm^{-1}
$\gamma_{11}\approx 0$ (assumed value)
$\gamma_{33}>-0.3\times10^{-5}$
$\gamma_{22}=-0.05$[a]$\times10^{-5}$
$\gamma_{12}=+0.68$[a]$\times10^{-5}$
$\gamma_{23}=+0.35\times10^{-5}$
$\gamma_{13}=10\times10^{-5}$ or 5×10^{-5}
$O^{16}C^{13}S^{32}$
α_3[b] $=0.001142$ cm^{-1}
$O^{18}C^{12}S^{32}$
α_3[b] $=0.001177$ cm^{-1}
$O^{16}C^{12}S^{34}$
α_3[b] $=0.001182$ cm^{-1}

[a] Calculated from microwave frequencies using $c=2.997930\times10^{10}$ cm/sec.
[b] These were determined by neglecting the γ_{ij} terms.

4. Vibrational Analysis and Vibrational Constants

Table 1 contains a list of the absorption bands and constants which have now been measured for OCS. Included in this list are a number of transitions in which the lower state is a vibrationally excited state. By using the following combinations:

$$(400\text{–}000)-(400\text{–}100)=3393.95-2535.00=858.95 \text{ cm}^{-1}$$
$$(002\text{–}000)-(002\text{–}100)=4101.387-3242.439=858.948 \text{ cm}^{-1}$$
$$(201\text{–}000)-(201\text{–}100)=3768.48-2909.511=858.97 \text{ cm}^{-1}$$

a weighted average value of 858.954 cm^{-1} is found for ν_1. This is in very good agreement with a value of 859.03 which we have measured on a small commercial grating spectrometer. The value of ν_2 is determined to be 520.41 cm^{-1} by using (01^11–000)

$-(01^{1}1-01^{1}0)$. This may be compared with the value of 521.5 found by Bartunek and Barker [10]. The $2\nu_2^0$ band has also been measured in this laboratory on a small commercial grating spectrometer and the band center was found to be 1047.1 cm^{-1}. The rotational structure of this band was rather poorly resolved so that the band center could only be determined with certainty within one value of J.

Seven absorption bands have also been measured and assigned to isotopic species other than $O^{16}C^{12}S^{32}$. These are given in table 3. More absorption bands have been found for $OC^{13}S$ than for OCS^{34}, although the abundance ratio is 1:4. This is undoubtedly due to the greater shift in absorption frequencies for $OC^{13}S$.

TABLE 3. *Observed infrared bands of isotopic OCS*

All frequencies given in wavenumbers

Upper state	Lower state	Freq.	$B'-B''$	$D'-D''\times10^8$
$O^{16}C^{13}S^{32}$				
0 1^{1} 1	0 1^{1} 0	2002.425	−0.00111	----------
0 0 1	0 0 0	2009.249	−0.00115	−0.6
1 0 1	0 0 0	2861.08	−0.001635	−2
0 2^{0} 1	0 0 0	3012.89	−0.000517	----------
0 0 2	0 0 0	3996.50	−0.00228	----------
$O^{18}C^{12}S^{34}$				
0 0 2	0 0 0	4099.873	−0.002364	−0.5
$O^{18}C^{12}S^{32}$				
0 0 2	0 0 0	4030.390	−0.002354	----------

With the large amount of vibrational data now available, it is possible to calculate some of the quadratic vibrational constants by two or more independent methods. Upon neglecting the cubic terms (y_{ijk}) three different values are found for the combination $x_{11}+4x_{22}+x_{12}$. These are −5.37, −5.01, and −3.63 cm^{-1}. The disagreement indicates that either the cubic terms must be taken into account, or else an unexpected perturbation is present. For the series ν_3, $2\nu_3$, $3\nu_3$ it has previously been shown [2] that only a very small cubic term is required to give nearly perfect agreement between calculated and observed frequencies. This is also the case for the "hot bands" of these transitions. From these bands the pertinent cubic constants are found to be $y_{233}=-0.03$ cm^{-1} and $y_{333}=+0.01$ cm^{-1}. Both of these are of the expected order of magnitude. These are the only cubic terms which can be determined explicitly from the available data without determining the unperturbed frequencies of the resonating vibrations.

One can also evaluate various combinations of quadratic and cubic constants by suitable combinations of the sums of various Fermi resonant multiplets but the resulting values are of dubious accuracy. One such combination yields $y_{113}+4y_{233}+y_{123}=1.38$ cm^{-1} which seems rather large for such a heavy molecule.

Because of inconsistencies in the values of the ΔB's for the Fermi resonant bands, it seems premature at this time to find the unperturbed frequencies of these vibrations. Further very careful work must be done on OCS in order to ascertain whether any further perturbations are present.

5. References

[1] H. J. Callomon and H. W. Thompson, Proc. Roy. Soc. **A222,** 431 (1954).
[2] H. C. Allen, E. K. Plyler, and L. R. Blaine, J. Chem. Phys. **26,** 400 (1957).
[3] G. D. Saksena, T. A. Wiggins, and D. H. Rank, J. Chem. Phys. **31,** 839 (1959).
[4] E. K. Plyler and L. R. Blaine, J. Research NBS **62,** 7 (1959).
[5] E. K. Plyler, L. R. Blaine, and E. D. Tidwell, J. Research NBS **55,** 183 (1955).
[6] G. Herzberg, Infrared and Raman spectra of polyatomic molecules (D. Van Nostrand Co., Inc., New York, 1954).
[7] C. H. Townes and A. H. Schawlow, Microwave Spectroscopy (McGraw-Hill Book Co., Inc., New York, 1955).
[8] W. C. King and W. Gordy, Phys. Rev. **93,** 407 (1954).
[9] M. Peter and M. W. P. Strandberg, Phys. Rev. **95,** 622 (1954).
[9a] G. Amat and H. H. Nielsen, J. Mol. Spectroscopy **2,** 163 (1958).
[10] P. Bartunek and E. F. Barker, Phys. Rev. **48,** 516 (1935).

(Paper 66A2–147)

JOURNAL OF RESEARCH of the National Bureau of Standards—A. Physics and Chemistry
Vol. 66A, No. 2, March–April 1962

Ionization in the Plasma of a Copper Arc

Charles H. Corliss

(December 8, 1961)

From the relative intensities of arc and spark lines observed in a d-c arc in air between copper electrodes, the degree of ionization of eleven elements added to the copper has been determined. With the aid of Saha's ionization equation, the electron density in the arc was calculated to be 2.4×10^{14} cm^{-3}. Partition functions for atoms and ions of 29 elements are newly calculated or estimated and a table of first ionization potentials and partition functions of atoms and ions for seventy elements is presented. The degree of ionization of seventy elements separately added to the arc is calculated. The electron density in the arc is confirmed by three independent spectroscopic and electrical determinations. The data developed in this paper will enable the calculation of relative transition probabilities from the intensities in the NBS Tables of Spectral-Line Intensities.

1. Introduction

It is possible to determine the relative transition probabilities for the lines of a particular spectrum emitted by a hot gas, from measurements of the relative intensities of those lines, provided that the excitation in the radiating gas can be described by Boltzmann's law. It is necessary to know only the temperature of the gas. If the relative transition probabilities for lines of both the first and second spectra of an element are to be determined on the same scale, the degree of ionization in the radiating gas must be found.

In this paper we shall investigate the ionization in the positive column or plasma of a 10 amp d-c arc in air between copper electrodes. This is the arc which served as the light source for obtaining the intensity values reported in the NBS Tables of Spectral-Line Intensities [1][1].

In that work, an element under investigation was mixed with pure copper powder in the atomic ratio of 1 to 1,000. The mixtures were pressed into solid cylindrical pellets ¼ in. in diameter, ¼ in. in length, and weighing about 1½ g. The pellets were mounted as electrodes in water-cooled clamps and a direct current of 10 amp passed between them from a 220-v line with a resistive ballast. A 3-mm gap between the electrodes was imaged entirely within the aperture of a stigmatic grating spectrograph by a lens at the slit. In this arrangement light from all parts of the arc stream contributed to the spectral-line intensities. Although the temperature and electron density in the arc stream are functions of the axial and radial positions, we deal here only with mean values which are inherently weighted according to the intensity distribution in the arc. The excitation in this light source has been shown in a previous paper [2] to follow Boltzmann's law.

2. Relative Intensities of Arc and Spark Lines

When the intensity ratio of lines from neutral atoms and ions of an element is known in such a light source, it is possible to calculate the relative particle density of atoms and ions for that element, if the absolute transition probabilities or absolute gf-values for those lines are available. Designating quantities associated with a neutral atom and its spectrum by the superscript ° we can write the Einstein-Boltzmann equation for the intensity of a line of that spectrum in the form

$$I^\circ=\frac{N^\circ}{u^\circ}h\nu^\circ g^\circ A^\circ e^{-\frac{E^\circ}{kT}}. \tag{1}$$

In this equation N° is the particle density of neutral atoms, u° is the partition function for the atom which expresses the distribution of neutral atoms over their possible energy states, $h\nu^\circ$ is the energy of a single photon, g° is the statistical weight of the upper state, A° is Einstein's transition probability for the particular line, E° is the energy of the upper state, k is Boltzmann's constant and T is the temperature of the copper arc. If we write a similar equation, designating quantities associated with an ion and its spectrum by the superscript $^+$, and take the ratio of the two equations, we obtain

$$\frac{I^\circ}{I^+}=\frac{N^\circ}{N^+}\frac{u^+}{u^\circ}\frac{\nu^\circ}{\nu^+}\frac{g^\circ A^\circ}{g^+A^+}e^{+\frac{E^+-E^\circ}{kT}}. \tag{2}$$

For convenience we make appropriate substitutions of λ instead of ν and gf instead of gA and solve for N^+/N°.

$$\frac{N^+}{N^\circ}=\frac{(I\lambda^3)^+}{(I\lambda^3)^\circ}\frac{u^+}{u^\circ}\frac{(gf)^\circ}{(gf)^+}e^{+\frac{E^+-E^\circ}{kT}}. \tag{3}$$

For computation we take common logarithms and insert a numerical value for Boltzmann's constant.

$$\log\frac{N^+}{N^\circ}=\log\frac{(I\lambda^3)^+}{(I\lambda^3)^\circ}+\log\frac{u^+}{u^\circ}+\log\frac{(gf)^\circ}{(gf)^+}+\frac{625}{T}(E^+-E^\circ). \tag{4}$$

In (4), E is in kilokaysers and T is in °K.

[1] Figures in brackets indicate the literature references at the end of this paper.

Of the 70 elements in the NBS Tables of Spectral-Line Intensities, there are, at present, only 11 for which all the quantities on the right side of eq (4) are known. The data used in obtaining the numerical solutions are given in table 1. The 11 atoms and ions are listed in order of atomic number in column 1. The wavelengths and intensities for the first term of the right member of eq (4) are taken from the Tables of Spectral-Line Intensities and given in columns 2 and 3. In most cases, the total intensity for a multiplet is used; and only the first 4 figures of the wavelength of the leading line in the multiplet are listed. When f-values were available for more than one multiplet, an attempt was made to select multiplets of moderately high intensity for each spectrum. In cases where a single line is used, the decimals are given also. For the second term we list in column 4 the partition functions calculated by Claas and given in tables 27 and 29 of his paper [3]. In column 5 are found the sums of the absolute gf-values for the lines. With two exceptions, only theoretical gf-values or experimental relative values adjusted to a theoretical absolute scale are employed. This is done because of the scarcity of experimental absolute values, especially for second spectra. The value for Cd I, however, is a measurement in absorption by King and Stockbarger [4]. The value used for Pb II is Stephenson's measurement [5] for the corresponding transition in isoelectronic Tl I. References to the origin of the absolute gf-values are given in column 6.

The energy levels of the upper states given in column 7 are taken from the Tables of Spectral-Line Intensities and are given in units of kilokaysers (1 kK=1000 cm^{-1}). For multiplets, weighted mean values are given. These values are used in the last term of eq (4) along with the temperature of the copper arc determined in a previous paper [2]. This temperature (5,100 °K) was determined by comparing 31 sets of experimental relative transition probabilities with the corresponding spectral-line intensities measured in the copper arc and reported in the Tables of Spectral-Line Intensities. The log ratio N^+/N° calculated from the data in the table by means of eq (4) is given in column 8 and the percent ionization of the element in column 9 is simply

$$\frac{100N^+}{N^\circ+N^+}=\frac{100N^+/N^\circ}{1+N^+/N^\circ}.$$

The principal source of error in these determinations of ionization lies in the absolute gf values, which are uncertain by more than a factor of 2. The intensities contribute an uncertainty of 20 percent, and the temperature of the copper arc contributes from 2 percent to 12 percent, depending on the value of (E^+-E°).

3. The Ionization Equation

The procedure used for the 11 elements discussed in the previous section cannot be employed for the determination of the degree of ionization of the remaining 59. For these latter elements, the equation of ionization first developed by Saha [11] will be used. This is an equation describing the equilibrium existing, in a hot gas, between the relative concentration of atoms and ions of any particular atomic species and the concentration of free electrons, as a function of the temperature of the gas and the ionization potential of the atom under study. For our purpose it is convenient to write it in the form

$$\frac{N^+}{N^\circ}N_e=\frac{(2\pi mkT)^{3/2}}{h^3}\frac{2u^+}{u^\circ}e^{-\frac{V}{kT}} \qquad (5)$$

where N_e is the electron density, m is the mass of the electron, and V is the ionization potential of the atom.

TABLE 1. *Experimental determination of ionization for eleven elements in the copper arc*

Atom or ion	Wavelength	Intensity	u	gf	Reference	E	$\text{Log}\frac{N^+}{N^\circ}$	Percent ionization
	A					kK		
Be°	3321	160	1.0	3.06	[6]	52.082	−1.236	5.5
Be+	3130	800	2.0	1.50	[6]	31.932		
Mg°	3838	940	1.0	6.0	[7]	47.957	−0.852	12
Mg+	2795	1,600	2.0	1.80	[7]	35.72		
Ca°	4226.73	1,100	1.2	1.46	[8]	23.652	.957	90
Ca+	3933	6,400	2.2	2.20	[9]	25.3		
Sc°	5671	598	12.1	11.	[7]	29.16	.761	85
Sc+	3613	6,606	23.2	6.9	[7]	27.65		
Ti°	4305	1,636	30.4	7.4	[7]	29.98	−.056	47
Ti+	3759	532	55.9	5.	[7]	31.36		
V°	4111	2,760	48.8	7.3	[7]	26.59	.284	66
V+	3093	1,936	43.0	11.2	[7]	35.06		
Zn°	4810	280	1.0	1.0	[7]	53.672	−2.931	0.12
Zn+	2061	15.5	2.0	1.8	[10]	48.62		
Sr°	4607.33	650	1.3	1.8	[7]	21.698	1.564	97
Sr+	4077	7,800	2.2	1.87	[7]	24.19		
Cd°	3261.06	32	1.0	0.0022	[4]	30.656	−0.608	20
Cd+	2265	170	2.0	1.8	[10]	45.01		
Ba°	5535.48	650	2.5	1.92	[7]	18.060	1.569	97
Ba+	4554	8,500	4.3	2.0	[7]	21.65		
Pb°	2401.95	36	1.6	0.064	[10]	49.440	−0.260	35
Pb+	2203.53	9	2.1	.604	[5]	59.448		

3.1. Electron Density

For the 11 elements treated in the previous section all quantities in eq (5) are known except N_e. The mean value of N_e determined from the evaluation of these 11 cases can be used to calculate N^+/N° for other elements for which partition functions and ionization potentials are known or can be estimated.

For computation we write eq (5) in the form

$$\log N_e=21.245-0.988\text{V}-\log\frac{N^+}{N^\circ}-\log\frac{u^\circ}{u^+} \qquad (6)$$

in which T is taken to be 5,100 °K, and V is in volts. The 11 values of N_e are given in table 2. Logarithmic averaging is appropriate here because errors proportional to the magnitudes of the quantities are involved.

TABLE 2. *Calculation of electron density* N_e

Element	V	u°/u^+	log N_e
Be	9.320	0.500	13.574
Mg	7.644	.500	14.846
Ca	6.111	.545	14.514
Sc	6.54	.522	14.306
Ti	6.82	.544	14.825
V	6.74	1.135	14.246
Zn	9.391	0.500	15.199
Sr	5.692	.591	14.285
Cd	8.991	.500	13.271
Ba	5.210	.582	14.764
Pb	7.415	.762	14.297
Average			14.375±0.413

The average value of electron density determined from the values in table 2 is 2.4×10^{14} electrons/cm^3. This corresponds to an electron pressure of 170 dynes/cm^2 or 1.7×10^{-4} atm at 5,100 °K. The average deviation in log N_e, given in table 2, corresponds to a range of N_e from 0.9 to 6×10^{14} cm^{-3}.

This large uncertainty originates in the uncertainty of the absolute values of gf. Consequently, it appears that the degree of ionization of the 11 elements listed in table 1 would be more accurately determined by recalculating N^+/N° from eq (6), using the mean value of N_e obtained in table 2. We will adopt this procedure and calculate the degree of ionization for all 70 elements. Rewriting eq (6) and substituting the mean value of log N_e, we have

$$\log \frac{N^+}{N^\circ}=6.870-0.988V-\log \frac{u^\circ}{u^+}. \qquad (7)$$

The straight line in figure 1 is a plot of this equation. The points represent the directly determined experimental values from table 1. The slope of the line is fixed by the temperature (5,100 °K) determined in a previous paper [2] on the assumption of a Boltzmann distribution of energy. The location of the points with respect to this slope indicates that this temperature is appropriate to the calculation of ionization as well as excitation.

3.2. Ionization Potentials and Partition Functions

For accurate solutions of eq (7) we need good values of the ionization potentials and the partition functions. Ionization potentials listed in table 3, column 3 are taken from volume III, table 34 of C. E. Moore's Atomic Energy Levels [12] with the exception of those for the rare earths and the more recent values for Ge [13], Hf [14], Os [15], and Ir [16]. For the rare earths, fairly good spectroscopic values are available for Sm [17], Eu [18], Gd [19], Yb [14], and Lu [20]. The ionization potentials of the remaining rare earths are unknown, but as a group

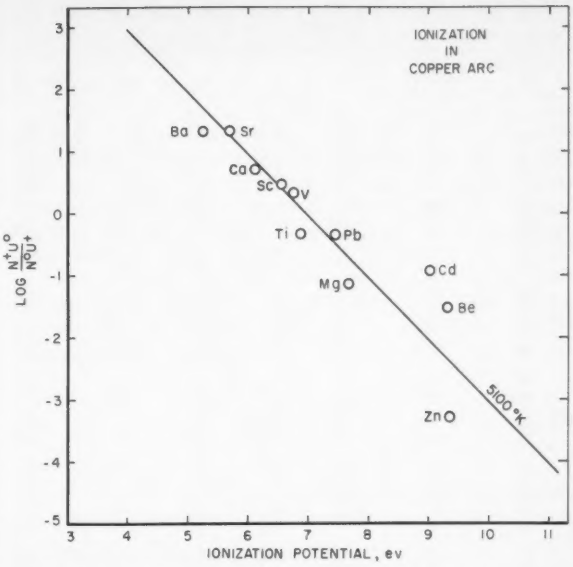

FIGURE 1. *Degree of ionization in a copper arc in air.*
The points are the experimentally determined values for eleven elements. The straight line represents Saha's ionization equation for a temperature of 5,100 °K and an electron density of 2.4×10^{14} cm^{-3}.

these elements are remarkably uniform in their ease of ionization. The values given in parentheses are estimates based in some cases on adjusted nonspectroscopic values [21], [22]. They are likely to be not more than 10 percent from the true value.

The partition functions at 5,100 °K for the 41 elements Li through Ge, Rb through Mo, Pd through Sn, Cs through La, and Hg through Bi in columns 4 and 5 of table 3 are taken from Claas [3]. Partition functions for 18 additional elements for which knowledge of the spectral terms is reasonably complete were calculated from the equation

$$\mu=\sum_n g_n e^{-\frac{E_n}{kT}}=\sum_n g_n\, 10^{-0.1225E_n} \qquad (8)$$

for all levels up to 14 kK. Above that value the Boltzmann factor is less than 2 percent. The partition functions for the 11 remaining elements could not be accurately determined because knowledge of the spectral terms is incomplete or wholly lacking. Estimated or assumed values, based partly on spectral structures predicted by Klinkenberg [23], and partly on comparison of the character of the observed spectrum with that of similar analysed spectra are given in parentheses.

The method given above for calculating partition functions for well-analysed spectra gives values in agreement to about 5 percent with those calculated by Claas. The assumed values (in parentheses) probably differ from the true values by less than a factor of 2. The more reliable values and estimates suggest that for most of the rare earths the value of u°/u^+ lies between 0.4 and 0.8; accordingly, a value of 0.6 has been assumed for the inadequately analysed rare earths. This may be accurate to 50 percent.

TABLE 3. *Ionization potentials and partition functions for seventy elements*

Z	Element	V	u°	u^+	u°/u^+	log u°/u^+
3	Li	5.390	2.1	1.0	2.1	0.322
4	Be	9.320	1.0	2.0	0.50	−.301
5	B	8.296	6.0	1.0	6.0	.778
6	C	11.256	9.3	6.0	1.55	.190
11	Na	5.138	2.1	1.0	2.1	.322
12	Mg	7.644	1.0	2.0	0.50	−.301
13	Al	5.984	5.9	1.0	5.9	.771
14	Si	8.149	9.5	5.7	1.67	.223
15	P	10.484	4.5	8.2	0.55	−.260
19	K	4.339	2.2	1.0	2.2	.342
20	Ca	6.111	1.2	2.2	0.55	−.260
21	Sc	6.54	12.1	23.2	.522	−.282
22	Ti	6.82	30.4	55.9	.544	−.264
23	V	6.74	48.8	43.0	1.135	.055
24	Cr	6.764	10.6	7.3	1.45	.161
25	Mn	7.432	6.5	7.8	0.83	−.081
26	Fe	7.87	28.5	43.6	0.654	−.184
27	Co	7.86	33.1	30.0	1.103	.042
28	Ni	7.633	30.6	11.0	2.78	.444
29	Cu	7.724	2.4	1.0	2.4	.380
30	Zn	9.391	1.0	2.0	0.50	−.301
31	Ga	6.00	5.2	1.0	5.2	.716
32	Ge	7.899	7.7	4.4	1.75	.243
33	As	9.81	4.6	6.0	0.77	−.114
34	Se	9.75	7.5	4.2	1.8	.255
37	Rb	4.176	2.3	1.0	2.3	.362
38	Sr	5.692	1.3	2.2	0.59	−.229
39	Y	6.38	12.1	16.2	.75	−.125
40	Zr	6.84	35.3	46.6	.758	−.120
41	Nb	6.88	25.4	23.2	1.095	.039
42	Mo	7.10	8.7	7.5	1.16	.064
44	Ru	7.364	33.6	23.3	1.44	.158
45	Rh	7.46	26.2	15.0	1.75	.243
46	Pd	8.33	3.1	7.5	0.41	−.387
47	Ag	7.574	2.0	1.0	2.0	.301
48	Cd	8.991	1.0	2.0	0.50	−.301
49	In	5.785	4.2	1.0	4.2	.623
50	Sn	7.342	5.3	3.2	1.66	.220
51	Sb	8.639	4.74	3.43	1.38	.140
52	Te	9.01	6.30	4.40	1.43	.155
55	Cs	3.893	2.5	1.0	2.5	.398
56	Ba	5.210	2.5	4.3	0.58	−.237
57	La	5.61	20.2	30.2	.67	−.174
58	Ce	(5.6)	(110)	190	(.6)	−.22
59	Pr	(5.5)	(50)	(86)	(.6)	−.22
60	Nd	(5.5)	(50)	(86)	(.6)	−.22
62	Sm	5.6	(35)	(57)	(.6)	−.22
63	Eu	5.67	9.2	15.7	.59	−.229
64	Gd	6.16	51	78	.65	−.187
65	Tb	(6)	(50)	(80)	(.6)	−.22
66	Dy	(6)	(36)	(60)	(.6)	−.22
67	Ho	(6)	(36)	(60)	(.6)	−.22
68	Er	(6)	(50)	(80)	(.6)	−.22
69	Tm	(6)	(10)	(17)	(.6)	−.22
70	Yb	6.2	1.00	2.00	.50	−.301
71	Lu	6.15	8.52	1.39	6.13	.788
72	Hf	6.8	13.9	12.3	1.13	.053
73	Ta	7.88	16.4	22.1	0.74	−.131
74	W	7.98	11.9	12.8	.93	−.032
75	Re	7.87	6.7	7.0	.96	−.018
76	Os	8.5	19.0	17.6	1.08	.033
77	Ir	9.1	20.9	(14)	(1.5)	.18
78	Pt	9.0	19.8	9.65	2.05	.312
79	Au	9.22	2.45	1.10	2.23	.348
80	Hg	10.43	1.0	2.0	0.50	−.301
81	Tl	6.106	2.5	1.0	2.5	.398
82	Pb	7.415	1.6	2.1	0.76	−.119
83	Bi	7.287	4.3	1.1	3.9	.591
90	Th	(6)	19.0	34.3	0.554	−.256
92	U	(6)	(54)	(80)	(.67)	−.17

TABLE 4. *Degree of ionization for seventy elements*

Z	Element	log N^+/N°	N^+/N°	Percent ions	Percent atoms
3	Li	1.223	16.7	94.4	5.65
4	Be	−2.037	0.0092	0.91	99
5	B	−2.104	.0079	.78	99
6	C	−4.441	.000036	.0036	100
11	Na	1.472	29.6	96.7	3.26
12	Mg	−0.381	0.42	29.4	71
13	Al	.187	1.54	61	39.4
14	Si	−1.404	0.039	3.8	96
15	P	−3.228	.00059	0.059	100
19	K	2.241	174	99.4	0.571
20	Ca	1.092	12.4	92.5	7.5
21	Sc	0.692	4.9	83	16.9
22	Ti	.394	2.48	71	28.8
23	V	.155	1.43	59	41
24	Cr	.026	1.06	51.5	49.5
25	Mn	−.392	0.406	28.9	71
26	Fe	−.726	.188	15.8	84
27	Co	−.942	.114	10.3	90
28	Ni	−1.115	.077	7.1	93
29	Cu	−1.141	.0723	6.74	93
30	Zn	−2.107	.0078	0.776	99.2
31	Ga	0.226	1.68	62.7	37.3
32	Ge	−1.177	0.066	6.24	93.8
33	As	−2.706	.00197	0.197	99.8
34	Se	−3.015	.00097	.097	99.9
37	Rb	2.382	241	99.6	0.413
38	Sr	1.475	29.8	97	3.24
39	Y	0.695	5.0	83	16.8
40	Zr	.230	1.70	63	37
41	Nb	.031	1.07	52	48
42	Mo	−.204	0.62	38	62
44	Ru	−.564	.273	21.4	79
45	Rh	−.743	.181	15.3	85
46	Pd	−.973	.106	9.6	90
47	Ag	−.914	.122	10.9	89.1
48	Cd	−1.712	.0194	1.90	98.1
49	In	0.531	3.40	77.3	22.7
50	Sn	−.604	0.249	19.9	80.1
51	Sb	−1.805	.0157	1.55	98.4
52	Te	−2.185	.0065	0.65	99
55	Cs	2.626	423	99.8	0.236
56	Ba	1.960	91.2	98.9	1.08
57	La	1.504	31.9	97	3.0
58	Ce	1.56	36	97	2.8
59	Pr	1.69	49	98	2.0
60	Nd	1.66	45	98	2.2
62	Sm	1.59	39	98	2.5
63	Eu	1.499	31.6	96.9	3.1
64	Gd	0.967	9.3	90.3	9.7
65	Tb	1.09	12.	92	8
66	Dy	1.09	12	92	8
67	Ho	1.09	12	92	8
68	Er	1.09	12	92	8
69	Tm	1.09	12	92	8
70	Yb	1.07	11.8	92	7.8
71	Lu	0.002	1.00	50.1	49.9
72	Hf	.117	1.31	57	43
73	Ta	−.789	0.163	14.0	86
74	W	−.978	.105	9.5	90
75	Re	−.892	.128	11.4	89
76	Os	−1.56	.027	2.7	97
77	Ir	−2.31	.0049	0.49	99
78	Pt	−2.34	.0046	.45	99
79	Au	−2.588	.00258	.257	99.7
80	Hg	−3.129	.00074	.074	99.9
81	Tl	0.439	2.75	73.3	26.7
82	Pb	−.337	0.46	31.5	68.5
83	Bi	−.921	.120	10.71	89.3
90	Th	1.13	13.5	93	7
92	U	1.04	11	92	8

3.3. Degree of Ionization for 70 Elements

Using the ionization potentials and the ratios of the partition functions from table 3, we have evaluated eq (7) for each of the 70 elements added to the copper arc. The results are given in table 4. Values in this table are to be preferred to the 11 individually determined values in table 1. It is interesting to note in table 4 the periodicities of N^+/N° versus atomic number. This ratio varies more smoothly than the well known variation of the ionization potential with atomic number.

At this point we may remark that for every 1,000 copper atoms in the copper arc stream, 67 electrons are contributed from copper ions. Even in the case of the most highly ionized added element not more than one electron can be contributed for every 1,000 atoms of copper. It is clear, then, that the added elements cannot affect the electron density in the arc.

It should also be pointed out that the degree of double ionization in the arc is negligible in its effect on the ratio of atoms to ions. Of the elements added to the copper, the one which may be expected to yield the largest number of doubly charged ions is barium. An evaluation of eq (7) for the ratio Ba^{++}/Ba^{+} shows that the proportion of barium which will be doubly ionized is only 0.02 percent.

4. Independent Estimates of Electron Density

To confirm the value of electron density determined in the foregoing section, we have estimated N_e by three other methods, two of which do not involve spectroscopic observations.

4.1. Relative Intensities of Copper and Oxygen Lines

In the spectrum of the copper arc in air, several lines of O I are observed in the infrared. By comparing the relative intensities of these lines with those of Cu I by the method given in section 2 for arc and spark lines, we may derive the relative particle density of copper and oxygen atoms. If we know the composition of air at 5,100 °K, we know the particle density of oxygen in the plasma and can calculate that of copper.

TABLE 5. *Determination of relative particle density of oxygen and copper atoms*

Spectrum	Wavelength	Intensity	u°	gf	Ref	E	$\log \frac{N^\circ_O}{N^\circ_{Cu}}$
	A					*kK*	
O I	7774	68	8.9	5.2	[10]	86.6	2.660
Cu I	8408.15	4.5	2.3	0.007	[10]	55.0	

The pertinent data for the lines of oxygen and copper are given in table 5, which is similar in presentation to table 1. Evaluating the analog of eq (4) for N°_{Cu}/N°_O, we find that there are about 457 oxygen atoms for every copper atom in the arc. According to Hilsenrath et al. [24], the atomic oxygen content of air at 5,100 °K is 30 mole percent so that there are 1,500 particles of air for every atom of copper. If we divide the particle density of air at atmospheric pressure and 5,100 °K (1.44×10^{18} cm^{-3}) by 1,500, we find that the particle density of copper atoms is 9.6×10^{14} cm^{-3}. Now if in eq (6) we were to let $N^+_{Cu}=N_e$ and $N^\circ_{Cu}=9.6\times10^{14}$, introduce the ionization potential and partition functions for copper and solve for N_e, we would find $N_e=1.3\times10^{14}$ cm^{-3}.

However, it may be that not all of the electrons come from the ionization of copper. According to Gilmore's tables of the equilibrium composition of air [25], the electron concentration in air at atmospheric pressure and 5,100 °K is 0.007 mole percent or 1.0×10^{14} cm^{-3}. This represents the difference between the concentrations of the positive ions of NO and the negative ions of O. No account is taken of the possible formation of NO_2^-. The electron concentration is strongly dependent on the ionization potential for NO. Hilsenrath's tables show a nearly negligible electron concentration because he uses an older value of 9.4 v, but Gilmore uses a more recent value of 9.25 v.

To calculate the electron density resulting from the ionization equilibrium of both copper and NO in the arc we write the equilibrium constants for the ionization of copper and of nitric oxide.

$$\frac{N^+_{Cu}N_e}{N^\circ_{Cu}}=K_{Cu}; \tag{9a}$$

$$\frac{N^+_{NO}N_e}{N^\circ_{NO}}=K_{NO}. \tag{9b}$$

Furthermore we can write

$$N_e=N^+_{Cu}+N^+_{NO} \tag{10}$$

since other charged particles are in negligible concentration. Now substituting from (9a) and (9b) in (10) we have

$$N_e=K_{Cu}\frac{N^\circ_{Cu}}{N_e}+K_{NO}\frac{N^\circ_{NO}}{N_e}. \tag{11}$$

Multiplying through by N_e we obtain

$$(N_e)^2=K_{Cu}N^\circ_{Cu}+K_{NO}N^\circ_{NO}. \tag{12}$$

The equilibrium constant for copper we obtain from Saha's equation, eq (5). (Note that this does not involve a knowledge of N_e.) We have just calculated the density of copper atoms from the relative intensities of copper and oxygen lines. The data for NO are obtained from Gilmore's tables. The last factor will not be affected by a change of N_e because of the very small degree of ionization of NO. Evaluating (12) we find

$$N_e^2=1.6\times10^{28}+1.2\times10^{28}=2.8\times10^{28}$$

and

$$N_e=1.7\times10^{14}\text{ cm}^{-3}.$$

This means that the total electron density reported in section 3.1 may consist of two approximately equal components, one arising from the ionization of copper atoms, the other from the equilibrium composition of air.

Bearing in mind the uncertainties in the absolute gf-values for copper and oxygen, the value of N_e determined by this method is in tolerable agreement with the mean value of 2.4×10^{14} cm^{-3} for the total concentration of electrons obtained in section 3.1 from the relative intensities of arc and spark lines. In fact, within the uncertainties mentioned above, the agreement provides a quantitative experimental

demonstration of the validity of Saha's ionization equation, in application to our arc.

4.2. Ratio of Current Density to Electron Velocity

In this section we attempt to confirm the spectroscopically determined electron density by using electrical and geometrical observations of the copper arc.

The current density in the positive column of the arc was measured by forming a magnified image of the arc in which instantaneous comparisons of the diameter were made against a centimeter scale. With a 3.0-mm gap and a current of 9.8 amp, the diameter of the column midway between the electrodes was 2.7 mm, corresponding to an average current density of 170 amp/cm^2.

The axial field of an arc is composed of three parts: A very strong field very close to the anode, a weak field over most of the space between the electrodes, and a strong field very close to the cathode. The thickness of the anode and cathode fields is independent of the total gap so that changes in the total arc voltage with gap length reflect only changes in the voltage drop and length of the positive column. The axial field in the column can be determined from the slope of a plot of total arc voltage versus gap length. Twenty observations of our arc at gaps from 1 to 7 mm showed an increase of voltage from 23 to 41 v in a strictly linear fashion. This corresponds to a field of 30 v/cm in the plasma.

With the aid of the measurements reported above and some rather dubious assumptions about the behavior of electrons, we can obtain an independent determination of the electron density.

a. Macroscopic Point of View

The density of any electric current is equal to the product of the electronic charge, the density of electrons in the current, and the average velocity of the electrons in the direction of current flow. Algebraically stated,

$$j=eN_e v. \tag{13}$$

Good measurements of the drift velocities of electrons in air at 273 °K have been made by Nielson and Bradbury [26]. They present their data as a function of E/p in v/cm/mm Hg. Comparison of the high-temperature experiment with that of Nielson and Bradbury should be made at constant density, so we define an effective pressure

$$P_0=P(273/T)=760\times 273/5{,}100=40.7 \text{ mm Hg}$$

corresponding to the density of our arc plasma. Now our value of E/p_0 is 30/40.7=0.74 v/cm/mm Hg. The drift velocity from the data of Nielson and Bradbury at this ratio of E/p_0 and T=273 °K is 1.03×10^6 cm/sec. This velocity may be affected slightly by the different composition of air at 5,100 °K.

The electron velocity further depends on temperature through the velocity dependence on cross sections. Because of poor information available on scattering cross sections, we can only make a crude guess as to how v depends on T. On the basis of simple kinetic theory arguments, Loeb [27] suggests dependence on $T^{\frac{1}{2}}$. On this assumption we find at 5,100 °K that

$$v=1.03\times 10^6(5{,}100/273)^{\frac{1}{2}}=4.46\times 10^6 \text{ cm/sec}.$$

Solving eq (13), we find that

$$N_e=170/1.6\times 10^{-19}\times 4.46\times 10^6=2.4\times 10^{14} \text{ cm}^{-3},$$

which is the same as the spectroscopic value.

b. Microscopic Point of View

In the paper in which he originally applied the term plasma to a neutral region of ionized gas [28], Langmuir gave an expression for the random current density passing through a plane arbitrarily oriented in the plasma:

$$j=eN_e\left(\frac{kT}{2\pi m}\right)^{\frac{1}{2}}=2.5\times 10^{-14}N_e T^{\frac{1}{2}}. \tag{14}$$

The derivation, based on a Maxwell-Boltzmann distribution, is given by Langmuir and Compton [29].

Consider the electrons passing through such a plane erected perpendicular to the axis of the arc column at its positive terminus, close to the beginning of the anode drop. The electrons which pass through the plane into the anode drop will be collected at the anode and measured in our ammeter. Those passing in the opposite direction will not reach an electrode and will not affect the measured arc current. If this in fact happens, we can calculate N_e from eq (10) by letting j=170 amp/cm^2 and T=5,100 °K.

$$N_e=4.0\times 10^{13} jT^{-\frac{1}{2}}=1.0\times 10^{14} \text{ cm}^{-3}.$$

This is within the uncertainty of the spectroscopic value.

5. Discussion

Unfortunately it is not possible to prove that the necessary local thermodynamic equilibrium obtains in this arc, justifying the use of the Saha equation to determine the ionization balance. As has been pointed out in this and the preceding paper [2], the population of excited states in the arc follows a Boltzmann distribution at a temperature which gives a very reasonable value of the electron density when the Saha equation is assumed. One might be tempted to avoid the assumption of LTE in the analysis of the data and apply a more generalized equation for the ionization balance, such as that developed by Dewan [30]. If one applies, blindly, the Dewan equations to the metallic constituents of the arc alone, then the relatively high degree of ionization and low electron density would suggest the applicability of the coronal formula [31]. The coronal formula can be fitted to the data of table I, with about

the same residual scatter as when the Saha equation is used, but only if a temperature of 7,500 °K is assumed. Not only is this temperature in conflict with that determined from the excitation distribution but the coronal formula also ignores the effect of the predominate abundance of neutral atoms and molecules of air at atmospheric pressure in the arc. Although the processes of excitation and ionization in such an arc involving neutral particles primarily are so complex that not enough of the rate coefficients are known to permit a non-LTE treatment, it does not seem implausible that these three-body reactions do bring the plasma into LTE and justify the use of the Saha equation.

6. Conclusion

The relative numbers of ions and atoms in an arc plasma can be determined if intensities, wavelengths, partition functions, absolute *gf*-values and energy levels associated with the ions and atoms and the temperature of the plasma are known. Enough of these quantities are known for 11 of 70 elements excited in our arc to permit these relative numbers to be found. A solution of Saha's equation for each of these cases gives an average value of electron density of 2.4×10^{14} cm^{-3} in our arc. With the aid of partition functions, some of which are here calculated for the first time, the degree of ionization for each of 70 elements in our copper arc is calculated.

The electron density determined in this manner is, within expected uncertainties, in agreement with the density determined by independent spectroscopic and electrical measurements. The agreement demonstrates the applicability of Saha's ionization equation to our arc. It should be pointed out that the degree of ionization of our 70 elements could have been determined empirically from the data of figure 1 without any assumptions regarding equations or mechanisms of ionization.

The information on the degree of ionization reported in this paper enables us to calculate, on a single scale, relative transition probabilities for all the classified lines of both first and second spectra which appear in the NBS Tables of Spectral-Line Intensities. If proper normalization factors can be found, this scale will be put on an absolute basis. Such a calibration will be discussed in a forthcoming paper. At the conclusion of these studies, we expect to publish transition probabilities and *gf*-values for the 25,000 classified lines in the NBS Tables, if possible, on an absolute scale.

(Paper 66A2–148)

The author acknowledges the help of Earl Beaty in interpreting data on electron velocities, of Joseph Hilsenrath concerning the data on the equilibrium composition of air, and of R. H. Garstang with regard to theoretical aspects of ionization and *f*-values. I also thank L. M. Branscomb for the many lively discussions he engendered.

7. References

[1] W. F. Meggers, C. H. Corliss, and B. F. Scribner, Tables of spectral-line intensities, NBS Mono. 32 (1961) (U.S. Government Printing Office, Washington, D.C.).
[2] C. H. Corliss, J. Research NBS **66A**, 5 (1962).
[3] W. J. Claas, Recherches Astronomiques de l'Observatoire d'Utrecht, Vol. XII, Pt. 1 (1951).
[4] R. B. King and D. C. Stockbarger, Astrophys. J. **91,** 488 (1940).
[5] G. Stephenson, Proc. Phys. Soc. (London) **64A,** 458 (1951).
[6] J. L. Greenstein and E. Tandberg-Hanssen, Astrophys. J. **119,** 113 (1954).
[7] C. W. Allen, Astrophysical Quantities, Univ. London (The Athlone Press, 1955).
[8] E. Trefftz, Zeits. f. Astrophysik **29,** 287 (1951).
[9] E. Trefftz and L. Biermann, Zeits. f. Astrophysik **30,** 275 (1952).
[10] R. H. Garstang (unpublished).
[11] M. N. Saha, Phil. Mag. **40,** 472 (1920).
[12] C. E. Moore, Atomic energy levels, NBS Circ. 467, Vol. I (1949), Vol. II (1952), Vol. III (1958) (U.S. Government Printing Office, Washington, D.C.).
[13] K. L. Andrew and K. W. Meissner, J. Opt. Soc. Am. **49,** 146 (1959).
[14] W. F. Meggers (unpublished).
[15] T. A. M. van Kleef and P. F. A. Klinkenberg, Physica **27,** 83 (1961).
[16] T. A. M. van Kleef, Physica **23,**, 843 (1957).
[17] W. Albertson, Phys. Rev. **52,** 644 (1937).
[18] H. N. Russell and A. S. King, Astrophys. J. **90,** 155 (1939).
[19] H. N. Russell, J. Opt. Soc. Am. **40,** 550 (1950).
[20] P. F. A. Klinkenberg, Physica **21,** 53 (1955).
[21] L. Rolla and G. Piccardi, Phil. Mag. **7,** 286 (1929).
[22] I. N. Bakulina and N. I. Ionov., Soviet Phys. J. E. T. P. **9,** 709 (1959); N. I. Ionov and M. A. Mittsev., ibid. **11,** 972 (1960) and **13,** 518 (1961).
[23] P. F. A. Klinkenberg, Physica **13,** 1 (1947).
[24] J. Hilsenrath, M. Klein, and H. Woolley, Tables of thermodynamic properties of air including dissociation and ionization from 1500 °K to 15000 °K, AEDC–TR–59–20, Arnold Engineering Development Center, Air Research and Development Command. U. S. A. F. (1959) (Dept. of Commerce, OTS PB161311).
[25] F. R. Gilmore, Equilibrium composition and thermodynamic properties of air to 24000 °K, RM–1543 (1955) Rand Corp., Santa Monica, Calif.
[26] R. A. Nielson and N. E. Bradbury, Phys. Rev. **51,** 69 (1937).
[27] L. B. Loeb, Basic processes of gaseous electronics, Univ. Calif. Press (1955).
[28] I. Langmuir, Phys. Rev. **33,** 954 (1929).
[29] I. Langmuir and K. T. Compton, Rev. Mod. Phys. **3,** 220 (1931).
[30] E. M. Dewan, Phys. of Fluids **4,** 759 (1961).
[31] G. Elwert, Z. Naturforsch. **7a,** 432, 703 (1952).

JOURNAL OF RESEARCH of the National Bureau of Standards—A. Physics and Chemistry
Vol. 66A, No. 2, March–April 1962

The Vapor Pressure of Palladium

R. F. Hampson and R. F. Walker

(December 6, 1961)

The vapor pressure and heat of sublimation of palladium were measured using a vacuum microbalance technique. The mean heat of sublimation obtained was 89.2 ±0.8 kcal/mole. Over the temperature range of 1,294 to 1,488 °K the measured vapor pressures may be represented by: Log $P_{mm} = 8.749 - 18655/T$. The normal boiling point is estimated to be 3,200 °K.

The vapor pressure of palladium was measured by Haefling and Daane [1],[1] using a modified Knudsen effusion technique which incorporated a microbalance. Their data yielded a mean heat of sublimation at 298 °K, ΔH_s° (298), of 80 kcal/mole. Walker, Efimenko, and Lofgren [2], used the Langmuir technique with a microbalance to obtain a mean ΔH_s° (298) of 103 kcal/mole. The latter authors pointed out that since both sets of data yielded values of ΔH_s° (298) which tended to vary with the temperatures at which the measurements were made, unresolved systematic errors were probably involved in both techniques.

More recently, Dreger and Margrave [3] measured the rate of sublimation by suspending a sample from a microbalance into a graphite tube furnace. The furnace approximated blackbody conditions. The mean value of ΔH_s° (298) and its average deviation were 91.0 and ±0.8 kcal/mole. These authors suggested that erroneous assumptions were made by Walker et al., concerning the emissivity of Pd and that these errors could account for the disagreement between the respective sets of data. However, further investigation in this laboratory strongly indicated that a slow change in the calibration of the microbalance was responsible for the systematic errors in the measurements of Walker et al. Subsequent improvements in the design of the apparatus eliminated this problem.

The technique, sample, and experimental procedure used for the present measurements were generally similar to those recently described [4]. Two significant changes were made to reduce the uncertainty in the temperature measurements: a small hole 0.02 in. diam × 0.16 in. deep was drilled into the wall of the 0.085 in. diam × 0.75 in. long sample rods at an angle of 75° to the normal (the angle of sighting with the optical pyrometer); the U-shaped hooks on the sapphire-rod suspension were replaced with V-shaped hooks. The first change permitted observations of the temperature of the sample under approximately black body conditions to be compared with observations of the surface brightness temperature. The second change prevented the small sight-hole twisting out of the line of sight during the course of a run. It was assumed that for a substance having a sublimation coefficient of unity the sight-hole would not contribute to the effective area of the vaporizing surface.

Measurements of the rates of sublimation were made according to the procedure described [4], and were converted to equilibrium vapor pressures using the well-known Langmuir equation. The sublimation coefficient was assumed to be unity, and palladium was assumed to vaporize solely to the monomeric gaseous species.

Spectrochemical analysis of the sample showed it to be better than 99.9 percent pure with small amounts of the following as impurities: Si, B, Cu, Fe, Pt, and Rh.

The vapor pressures calculated from the measured rates of vaporization are given in the table, together with the corresponding values of ΔH_s° (298). The free energy functions of Stull and Sinke [5] were used to obtain the heats of sublimation. Only those temperatures obtained from observations down the sight-hole are reported in the table. The relative values of these temperatures and the observed surface brightness temperatures were generally consistent with normal spectral emissivities assumed in the previous work [2]. Figure 1 shows a Clausius-Clapeyron plot of the data given in the table.

The mean value and standard deviation of ΔH_s° (298), obtained from the data of table 1, are 89.2 and 0.2 kcal/mole respectively. The normal boiling point is estimated to be 3,200 °K.

The least squares line through the data shown in figure 1 is represented by log $P_{mm} = 8.749 - 18655/T$.

If the value of the sublimation coefficient is less than unity, the equilibrium vapor pressures given in table 1 are too low, and the corresponding values of ΔH_s° (298) are too high. Neglecting uncertainties in the free energy functions and assuming a sublimation coefficient of unity, the overall limits of error in the absolute value of ΔH_s° (298) are estimated to be ±0.8 kcal/mole, which corresponds to an error of ±35 percent in the vapor pressures.

[1] Figures in brackets indicate the literature references at the end of this paper.

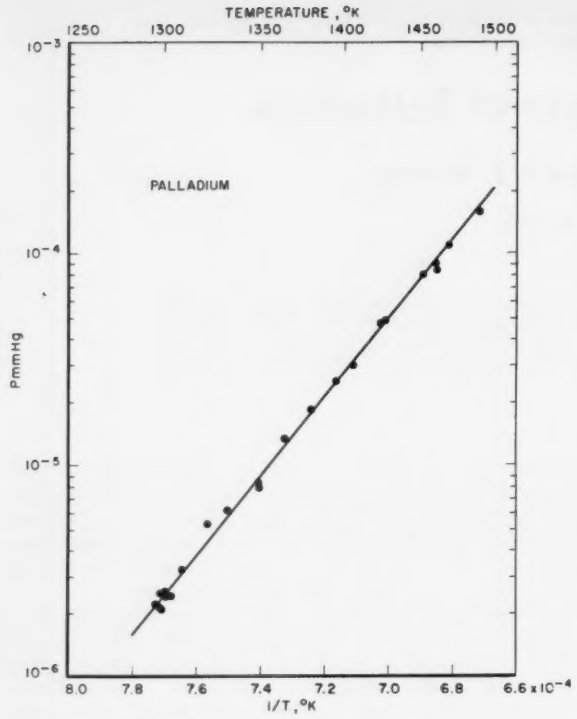

FIGURE 1. *Equilibrium vapor pressure of palladium versus the reciprocal of the absolute temperature.*

(Paper 66A2–149)

TABLE 1. *Vapor pressures and heats of sublimation of palladium**

Temperature	Vapor pressure	ΔH_s° (298)
°K	*mm* Hg	*kcal/mole*
1296	2.10×10^{-6}	89.3
1294	2.17×10^{-6}	89.1
1299	2.50×10^{-6}	89.1
1302	2.37×10^{-6}	89.4
1299	2.40×10^{-6}	89.2
1350	8.22×10^{-6}	89.3
1351	7.69×10^{-6}	89.6
1426	4.78×10^{-5}	89.2
1396	2.45×10^{-5}	89.3
1459	8.21×10^{-5}	89.7
1488	1.68×10^{-4}	89.3
1467	1.09×10^{-4}	89.3
1450	7.84×10^{-5}	89.3
1365	1.31×10^{-5}	89.0
1297	2.09×10^{-6}	89.4
1423	4.61×10^{-5}	89.2
1381	1.80×10^{-5}	89.2
1333	6.01×10^{-6}	89.0
1308	3.19×10^{-6}	89.0
1296	2.48×10^{-6}	88.9
1459	8.86×10^{-5}	89.5
1406	2.90×10^{-5}	89.4
1322	5.23×10^{-6}	88.7
Mean ΔH_s° (298)		89.2
Standard deviation		0.2

*Data are presented in experimental sequence and assume the sublimation coefficient is unity.

References

[1] J. F. Haefling and A. H. Daane, Trans. Amer. Inst. Min. (Metall.) Engrs. **212,** 115 (1958).

[2] R. F. Walker, J. Efimenko, and N. F. Lofgren, Rate of vaporization of refractory substances, Physical Chemistry in Aerodynamics and Space Flight, p. 24 (Pergamon Press, 1961).

[3] L. H. Dreger and J. L. Margrave, J. Phys. Chem. **64,** 1323 (1960).

[4] R. F. Hampson and R. F. Walker, J. Research NBS. **65A** (Phys. and Chem.), No. 4, 289 (1961).

[5] D. R. Stull and G. C. Sinke, Thermodynamic properties of the elements, American Chemical Society, Washington, D.C., 1956.

JOURNAL OF RESEARCH of the National Bureau of Standards—A. Physics and Chemistry
Vol. 66A, No. 2, March–April 1962

Revised Standard Values for *p*H Measurements from 0 to 95 °C

Roger G. Bates

(December 6, 1961)

Seven standard solutions serve to fix the NBS conventional activity scale of *p*H (termed pH_s) from 0 to 95° C. The original emf data have been re-examined and the values of the acidity function $p(a_H\gamma_{Cl})$, from which pH_s is derived, have been recalculated with the use of a single consistent set of standard potentials and electrochemical constants. The convention proposed recently by Bates and Guggenheim for the numerical evaluation of the individual activity coefficient of chloride ion in the buffer solutions has been adopted, and by this means pH_s values to the third decimal have been assigned. These "experimental" pH_s values in the temperature range 0 to 95 °C have been smoothed as a function of temperature by least-squares treatment. The properties and uses of the standards are discussed and directions for the preparation of the solutions are given.

1. Introduction

For a number of years the National Bureau of Standards has recommended a standard *p*H scale defined in terms of six reference points (see, for example, [1][1]). A seventh standard (*E* below) has recently been established to aid in the accurate measurement of *p*H in the physiologically important range *p*H 7 to 8 [2]. The compositions of these seven solutions are as follows, where *m* is molality:

A, potassium tetroxalate, 0.05 *m*,
B, potassium hydrogen tartrate, saturated at 25 °C,
C, potassium hydrogen phthalate, 0.05 *m*,
D, a solution 0.025 *m* with respect to both potassium dihydrogen phosphate and disodium hydrogen phosphate,
E, a solution 0.008695 *m* with respect to potassium dihydrogen phosphate and 0.03043 *m* with respect to disodium hydrogen phosphate,
F, borax, 0.01 *m*,
G, calcium hydroxide, saturated at 25 °C.

The assignment of *p*H values to these standards has been described in detail in earlier papers (citations are given in [1]). The necessity of estimating the individual activity coefficient of chloride ion in each reference solution deprives the standard *p*H value (termed pH_s) of exact fundamental meaning. The numerical value of this activity coefficient must rest upon an arbitrary convention, chosen in part for its reasonableness but largely for its utility [3].

Heretofore, the assigned *p*H values have been made consistent with several reasonable conventions for the single ionic activity coefficient of chloride ion. In order to do this, *p*H values had to be assigned with only second decimal accuracy. Recently, however, the adoption of a single convention has been recommended [4]. For the assignment of standard *p*H values it has thus been proposed that the activity coefficient of chloride ion (γ_{Cl}) be defined by the equation

$$\log \gamma_{Cl} = \frac{-AI^{1/2}}{1+1.5I^{1/2}}, \qquad (1)$$

where I is the ionic strength and A is a parameter of the Debye-Hückel theory having a different value at each temperature. It was intended that this convention be applied when I is equal to, or less than, 0.1.

This convention is both simple and useful. It is also reasonable in that it makes the activity coefficient of chloride ion nearly equal to the mean ionic activity coefficient of sodium chloride in its pure aqueous solution of ionic strength I. Furthermore, the values of pH_s for the four standards in the intermediate *p*H range, obtained by the use of this convention, agree quite well with the experimental *p*H values furnished by a *p*H cell with liquid junction standardized with the phosphate buffer at *p*H 6.865, as the following data illustrate [5]:

Standard	pH_s at 25° C	*p*H (l.j.) at 25° C
B, tartrate	3. 557	3. 566
C, phthalate	4. 008	4. 009
D, phosphate	6. 865	[a] (6. 865)
F, borax	9. 180	9. 185

[a] Reference value.

The values of $-\log(\gamma_H\gamma_{Cl}m_H)$ or $p(a_H\gamma_{Cl})$, used to derive pH_s, can be obtained with an accuracy of a few thousandths of a unit. With the adoption of the new convention it becomes possible to assign pH_s values with an accuracy dependent only upon the precision of the primary data. The reproducibility of the *p*H of the standards justifies this move.

It is the purpose of this paper to report a critical re-examination of the original emf data, a recalculation of the values of $p(a_H\gamma_{Cl})$ with the use of consistent values for the natural constants involved, and finally an assignment of pH_s values given to the third decimal place in terms of the new convention for γ_{Cl}. The properties of the seven standard

[1] Figures in brackets indicate the literature references at the end of this paper.

solutions are summarized, and instructions for the preparation and use of the solutions are given.

2. Method

The acidity function $p(a_H\gamma_{Cl})$ is calculated from the electromotive force (E) of cells containing hydrogen and silver–silver chloride electrodes by the equation

$$p(a_H\gamma_{Cl}) \equiv -\log\ (\gamma_H\gamma_{Cl}m_H) = \frac{E-E^\circ}{2.30259RT/F} + \log\ m_{Cl}, \tag{2}$$

where E° is the standard potential of the cell [6], F is the Faraday, R is the gas constant, and T is the temperature in degrees Kelvin.[2] The $p\mathrm{H_s}$ of the chloride-free buffer solution is computed from the equation

$$p\mathrm{H_s} = p(a_H\gamma_{Cl})^\circ + \log\ \gamma^\circ_{Cl}, \tag{3}$$

where $p(a_H\gamma_{Cl})^\circ$ is the value of $p(a_H\gamma_{Cl})$ in the limit of zero concentration of added chloride. Similarly, γ°_{Cl} is the limit of γ_{Cl} as the concentration of chloride in the buffer solution is reduced to zero. Values of $p(a_H\gamma_{Cl})^\circ$ are obtained readily by extrapolation of emf data obtained for the same buffer solution with two or more added small concentrations of a soluble chloride; γ°_{Cl} is computed by the convention set forth in eq (1).

The values of E°, $2.30259RT/F$, and of the Debye-Hückel slope A on the molal scale from 0 to 95 °C are summarized in table 1. For this calculation, R was taken to be 8.3147 j mole^{-1} deg^{-1}, F was taken to be 96,495.4 coulomb equiv^{-1}, while T is t °C+273.150 [7]. It should be noted that the recent shift to the carbon 12 scale of atomic weights is without effect on the magnitude of the quantity $2.30259RT/F$, inasmuch as R and F are changed in the same proportion. The values of A have been recalculated by Robinson and Stokes [8] with the use of a recent redetermination of the dielectric constant of water [9]. Their figures, given for the volume scale of concentration, have been converted to the molal scale through multiplication by $\sqrt{d^\circ}$, where d° is the density of pure water. All emf values recorded prior to January 1, 1948, have been corrected to absolute volts through multiplication by the conversion factor 1.00033 [10].

The recalculated values of $p(a_H\gamma_{Cl})^\circ$ for the seven standard buffer solutions from 0 to 95 °C are collected in table 2. The $p\mathrm{H_s}$ values given in table 3 were calculated from these values of $p(a_H\gamma_{Cl})^\circ$ together with the convention for γ_{Cl} given in eq (1).

The relation between $p\mathrm{H_s}$ for each buffer solution and the absolute temperature T was found to be represented closely by a four-constant equation of the form

[2] This acidity function was formerly called $p_c\mathrm{H}$ (see [3] and later papers).

Table 1. *Values of* E°, 2.30259RT/F, *and the Debye-Hückel slope* A (*molal scale*) *from 0 to 95 °C*

t	E°	$2.30259RT/F$	A
°C	v	v	
0	0.23655	0.054195	0.4918
5	.23413	.055187	.4952
10	.23142	.056183	.4988
15	.22857	.057171	.5026
20	.22557	.058163	.5066
25	.22234	.059155	.5108
30	.21904	.060147	.5150
35	.21565	.061139	.5196
40	.21208	.062131	.5242
45	.20835	.063123	.5291
50	.20449	.064115	.5341
55	.20056	.065107	.5393
60	.19649	.066099	.5448
70	.18782	.068083	.5562
80	.17873	.070067	.5685
90	.16952	.072051	.5817
95	.16511	.073043	.5886

$$p\mathrm{H_s} = \frac{A}{T} + B + CT + DT^2. \tag{4}$$

The constants A, B, C, and D of this empirical equation were obtained for each of the buffer solutions with the aid of the IBM 704 computer. They are summarized in table 4, the last column of which gives the standard deviation of a single value of $p\mathrm{H_s}$ based on the deviations from the least-squares line. The "recommended" values of $p\mathrm{H_s}$ are those calculated by eq (4) and, hence, smoothed temperature-wise. The summary given in table 5 includes $p\mathrm{H_s}$ for 38° C, in view of the frequent use of this temperature in biological studies.

A consideration of the standard deviations of the values of $p(a_H\gamma_{Cl})^\circ$ given in table 2 (where available) together with the fit of $p\mathrm{H_s}$ to eq (4) as represented by the standard deviations given in table 4, leads to the following estimated limits to the effects of random errors in the recommended standard $p\mathrm{H_s}$ values: 0.003 for the range 0 to 60 °C and 0.005 for the range 60 to 95 °C. If, in addition, 0.002 is allowed for the maximum uncertainty in the constants of eq (2) below 60 °C and 0.003 above 60 °C, the total uncertainties in $p\mathrm{H_s}$ (table 5) become 0.005 unit (0 to 60 °C) and 0.008 unit (60 to 95 °C).

3. Properties of the Standards

Compositions on the molal scale of the solutions to which $p\mathrm{H_s}$ values have been assigned are given above. Furthermore, the $p\mathrm{H_s}$ represents $-\log\ a_H$, where a_H is an activity in molal units. It is nonetheless usually convenient to prepare buffer solutions by volume methods rather than weight methods, and it has been noted in earlier publications that the error in $p\mathrm{H_s}$ that results from use of an *x molar* solution in place of the prescribed *x molal* solution is negligible, in view of the tolerance of ± 0.01 unit placed on the values of $p\mathrm{H_s}$. If, however, third-decimal accuracy is to be ascribed to the values of $p\mathrm{H_s}$, the compositions of the solutions must be adjusted somewhat more carefully.

TABLE 2. *Values of $p(a_H \gamma_{Cl})^\circ$ for seven standard buffer solutions from 0 to 95 °C*

t	*A*	*B*	*C*	*D*	*E*	*F*	*G*
	Tetroxalate	Tartrate	Phthalate	Phosphate	Phosphate	Borax	Calcium hydroxide
°C							
0	1.765	----------	4.090	7.091	7.640	9.522	13.510
5	1.764	----------	4.084	7.057	7.605	9.450	13.291
10	1.765	----------	4.082	7.029	7.579	9.390	13.088
15	1.769	----------	4.083	7.006	7.555	9.336	12.893
20	1.773	----------	4.087	6.988	7.537	9.287	12.712
25	1.780	3.637	4.096	6.974	7.523	9.240	12.537
30	1.785	3.631	4.104	6.965	7.511	9.200	12.381
35	1.792	3.628	4.113	6.956	7.498	9.162	12.219
40	1.797	3.627	4.125	6.951	7.493	9.130	12.070
45	1.803	3.628	4.138	6.949	7.486	9.100	11.926
50	1.811	3.631	4.155	6.948	7.482	9.072	11.790
55	1.819	3.639	4.172	6.950	----------	9.044	11.661
60	1.824(1.827)	3.647(3.643)	4.188(4.175)	6.954(6.948)	----------	9.021(9.026)	11.540
70	1.849	3.664	4.219	6.962	----------	8.990	----------
80	1.877	3.698	4.259	6.979	----------	8.953	----------
90	1.904	3.738	4.301	7.001	----------	8.920	----------
95	1.919	3.767	4.331	7.014	----------	8.899	----------
Reference, 0 to 60 °C	[11]	[12]	[13]	[14]	[2]	[15]	[16]
Reference, 60 to 95 °C (value at 60 °C enclosed in parentheses)	[1]	[1]	[1]	[1]		[1]	

TABLE 3. *"Experimental" values of pH_s for seven standard buffer solutions from 0 to 95 °C*

t	*A*	*B*	*C*	*D*	*E*	*F*	*G*
	Tetroxalate	Tartrate	Phthalate	Phosphate	Phosphate	Borax	Calcium hydroxide
°C							
0	1.669	----------	4.006	6.986	7.534	9.465	13.425
5	1.667	----------	3.999	6.951	7.499	9.392	13.206
10	1.667	----------	3.996	6.922	7.472	9.332	13.003
15	1.671	----------	3.997	6.898	7.447	9.277	12.808
20	1.674	----------	4.000	6.879	7.429	9.228	12.627
25	1.680	3.558	4.008	6.864	7.414	9.180	12.452
30	1.685	3.552	4.016	6.855	7.400	9.140	12.296
35	1.691	3.548	4.024	6.845	7.387	9.101	12.133
40	1.695	3.546	4.035	6.839	7.381	9.069	11.984
45	1.700	3.547	4.047	6.836	7.373	9.038	11.839
50	1.707	3.549	4.063	6.833	7.367	9.010	11.703
55	1.714	3.556	4.080	6.834	----------	8.981	11.573
60	1.719(1.722)	3.563(3.559)	4.095(4.082)	6.837(6.831)	----------	8.957(8.962)	11.451
70	1.742	3.578	4.124	6.843	----------	8.925	----------
80	1.767	3.610	4.162	6.857	----------	8.887	----------
90	1.792	3.648	4.202	6.876	----------	8.852	----------
95	1.806	3.676	4.231	6.888	----------	8.830	----------

The density of each of the seven standard solutions at 25 °C is listed in table 6, together with the corresponding molarity of each of the buffer components. The fifth column of the table gives the dilution value [17] or change of pH_s resulting from dilution of the buffer with an equal volume of pure water. The difference of pH_s between two solutions of numerically equal molality and molarity can therefore be derived, and it is given in the sixth column of the table. The Van Slyke buffer value, $\beta = db/dp\text{H}$ (where db is an increment of strong acid or strong base, in equivalents, added to 1 liter of buffer solution) [18], is given in the seventh column and the temperature coefficient of the pH_s value in the last column.

It is evident from the results given in table 6 that only the tetroxalate solution and the calcium hydroxide solution (solutions *A* and *G*) have sufficiently large dilution values to require that a distinction between molal (m) and molar (M) scales be made. Indeed, this difference is of only academic interest as it applies to the standard solution of calcium hydroxide, which is a saturated solution prepared without the necessity of weighing the calcium hydroxide itself. On the other hand, the pH_s of a 0.05 M solution of potassium tetroxalate is lower by about 0.003 unit than that of the standard 0.05 m solution, and allowance should be made for this difference.

TABLE 4. *Values of the constants of the equation:* $pH_s = A/T + B + CT + DT^2$, *for seven standard buffer solutions from 0 to 95 °C*

Solution	Temperature range	A	B	C	$10^3 D$	Standard deviation
	°C					
A, Tetroxalate	0 to 95	−362.76	6.1765	−0.018710	2.5847	0.0019
B, Tartrate	25 to 95	−1727.96	23.7406	−.075947	9.2873	.0016
C, Phthalate	0 to 95	1678.30	−9.8357	0.034946	−2.4804	.0027
D, Phosphate	0 to 95	3459.39	−21.0574	.073301	−6.2266	.0017
E, Phosphate	0 to 50	5706.61	−43.9428	.154785	−15.6745	.0011
F, Borax	0 to 95	5259.02	−33.1064	.114826	−10.7860	.0025
G, Calcium hydroxide	0 to 60	7613.65	−38.5892	.119217	−11.2918	.0028

TABLE 5. *Recommended standard values of* pH_s, *calculated by eq (4)*

t	A	B	C	D	E	F	G
	Tetroxalate	Tartrate	Phthalate	Phosphate	Phosphate	Borax	Calcium hydroxide
°C							
0	1.666	----------	4.003	6.984	7.534	9.464	13.423
5	1.668	----------	3.999	6.951	7.500	9.395	13.207
10	1.670	----------	3.998	6.923	7.472	9.332	13.003
15	1.672	----------	3.999	6.900	7.448	9.276	12.810
20	1.675	----------	4.002	6.881	7.429	9.225	12.627
25	1.679	3.557	4.008	6.865	7.413	9.180	12.454
30	1.683	3.552	4.015	6.853	7.400	9.139	12.289
35	1.688	3.549	4.024	6.844	7.389	9.102	12.133
38	1.691	3.548	4.030	6.840	7.384	9.081	12.043
40	1.694	3.547	4.035	6.838	7.380	9.068	11.984
45	1.700	3.547	4.047	6.834	7.373	9.038	11.841
50	1.707	3.549	4.060	6.833	7.367	9.011	11.705
55	1.715	3.554	4.075	6.834	----------	8.985	11.574
60	1.723	3.560	4.091	6.836	----------	8.962	11.449
70	1.743	3.580	4.126	6.845	----------	8.921	----------
80	1.766	3.609	4.164	6.859	----------	8.885	----------
90	1.792	3.650	4.205	6.877	----------	8.850	----------
95	1.806	3.674	4.227	6.886	----------	8.833	----------

TABLE 6. *Properties of seven standard buffer solutions at 25 °C*

Solution	m	Density	Molarity	Dilution value, $\Delta pH_{1/3}$	[a] ΔpH_s	Buffer value, β	Temperature coeff., dpH_s/dt
		g/ml				*equiv./pH*	*units/°C*
A, Tetroxalate	0.05	1.0032	0.04962	+0.186	−0.0028	0.070	+0.001
B, Tartrate	.0341	1.0036	.034	+.049	−.0003	.027	−.0014
C, Phthalate	.05	1.0017	.04958	+.052	−.0009	.016	+.0012
D, Phosphate	[b] .025	1.0028	[b] .02490	+.080	−.0006	.029	−.0028
E, Phosphate	[c] .008695 [d] .03043	1.0020	[c] .008665 [d] .03032	[e] +.07	−.0005	.016	−.0028
F, Borax	.01	0.9996	.009971	+.01	−.0001	.020	−.0082
G, Calcium hydroxide	.0203	0.9991	.02025	−.28	+.0014	.09	−.033

[a] $\Delta pH_s = pH_s$ (*M Molar* solution) $- pH_s$ (*m molal* solution).
[b] Concentration of each phosphate salt.
[c] KH_2PO_4.
[d] Na_2HPO_4.
[e] Calculated value.

Accordingly, from the molarities given in table 6 have been calculated the weights of buffer substance that should be taken in order to prepare (by volume methods) 1 liter of buffer solution of the prescribed molality at 25 °C. The weights (in air near sea level) are given in table 7. The preparation of a sample of calcium hydroxide suitable for use as a standard buffer substance has been described in an earlier paper [16]. The other buffer substances are available as certified standard samples from the National Bureau of Standards. Carbon dioxide-free water should be used to prepare the standards composed of phosphate salts or borax.

TABLE 7. *Compositions of seven standard buffer solutions*

Weight of buffer substance (in air) per liter of buffer solution at 25 °C

Solution		Buffer substance	Weight in air
			g
A, Tetroxalate,	0.05 *m*	$KH_3(C_2O_4)_2 \cdot 2H_2O$	12.61
B, Tartrate,	about 0.034 *m*	$KHC_4H_4O_6$	Saturated at 25 °C
C, Phthalate,	0.05 *m*	$KHC_8H_4O_4$	10.12
D, Phosphate,	0.025 *m*	KH_2PO_4	3.39
	0.025 *m*	Na_2HPO_4	3.53
E, Phosphate	0.008695 *m*	KH_2PO_4	1.179
	0.03043 *m*	Na_2HPO_4	4.30
F, Borax,	0.01 *m*	$Na_2B_4O_7 \cdot 10H_2O$	3.80
G, Calcium hydroxide,	0.0203 *m*	$Ca(OH)_2$	(Saturated at 25 °C)

4. Discussion

It is evident from the foregoing sections that the NBS standard *p*H scale can be characterized as a scale of conventional hydrogen ion activity (on the molal scale), defined in terms of certain specified standard solutions. The special nature of these standard values is indicated by use of the symbol pH_s or *p*H(S) to avoid confusion with the *p*H, a quantity that is determined operationally, usually by a *p*H cell with a liquid junction and a glass electrode. Although the precise meaning of pH_s is set forth in eqs (1) and (2), it cannot be said that experimental *p*H values possess this same significance in the same degree. The unavoidable variations in the liquid-junction potential are largely responsible for the indeterminate nature of operational *p*H values. Only under certain very restricted experimental conditions is it wise to attempt an interpretation of *p*H values in terms of the conventional scale of pH_s.

The *p*H response of glass electrodes (that is, the change in the surface potential with change of *p*H) is often somewhat less than the theoretical Nernst slope. Fortunately, however, the voltage response is usually linear with *p*H over considerable ranges. For these reasons, two or more standards are needed to furnish a useful calibration of the glass electrode function. The *p*H values of "unknowns" X then are determined, in effect, by interpolation between two electromotive forces (E_1 and E_2) furnished by two standard solutions, S_1 and S_2 [4]:

$$\frac{pH(X)-pH(S_1)}{pH(S_2)-pH(S_1)}=\frac{E_X-E_1}{E_2-E_1}. \qquad (5)$$

This procedure serves admirably for the standardization of *p*H cells with a glass electrode between a lower limit of about *p*H 2.5 and an upper limit of about *p*H 11.5, corrections for the alkaline error of the glass electrode being applied where necessary. With the availability of the tetroxalate standard and the calcium hydroxide standard, it seemed possible to extend this standardization procedure to *p*H 1.7 at the low end and to *p*H 12.4 at the high end [19].

If this procedure were followed, however, the calibration of the assembly would correct not only for deficiencies in the response of the glass electrode but also for the variability of the liquid-junction potential when a standard of intermediate *p*H is replaced by the tetroxalate solution or by the calcium hydroxide solution. It may be anticipated that the response of the glass electrode will be nearly the same in all solutions of *p*H 1.7 or in all solutions of *p*H 12.4, but it is a well-known fact that the liquid-junction potential does not necessarily show this regularity and cannot, therefore, be effectively "calibrated out."

For the standardization of glass electrode assemblies with a liquid junction, therefore, a distinction has been made between "primary standards" and "secondary standards." The five solutions of *p*H 3.5 to 9.5 are considered to be *primary* standards intended for establishing the response of glass electrode *p*H cells. On the other hand, the tetroxalate solution and the calcium hydroxide solution are considered to be *secondary* standards, for confirmatory purposes, only when the usual *p*H cell is used. Experiments have shown that a *p*H assembly with liquid junction, standardized in the approved fashion in the intermediate range of *p*H, will indicate a *p*H value for the tetroxalate solution that is about 0.03 unit lower than the value of pH_s given in table 5 [20].

Similarly, the calcium hydroxide solution will also have a *p*H value about 0.03 unit lower than pH_s [16]. (The equality of these two figures is, of course, fortuitous.) In spite of these deviations, it should be realized that the pH_s values of these two solutions are as accurate as those for the other five, and all seven may be used with equal confidence when the variability of the liquid-junction potential is not a factor.

Inasmuch as pH_s is assigned independently for each buffer solution, the possibility of the existence of inconsistencies in the standardization of practical *p*H assemblies, even in the intermediate *p*H range, must be recognized. These inconsistencies, if they exist, would be attributable to one or both of the following causes: The first is the unavoidable oversimplification inherent in eq (1), which recognizes a single formula for the variation of γ_{Cl} with I in seven solutions of different compositions. The second is that the concentrations and mobilities of the ions in the several buffer solutions are different. No effort has been made to match the buffer solutions carefully in these respects, since the "unknowns" cannot in any case be expected to match the standards.

At any rate, the concentrated solution of potassium chloride used as a bridge solution, together with a properly designed junction, can be depended upon to smooth out variations in the liquid-junction potential rather successfully between *p*H 3.5 and 10.5. The data reproduced in section 1 of this paper indicate that the inconsistency is not large for one particular design of liquid junction of the free-diffusion type. Further studies are, however, desirable at other temperatures and for other junctions, including those of the commercial types most commonly used.

5. References

[1] V. E. Bower and R. G. Bates, J. Research NBS **59,** 261 (1957) RP2797.

[2] V. E. Bower, M. Paabo, and R. G. Bates, J. Research NBS **65**A, 267 (1961).

[3] R. G. Bates, Chem. Revs. **42,** 1 (1948).

[4] R. G. Bates and E. A. Guggenheim, Pure and Applied Chemistry **1,** 163 (1960).

[5] R. G. Bates, Chimia **14,** 111 (1960).

[6] R. G. Bates and V. E. Bower, J. Research NBS **53,** 283 (1954) RP2546.

[7] E. R. Cohen, K. M. Crowe, and J. W. M. DuMond, Fundamental constants of physics (Interscience Publishers, Inc., New York, 1957).

[8] R. A. Robinson and R. H. Stokes, Electrolyte solutions, 2d ed., appendix 7.1 (Academic Press, Inc., New York, 1959).

[9] C. G. Malmberg and A. A. Maryott, J. Research NBS **56,** 1 (1956) RP2641.

10] Announcement of changes in electrical and photometric units, NBS Circular 459 (May 15, 1947).

[11] V. E. Bower, R. G. Bates, and E. R. Smith, J. Research NBS **51,** 189 (1953) RP2450.
[12] R. G. Bates, V. E. Bower, R. G. Miller, and E. R. Smith, J. Research NBS **47,** 433 (1951) RP2268.
[13] W. J. Hamer and S. F. Acree, J. Research NBS **32,** 215 (1944) RP1586.
[14] R. G. Bates and S. F. Acree, J. Research NBS **34,** 373 (1945) RP1648.
[15] G. G. Manov, N. J. DeLollis, P. W. Lindvall, and S. F. Acree, J. Research NBS **36,** 543 (1946) RP1721.
[16] R. G. Bates, V. E. Bower, and E. R. Smith, J. Research NBS **56,** 305 (1956) RP2680.
[17] R. G. Bates, Anal. Chem. **26,** 871 (1954).
[18] D. D. Van Slyke, J. Biol. Chem. **52,** 525 (1922).
[19] R. G. Bates, Symposium on *p*H Measurement, Spec. Tech. Pub. No. 190, p. 1 (Am. Soc. Testing Materials, Philadelphia, Pa., 1956).
[20] R. G. Bates, G. D. Pinching, and E. R. Smith, J. Research NBS **45,** 418 (1950) RP2153.

(Paper 66A2–150)

JOURNAL OF RESEARCH of the National Bureau of Standards—A. Physics and Chemistry
Vol. 66A, No. 2, March–April 1962

Conductometric Determination of Sulfhydryl Groups in Swollen Polycaprolactam Fibers Having Disulfide and Alkylene Sulfide Crosslinks

Stephen D. Bruck and Sylvia M. Bailey

(December 6, 1961)

A simple conductometric titration method is discussed for the determination of sulfhydryl groups in nonionic polymer networks, such as disulfide and alkylene sulfide crosslinked polycaprolactam fibers. The diffusion of the titrant into the crosslinked polymer is accomplished by swelling the network structure, thereby eliminating the necessity of destroying the crosslinks and/or breaking the polymer chains.

1. Introduction

In current communications [1, 2, 3] [1] a method is discussed for producing macroscopic deformations (such as crimping and coiling) in polycaprolactam fibers by crosslinking. The disulfide and alkylene sulfide crosslinks used were introduced into the oriented, swollen, *N*-methylmethoxylated fibers (swelling agent: methyl alcohol) and consisted primarily of the following structures:

Fiber A

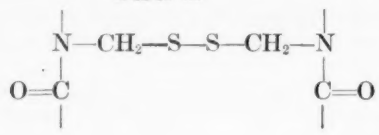

(1)

Fiber B

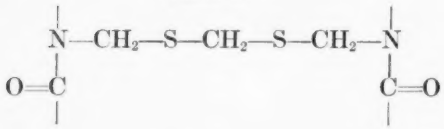

(2)

Fiber C

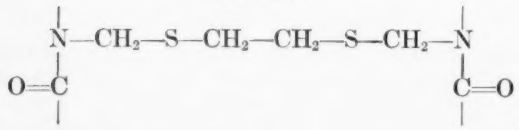

(3)

In addition to the above crosslinks, various amounts of unreacted sulfhydryl or potassium mercaptide groups having the following structure may also be present:

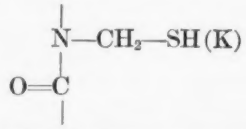

(4)

[1] Figures in brackets indicate the literature references at the end of this paper.

A knowledge of the number of sulfhydryl groups in the crosslinked fibers is valuable because one can then estimate the number of crosslinks from the total sulfur content and the number of sulfhydryl groups.

2. Discussion

There are numerous methods for the determination of sulfhydryl groups in organic compounds [4, 5]. These include visual titrimetric [6], potentiometric [7], and amperometric [8] techniques, as well as oxidation methods [9, 10]. Similarly, various methods exist for the determination of disulfides and sulfides [4, 5, 11, 12]. There are difficulties, however, when both sulfhydryl groups and disulfide groups (or other sulfur-containing functional groups) are present in the same molecule. In such a case, in order to determine the number of disulfide groups, one must first remove or analyze the sulfhydryl groups (for example, by potentiometric titration with Ag^+), then quantitatively reduce the disulfides to sulfhydryls, followed by analysis of the resulting sulfhydryl groups. Apart from the complexity of this approach, a further difficulty arises if all excess silver ions are not removed from the system after the initial analysis of sulfhydryl groups; any excess Ag^+ will combine with those sulfhydryls that are produced from the reduction of disulfides, thus making an accurate analysis impossible.

In the systems discussed here the unmodified polyamides are essentially nonionic, and the sulfhydryls and crosslinks were introduced into the swollen *N*-methylmethoxylated fibers in the presence of methyl alcohol as swelling agent. It should be possible then to reach the free sulfhydryl (or potassium mercaptide) groups with a specific reagent, provided that the system is in the swollen state. Thus, conductometric titration methods with Ag^+ offer a promising approach. Diffusion of the titrant into the crosslinked polymer is accomplished by swelling the network structure, thereby eliminating the necessity of destroying the crosslinks or breaking the polymer chains. Conductometric techniques are not ordinarily used in sulfhydryl

analyses partly because of the interfering effect of electrolytes that do not take part in the analytical reaction. However, in the present work, the unmodified polymer is nonionic and because it is not dissolved, it should not contribute significantly to the total conductance of the solution. Consequently the titration of the sulfhydryl groups with Ag^+ should be free of disturbances provided that the swelling agent is also a suitable medium for the conductance of silver ions.

To ascertain the applicability of such a procedure the effect of increased swelling periods on the diffusion of the titrant into the polymer must be assessed, and evidence must be obtained that the observed end-points are truly indicative of sulfhydryl groups. The first parameter can be checked by carrying out titrations on the system after it has been swollen for different periods in a swelling agent; the second parameter can be ascertained by analyzing the titrated samples for silver. One equivalent of silver corresponds to one equivalent of mercaptide (or sulfhydryl) groups, according to the reaction:

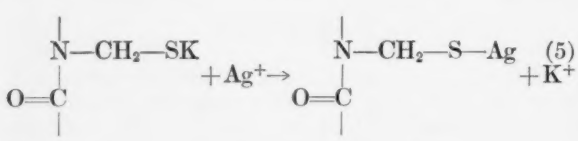

(5)

The following experimental procedure was thus adopted.

3. Experimental Details

Samples of crosslinked polycaprolactam fibers were cut to lengths of approximately 1 to 2 mm and swollen in 100 ml of methyl alcohol for periods of 15 min, 2 hr, and 4 hr, respectively, in 250 ml beakers. Such small, cut filaments are subject to a relatively rapid rate of swelling as has already been shown [13,14]. The suspended and swollen filaments were stirred with a magnetic stirrer. The titrant, a solution of 0.0014 N $AgNO_3$ in methanol-distilled water (99:1 by volume), was added in approximately 0.1 ml amounts at 2-min intervals to allow diffusion into the fiber. A Serfass conductometric bridge and platinum electrodes (¼ cm^2, 1 in. apart) were used, and the titrations were carried out at room temperature. The use of other swelling agents, such as benzyl alcohol, *m*-cresol, or mixtures of these gave poor titration curves due probably to insufficient conductance of Ag^+ in these media. Figure 1, curve A shows a typical conductometeric titration curve for the uncrosslinked (control) sample after 2 hr of swelling. Curve B is a typical plot for the crosslinked fibers that contain both disulfide and alkylene sulfide crosslinks, after 2 hr of swelling. Similar plots were also obtained for fibers that had been swollen for 4 hr in methanol. No satisfactory end-points were obtained for those crosslinked samples that had been swollen for only 15 min.

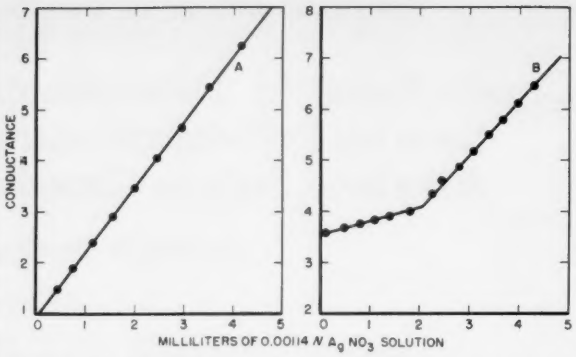

FIGURE 1. *Typical conductometric titration curves for an uncrosslinked polycaprolactam fiber (curve A), and a sulfhydryl containing disulfide crosslinked polycaprolactam fiber (curve B).*

After the titrations were completed (carried sufficiently past the end-point), the swollen polymer samples were immediately filtered with suction on medium-porosity sintered glass filters, thoroughly washed with ethanol, and dried. Care was exercised to avoid prolonged standing of the samples in light, as the excess silver ions present in the solution from additions past the end-point could be reduced to free silver thus becoming part of the samples after filtration. Each titrated sample was then analyzed for silver. Table 1 gives the equivalents of sulfhydryl groups per 10^6 g of polymer calculated from the titration curves and silver analyses, respectively.

TABLE 1. *Equivalents of sulfhydryl groups per 10^6 g of polymer calculated from conductometric titrations and silver analyses*

Experiment	Swelling time prior to titration	Sample wt used in titration	Equivalents of sulfhydryls per 10^6 g of polymer	
			Titration	Ag analysis
	hr	*g*		
1	2	0.0314	54	51
2	2	.0283	47	51
3	2	.0479	51	
4	2	.0348	46	47
5	4	.0581	44	
6	4	.0502	44	46

There is good agreement between the equivalents of sulfhydryl groups obtained from titration curves and from corresponding silver analyses. The fact that the number of equivalents of sulfhydryls did not show significant changes for the samples that had been swollen for 2 and 4 hrs, respectively, indicates that the polymer network was sufficiently swollen after only 2 hrs for the diffusion of silver ions and for their subsequent reaction with the sulfhydryl groups. Cross sections of the titrated fibers indicated that the penetration of the Ag^+ was not restricted to the surface of the fiber, inasmuch as greying of the entire section was observed, instead of a so-called surface "ring." Furthermore, if any untitrated sulfhydryl groups remained in the

polymer, some of these would have reacted with the excess silver ions present in the solution from additions past the end point. In this case the silver analyses would have been higher in contrast to the results in table 1.

It can be concluded, therefore, that it is feasible to determine sulfhydryl groups in a swollen disulfide or alkylene sulfide crosslinked polyamide by conductrometric titration with $AgNO_3$. The accuracy of the method compares favorably with usual end-group analyses in polymers, and suggests its possible wider applicability.

The authors thank R. A. Paulson, Applied Analytical Research Section, National Bureau of Standards, for the silver analyses.

4. References

[1] S. D. Bruck, J. Research NBS **65A** (Phys. and Chem.), No. 6, 489 (Nov.–Dec. 1961).

[2] Structural modification of synthetic fibers, NBS Tech. News Bull. **45,** 152 (1961); Cross-links crimp and coil nylon-6 fiber, Chem. Engr. News pp. 50–51 (Oct. 23, 1961).

[3] S. D. Bruck, J. Research NBS **66A** (Phys. and Chem.), No. 1, 77 (Jan.–Feb. 1962).

[4] S. Dal Nogare, Organic Analysis, Vol. I, p. 329 (Interscience Publishers, Inc., New York, 1953).

[5] S. Siggia, Quantitative Organic Analysis Via Functional Groups (John Wiley & Sons, Inc., New York, 1949).

[6] W. M. Malisoff and C. E. Anding, Jr., Ind. Eng. Chem. Anal. Ed. **7,** 86 (1935).

[7] E. R. H. Davies and J. W. Armstrong, J. Inst. Petroleum **29,** 323 (1943).

[8] I. M. Kolthoff and W. E. Harris, Ind. Eng. Chem. Anal. Ed. **18,** 161 (1946).

[9] J. R. Sampey and E. E. Reid, J. Am. Chem. Soc. **54,** 3404 (1932).

[10] I. M. Kolthoff and W. Stricks, Anal. Chem. **23,** 763 (1951).

[11] I. M. Kolthoff, D. R. May, P. Morgan, H. A. Laitinen, and A. S. O'Brien, Ind. Eng. Chem. Anal. Ed. **18,** 442 (1946).

[12] R. L. Hubbard, W. E. Haines, and J. S. Ball, Anal. Chem. **30,** 91 (1958).

[13] S. D. Bruck, J. Polymer Sci. **55,** S 29 (1961).

[14] S. D. Bruck, J. Research NBS **65A** (Phys. and Chem.) No. 6, 485 (Nov.–Dec. 1961).

(Paper 66A2–151)

JOURNAL OF RESEARCH of the National Bureau of Standards—A. Physics and Chemistry
Vol. 66A, No. 2, March–April 1962

Chromatographic Analysis of Petroleum Fractions Used in Oil-Extended Rubber[1]

Dominic J. Termini and Augustus R. Glasgow

(October 10, 1961)

The classification of oils with respect to differences in composition is important in their use in the manufacture of oil-extended butadiene-styrene rubber. A rapid chromatographic method of analysis has been developed in which 2.5- to 3.0-gram samples of oil are desorbed from silica gel into five different fractions by successive elution with pentane, benzene, carbon tetrachloride, and ethanol as eluents. Six extender-oils were analyzed by this method. Physical properties of the separated fractions showed marked differences between fractions of the same oil and similarities between corresponding fractions of the different oils. The chromatographic separation of extender-oils into compositionally different fractions provides a method for evaluation of the effect of different components on specific properties of the finished rubber product.

1. Introduction

High-boiling oils of petroleum origin are used in the preparation of oil-extended rubber. The oils are complex mixtures of hydrocarbons and also contain compounds of nitrogen, sulfur, and oxygen [1, 2, 3, 4].[2] The different components in these oils impart certain desirable and undesirable properties to butadiene-styrene copolymer. Classification of the composition of these materials is necessary for proper formulation of such rubbers [5, 6].

Rostler and associates [7, 8] classify these oils according to the solubility of the oil with sulfuric acid of varying concentration into four groups; namely, nitrogen bases, first acidaffins, second acidaffins, and paraffins. Kurtz and associates have published data supporting a classification of these oils based on the relationship between the viscosity-gravity constant and viscosity [9, 10], the viscosity-gravity constant and refractivity intercept [11, 12], and the density and refractivity intercept [13]. Chromatographic techniques [14, 15, 16, 17] with measurements of the physical properties of the separated fractions have also been used to classify these oils.

The chromatographic method of analysis described in this paper was developed as a rapid method for characterizing these oils. It differs from previous silica-gel adsorption methods for viscous oils [14, 17, 18] in that the oil is separated into five compositionally different fractions instead of two fractions. Samples of six oils certified for use as rubber-processing oils by the Federal Facilities Corporation were analyzed by this procedure.

2. Adsorption and Elution

The adsorption column used was 85×1.5 cm, and was fitted with a reservoir at the top and a 1 mm capillary 0.5 cm long at the bottom. It was packed in the usual way with about 90 g of silica gel (28–200 mesh). Removal of the lower boiling solvents from the eluted oil in each fraction was accomplished by distillation in a stream of nitrogen from a pot heated by a water bath.

In preliminary tests of the effectiveness of removal of the solvent by distillation, it was found that a solution of 100 ml pentane and 3 g *n*-dotriacontane allowed a substantially complete recovery of the high boiling compound; the amount recovered was the same within 0.02 percent of the amount added.

The eluting agents (pentane, benzene, carbon tetrachloride, and absolute alcohol) were redistilled solvents. Preliminary tests indicated that these agents would remove small amounts of nonvolatile material from the gel. On the basis of 2.5–3.0 g samples of oils separated, the error introduced by alcohol extraction of the gel amounted to about 0.2 weight percent; with the other eluting agents, the error was about 0.02 weight percent.

3. Chromatographic Separation

3.1. Procedure

A sample of 2.5 to 3.0 g of the whole oil was weighed in a 10 ml beaker and transferred to the column by a few washings of 5 ml pentane each. The reservoir was then filled with 250 ml pentane and this solution allowed to drain. This elution was followed successively by 100 ml pentane, 160 ml benzene, 160 ml carbon tetrachloride, and 250 ml ethanol. Each solvent was added just before the last of the preceding liquid entered the adsorbent; the reservoir was not allowed to become completely empty. The collection of a fraction was terminated when the next eluent was about two-thirds down the adsorption section. The visibility of the fronts between the different eluents in the column made it easy to observe the above condition. Before exchanging receivers, the tip of the adsorption column was washed

[1] This work was performed under the sponsorship of the Federal Facilities Corporation, Office of Synthetic Rubber, as part of the Government Synthetic Rubber Program.

[2] Figures in brackets indicate the literature references at the end of this paper.

with some of the appropriate solvent to redissolve deposited material. After the final fraction had been collected, carbon tetrachloride was used to wash the tip because of the very slight solubility of the last fraction in ethanol. In the separation, the less strongly adsorbed components are eluted first, followed by those more strongly adsorbed. An important function of the carbon tetrachloride, as an eluent preceding ethanol, is to solubilize the ethanol-desorbable constituents which are very slightly soluble in ethanol. By this procedure, the entire sample was recovered. The volatile solvents in the eluted fraction were removed by distillation and the weights of the oil residues were determined.

3.2. Evaluation of Procedure

The effectiveness of the chromatographic separation was evaluated from experiments performed on solutions containing known amounts by weight of "saturates" (paraffins and cycloparaffins) and "aromatics" that were separated from an aromatic type oil (Sundex 53). For this separation, 150 g of the oil was processed according to the program shown in figure 1. For this large-scale separation, a 70 mm diam column, packed with 1,750 g of silica gel (28–200 mesh) was used. Five main fractions (I-P, II-B, III-B, IV-B, and V-M) were eluted from this column with pentane, benzene, and methanol, respectively. Fractions I–P and III–B were rechromatographed in smaller columns. The refractive indices given in figure 1 refer to those of the oil portions. A still further separation of lot II–P was made in order to remove some material having a higher refractive index. The amounts of these fractions in lot II–P, expressed as weight percent, were: II–P1, 96.6; II–P2, 1.5; II–P3, 1.0; and II–P4, 0.6.

The saturate portion, lot II–P2, used in preparing known solutions A through H (table 1) was investigated for possible inclusion of some 1-ring aromatic material. The refractive index of this portion was 1.4797 at 25 °C, whereas the refractive index of the eluted portions of the test solution E was 1.4790. Some of lot II–P was further fractionated by adsorption as shown in figure 1. The infrared analysis of these fractions showed that benzene ring compounds were present in fraction II-P4 and absent in fraction II-P1. A second series of solutions, I through K in table 1, was prepared from lot II-P1, which was substantially free of aromatics.

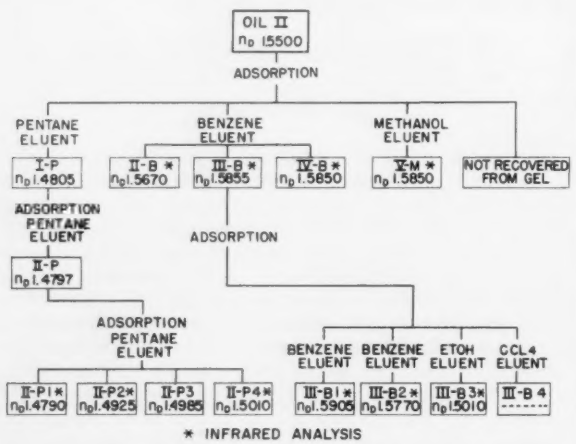

FIGURE 1. *Chromatographic separation of 150 g of a rubber-processing oil.*

II-P, II-P1, III-B and III-B1 are portions used in preparing test solutions of saturates and aromatics for evaluating the analytical chromatographic procedure. n_D=refractive index at 25 °C.

TABLE 1. *Chromatographic separations of test solutions of saturates (paraffins and cycloparaffins) and aromatics*

Solution	Amount of solution chromatographed	Saturates in solution	Saturates found by analysis	Difference [c] (calc-found)
	Series 1 [a]			
	g	*wt%*	*wt%*	*wt%*
A	2.5	5.86	6.28, 6.22, 6.00	−0.3(−0.5)
B	2.5	10.28	10.36, 10.42, 10.43	−.1(−0.4)
C	2.5	25.93	25.71, 25.65	.3(−0.5)
D	2.0	45.97	44.48	1.5(0.1)
E	0.5	49.51	47.50, 47.15, 47.80	2.0(0.5)
	2.5	49.51	47.72, 47.75, 47.43	1.9(0.4)
	4.5	49.51	47.67	1.8(0.3)
F	2.5	52.25	50.47	1.8(0.2)
G	2.5	75.47	73.54	1.9(−0.3)
H	2.5	89.81	86.44	3.4(0.7)
	Series 2 [b]			
I	2.5	26.28	26.02	0.3
J	2.5	47.18	46.71	.5
K	2.5	74.26	73.41	.9

[a] These solutions were prepared from lots II–P (saturates) and III–B (aromatics). It was later found that this saturate portion contained some aromatics.
[b] These solutions were prepared from lots II–P1 (saturates) and III–B1 (aromatics). This saturate portion was free of aromatics.
[c] Values in parentheses corrected for about 3 percent aromatics in saturate portion II–P.

A summary of the results of a study of the infrared spectra [3] of the fractions separated from this oil follows:

1. Lot II–P1: no aromatic rings.
2. Lot II–P2: indication of aromatic ring compounds.
3. Lot II–P4: polynuclear aromatic or single-ring aromatic with long straight chain.
4. Lot III–B1: large aromatic type molecules with few side chains, slight indication of NH group.
5. Lot III–B2: aromatic pattern about the same as lot III–B1, but indicates more NH or possibly OH; possible presence of carbonyls which were not present in lot III–B1. The combination of NH, OH, and carbonyl would indicate the presence of carboxylic acid or acid amide.

[3] The infrared analyses were performed by J. E. Stewart, formerly of the Gas Chemistry Section, Chemistry Division.

6. Lot III–B3: greatest number of aromatic rings, different from lots III–B1 and III–B2; possible presence of a sulfoxide or a sulfone.
7. Lots II–B, III–B, and IV–B: largely aromatic; no indication of oxygen, sulfur, or nitrogen compounds.
8. Lot V–M: resembles lot III–B2.

Experiments were performed to determine the relation between the volume of eluent and the amount of oil desorbed. In the first of these experiments about 0.7 g of saturated hydrocarbons (lot P–1, fig. 1) was adsorbed on 90 g of silica gel in the small column and eluted with pentane. A series of 20 ml fractions were collected and the weight of oil in each determined. These results are shown in figure 2. The bulk of the oil was recovered in the first two fractions; the amount recovered in each of the succeeding fractions is shown on an expanded scale.

Similar experiments were performed in which 0.84 g of aromatic hydrocarbons (lot III–B, fig. 3) were adsorbed and then eluted with pentane and benzene. The results are shown in figure 3. The amounts of material recovered in successive 20-ml fractions of the pentane eluent are shown on an expanded weight scale. It will be noted that only 0.012 g was eluted by pentane; the remainder was rapidly eluted by benzene, the bulk appearing in the first 20 ml.

In a third experiment, a solution containing both saturates and aromatics was adsorbed and eluted, first with pentane, followed by benzene; the results are shown in figure 4. The original solution was prepared from 0.2875 g of fraction I–P (saturates) and 0.9845 g of fraction III–B (aromatics). These experiments established the volumes of pentane and benzene required to separate a saturate portion and an aromatic portion.

Experiments were also performed to establish the reliability of the method for the determination of saturates (paraffins and cycloparaffins) in an extender-oil. Binary solutions of saturates and aromatics were prepared from fractions II–P and III–B for series 1 and from fractions II–P1 and III–B1 for series 2. These solutions were chromatographed and the results are given in table 1.

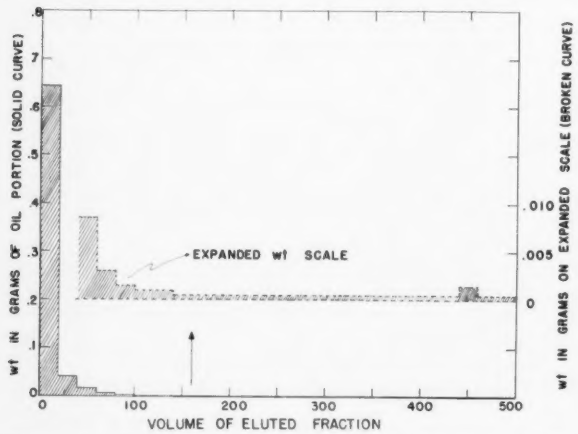
wt IN GRAMS OF OIL PORTION (SOLID CURVE)
wt IN GRAMS ON EXPANDED SCALE (BROKEN CURVE)
EXPANDED wt SCALE
VOLUME OF ELUTED FRACTION

FIGURE 2. *Weight of oil eluted with pentane from test solution of saturates.*

Source of saturates; lot II–P, figure 1.

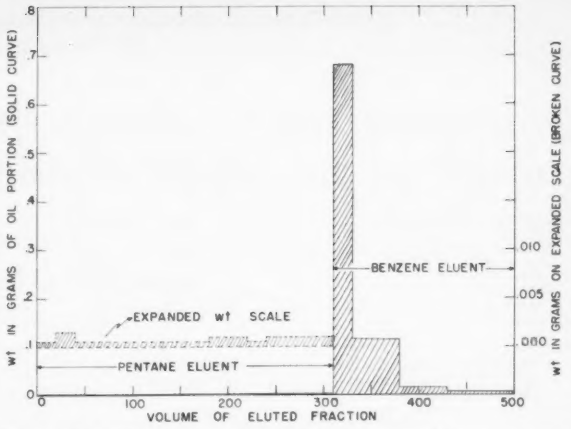
wt IN GRAMS OF OIL PORTION (SOLID CURVE)
wt IN GRAMS ON EXPANDED SCALE (BROKEN CURVE)
BENZENE ELUENT
EXPANDED wt SCALE
PENTANE ELUENT
VOLUME OF ELUTED FRACTION

FIGURE 3. *Weight of oil eluted with pentane and benzene from test solution of aromatics.*

Source of aromatics; lot III–B, figure 1.

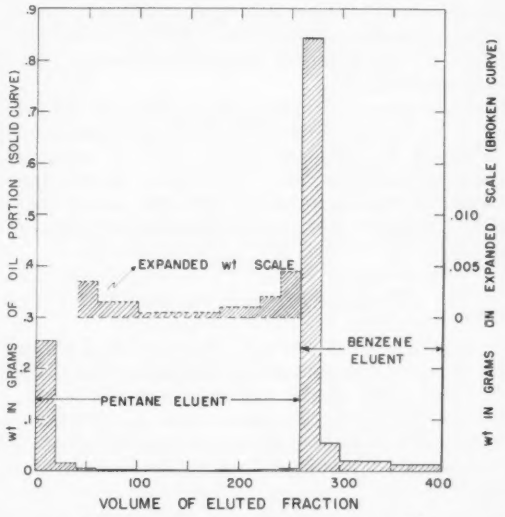
wt IN GRAMS OF OIL PORTION (SOLID CURVE)
wt IN GRAMS ON EXPANDED SCALE (BROKEN CURVE)
EXPANDED wt SCALE
BENZENE ELUENT
PENTANE ELUENT
VOLUME OF ELUTED FRACTION

FIGURE 4. *Weight of oil eluted with pentane and benzene from test solution of saturates and aromatics.*

Source of saturates; lot II–P, figure 1.
Source of aromatics; lot III–B, figure 1.

The large differences found for solutions of 50 to 90 percent saturates (solutions D–H) can be explained by the presence of a small amount of aromatic-type material in lot II–P. One-ring aromatic compounds containing paraffin side chains are adsorbed on silica gel only slightly more strongly than three- or four-ring cycloparaffins containing paraffin side chains. In solutions D through H, such aromatic compounds would be retained on the silica gel; but in solutions (A through C) having a lower content of saturated hydrocarbons, they

TABLE 2. *Results of the chromatographic separations of six extender-oils*

Extender-oil type	Oil portions in eluted fractions										Total wt % recovered
	1st pentane		2d pentane		Benzene		Carbon tetrachloride		Ethanol		
	wt%[a]	n_D^{25}[b]	wt%[b]	n_D^{25}[b]	wt%[a]	n_D^{25}[b]	wt%[a]	n_D^{25}[b]	wt%[b]	n_D^{25}[b]	
Naphthenic: Circosol 2XH	53.4	1.4882	2.0	1.5017	41.3	1.5635	0.7	1.5552	2.6	(c)	100.0
Aromatic:											
Sundex 53 (Oil II)	25.1	1.4805	1.7	1.4992	68.0	1.5796	.9	1.5630	6.0	(c)	101.7
Shell SPX97	26.0	1.4800	4.8	1.4995	64.3	1.5865	.8	----------	5.0	(c)	100.9
Highly Aromatic:											
Philrich 5	11.0	1.4845	6.2	1.5015	75.7	1.5780	.3	----------	6.3	(c)	99.5
Dutrex 20	5.9	1.4915	1.2	1.5020	80.6	1.6065	.8	1.6070	10.6	(c)	99.1
Califlux TT	11.8	1.4923	0.7	1.5018	74.9	1.5885	.5	----------	11.8	(c)	99.7

[a] Expressed in terms of weight of sample of oil chromatographed.
[b] Refractive index of components from oil in eluted fractions.
[c] Refractive index not determined because these fractions were highly colored liquids which contained dispersed solids.

would be eluted. When lot II–P1, which had been further fractionated to remove aromatics, was used for the saturate portion these large differences did not appear (solutions I through K). When the compositions of solutions A through H are corrected for the 3 percent of aromatics found to be present in lot II–P, much better agreement results (see last column of table 1).

Analyses given in table 1 show that oils containing about 5 to 75 percent saturated hydrocarbons may be analyzed by this procedure with an uncertainty of less than one percent. This range of composition embraces all oils now being used in the manufacture of oil-extended rubbers of the butadiene-styrene types.

3.3. Analysis of Extender Oils

A summary of the weight percent and refractive index of the five fractions separated chromatographically from each of the six extender-oils is given in table 2. The infrared absorption spectra of these fractions [19] showed that there were marked differences between fractions separated from the same oil and marked similarities between corresponding fractions separated from the different oils. The spectra have been compared with those [20] for fractions separated from asphalts [21] and by acid extraction of an extender-oil [22]. A more complete study of the composition of the extender oils will be given in another report [1].

4. Conclusions

The chromatographic procedure described in this report provides a simple, reproducible, and relatively rapid method of analyzing rubber-processing oils. The selective solvents, pentane, benzene, carbon tetrachloride, and ethanol, separate the oil adsorbed on silica gel into five compositionally different fractions. The analyses provide a means for evaluation of the oils as rubber extenders.

(Page 66A2–152)

5. References

[1] A. R. Glasgow and D. J. Termini, Chemical constitution of petroleum fractions used in oil-extended rubber, to be published in J. Research NBS.
[2] F. D. Rossini, B. J. Mair, and A. J. Streiff, Hydrocarbons from Petroleum (Reinhold Publishing Corp., New York, 1953).
[3] K. Van Nes and H. A. Van Weston, Aspects of the constitution of mineral oils (Elsevier Publishing Co., Inc., New York, 1951).
[4] A. N. Sachanen, The chemical consitutents of petroleum (Reinhold Publishing Corp., New York, 1945).
[5] W. K. Taft, J. Duke, A. D. Snyder, M. Feldon, and R. W. Laundrie, Ind. Eng. Chem. **45,** 1043 (1953).
[6] K. V. Weinstock, E. B. Storey, and J. S. Sweely, Ind. Eng. Chem. **45,** 1035 (1953).
[7] F. S. Rostler and R. M. White, Rubber Age **70,** 735 (1952).
[8] F. S. Rostler and H. W. Sternberg, Ind. Eng. Chem. **41,** 598 (1949).
[9] Sun Oil Company, Marcus Hook, Pennsylvania, A method of classifying oils in oil-extended rubbers, 1954.
[10] S. S. Kurtz, Jr., R. W. King, W. J. Stout, D. G. Partikian, and E. A. Skrabek, Anal. Chem. **28,** 1928 (1956).
[11] S. S. Kurtz, Jr., R. W. King, and J. S. Sweely, Ind. Eng. Chem. **48,** 2232 (1956).
[12] Sun Oil Company, Marcus Hook, Pennsylvania, A graphical method of selecting oils used in compounding and extending butadiene-styrene rubbers, 1958.
[13] S. S. Kurtz, Jr., R. W. King, W. J. Stout, and M. E. Peterkin, Anal. Chem. **30,** 1224 (1958).
[14] S. S. Kurtz, Jr., and C. C. Martin, India Rubber World **126,** 495 (1952).
[15] W. L. Dunkel, F. P. Ford, and J. N. McAteer, Ind. Eng. Chem. **46,** 578 (1954).
[16] T. F. Mika, F. M. McMillan, and S. H. Page (Shell Development Company, Emeryville, Calif.), Chromatographic separation of rubber-processing oils from Petroleum sources, presented at 63rd meeting of the Division of Rubber Chemistry, Am. Chem. Soc. (May 27, 1953).
[17] W. J. Stout, R. W. King, M. E. Peterkin, and S. S. Kurtz, Jr., Symposium on Composition of Petroleum Oils, Adsorption and physical property methods, Spe. Tech. Pub. No. 224, Am. Soc. for Testing Materials (1958).
[18] M. R. Lipkin, W. A. Hoffecker, C. C. Martin, and R. E. Ledley, Anal. Chem. **20,** 130 (1948).
[19] F. J. Linnig and J. E. Stewart, J. Research NBS **59,** 27 (1957) RP2771.
[20] J. E. Stewart, J. Research NBS **58,** 265 (1957) RP2759.
[21] L. R. Kleinschmidt, J. Research NBS **54,** 163 (1955) RP2577.
[22] F. S. Rostler and R. M. White, Ind. Eng. Chem. **46,** 610 (1954).

JOURNAL OF RESEARCH of the National Bureau of Standards—A. Physics and Chemistry
Vol. 66A, No. 2, March–April 1962

Cross-Sectional Correction for Computing Young's Modulus From Longitudinal Resonance Vibrations of Square and Cylindrical Rods

Wayne E. Tefft and Sam Spinner

(December 8, 1961)

The cross-sectional correction involved in the calculation of Young's modulus from the longitudinal resonance vibrations of both square and cylindrical bars has been determined by an empirical method.

On an order of accuracy of 1 part in 1,000, Bancroft's correction, developed for longitudinal waves in cylinders of infinite length was found to be satisfactory. For this purpose the thickness of square bars is related to the diameter of cylindrical bars of the same length by $4t^2=3d^2$.

For accuracies of 1 part in 10,000, modifications in Bancroft's correction must be applied. These modifications take a different form for the square rods than for the cylindrical rods. The relation, $2l=n\lambda$ held for both shapes and on the higher order of accuracy, i.e., the cross-sectional correction was the same for the fundamental and overtones on specimens of the same effective length.

1. Introduction

This is the fourth in a series of papers [1,2,3] [1] dealing with the empirical establishment of accurate [2] relations for computing elastic moduli from the various types of resonance vibrations of isotropic solids. The experimental technique and general approach have been fully described in these previous papers and will not be elaborated here. In one of these papers [2] the problem of the cross-sectional correction factors involved in the computation of Young's modulus from both the fundamental and overtones of the longitudinal resonance vibrations of cylindrical bars has already been treated. The present investigation extends this treatment by considering longitudinal vibrations of square as well as cylindrical bars; and on a higher order of accuracy for both shapes (by a factor of 10) than in the previous work.

Bancroft [4] has obtained an accurate numerical solution of the Pochhammer-Chree equations for the case of longitudinal waves in cylinders of infinite length. However, it is known [5] that these equations cannot be applied rigorously for longitudinal resonance vibrations in bars of finite length (where the ends of the bar are at zero stress). The problem of the present investigation is to determine experimentally the degree to which Bancroft's solution, developed for longitudinal waves in cylinders of infinite length, fits the case for longitudinal resonance vibrations in cylindrical and square bars of finite length; and to what degree modification is required.

[1] Figures in brackets indicate the literature references at the end of this paper.
[2] As accurate as the determination of the relevant parameters permit.

2. Experiment

Of the eight steel specimens used in this investigation, (table 1) the first six were the same ones used in a previous study [3], and have the same designation. A description of their method of preparation and characterization is given in that reference. This description applies also to the remaining two specimens. The longitudinal modes of vibration were obtained concurrently with the torsional modes discussed in [3]. Consequently, the advantage which was gained in the previous study by cutting down certain larger specimens after a series of resonance frequencies had been determined, and obtaining the resonances on the shortened specimens thus formed (enabling one to obtain a fairly large number of experimental points from a fairly small piece of original stock), is also retained here.

The number of experimental points obtained here, however, was more limited than in the study on torsion because the fundamental and overtones of the longitudinal resonance frequencies of bars are higher than the corresponding torsional ones. It is recalled from the previous paper that the upper frequency limit of the resonance determinations is about 50 kc/s. Consequently, fewer overtones of longitudinal resonances could be obtained before this upper frequency limit was attained; and for the shortest specimen (A_{11}, actually a cube) for which only the fundamental torsional resonance could be determined, not even the fundamental longitudinal resonance frequency could be detected.

The same precautions to insure accuracy, including waiting for the specimens to attain thermal equilibrium with a controlled ambient temperature, that were taken for the torsional resonance determinations, were also used here. The accuracy of these

resonance determinations, was conservatively estimated to be about 1 part in 10,000, as was the case for torsional resonance.

3. Results and Analysis

The frequency of the fundamental and overtones of the longitudinal resonance vibrations of all the specimens is given in table 1.

TABLE 1. *Dimensions and longitudinal resonance frequencies of specimens of this investigation*

Specimen*	Length	Thickness	Resonance frequencies (c/s)			
			f_1**	f_2	f_3	f_4
	cm	cm				
A	28.5902	3.4950	9043.6	18030.5	26890	35529
A 1	19.9753	3.4950	12931.2	25686	38016	----
A 12	16.1737	3.4950	15953.1	31555	46234	----
A 2	8.2550	3.4950	30932	59437	----	----
B	5.7142	2.5737	44807	----	----	----
C	9.2341	2.5737	27927	55075	----	----
D	9.2340	2.2285	27924	55057	----	----
F	5.7144	2.2285	44795	----	----	----

*Specimens B and C are cylindrical; all others are square in cross section.
**f_1=fundamental resonance frequency, f_2=first overtone, etc.

We proceed with an analysis of the data by recalling certain well-known relations, some of which have been used previously [2] in studying this mode of vibration. First, the relation between the velocity, v_0, of a longitudinal wave in an infinitely thin rod, of infinite length, and the Young's modulus, E, and density, ρ, of the medium is given by

$$v_0=\sqrt{E/\rho}. \tag{1}$$

In a cylinder of finite diameter, d, and infinite length, the velocity of a longitudinal wave, v, is reduced from v_0. Bancroft's [4] numerical solution of the Pochhammer-Chree equations for this particular case has already been mentioned. His results can be conveniently expressed in the form of a table, such as table 2, which gives numerical values of the reduction factor,

$$K_n=(v_B/v_0)^2, \tag{2}$$

as a function of d/λ (λ being the wavelength of the wave) and Poisson's ratio, μ, of the medium; v_B is the velocity from Bancroft's correction.

For square bars, no theory comparable in accuracy to that developed for cylinders (for this cross-sectional correction) appears to be available. However, it seems that the correction factors from table 2 could be applied to square bars if an appropriate assumption were made as to what cross-sectional dimension of a square bar should be taken to correspond to d for a cylinder of the same length. There appears to be some theoretical justification [5] for assuming that the correction would be the same if the polar moments of inertia of the square and circular cross-sectional areas were the same. This assumption was adopted here. Such a condition would require the following relation between the thickness, t, of a square bar, and the diameter, d, of a cylinder of the same length.

$$d^2=\frac{4}{3}t^2. \tag{3}$$

In longitudinal resonance vibrations in cylindrical or square rods (associated with standing waves) the following set of relations are usually adopted,

$$\lambda=2l/n,\ v_s=f_n\lambda=2lf_n/n \tag{4}$$

where l is the length of the specimen, v_s the "velocity" of the wave, f the longitudinal resonance frequency, and the letter n, either as a subscript, or independently, indicates the order of the resonance vibration; for the fundamental, $n=1$; for the first overtone, $n=2$, etc.

Assuming that $v_B=v_s$, and combining eqs (1), (2), and (4), one obtains the following relation,

$$E/\rho=(1/K_n)(2lf_n/n)^2. \tag{5}$$

Here the subscript in K_n takes on the added significance of indicating the order of vibration to which this correction factor applies.

All the parameters in the parentheses in eq (5) may be determined experimentally and E/ρ for a carefully selected group of specimens from the same source should be the same.

The remainder of this paper, then, reduces itself to the problem of determining the degree to which the factor, K_n, developed for longitudinal waves in cylinders of infinite length also applies to longitudinal resonance vibrations (in rods of finite length). This is equivalent to finding the degree to which the assumption that $v_B=v_s$ holds. Also to be tested is the assumption that square and cylindrical rods of the same length, having the same polar moments of inertia of cross sectional area, undergo the same reduction in velocity.

In figure 1, the data of table 1 are plotted on a scale comparable in precision (about 1 part in 1,000) to that of the previous study (fig. 1 of [2]). The square of the parameters comprising the ordinate and abscissa are selected, rather than the first power, as in the previous study, to show the approximately linear relationship that then exists between these variables. Such a presentation is in conformity with table 2 which facilitates accurate interpolation. For the highest accuracy of interpolation from Bancroft's values Aitken's [6] method of interpolation must be used. In order to include square as well as cylindrical specimens, β, in the figure, is chosen so that $\beta^2=(d/2)^2$, or $t^2/3$.

The line in the figure is obtained by plotting Bancroft's values from table 2 for an appropriate value of μ. Such a value may be selected in two independent ways, and the degree to which the values so obtained agree provides a check of the consistency of the data. On the one hand, one may select that value of μ from table 2 for which the associated values of ordinate and abscissa give the best fit to the experimental data. The value of μ so obtained was 0.2906. On the other hand, one may extrapolate

the experimental values to obtain the best estimate of v_0; then, knowing ρ for the specimens[3] from the previous study [3], E may be computed from eq (1). Since G for these specimens is also known from [3], μ may be computed from the well-known relation, $\mu=(E/2G)-1$. The value of μ so obtained was 0.2880. This was the value used in the figure. The two values are seen to be in excellent agreement with each other and also with the ones given in the literature for steel.

Examination of figure 1 leads to the following conclusions:

(1) The data of the previous study for cylinders is confirmed in that Bancroft's cross-sectional correction for longitudinal waves in cylinders of infinite length may also be applied to longitudinal resonance vibrations (in cylinders of finite length).

(2) For square specimens, this correction also applies, if the assumption previously made is adopted, namely, that $d^2=(4/3)t^2=4\beta^2$.

The above two conclusions hold only on the order of accuracy of figure 1, i.e., 1 part in 1,000. Small deviations are noted when the data are plotted on a more expanded scale as will be shown in figures 2 and 3.

(3) For both square as well as cylindrical specimens, the observation previously made for cylindrical specimens with respect to overtones still holds. This is that the points for overtones fall on the same line as for fundamental resonance vibrations. This means that the relation, $\lambda=2l/n$, holds and that the correction factor for the overtones of a longer specimen is the same as for that of a shorter specimen having the same effective length (i.e., having the same value of abscissa).

In figure 2, the experimental points are plotted on a more extended scale, comparable to the full accuracy of the data itself, namely, about 1 part in 10,000. A convenient way to present such a plot

[3] Actually, since the same set of specimens is involved, ρ should be the same for all specimens and need not be known. Poisson's ratio may then also be computed using r_0 (longitudinal) and r_0 (torsional) in place of E and G, respectively; r_0 (torsional) is also known from [3].

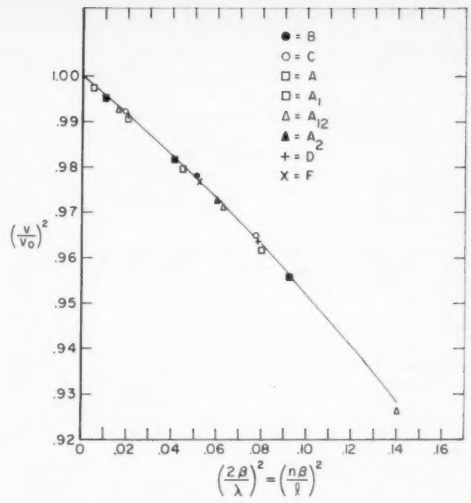

FIGURE 1. *Plot showing the reduction in longitudinal velocity, v, in a square or cylindrical rod of finite cross section from v_0, the corresponding velocity in an infinitely thin rod of the same length l.*

β is related to the diameter, d, of cylinders, and the thickness, t, of square rods by $4\beta^2=d^2$ and $3\beta^2=t^2$. Also the wavelength, $\lambda=2l/n$ (n being the overtone). The line is drawn through Bancroft's values for Poisson's ratio=0.2880, showing the agreement between Bancroft's correction, developed for longitudinal waves in cylinders of infinite length, and resonance vibrations in cylinders or square bars of finite length on this scale of accuracy (1 part in 1,000).

is in terms of possible departures of the experimental points from the velocities resulting from Bancroft's correction, v_B. This would correspond geometrically to making a horizontal line of the one given in figure 1 at $(v/v_B)^2=1$, and plotting the ratio $(v/v_B)^2$ as a function of $(\beta n/l)^2$ for all the experimental points in table 1.

When this procedure is followed, certain significant departures from Bancroft's correction become evident. The upper line shows that the cross-sectional correction factor for cylinders deviates linearly from Bancroft's correction as $(\beta n/l)^2$ increases.

TABLE 2. *Bancroft's cross-sectional correction factor, $K_B=(v_B/v_0)^2$ [a], as a function of Poisson's ratio, μ, and diameter to wavelength ratio, d/λ*

d/λ	μ / $(d/\lambda)^2$	.10	.15	.20	.25	.30	.35	.40
0.00	0.0000	1.00000	1.00000	1.00000	1.00000	1.00000	1.00000	1.00000
.05	.0025	0.99988	0.99972	0.99950	0.99922	0.99888	0.99848	0.99802
.10	.0100	.99950	.99886	.99798	.99686	.99549	.99389	.99206
.15	.0225	.99882	.99736	.99533	.99277	.98967	.98609	.98202
.20	.0400	.99780	.99509	.99138	.98670	.98117	.97480	.96772
.25	.0625	.99632	.99184	.98579	.97830	.96956	.95975	.94903
.30	.0900	.99421	.98728	.97810	.96702	.95435	.94049	.92571
.35	.1225	.99114	.98085	.96759	.95203	.93486	.91660	.89770
.40	.1600	.98651	.97158	.95310	.93236	.91031	.88770	.86503
.45	.2025	.97913	.95778	.93300	.90668	.88003	.85372	.82812
.50	.2500	.96621	.93646	.90503	.87383	.84372	.81499	.78780

[a] v_0 is the velocity of a longitudinal wave in an infinitely thin cylinder, and v_B is the velocity in a cylinder of finite diameter and infinite length.

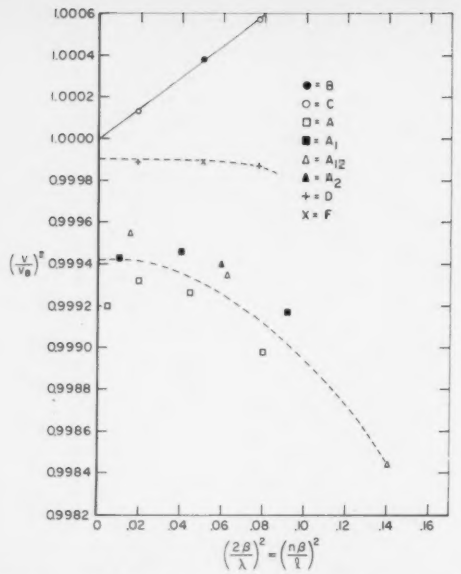

FIGURE 2. *Expanded plot showing departure of longitudinal velocities, associated with resonance vibrations, from values obtained using Bancroft's correction for longitudinal waves, v_B, as a function of cross section to length.*

Upper line is a least square solution of points for cylindrical specimens while lower two curves are simply drawn through experimental points for smaller and larger square specimens.

This line is obtained by a least squares fit of the experimental points yielding the following relation:

$$(v/v_B)^2 = 1 + 0.0075(nd/2l)^2. \quad (6)$$

The two lower curves are for the square specimens. The fact that two such curves, one for the larger specimens and one for the smaller ones, appear is disconcerting but presents no serious problem. If the reasonable assumption is made that the separation of these curves is caused by real differences in intrinsic elastic moduli (or E/ρ) of the large and small specimens due to differences in work hardening or some other cause [4] and the two curves are brought into coincidence by changing the base value for the lower curve, say, then figure 3 results. Following the procedure of the other figures, the abscissa is again squared in order to obtain an approximately linear relationship. The line in figure 3 is also a least square solution of the experimental points, represented by the equation,

$$(v/v_B)^2 = 1 - 0.055[1/3(nt/l)^2]^2. \quad (7)$$

It is emphasized that these departures from Bancroft's correction do not mean that this factor is in

[4] It is recalled from [3] that the large and small square specimens were cut from opposite ends of the original stock. It is also important to remember that these differences only show themselves on the highly expanded scale of figure 2.

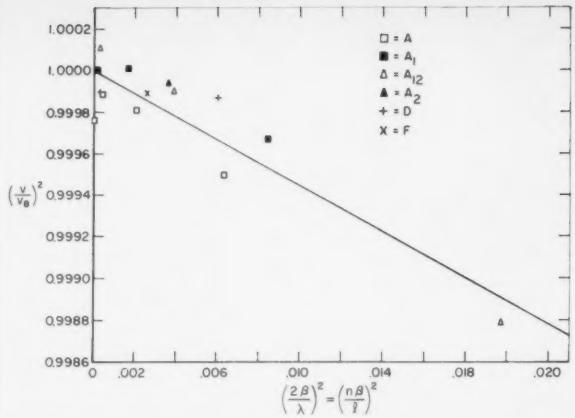

FIGURE 3. *Expanded plot showing reduction in longitudinal velocities of square bars, associated with longitudinal resonance vibrations, from that obtained using Bancroft's correction, after adjustment in the base value of the larger specimens.*

The line is a least square solution of the experimental points.

error. Rather they are a measure of the degree to which the experimental points depart from Bancroft's values when the conditions of his analysis are not fulfilled.

It is also noted that the third observation on figure 1 concerning the identity of the correction factor for overtones and fundamental resonance vibrations still holds on the expanded scale of figures 2 and 3. It is recalled from the previous study [3] that this was not the case for torsional resonance vibrations in square rods in which the cross-sectional correction for overtones followed a different pattern from that for the fundamental of specimens of the same effective length. For cylindrical specimens in torsional resonance, on the other hand, no cross-sectional correction at all is required theoretically either for the fundamental or for overtones and this is borne out by experiment.

4. Summary

The foregoing analysis may now be summarized in the following way.

In making the cross-sectional correction for longitudinal resonance vibrations of square or cylindrical bars, Bancroft's theoretical correction (developed for longitudinal waves in cylinders of infinite length) may be safely used if accuracy not higher than 1 part in 1,000 is sought. Bancroft's values are presented in such a manner that linear interpolations can also be made to this order of accuracy.

In making a similar correction to an accuracy of 1 part in 10,000, an adjustment in Bancroft's correction factor is required. In computing E, from this mode of vibration, then, the following two equations fit the data.

(a) For cylinders

$$E=\rho/K_n(2lf_n/n)^2\,[1+0.0075(nd/2l)^2].$$

(b) For square bars

$$E=\rho/K_n(2lf_n/n)^2\,[1-0.055(1/3\{nt/l\}^2)^2].$$

Linear interpolation of Bancroft's values is accurate to 1 part in 10,000 except at the highest values of $d/\lambda=n\beta/l$. In this range Aiken's method of interpolation must be used.

(Paper 66A2–153)

5. References

[1] S. Spinner and R. C. Valore, Jr., Comparison of theoretical and empirical relations between the shear modulus and torsional resonance frequencies for bars of rectangular cross section, J. Research NBS **60,** 459 (1958) RP2861.

[2] S. Spinner, T. W. Reichard, and W. E. Tefft, A comparison of experimental and theoretical relations between Young's Modulus and the flexural and longitudinal resonance frequencies of uniform bars, J. Research NBS **64A** (Phys. and Chem.), No. 2, 147–155 (Mar.–Apr. 1960).

[3] W. E. Tefft and S. Spinner, Torsional resonance vibrations of uniform bars of square cross section, J. Research NBS **65A** (Phys. and Chem.), No. 3, 167–171 (May–June 1961).

[4] D. Bancroft, The velocity of longitudinal waves in cylindrical bars, Phys. Rev. **59,** 588–593 (1941).

[5] A. E. H. Love, A treatise on the mathematical theory of elasticity, Fourth Edition, pp. 287–290, Footnote p. 290 (Dover Publications, New York).

[6] A. C. Aitken, Proc. Edinburgh Math. Soc. Ser. 2, **3,** 56 (1932).

JOURNAL OF RESEARCH of the National Bureau of Standards—A. Physics and Chemistry
Vol. 66A, No. 2, March–April 1962

Publications of the National Bureau of Standards*

(Including papers in outside journals)

Selected Abstracts

Tables of spectral-line intensities arranged by wavelengths, W. F. Meggers, C. H. Corliss, and B. F. Scribner, *NBS Mono. 32, Pt. II (1961) $3.00.*
The relative intensities, or radiant powers, of 39,000 spectral lines with wavelengths between 2000 and 9000 Angstroms have been determined on a uniform energy scale for seventy chemical elements. This was done by mixing 0.1 atomic percent of each element in powered copper, pressing the powder mixture to form solid electrodes which were burned in a 10 ampere, 220 volt direct-current arc, and photographing the spectra with a stigmatic concave grating while a step sector was rotating in front of the slit. The sectored spectrograms facilitated the estimation of intensities of all elements lines relative to copper lines which were then calibrated on an energy scale provided by standardized lamps, and all estimated line intensities were finally adjusted to fit this calibration. Comparisons with other intensity measurements in individual spectra indicate that the National Bureau of Standards spectral-line intensities may have average errors of 20 percent, but first of all they provide uniform quantitative values for the seventy chemical elements commonly determined by spectrochemists. These data are presented by element in part I, and all 39,000 observed lines are given in order of wavelength in part II.

Tables of chemical kinetics. Homogeneous reactions (Supplementary tables), *NBS Mono. 34 (Sept. 15, 1961) $2.75.*
A description of these tables and definition of the terms and abbreviations used may be found in the introduction to the 1951 publication. A brief description of the method used in compiling these tables and the limitation of coverage is given in the preface to Supplement 1. A description of the numbering system used in classifying reactions for the tables is given in Supplement 2. The present supplement contains information pertaining to Substitution, Exchange, and Elimination reaction types. It is not complete as still more material falling in these groups is being prepared. The amount of kinetic data to be studied made it seem advisable to present all the material completed to date without further delay. The data on each section give the year and month to which the literature has been surveyed.

Ultraviolet absorption spectrum of ammonia in solid argon at 4.2 °K, K. Dressler, *J. Chem. Phys.* **35** *No. 1, 165–169 (July 1961).*
A series of absorption bands in the region 1600 A to 1900 A has been observed in thin films of solid argon containing between 0.3% and 3% of ammonia. The bands are attributed to isolated NH_3, and the missing of alternate bands in the observed vibrational progression shows that in the ground state only the $J=0$ level is appreciably populated. Thermal equilibration of NH_3 at 4.2 °K involves the interconversion of nuclear spin species. It is suggested that the observed rapid equilibration is due to coupling between the proton spins and the spin of the nitrogen nucleus.

Photon-dissociation of water: initial nonequilibrium populations of rotational states of OH ($^2\Sigma^+$), I. Tanaka, T. Carrington, and H. P. Broida, *J. Chem. Phys.* **35** *No. 2, 750–751 (Aug. 1961).*
The irradiation of water vapor by 10 volt photons leads to an excited state which eventually dissociates into a normal hydrogen atom and an electronically excited OH radical. Our spectroscopic observations of the rotational and vibrational distributions of these OH radicals show that different excitation energies affect the initial state of the water molecule, and that added inert gases influence the dissociation of this molecule.

Repulsion of energy levels in complex atomic spectra, R. E. Trees, *Phys. Rev.* **123,** *No. 4, 1293–1300 (Aug. 15, 1961).*
Rosenzweig and Porter have shown a "repulsion of energy levels" in spacing distributions determined from energy levels in complex atomic spectra. The present paper extends their work by showing that these spacing distributions can be determined from calculated positions of the levels in these spectra. Since calculated data are available for spectra where the observed data are scarce or incomplete, this partially overcomes limitations imposed by statistical inaccuracy when direct use is made of the observed data. The equivalence of the two approaches is demonstrated by showing that calculated data for Ta II yield the same spacing distribution as obtained from observed data for Ta II and Re I combined. These are complex spectra in which a fully developed repulsion effect is present. A similar demonstration of equivalence is carried out for spectra of Ru I and Mo I, where the repulsion effect is in an intermediate state of development. The results also indicate that numbers easily evaluated from the radial parameters of the theory will indicate roughly the degree of repulsion, replacing to some extent the need for an explicit calculation of the spacing distribution.

Infrared spectrum and structures of the NF_2 radical, M. D. Harmony, R. J. Myers, L. J. Schoen, D. R. Lide, Jr., and D. E. Mann, *J. Chem. Phys.* **35,** *No. 3, 1129 (Sept. 1961).*
The infrared spectrum of the NF_2 radical has been detected in a heated sample of N_2F_4. The stretching vibrations ν_1 and ν_3 are assigned as 1074 cm^{-1} and 935 cm^{-1}, respectively. The former band shows well-resolved rotational structure, from which one obtains $A-(B+C)/2=1.93\pm0.01$ cm^{-1}. This constant implies an FNF angle of about 104°.

Statistical dynamics of simple cubic lattices. Model for the study of Brownian motion II, R. J. Rubin, *J. Math. Phys.* **21,** *No. 3, 373–386 (May–June 1961).*
New results concerning the statistical dynamics of a heavy particle in an n-dimensional (nD) cubic lattice are presented. In a well-defined sense, the random motions of a heavy particle in a 1D lattice and a 3D lattice are accurately described by Kramers' equation for a free particle and a harmonically bound particle, respectively. A related, but not independent, result, is that the velocity $v(t)$ and position $u(t)$ of a heavy particle in a 1D lattice and a 3D lattice constitute two dimensional stationary gaussian Markoff processes. It is definitely established that in the case of a 2D lattice the stationary gaussian process $\begin{pmatrix} v(t) \\ u(t) \end{pmatrix}$ is non-Markoffian. In the course of the analysis, several interesting connections between solutions of the discrete lattice equations of motion and solutions of the corresponding continuum equation of motion (the nD wave equation) are uncovered.

Mass spectrometric study of the thermal dissociation of N_2F_4, J. T. Herron and V. H. Dibeler, *J. Chem. Phys.* **35,** *No. 2, 747–748 (Aug. 1961).*
The bond dissociation energy $D(F_2N\text{-}NF_2)$ has been measured by a mass spectrometric method to be 21.5 kcal/mole. This is considered accurate within 1.6 kcal/mole.

Effect of branching on the thermal decomposition of polymers, L. A. Wall, *Soc. Chem. Ind. Mono.* **13,** pp. 146–162 (Page Bros. (Norwich) Ltd., England, 1961).

The rates of volatilization for certain linear polymers, for example, polyethylene and polypropylene and copolymers of ethylene and propylene, prepared using Ziegler-type catalyst, show maxima in the region of 20 to 40% volatilization, or conversion. On the other hand, polymers prepared from the same monomers under conditions that produce branched molecules show a continuous decrease in the rate of volatilization with conversion. The presence of a maximum indicates the operation, at least partially, of an overall random mechanism of scission. Theoretical treatments have previously been made by Simha on the random breakdown of branched chains and on the random breakdown perturbed by allowing chain bonds at branched points to rupture more rapidly than the other chain bonds. The net result was that branched chains *per se* do not account for the lack of maxima in the rate curves, although experimentally the influence of the branches is apparent. From a study of degradation rates of approximately forty polymers having varying numbers and lengths of branches, the results show that in paraffinic hydrocarbon polymers containing three or more methyl end groups per 100 methylene chain groups, the maxima are eliminated provided the branches contained two or more carbon atoms.

Phase equilibria research in systems involving the rare earth oxides, R. S. Roth, *Book, Rare Earth Research Pt. II, pp. 88–95 (The MacMillan Company, New York, N.Y., 1961).*

This manuscript is a review of the unpublished phase equilibria research at present being conducted at the National Bureau of Standards on systems involving rare earth oxides with: (1) oxides of other trivalent ions, (2) Nb_2O_5 or Ta_2O_5, and (3) B_2O_3. Simplified solid-state phase diagrams are shown for the systems involving oxides of trivalent rare earth ions and Al_2O_3, Ga_2O_3, Cr_2O_3, Fe_2O_3, Sc_2O_3 and In_2O_3.

Degradation of poly (2,3,4,5,6-pentafluorostyrene), L. A. Wall, J. M. Anotnucci, S. Straus, and M. Tyron, *Soc. Chem. Ind. Mono. No.* **13,** *295–302 (1961).*

The rates of thermal decomposition of a ploymer of 2,3,4,5,6-pentafluorostyrene have been measured, and from these data an activation energy value of 65 kcal per mole was calculated. A qualitative evaluation was also made of the behavior of the polymer in photo-oxidation. The results of both studies indicate that the material is to a surprising degree more stable than polystyrene. Although further mechanism studies are necessary for a complete understanding of the effects observed, it seems evident that the alpha C–H bonds and the C–C bonds of the polymer chain are stronger in the poly, pentafluorostyrene. This is interpreted to be the result of decreased resonance interaction between the chain bonds and the phenyl groups due to the presence of fluorine atoms on the phenyl ring.

The half-life of carbon-14, W. B. Mann, W. F. Marlow, and E. E. Hughes, *Intern. J. Appl. Radiation and Isotopes* **11,** *No. 2, 57–67 (1961).*

The half-life of carbon-14 has been determined with an accuracy believed to be higher than that of previously reported values. Carbon dioxide was liberated by the action of perchloric acid on barium carbonate which contained C^{14} in approximately 44 percent isotopic abundance. Samples of this C^{14} dioxide were analyzed mass spectrometrically, and other portions were diluted quantitatively with inert carbon dioxide and counted in the NBS length-compensated internal gas counters. Technical difficulties encountered in this work, which are characteristic of this type of experiment, particularly problems of adsorption and the methods used to overcome them, are discussed in detail. On the basis of a thorough analysis of all results obtained, the half-life of C^{14} is believed to be 5760 ± 50 years, where the indicated uncertainty denotes an estimated overall probable error of the result.

Rate of the reaction NO + N, J. T. Herron, *J. Chem. Phys.* **35,** *No. 3, 1138–1139 (Sept. 1961).*

The rate of the reaction NO+N has been measured to be $k = 1.0 \pm 0.5 \times 10^{13}$ cc. mole^{-1} sec^{-1}.

Transition probabilities in multilevel system: calculation from impulsive and steady-state experiments, T. Carrington, *J. Chem. Phys.* **35,** *No. 3, 807–816 (Sept. 1961).*

The study of collison induced transitions of molecules in a system of many energy levels is discussed in an analysis of time dependent and steady state experiments. These results are used in a discussion, with numerical examples, of the difficulties in calculating the transition probabilities from observed population distributions.

An intimate conceptual and mathematical relationship is established between two types of experiments which are possible at present. One is an impulse, or time dependent experiment such as excitation with a fast flash lamp and snapshot observation after a known delay time. The other is a steady state experiment in which molecules are fed into the system (a gas or a surface) at a single energy level, for example, and undergo transitions among the available levels in competition with a first order removal process such as spontaneous radiation or description from a surface.

The ideas summarized above are used to develop procedures for calculating transition probabilities from observed population distributions. Numerical examples and qualitative considerations indicate that when transitions involving more than single quantum jumps are involved, the experimental data must be known to much higher accuracy than that desired in the transition probabilities. The difficulties increase rapidly as the number of levels in the system increases.

Perturbations and rotational intensities observed in CN bands emitted by reactions of organic molecules with nitrogen atoms, N. H. Kiess and H. P. Broida, *J. Mole. Spect.* **7,** *No. 3, 194–208 (Sept. 1961).*

The rotational perturbations between the $v=0$ level of the $B^2\Sigma^+$ electronic state and the $v=10$ level of the $A^2\pi_i$ electronic state of CN have been re-investigated. Rotational analyses of the 10.3 and 10.5 bands of the $A^2\pi$—$X^2\Sigma$ system and of the 0.0 band of the $B^2\Sigma$—$X^2\Sigma$ system have been made. The relative intensities of the perturbed lines, extra lines, and neighboring unperturbed lines have been studied as a function of pressure from 0.1 to 100 mm Hg. A new pair of extra lines has been found. At the higher pressures the populations of the excited rotational levels of CN approach a Boltzmann distribution. As the pressure is lowered the intensities of the perturbed and extra lines become continually more anomalous. The interpretation is given that CN is formed in the $A^2\pi$ state more than 20 times as readily as it is formed in the $B^2\Sigma$ state in reactions of organic molecules with the nitrogen afterglow.

Molecular structure of propylene, D. R. Lide and D. Christensen, *J. Chem. Phys.* **35,** *No. 4, 1374–78 (Oct. 1961).*

The microwave spectra of seven isotopic species of propylene have been studied in order to obtain an accurate molecular structure. The complete r_s (substitution) structure has been calculated. The more important parameters are: r (C—C) $= 1.336 \pm 0.004$ A, r (C—C) $= 1.501 \pm 0.004$ A, $\angle CCC = 124.3° \pm 0.3°$. The structure is compared with those of related molecules. It is concluded that no difference can be detected in the double-bond lengths in ethylene, propylene, and the vinyl halides. The CC single-bond length in propylene is indistinguishable from that in acetaldehyde and other acetyl compounds, and is 0.025 A shorter than the CC distance in saturated hydrocarbons. In the $—CH_2$ group in propylene the CH bond *trans* to the methyl group appears slightly shorter than the *cis* CH bond; a similar effect occurs in the vinyl halides.

Low-angle X-ray diffraction of crystalline nonoriented polyethylene and its relation to crystallization mechanisms, L. Mandelkern, A. S. Posner, A. F. Diorio, and D. E. Roberts, *J. Appl. Phys.* **32,** *No. 8, 1509–1517 (Aug. 1961).*

X-ray diffraction maxima at low angles have been observed in crystalline but non-oriented linear polyethylene, the crystallization process being conducted from the melt of the pure undiluted polymer. Several orders of diffraction are observed in favorable cases, and the spacings corresponding

to the first-order reflections range from 150 to 850A. The values of the maxima depend on the mode of crystallization. Previous assertions that in such systems the maxima are limited to 100–200A are shown to be overly restrictive and typical only of crystallization processes conducted at very large undercoolings.

Major attention is focused on the properties of specimens crystallized isothermally at relatively low values of the undercooling. The spacings are very sensitive to the crystallization temperature in this range. The highest values are observed at low undercooling and substantial decreases occur as the temperature is lowered. Concomitantly, the density observed after isothermal crystallization significantly decreases with a lowering of the crystallization temperature.

The fact that a periodicity can be developed in such systems, the magnitude of the maxima, and their dependence on the crystallization temperature, is explicable by the application of nucleation theory. It is assumed that subsequent to the formation of critical-size nuclei from a bundle of polymer chains, crystal growth along the chain direction is severely retarded, while in the transverse direction essentially unimpeded crystallization occurs. From the observed temperature coefficient of the low angle spacings the ratio of the excess free energy (due to the junction of crystalline and amorphous regions at the crystallite ends) to the bulk enthalpy of fusion is found to be 2.6. The magnitude of this ratio receives confirmation from other types of experiments.

Intramolecular rearrangements. II. Photolysis and radiolysis of 4-methyl-2-hexanone, P. J. Ausloss, *J. Phys. Chem.* **65,** *1616–1618 (1961).*

In the photolysis and radiolysis of 4-methyl-2-hexanone, three butene isomers are formed by an intramolecular rearrangement process in which a secondary or primary γ-hydrogen is transferred to the carbonyl group.

In the vapor-phase photochemical decomposition, the ratios 1-butene/2-butene and *cis*-2-butene/*trans*-2-butene increase with decrease in wavelength and increase in temperature. In the liquid-phase photolysis, however, no dependence on wavelength was observed, although the effect of temperature on the butene distribution was very pronounced. Similar results were obtained in the photochemical decomposition of *sec*-butyl acetate. In the transition of the liquid to the solid phase there was a drastic change in the butene distribution. The butene distribution obtained in the photosensitized decomposition at 2537A agrees closely with the one obtained in the nonsensitized decomposition at the same wavelength.

A comparison of the results obtained in the photolysis with those obtained in the radiolysis in the vapor and liquid phase indicates that in the latter case the butenes may be formed by way of a highly electronically excited molecule.

Infrared spectra of carbon monoxide as a solid and in solid matrices, A. G. Maki, *J. Chem. Phys.* **35,** *No. 3, 931–935 (Sept. 1961).*

The fundamental infrared absorption frequency of several isotopes of CO has been observed in solid carbon monoxide and in the solid matrices N_2, Ar, and CH_4. In addition, the overtone in solid carbon monoxide has been measured. It is shown that frequency shifts due to isotopic substitution in the solid state follow the formulas developed for the gas phase only when molecules of the same isotopic species are not adjacent to each other, i.e., only in dilute solutions.

Other NBS Publications

Journal of Research 66B (Math. and Math. Phys.) No. 1 (Jan.–Mar. 1962) 75 cents.

Error bounds for eigenvectors of self-adjoint operators. N. W. Bazley and D. W. Fox.

Intermediary equatorial orbits of an artificial satellite. J. P. Vinti.

Selected bibliography of statistical literature 1930 to 1957: V. Frequency functions, moments, and graduation. L. S. Deming.

Measurement of wave fronts without a reference standard: Part 2. The wave front-reversing interferometer. J. B. Saunders.

Journal of Research 66C (Eng. and Instr.) No. 1 (Jan.–Mar. 1962) 75 cents.

Reference tables for 40 percent iridium-60 percent rhodium versus iridium thermocouples. G. F. Blackburn and F. R. Caldwell.

A method for the self-calibration of attenuation-measuring systems. R. L. Peck.

Special shielded resistor for high-voltage d-c measurements. J. H. Parks.

Voltage ratio measurements with a transformer capacitance bridge. T. L. Zapf.

Weight calibration schemes for two-knife-edge direct-reading balances. H. E. Almer, L. B. Macurdy, H. S. Peiser, and E. A. Weck.

Tunnel diode large-signal equivalent circuit study and the solutions of its nonlinear differential equations. S. B. Geller and P. A. Mantek.

A missile technique for the study of detonation waves. F. W. Ruegg and W. W. Dorsey.

Creep of cold-drawn nickel, copper, 70 percent nickel-30 percent copper, and 30 percent nickel-70 percent copper alloys. W. D. Jenkins and W. A. Willard.

Journal of Research 66D (Radio Prop.) No. 2 (Mar.–Apr. 1962) 70 cents.

Atmospheric phenomena, energetic electrons, and the geomagnetic field. J. R. Winckler.

The summer intensity variations of [OI] 6300 A in the tropics. D. Barbier, F. E. Roach, and W. R. Steiger.

Generation of radio noise in the vicinity of the earth. P. A. Sturrock.

Fading characteristics observed on a high-frequency auroral radio path. J. W. Koch and H. E. Petrie.

Some problems connected with Rayleigh distributions. M. M. Siddiqui.

Impedance of a monopole antenna with a radial-wire ground system on an imperfectly conducting half space, Part I. S. W. Maley and R. J. King.

Theory of the infinite cylindrical antenna including the feed-point singularity in antenna current. R. H. Duncan.

The E-field and H-field losses around antennas with a radial ground wire system. T. Larsen.

The electric field at the ground plane near a disk-loaded monopole. J. Hansen and T. Larsen.

An experimental study of phase variations in line-of-sight microwave transmissions, K. A. Norton, J. W. Herbstreit, H. B. Janes, K. O. Hornberg, C. F. Peterson, A. F. Barghausen, W. E. Johnson, P. I. Wells, M. C. Thompson, Jr., M. J. Vetter, and A. W. Kirkpatrick, NBS Mono. 33 (Nov. 1, 1961) 55 cents.

Bibliography and index on vacuum and low pressure measurement, W. G. Brombacher, NBS Mono. 35 (Nov. 10, 1961) 60 cents.

Effect of mortar properties on strength of masonry, C. C. Fishburn, NBS Mono. 36 (Nov. 20, 1961) 30 cents.

Tabulation of data on microwave tubes, C. P. Marsden, W. J. Keery, and J. K. Moffitt, NBS Handb. 70, (Nov. 1, 1961) $1.00.

Safety rules for the installation and maintenance of electric supply and communications lines. Comprising Part 2, the definitions, and the grounding rules of the sixth edition of the National Electrical Safety Code, NBS Handb. 81, (1961) $1.75.

Mean electron density variations of the quiet ionosphere, No. 6—August 1959, J. W. Wright, L. R. Wescott, and D. J. Brown, NBS Tech. Note 40–6 (PB151399–6) (1961) $1.50.

Techniques for computing refraction of radio waves in the troposphere, E. J. Dutton and G. D. Thayer, NBS Tech. Note 97 (PB161598) (1961) $1.50.

Performance predictions for single tropospheric communication links and for several links in tandem, A. P. Barsis, K. A. Norton, P. L. Rice, and P. H. Elder, NBS Tech. Note 102 (PB161603) (1961) $3.00.

Mode calculations for VLF propagation in the earth-ionosphere waveguide, K. P. Spies and J. R. Wait, NBS Tech. Note 114 (PB161615) (1961) $1.50.

Astrophysical and plasma physics research at the National Bureau of Standards, Highlights for 1961, L. M. Branscomb, K. E. Shuler, J. A. Suddeth, NBS Tech. Note 116 (PB161617) (1961) $1.00.

Variations in frequency of occurrence of sporadic *E* 1949–1959, W. B. Chadwick, NBS Tech. Note 117 (PB161618) (1961) 75 cents.

Electrical conduction in *p*-type titanium sesquioxide, J. Yahia and H. P. R. Frederikse, Phys. Rev. **123,** No. 4, 1257–1261 (Aug. 15, 1961).

Parameters α and β in the spectra of the iron group. R. E. Trees and C. K. Jorgensen, Phys. Rev. **132,** No. 4, 1278–1280 (Aug. 15, 1961).

Slow drift solar radio bursts: harmonic frequency ratios, solar longitude dependence, and frequency drift rates, M. B. Wood, Australian J. Phys. **14,** No. 2, 234–241 (1961).

Fibrous silica, W. Haller, Nature **191,** No. 4789, 662–663 (Aug. 12, 1961).

Control terminology—A report on U.S. standards activity H. L. Mason, Control Eng. **8,** No. 10, 67–70 (Oct. 1961).

Behavior and evaluation of rubber, R. D. Stiehler, Am. Concrete Pipe Assoc. Tech. Memo. (Oct. 1961).

Partial confounding in fractional replication, W. J. Youden, Technometric **3,** No. 3, 353–358 (Aug. 1961).

Welded butt joints with fine wires, L. Martz, Rev. Sci. Instr., **32,** No. 8, 990–991 (Aug. 1961).

Systematic errors in physical constants, W. J. Youden, Physics Today **14,** No. 9, 32–34, 36, 38, 40, 42 (Sept. 1961).

A study of solar activity associated with polar cap absorption (abstract), C. S. Warwick and M. B. Wood, Polar Cap Absorption Conf. (Kiruna, Sweden, Aug. 8–11, 1960), Arkiv Géofyski **3,** No. 21, 457 (1960).

Kr^{86} and atomic-beam-emitted Hg^{198} wavelengths, R. L. Barger and K. G. Kessler, J. Opt. Soc. Am. **51,** No. 8, 827–829 (Aug. 1961).

Excess noise in microwave detector diodes, J. J. Faris and J. M. Richardson, IRE Trans. Microwave Theory and Tech. **MTT–9,** No. 4, 312–314 (July 1961).

Conductance of solutions of water, acetic anhydride, and acetyl chloride in acetic acid, T. B. Hoover and A. W. Hutchinson, J. Am. Chem. Soc. **83,** No. 16, 3400–3405 (1961).

Amine buffers for *p*H control, R. G. Bates, Ann. N.Y. Acad. Sci. **92,** No. 2, 341–356 (June 1961).

Exact and approximate distributions for the Wilcoxon statistic with ties, S. Y. Lehman, J. Am. Stat. Assoc. **56,** 293–298 (June 1961).

Some geometrical theorems for abscissas and weights of gauss type, P. J. Davis and P. Rabinowitz, J. Math. Anal. Appl. **2,** No. 3, 428–437 (June 1961).

Some relationships between short-wave fadeouts, magnetic crochets, and solar flares, L. W. Acton, J. Geophys. Research **66,** 3060–3063 (Sept. 1961).

A simple calibration technique for vibrating sample and coil magnetometers, N. V. Frederick, Proc. IRE **49,** 1449 (Sept. 1961).

First pulsed radio soundings of the topside of the ionosphere, R. W. Knecht, T. E. Van Zandt, and S. Russell, J. Geophys. Research **66,** 3078–3081 (Sept. 1961).

Performance characteristics of turbine flowmeters, M. R. Shafer, Trans. ASME J. Basic Eng. Paper No. 61–WA–25 (1961).

Periodicity modulo *m* and diversibility properties of the partition function, M. Newman, Trans. Am. Math. Soc. **97,** No. 2, 225–236 (Nov. 1960).

The synthesis of food, A. T. McPherson, Ind. Research, pp. 20–27 (Nov. 1961).

Effect of mercury-alloy ratio on the physical properties of amalgams, W. T. Sweeney and C. L. Burns, J. Am. Dental Assoc. **63,** No. 9, 374–381 (Sept. 1961).

Measurement characteristics of farm milk tanks, M. W. Jensen, Scale J., pp. 4–5 (Oct. 1961).

Applications of statistics in Post Office automation, B. M. Levin and N. C. Severo, Am. Statistician **15,** No. 4, 14–18 (Oct. 1961).

Experimental design and the ASTM committees, W. J. Youden, Materials Research and Standards, 862–867 (Nov. 1961).

Present status of panoramic roentgenography, J. W. Kumpula, J. Am. Dental Assoc. **63,** No. 8, 194–200 (Aug. 1961).

Sun-time replaced by atomic clocks, R. S. Tipson, Capital Chemist **11,** 255 (Nov. 1961).

What is the best value? W. J. Youden, J. Wash. Acad. Sci. **51,** No. 6, 95–97 (Oct. 1961).

The permanent function as an innerproduct, M. Marcus and M. Newman, Bull. Am. Math. Soc. **67,** No. 2, 223–224 (March 1961).

Thermal conductivity of some commercial iron-nickel alloys, T. W. Watson and H. E. Robinson, Trans. ASME, Series C, J. Heat Transfer **83,** No. 4, 403–408 (Nov. 1961).

Exploratory research on demineralization, A. Rose, R. F. Sweeny, T. B. Hoover, V. N. Schrodt, Ch. in Book, Saline Water Conversion, Advances in Chemistry Series No. 27, 50–55 (American Chemical Society, Washington, D.C., 1960).

Measurement of the transition probability of the OI multiplet at 6157A, W. L. Wiese and J. B. Shumaker, Jr., J. Opt. Soc. Am. **51,** No. 9, 937–942 (Sept. 1961).

Deposition of metals from the vapor phase and similarity of the process to electrodeposition, A. Brenner, Trans. Inst. Metal Finishing **38,** No. 4, 123–130 (Aug. 1961).

Photographic response to successive exposures of different types of radiation, M. Ehrlich and W. L. McLaughlin, J. Opt. Soc. Am. **51,** No. 11, 1172–1181 (Nov. 1961).

On the possibility of rejecting certain modes in VLF Propagation, J. R. Wait, Proc. IRE, Letter **49,** 1429–1430 (Sept. 1961).

The relaxation times of some paramagnetic dispersions, P. H. Fang, Physica **27,** 68 (1961).

Multiple biologic recording for digital analysis, H. L. Mason, Proc. Interdisciplinary Clinic on the Instrumentation Requirements for Psychophysiological Research, FIER Clinic on Psychophysiological Instrumentation, Lafayette Clinic, pp. 65–67 (May 16–17, 1961).

**Publications for which a price is indicated (except for Technical Notes) are available only from the Superintendent of Documents, U.S. Government Printing Office, Washington 25, D.C. (foreign postage, one-fourth additional). Technical Notes are available only from the Office of Technical Services, U.S. Department of Commerce, Washington 25, D.C. (Order by PB number.) Reprints from outside journals and the NBS Journal of Research may often be obtained directly from the authors.*

UNIVERSITY MICROFILMS INC
EDITORIAL DEPARTMENT
313 NORTH FIRST ST
ANN ARBOR MICH
SUR-A OCT
UNIVERSITY OF

UNI
GOVERNMEN
DIVISION OF PUBLIC DOCUMENTS
WASHINGTON 25, D.C.

OFFICIAL BUSINESS

PENALTY FOR PRIVATE USE TO AVOID PAYMENT OF POSTAGE, $300 (GPO)

JOURNAL OF RESEARCH of the National Bureau of Standards Vol. 66A, No. 2 March–April 1962
A. Physics and Chemistry

Contents

Page

Correction factors for the calibration of encapsulated radium sources. R. M. Lee and T. P. Loftus. 103

Description and analysis of the second spectrum of tantalum, Ta II. C. C. Kiess. 111

Vibration-rotation bands of carbonyl sulfide. Arthur G. Maki, Earle K. Plyler, and Eugene D. Tidwell. 163

Ionization in the plasma of a copper arc. Charles H. Corliss. 169

The vapor pressure of palladium. R. F. Hampson and R. F. Walker. 177

Revised standard values for *p*H measurements from 0 to 95 °C. Roger G. Bates. 179

Conductometric determination of sulfhydryl groups in swollen polycaprolactam fibers having disulfide and alkylene sulfide crosslinks. Stephen D. Bruck and Sylvia M. Bailey. 185

Chromatographic analysis of petroleum fractions used in oil-extended rubber. Dominic J. Termini and Augustus R. Glasgow. 189

Cross-sectional correction for computing Young's modulus from longitudinal resonance vibrations of square and cylindrical rods. Wayne E. Tefft and Sam Spinner. 193

Publications of the National Bureau of Standards. 199

For sale by the Superintendent of Documents, U.S. Government Printing Office, Washington 25, D.C. Price 70 cents (single copy)
Subscription price: $4.00 a year; 75 cents additional for foreign mailing.
UNITED STATES GOVERNMENT PRINTING OFFICE, WASHINGTON : 1962